

## **Distribution Agreement**

In presenting this dissertation as a partial fulfillment of the requirements for an advanced degree from Emory University, I hereby grant to Emory University and its agents the non-exclusive license to archive, make accessible, and display my dissertation in whole or in part in all forms of media, now or hereafter known, including display on the world wide web. I understand that I may select some access restrictions as part of the online submission of this dissertation. I retain all ownership rights to the copyright of the dissertation. I retain all ownership rights to the copyright of the thesis. I also retain the right to use in future works all or part of this dissertation.

Signature:

---

Valarie M. Truax

---

Date

Design, Synthesis, and Biologic Evaluation of  
Tetrahydroisoquinoline-Based CXCR4 Modulators

By

Valarie M. Truax  
Doctor of Philosophy

Chemistry

---

Prof. Dennis C. Liotta, Ph.D.  
Advisor

---

Prof. Cora E. MacBeth, Ph.D.  
Committee Member

---

Prof. David G. Lynn, Ph.D.  
Committee Member

Accepted:

---

Lisa A. Tedesco, Ph.D.  
Dean of the James T. Laney School of Graduate Studies

---

Date

Design, Synthesis, and Biologic Evaluation of  
Tetrahydroisoquinoline-Based CXCR4 Modulators

By

Valarie M. Truax

Advisor: Prof. Dennis C. Liotta, Ph.D.

An abstract of  
A dissertation submitted to the Faculty of the James T. Laney School of Graduate Studies of  
Emory University in partial fulfillment of the requirements for the degree of  
Doctor of Philosophy  
in Chemistry  
2014

## Abstract

### Design, Synthesis, and Biologic Evaluation of Tetrahydroisoquinoline-Based CXCR4 Modulators

By Valarie M. Truax

CXCR4 is a G-protein coupled receptor (GPCR) that binds to the chemokine, CXCL12 (SDF-1, stromal cell derived factor -1). The CXCR4/CXCL12 signaling axis plays an essential role during embryogenesis as well as mediating immune cell trafficking and stem cell homing to the bone marrow. Dysregulation of the CXCR4/CXCL12 axis is also linked to several pathological conditions; including X4-tropic HIV-1 infection, cancer metastasis and inflammation. In an effort to discover potential treatments for these disorders, enormous efforts have been made by the research community to understand the mechanisms that govern CXCR4 signaling and develop novel and effective CXCR4 modulators.

In Chapter 2, the synthesis and structure activity relationship of novel AMD3100, 1,4-bis((1,4,8,11-tetraazacyclotetradecan-1-yl)methyl)benzene analogs are presented. These compounds have been evaluated for CXCR4 mediated effects in the viral attachment assay with HIV-1<sub>III-B</sub> in CCR5/CXCR4-expressing HeLa-CD4-LTR- $\beta$ -gal (MAGI) cells measuring each compound's ability to block potential viral entry as well as cellular toxicological properties. In Chapter 3, a novel series of highly potent and selective CXCR4 antagonists based on a chiral tetrahydroisoquinoline ((*R*)-THIQ)) scaffold are presented. This novel series made use of a GPCR chemotype with a chiral linkage that may exploit unique and efficient contacts with amino acid residues in the receptor. The data used to elucidate the structure activity relationships (SAR) of this series was generated by a combination of two assays: 1) blockade of HIV-1<sub>III-B</sub> attachment via the CXCR4 receptor in MAGI cells, and 2) inhibition of CXCL12 induced calcium ( $\text{Ca}^{2+}$ ) flux/release in Chem-1 cells. The compounds revealed a range of potencies and divergent SAR. The motif also provided compounds with unique biological selectivity and provided exciting insights for the design of X4-tropic HIV-1 selective modulators that do not interfere with CXCL12 based receptor signaling.

The CXCR4 receptor has a specific role in a wide range of human disease pathologies, but the interaction between CXCR4 and its natural ligand CXCL12 also synchronizes many essential physiological roles. Therefore, selective inhibition of X4-tropic HIV-1 entry without compromising the physiologically important signaling between CXCR4 and CXCL12 is crucial and therapeutically relevant. In Chapter 4, we describe the synthesis and biological activity of a new class of CXCR4 modulators. Within this series of compounds, certain analogues were identified with 2500-fold selectivity for blocking X4-tropic HIV-1 entry over inhibition of CXCL12 induced calcium flux. These compounds represent a novel class of CXCR4 modulators.

Design, Synthesis, and Biologic Evaluation of  
Tetrahydroisoquinoline-Based CXCR4 Modulators

By

Valarie M. Truax  
B.S., Salem College  
M.S., Georgetown University  
MBA, Emory University Goizueta Business School

Advisor: Prof. Dennis C. Liotta, Ph.D.

A dissertation submitted to the Faculty of the James T. Laney School of Graduate Studies of  
Emory University in partial fulfillment of the requirements for the degree of  
Doctor of Philosophy  
in Chemistry  
2014

## **Acknowledgements**

This dissertation is principally dedicated to my parents, Cynthia and John Truax, who have unconditionally supported me in every way throughout my life; without their loving, kind, and tireless encouragement, I would not have completed this work. I would also like to dedicate this work my grandparents Francis and Stephanie Hawke, and John and Edna Truax for their support and love; for encouraging me to pursue my dreams, to strive for greatness, and for always believing in me. I would also like to thank the Hawke Sisters, especially my godmother Pat Andrews and Wendy Lenz for their constant encouragement and support. I am incredibly grateful for having the opportunity to work in Dr. Dennis C. Liotta's research group, as well as to have had the opportunity to learn from Dr. James P. Snyder and the members of the computational lab. To Dr. Liotta, thank you for your unconditional support, for always believing in me, for your wise words, and for your unparalleled advisement. There are not words to express my gratitude or how much I have learned during my tenure under your tutelage. I will always be grateful for and think back on this time fondly. To Dr. Snyder, thank you for all the many engaging conversations that have been invaluable. I would also like to thank Dr. Cora E. MacBeth and Dr. David G. Lynn for all of your support and guidance throughout the years. Thank you to the Liotta group, current and past members for your friendship and an providing environment that has been an absolute pleasure to work in.

## Table of Contents

### List of Illustrations

Figures
Tables
Schemes
List of Graphs

## Chapter 1: Introduction and Background

---

1.1 CXCR4 and the Natural Ligand CXCL12	1
1.1.2 CXCX4 and CXCL12 Structures	3
1.1.3 Two-Site Ligand Binding	5
1.1.4 Signaling	6
1.2 Therapeutic Uses of CXCR4 Antagonists	
1.2.1 HIV Infection	8
1.2.2 Stem Cell Mobilization	9

## Chapter 2: Design of Novel AMD3100 Analogs

---

2.1 Statement of Purpose	15
2.2 Introduction and Background	16
2.3 Design Rational	19
2.4 Discussion & Biological Evaluation	21
2.5 Conclusions	29
2.6 Chemistry Experimental	30
2.7 Biological Experimental	45

## Chapter 3: Design of 1,2,3,4-tetrahydroisoquinoline-based CXCR4 Antagonists

---

3.1 Statement of Purpose	50
3.2 Introduction and Background	51
3.3 Design Rational	58
3.3.1 Tetrahydroisoquinoline Modifications	61
3.3.2 Butyl amine side chain Modifications	72
3.4 Discussion & Biological Evaluation	68
3.5 Conclusions	78
3.6 Chemistry Experimental	79
3.7 Biological Experimental	137

## Chapter 4: Design of Novel First-In-Class CXCR4 Allosteric Modulators

---

4.1 Statement of Purpose	147
4.2 Introduction and Background	149
4.3 Design Rational	151
4.4 Discussion & Biological Evaluation	152
4.5 Conclusions	157
4.6 Chemistry Experimental	158
4.7 Biological Experimental	187

## List of Illustrations

---

### List of Figures

Figure 1.1: Cartoon representation of CXCR4-IT1t structure	3
Figure 1.2: Cartoon representation of CXCL12 (SDF-1)	4
Figure 1.3: Proposed 2-step mechanism of the CXCR4/CXCL12 binding	5
Figure 1.4: CXCR4 signaling pathways	6
Figure 1.5: Mechanism of HIV-1 entry	8
Figure 1.6: Mechanism of stem cell mobilization	9
Figure 2.1: Structures of CXCR4 antagonists	15
Figure 2.2: Proposed binding mode of AMD3100 with CXCR4	17
Figure 2.3: CXCR4 antagonist template used to generate AMD3100 analogs	18
Figure 2.4: WZ-41 structure	18
Figure 2.5: Structures of select bioactive products that incorporate the bis-THF moiety	19
Figure 2.6: Structures of Brecanavir and Darunavir	20
Figure 2.7: Interaction in x-ray crystal structure of Darunavir bound to HIV protease	20
Figure 3.1: Selected orally bioavailable small-molecule CXCR4 antagonists.	50
Figure 3.2: Initial hit-to-lead efforts and general conclusions	52
Figure 3.3: General conclusions on initial hit-to-lead efforts.	53
Figure 3.4: Conclusions on hit-to-lead efforts	54
Figure 3.5: Overview of proposed N-THIQ and butyl amine analogs	57
Figure 3.6: Advanced intermediate scaffold	58
Figure 3.7: Retrosynthesis of N-TIC analogs	59
Figure 3.8: Retrosynthesis of butyl amine analogs <b>92-95</b>	64
Figure 4.1: Tetrahydroisoquinoline-based selective HIV compounds	
Figure 4.2: Allosteric and orthosteric ligands of G protein-coupled receptors; range of possible activities	65

### List of Tables

Table 2.1: Biological data for compounds <b>25, 29, 34, 36 &amp; 41</b>	21
Table 3.1: Tetrahydroisoquinoline analogs <b>45-64</b>	70
Table 3.2: Butyl amine analogs <b>74-84</b>	71
Table 3.3: Butyl amine analogs <b>92-95</b>	72

Table 3.4: Butyl amine analogs <b>102, 104, 108, &amp; 109</b>	73
Table 4.1: Tetrahydroisoquinoline analogs <b>125-139</b>	155

### List of Schemes

Scheme 2.1: Strategy for asymmetric synthesis of bis-THF alcohol	21
Scheme 2.2: Synthesis of fragment A1	22
Scheme 2.3: Retrosynthesis of bis-THF analogs	23
Scheme 2.4: Synthesis of fragment B1	24
Scheme 2.5: Synthesis of fragments A2 and A3	25
Scheme 2.6: Synthesis of analog <b>29</b>	25
Scheme 2.7: Synthesis of fragment B2	26
Scheme 2.9: Synthesis of analog <b>41</b>	27
Scheme 3.1: Synthesis of (S)-5,6,7,8-tetrahydroquinolin-8-amine	59
Scheme 3.2: Synthesis 4-(1,3,-dioxoisindolin-2-yl)butanol	60
Scheme 3.3: Synthesis of ( <i>R</i> )- <i>tert</i> -butyl 3-formyl-3,4-dihydroisoquinoline-2( <i>1H</i> )-carboxylate	60
Scheme 3.4: Synthesis of N-THIQ analogs <b>45-59</b>	61
Scheme 3.5: Synthesis of N-THIQ morpholine analog <b>63</b>	62
Scheme 3.6: Synthesis of butyl amine analogs <b>74-82</b>	63
Scheme 3.7: Synthesis of butyl amine analog <b>84</b>	64
Scheme 3.8: Synthesis of butyl amine analogs <b>102 &amp; 104</b>	65
Scheme 3.9: Synthesis of butyl amine analogs <b>108 &amp; 109</b>	66
Scheme 4.1: Synthesis of N-THIQ analogs <b>125-139</b>	152
Table 4.1: Tetrahydroisoquinoline analogs <b>125-139</b>	155

### List of Graphs

4.1: Inhibition of HIV-III <sub>B</sub> replication in PBMCs by <b>137</b>	181
4.2: Cytochrome P450 Assay on compound <b>137</b>	182
4.3: Displacement of <sup>125</sup> I-SDF-1 binding by compound <b>137</b>	185

# 1 Introduction and Background

## 1.1 CXCR4 and its Natural Ligand CXCL12

The C-X-C chemokine receptor type 4 (CXCR4) is a seven transmembrane (TM) protein that belongs to the superfamily of G-protein coupled receptors (GPCRs). GPCRs, with more than 1,000 members represent the largest family of vertebrate proteins grouped into six classes (A-F) on the basis of their sequence homology and functional similarity.<sup>1</sup> Perhaps more than any other type of protein, GPCRs have evolved to recognize a plethora of endogenous stimuli, and transmit signals encoded in stimuli from the exterior to the interior of the cell.<sup>2</sup> GPCRs mediate key physiological functions, and their dysfunction contributes to some of the most prevalent human diseases.<sup>3</sup> This emphasizes both the fundamental biological importance, as well as clinical importance of this family of membrane proteins. CXCR4 belongs to class A of GPCRs and is broadly expressed on most hematopoietic cell types including neutrophils, monocytes and macrophages, immature and mature T and B-lymphocytes, neurons, hematopoietic and endothelial progenitor and stem cells from blood and BM, and blood-derived dendritic cells.<sup>4</sup> It is also expressed at high levels on vascular endothelial cells,<sup>4c</sup> neurons and neuronal stem cells,<sup>5</sup> microglia, and astrocytes<sup>6</sup>.

The only known natural ligand for CXCR4 is the chemokine ligand 12 (CXCL12), also referred to as stromal-derived-factor-1 (SDF-1)<sup>7</sup>. Chemokines are small 70 amino acid long soluble proteins that chemoattract a variety of cell types to sites of inflammation or secondary lymphoid organs by interacting with chemokine receptors<sup>8</sup>. They are divided into four subfamilies based on the positions of two conserved cysteine residues on the amino (N)-terminus: CC, CXC, CX3C, and C.<sup>9</sup> CXCL12 belongs to the CXC class of chemokines and localized in the kidney, lungs, heart, liver, and bone marrow stromal cells, and is a key regulator

of hematopoietic stem cell (HSC) homing and retention in the bone marrow.<sup>9</sup> Importantly, the CXCR4/CXCL12 axis synchronizes many essential physiological roles, such as homeostatic regulation of leukocyte trafficking, hematopoiesis, and embryonic development.<sup>10</sup> Given the broad expression and function of CXCR4 and CXCL12, it is not surprising that CXCR4 was the first chemokine shown to be essential for life in mice.<sup>10b, 11</sup> Genetic disruption of CXCR4 and CXCL12 results in a similar lethal phenotype with defects in B cell lymphopoiesis, bone marrow colonization, cardiac septum formation, and abnormal hematopoiesis formation.<sup>12</sup>

From a historical perspective, it was the discovery elucidating CXCR4 as a co-receptor used along with CD4 by T cell-tropic (X4) HIV-1 strains for cellular entry that catalyzed the observed abundance of research.<sup>13</sup> This seminal discovery was concurrent with the elucidation of the mechanism of the anti-HIV-1 AMD3100, which a priori became the first small molecule CXCR4 antagonist.<sup>14</sup> Although, AMD3100 entered the clinic as an antiviral treatment of X4-HIV-1 strains, it was shown during clinical trials to mobilize various hematopoietic cells, including CD34+ cells. Through further clinical investigation the compound was subsequently approved by the FDA for use in mobilizing hematopoietic stem cells (HSCs) for autologous transplants in patients with non-Hodgkins lymphoma and multiple myeloma.<sup>15</sup> This unexpected finding resulted in an unprecedented therapeutic use and prompted a paradigm shift in CXCR4 research, significantly expanding the breadth and scope from both biological and medicinal chemistry standpoints. More recent CXCR4 discoveries include the involvement of the CXCR4/CXCL12 axis in the progression of 23 different types of cancer, where the interaction between CXCR4 and CXCL12 promotes metastasis, angiogenesis, and tumor growth via direct and indirect mechanisms.<sup>16</sup> Consequently, CXCR4 is an attractive target for therapeutic intervention and holds promise for a variety of clinical applications.

### 1.1.2 CXCR4 and CXCL12 Structure

CXCR4 consists of 352 amino acid residues comprising an N-terminal domain, seven TM alpha helices, three extracellular loops (ECL), three intracellular loops (ICL) and a C-terminal domain.

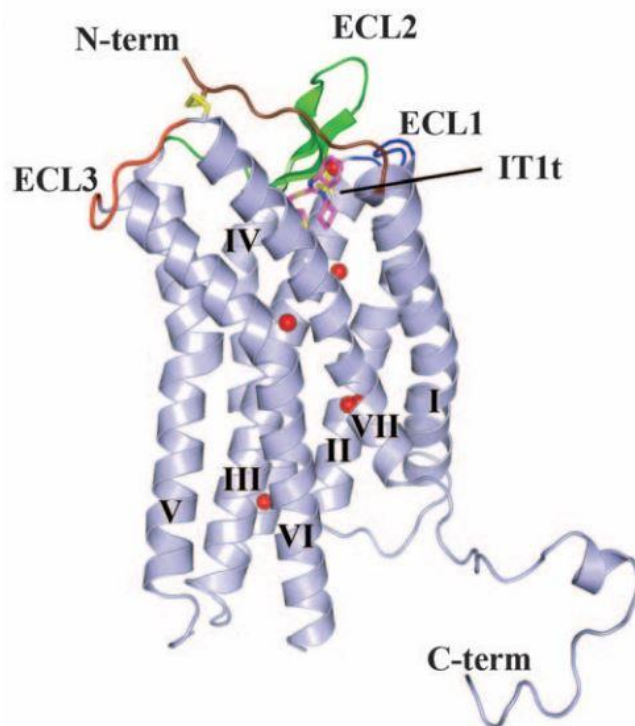


**Figure 1.1: Cartoon representation of the CXCR4-IT1t Structure.** The receptor is colored in blue. The N terminus, ECL1, ECL2, and ECL3 are highlighted in brown, blue, green, and red. The compound IT1t is shown in a magenta stick representation. The disulfide bonds are yellow. Water molecules are shown as red spheres.<sup>17</sup>

In 2010, five independent crystal structures of CXCR4 bound to an antagonist small molecule IT1t and a cyclic peptide CVX15 were reported.<sup>17</sup> This opened up new possibilities for structure-based drug design, and a detailed discussion of our efforts in this area are discussed *vide infra* (3.1.3).

The structures of multiple chemokines have also been determined by NMR and/or X-ray crystallography, including CXCL12. These structures demonstrate the highly conserved three-

dimensional structures of all chemokines.<sup>18</sup> In a typical structure, the first two cysteine are situated close together near the N-terminus, followed by a "N" loop. After the N-loop, there is a single-turn "3<sub>10</sub> helix", a  $\beta$ -sheet with three  $\beta$ -strands, connected by turns called "30s", "40s", and "50s" loops, and a C-terminal alpha helix.<sup>19</sup>

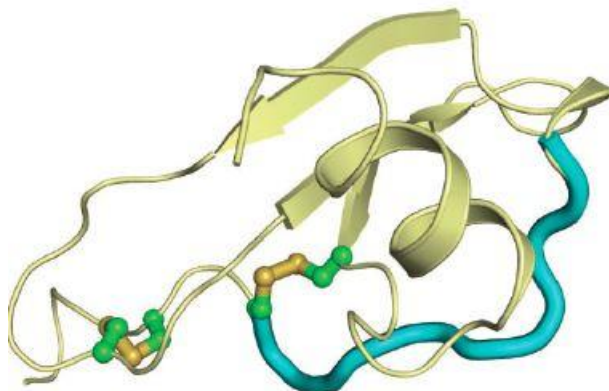


**Figure 1.2: CXCL12 from NMR solution structure.** The disulfide bonds are indicated in green and yellow. The N-loop is indicated in blue.<sup>19</sup>

### 1.1.3 Two-Site Ligand Binding

Understanding the mechanism of ligand binding and activation is of great importance and practical value for designing both antagonistic, agonistic, and allosteric ligands of CXCR4. A two-step/two-site theory for the binding of CXCL12 with CXCR4 was proposed in 2001 and has gained substantial experimental support with the release of the CXCR4 crystal structure (Figure 1.3).<sup>20</sup> In the two-step interaction, the first interaction between the SDF-1 (CXCL12)  $\beta$ -sheet, and N-loop and the CXCR4 extracellular region facilitates the anchoring of SDF-1 near the CXCR TM region.<sup>21</sup> After this, the SDF-1 N-terminus is postulated to search for the space of its binding through the well known "fly casting" mechanism of intrinsically disordered proteins.<sup>22</sup>

Consequently, the SDF-1 N-terminus binds to the cavities within the CXCR4 TM helices and triggers the conformational changes that leads to signaling and physiological responses.

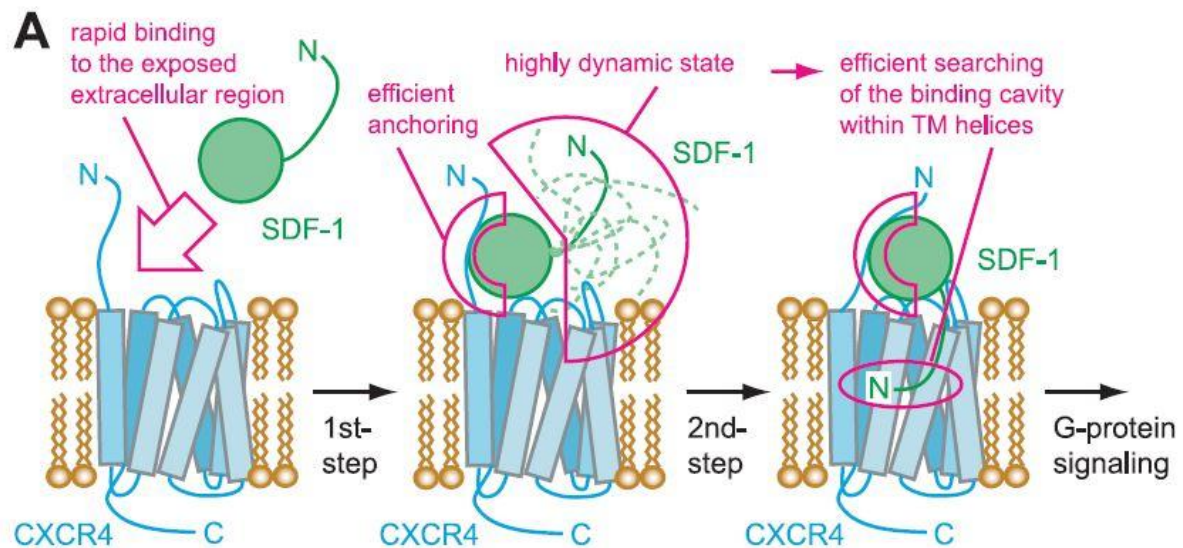
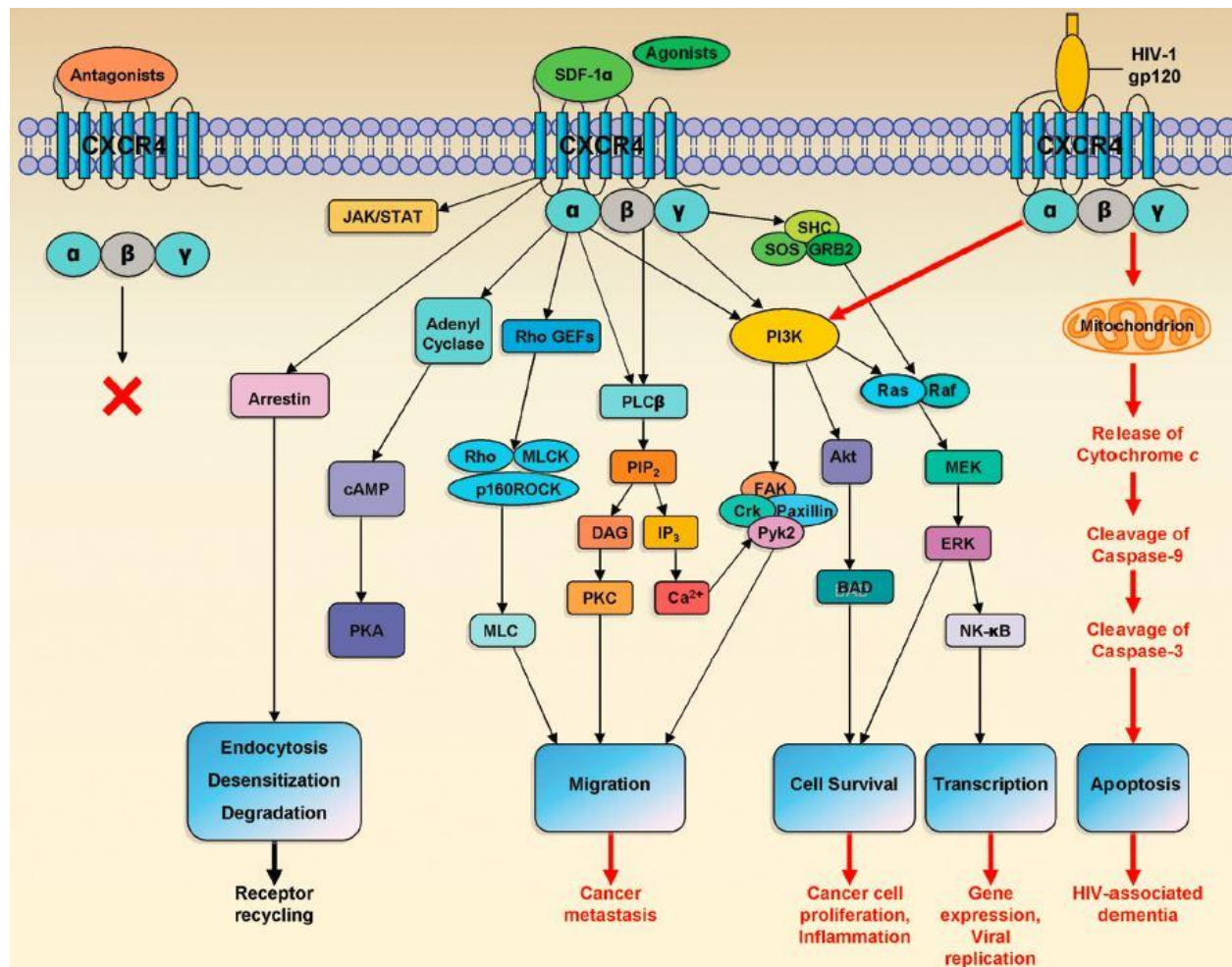


Figure 1.3: Proposed two-step mechanism for the CXCL12 (SDF-1) and CXCR4 interaction.<sup>21</sup>

### 1.1.4 Signaling

The activation of CXCR4 by CXCL12 (SDF-1) triggers different downstream signaling pathways that result in a variety of physiological responses, such as chemotaxis, cell survival and proliferation, intracellular calcium flux, and gene transcription. These normal physiological responses also share several downstream effectors with multiple pathological processes, including tumor cell metastasis, autoimmune, and inflammatory diseases (Figure 1.4).<sup>16c, 23</sup>



**Figure 1.4: CXCR4 intracellular signaling pathways.** CXCR4 activation by CXCL12 can trigger a variety of physiological responses such as chemotaxis, cell survival, and transcription, whereas CXCR4 antagonists fail to do so. The normal physiological responses also share several downstream effectors with multiple pathological processes, including tumor cell metastasis.<sup>24</sup>

The mechanism of CXCR4 receptor activation is mediated by coupling to an intracellular heterotrimeric G-protein associated with the inner surface of the plasma membrane. The heterotrimer is composed of  $G_\alpha$ ,  $G_\beta$ ,  $G_\gamma$  subunits. Upon CXCL12 binding the subunits dissociate into a  $\beta\gamma$  dimer and the  $\alpha$  monomer.<sup>25</sup> On the basis of sequence similarity, the  $G_\alpha$  subunits have been divided into four families  $G_{\alpha_s}$ ,  $G_{\alpha_i}$ ,  $G_{\alpha_q}$ ,  $G_{\alpha_{12}}$ . Each  $G_\alpha$  subunit relays the GPCR via different routes. One of the features of chemokine receptors is that they are primarily  $G_{\alpha_i}$ -

coupled receptors, and although it was originally thought CXCR4 was also limited to  $G\alpha_i$  signalling, more recent data suggests it can couple to other  $G\alpha$  proteins, such as  $G\alpha_q$ .<sup>26</sup>

## 1.2 Therapeutic Uses of CXCR4 Antagonists

### 1.2.1 HIV Infection

CXCR4 and CCR5 are the two major co-receptors for HIV entry into its target cells in the human immune system and play important physiological roles in viral infection. Through a series of steps, HIV enters the target cells by binding to the host surface receptor CD4 and a co-receptor, either CCR5 or CXCR4.<sup>27</sup> As the initiation step, the viral envelop (Env) glycoprotein gp120 (gp120) interacts with CD4, which in turn triggers the binding of gp120's V3 loop to the N-terminus, ECL2, ECL3, and the ligand binding cavity of CXCR4. These interactions lead to a conformational change in the viral TM protein gp41, cause a fusion of the viral and host membranes and the delivery of the viral payload.<sup>28</sup>

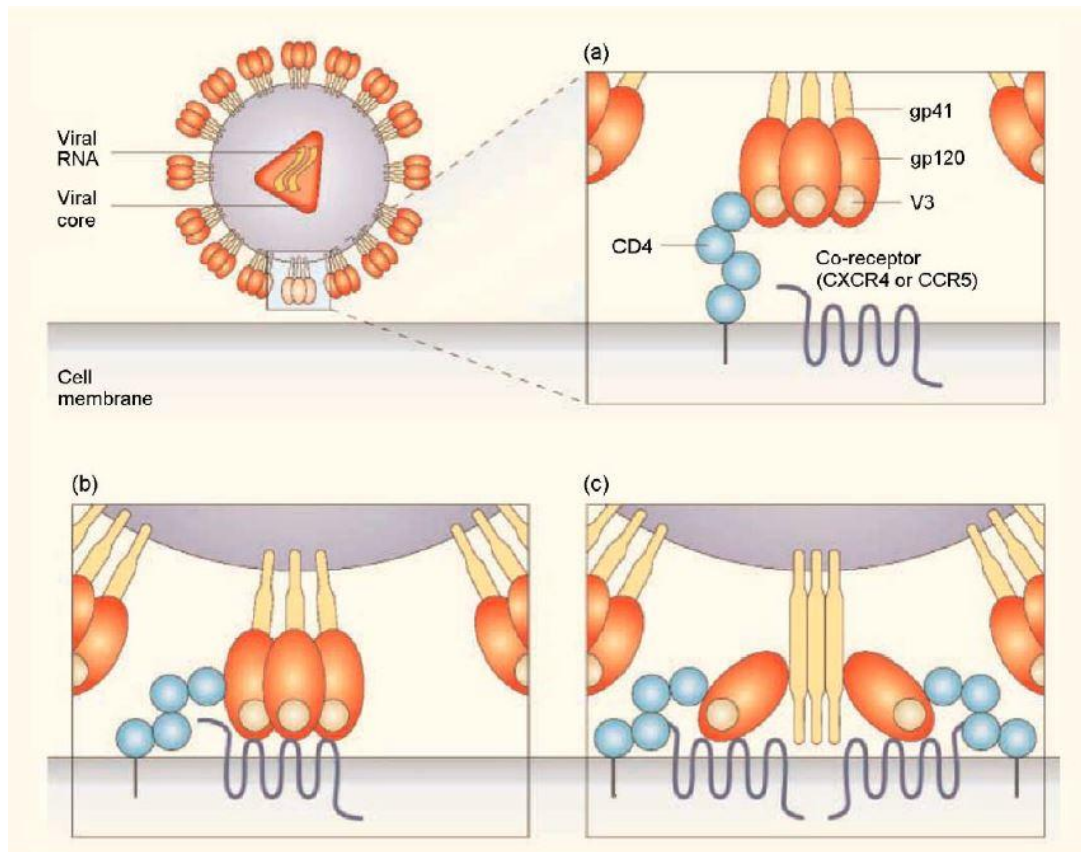


**Figure 1.5: Mechanism of HIV-1 entry.** During the viral entry process, (a) the viral envelop glycoprotein gp120 interacts with the CD4 receptor at the cell membrane, (b) Subsequently, gp120 interacts with the co-receptor CCR5 for M-tropic (R5) HIV strains, or the CXCR4 receptor for T-tropic (X4) HIV strains, whereupon (c), the viral glycoprotein gp41 anchors to the cell membrane.<sup>14</sup>

During the asymptomatic stage of the disease, M-tropic (R5) strains primarily use CCR5 as the entry co-receptor. However, during the course of the disease T-tropic (X4) strains, that use CXCR4 as the entry co-receptor, emerge and eventually replace the R5 strain.<sup>29</sup> This phenotypic switch from R5 to X4 is thought to arise from an X4/R5 intermediate strain capable of using both the CCR5 and CXCR4 receptor. This switch *in vivo* heralds the accelerated depletion of CD4<sup>+</sup> T cells and progression to AIDS, and exemplifies the importance of therapeutic intervention for X4 viral strains.<sup>30</sup>

### 1.2.2 Stem Cell Mobilization

Adult bone marrow (BM) is the primary source of hematopoietic stem cells (HSCs) that initiate hematopoiesis. The elevation of intermediates of HSCs, in the blood of patients recovering from chemotherapy or radiation led to the discovery that these mobilized cells could be collected and would rehome to the bone marrow and restore hematopoiesis.<sup>31</sup> The granulocyte colony-stimulating factor (G-CSF) is routinely used in the clinic as a mobilizing agent for HSCs, but it results in a broad individual variability in mobilization responsiveness and frequently requires repeated dosing with undesirable side effects.<sup>32</sup> The role of the CXCR4/CXCL12 axis in the trafficking of hematopoietic cells has been extensively studied, and thought to play a role in the mobilization induced by G-CSF.<sup>33</sup> The administration of CXCR4 antagonists such as AMD3100, induces a rapid and robust mobilization of hematopoietic cells, including hematopoietic stem and progenitor cells, pre-B cells, and as mature cells, such as neutrophils, monocytes, macrophages, T cells and NK cells in a variety of animal models and humans (Figure 1.6).<sup>34</sup>

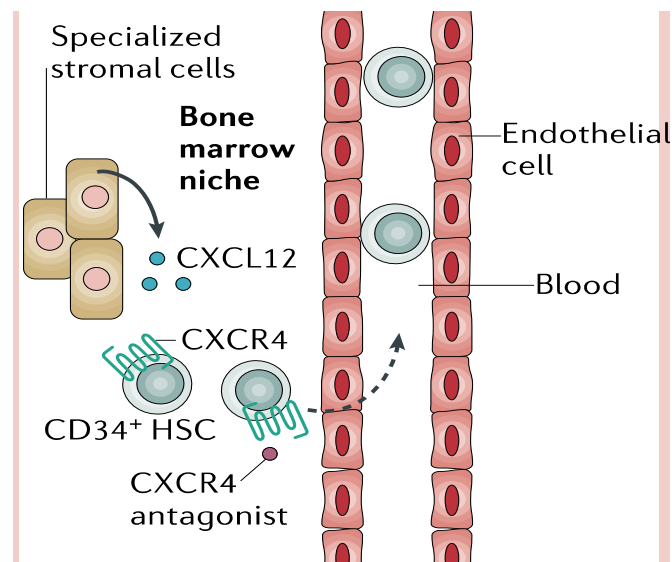


Figure 1.6: Mechanism of hematopoietic stem cell mobilization.

Whereas G-CSF treatment increases the mobility of stem cells and neutrophils and reduces retention signals in the bone marrow by reducing the levels of CXCL12, CXCR4 antagonists solely but strongly reduce the retention signals for hematopoietic cells. Therefore, CXCR4 antagonists, such as AMD3100, were shown to strongly synergize with G-CSF to increase the mobilization of stem cells and neutrophils.<sup>35</sup>

**References**

1. Rosenbaum, D. M.; Rasmussen, S. G.; Kobilka, B. K., The structure and function of G-protein-coupled receptors. *Nature* **2009**, *459* (7245), 356-63.
2. Dorsam, R. T.; Gutkind, J. S., G-protein-coupled receptors and cancer. *Nature reviews. Cancer* **2007**, *7* (2), 79-94.
3. Pierce, K. L.; Premont, R. T.; Lefkowitz, R. J., Seven-transmembrane receptors. *Nature reviews. Molecular cell biology* **2002**, *3* (9), 639-50.
4. (a) Bleul, C. C.; Wu, L.; Hoxie, J. A.; Springer, T. A.; Mackay, C. R., The HIV coreceptors CXCR4 and CCR5 are differentially expressed and regulated on human T lymphocytes. *Proceedings of the National Academy of Sciences of the United States of America* **1997**, *94* (5), 1925-30; (b) Zaitseva, M.; Blauvelt, A.; Lee, S.; Lapham, C. K.; Klaus-Kovtun, V.; Mostowski, H.; Manischewitz, J.; Golding, H., Expression and function of CCR5 and CXCR4 on human Langerhans cells and macrophages: implications for HIV primary infection. *Nature medicine* **1997**, *3* (12), 1369-75; (c) Zaitseva, M. B.; Lee, S.; Rabin, R. L.; Tiffany, H. L.; Farber, J. M.; Peden, K. W.; Murphy, P. M.; Golding, H., CXCR4 and CCR5 on human thymocytes: biological function and role in HIV-1 infection. *Journal of immunology* **1998**, *161* (6), 3103-13.
5. Gupta, S. K.; Lysko, P. G.; Pillarisetti, K.; Ohlstein, E.; Stadel, J. M., Chemokine receptors in human endothelial cells. Functional expression of CXCR4 and its transcriptional regulation by inflammatory cytokines. *The Journal of biological chemistry* **1998**, *273* (7), 4282-7.
6. Aiuti, A.; Webb, I. J.; Bleul, C.; Springer, T.; Gutierrez-Ramos, J. C., The chemokine SDF-1 is a chemoattractant for human CD34+ hematopoietic progenitor cells and provides a new mechanism to explain the mobilization of CD34+ progenitors to peripheral blood. *The Journal of experimental medicine* **1997**, *185* (1), 111-20.
7. Bleul, C. C.; Farzan, M.; Choe, H.; Parolin, C.; Clark-Lewis, I.; Sodroski, J.; Springer, T. A., The lymphocyte chemoattractant SDF-1 is a ligand for LESTR/fusin and blocks HIV-1 entry. *Nature* **1996**, *382* (6594), 829-33.
8. Proudfoot, A. E., Chemokine receptors: multifaceted therapeutic targets. *Nature reviews. Immunology* **2002**, *2* (2), 106-15.
9. Zlotnik, A.; Yoshie, O., Chemokines: a new classification system and their role in immunity. *Immunity* **2000**, *12* (2), 121-7.
10. (a) Tachibana, K.; Hirota, S.; Iizasa, H.; Yoshida, H.; Kawabata, K.; Kataoka, Y.; Kitamura, Y.; Matsushima, K.; Yoshida, N.; Nishikawa, S.; Kishimoto, T.; Nagasawa, T., The chemokine receptor CXCR4 is essential for vascularization of the gastrointestinal tract. *Nature* **1998**, *393* (6685), 591-4; (b) Zou, Y. R.; Kottmann, A. H.; Kuroda, M.; Taniuchi, I.; Littman, D. R., Function of the chemokine receptor CXCR4 in haematopoiesis and in cerebellar development. *Nature* **1998**, *393* (6685), 595-9.
11. Arenberg, D. A.; Keane, M. P.; DiGiovine, B.; Kunkel, S. L.; Morris, S. B.; Xue, Y. Y.; Burdick, M. D.; Glass, M. C.; Iannettoni, M. D.; Strieter, R. M., Epithelial-neutrophil activating peptide (ENA-78) is an important angiogenic factor in non-small cell lung cancer. *The Journal of clinical investigation* **1998**, *102* (3), 465-72.
12. (a) Doitsidou, M.; Reichman-Fried, M.; Stebler, J.; Kopranner, M.; Dorries, J.; Meyer, D.; Esguerra, C. V.; Leung, T.; Raz, E., Guidance of primordial germ cell migration by the chemokine SDF-1. *Cell* **2002**, *111* (5), 647-59; (b) Molyneaux, K. A.; Zinszner, H.; Kunwar, P. S.; Schaible, K.; Stebler, J.; Sunshine, M. J.; O'Brien, W.; Raz, E.; Littman,

- D.; Wylie, C.; Lehmann, R., The chemokine SDF1/CXCL12 and its receptor CXCR4 regulate mouse germ cell migration and survival. *Development* **2003**, *130* (18), 4279-86; (c) Raz, E., Primordial germ-cell development: the zebrafish perspective. *Nature reviews. Genetics* **2003**, *4* (9), 690-700.
13. Oberlin, E.; Amara, A.; Bachelier, F.; Bessia, C.; Virelizier, J. L.; Arenzana-Seisdedos, F.; Schwartz, O.; Heard, J. M.; Clark-Lewis, I.; Legler, D. F.; Loetscher, M.; Baggiolini, M.; Moser, B., The CXC chemokine SDF-1 is the ligand for LESTR/fusin and prevents infection by T-cell-line-adapted HIV-1. *Nature* **1996**, *382* (6594), 833-5.
  14. De Clercq, E., The bicyclam AMD3100 story. *Nature reviews. Drug discovery* **2003**, *2* (7), 581-7.
  15. DiPersio, J. F.; Uy, G. L.; Yasothan, U.; Kirkpatrick, P., Plerixafor. *Nature reviews. Drug discovery* **2009**, *8* (2), 105-6.
  16. (a) Balkwill, F., Cancer and the chemokine network. *Nature reviews. Cancer* **2004**, *4* (7), 540-50; (b) Burger, J. A.; Peled, A., CXCR4 antagonists: targeting the microenvironment in leukemia and other cancers. *Leukemia* **2009**, *23* (1), 43-52; (c) Teicher, B. A.; Fricker, S. P., CXCL12 (SDF-1)/CXCR4 pathway in cancer. *Clinical cancer research : an official journal of the American Association for Cancer Research* **2010**, *16* (11), 2927-31; (d) Zlotnik, A., New insights on the role of CXCR4 in cancer metastasis. *The Journal of pathology* **2008**, *215* (3), 211-3.
  17. Wu, B.; Chien, E. Y.; Mol, C. D.; Fenalti, G.; Liu, W.; Katritch, V.; Abagyan, R.; Brooun, A.; Wells, P.; Bi, F. C.; Hamel, D. J.; Kuhn, P.; Handel, T. M.; Cherezov, V.; Stevens, R. C., Structures of the CXCR4 chemokine GPCR with small-molecule and cyclic peptide antagonists. *Science* **2010**, *330* (6007), 1066-71.
  18. Viola, A.; Luster, A. D., Chemokines and their receptors: drug targets in immunity and inflammation. *Annual review of pharmacology and toxicology* **2008**, *48*, 171-97.
  19. Bleul, C. C.; Fuhlbrigge, R. C.; Casasnovas, J. M.; Aiuti, A.; Springer, T. A., A highly efficacious lymphocyte chemoattractant, stromal cell-derived factor 1 (SDF-1). *The Journal of experimental medicine* **1996**, *184* (3), 1101-9.
  20. Crump, M. P.; Gong, J. H.; Loetscher, P.; Rajarathnam, K.; Amara, A.; Arenzana-Seisdedos, F.; Virelizier, J. L.; Baggiolini, M.; Sykes, B. D.; Clark-Lewis, I., Solution structure and basis for functional activity of stromal cell-derived factor-1; dissociation of CXCR4 activation from binding and inhibition of HIV-1. *The EMBO journal* **1997**, *16* (23), 6996-7007.
  21. Kofuku, Y.; Yoshiura, C.; Ueda, T.; Terasawa, H.; Hirai, T.; Tominaga, S.; Hirose, M.; Maeda, Y.; Takahashi, H.; Terashima, Y.; Matsushima, K.; Shimada, I., Structural basis of the interaction between chemokine stromal cell-derived factor-1/CXCL12 and its G-protein-coupled receptor CXCR4. *The Journal of biological chemistry* **2009**, *284* (50), 35240-50.
  22. Wright, P. E.; Dyson, H. J., Linking folding and binding. *Current opinion in structural biology* **2009**, *19* (1), 31-8.
  23. (a) Bachis, A.; Biggio, F.; Major, E. O.; Mochetti, I., M- and T-tropic HIVs promote apoptosis in rat neurons. *Journal of neuroimmune pharmacology : the official journal of the Society on NeuroImmune Pharmacology* **2009**, *4* (1), 150-60; (b) Bardi, G.; Sengupta, R.; Khan, M. Z.; Patel, J. P.; Meucci, O., Human immunodeficiency virus gp120-induced apoptosis of human neuroblastoma cells in the absence of CXCR4 internalization. *Journal of neurovirology* **2006**, *12* (3), 211-8; (c) Busillo, J. M.; Benovic, J. L.,

- Regulation of CXCR4 signaling. *Biochimica et biophysica acta* **2007**, *1768* (4), 952-63; (d) Hesselgesser, J.; Halks-Miller, M.; DelVecchio, V.; Peiper, S. C.; Hoxie, J.; Kolson, D. L.; Taub, D.; Horuk, R., CD4-independent association between HIV-1 gp120 and CXCR4: functional chemokine receptors are expressed in human neurons. *Current biology : CB* **1997**, *7* (2), 112-21; (e) Sodhi, A.; Montaner, S.; Gutkind, J. S., Viral hijacking of G-protein-coupled-receptor signalling networks. *Nature reviews. Molecular cell biology* **2004**, *5* (12), 998-1012.
24. Choi, W. T.; Duggineni, S.; Xu, Y.; Huang, Z.; An, J., Drug discovery research targeting the CXC chemokine receptor 4 (CXCR4). *Journal of medicinal chemistry* **2012**, *55* (3), 977-94.
  25. Arai, H.; Charo, I. F., Differential regulation of G-protein-mediated signaling by chemokine receptors. *The Journal of biological chemistry* **1996**, *271* (36), 21814-9.
  26. (a) Mellado, M.; Vila-Coro, A. J.; Martinez, C.; Rodriguez-Frade, J. M., Receptor dimerization: a key step in chemokine signaling. *Cellular and molecular biology* **2001**, *47* (4), 575-82; (b) Rodriguez-Frade, J. M.; Mellado, M.; Martinez, A. C., Chemokine receptor dimerization: two are better than one. *Trends in immunology* **2001**, *22* (11), 612-617.
  27. Didigu, C. A.; Doms, R. W., Novel approaches to inhibit HIV entry. *Viruses* **2012**, *4* (2), 309-24.
  28. (a) Cervia, J. S.; Smith, M. A., Enfuvirtide (T-20): a novel human immunodeficiency virus type 1 fusion inhibitor. *Clinical infectious diseases : an official publication of the Infectious Diseases Society of America* **2003**, *37* (8), 1102-6; (b) Grande, F.; Garofalo, A.; Neamati, N., Small molecules anti-HIV therapeutics targeting CXCR4. *Current pharmaceutical design* **2008**, *14* (4), 385-404; (c) Seibert, C.; Sakmar, T. P., Small-molecule antagonists of CCR5 and CXCR4: a promising new class of anti-HIV-1 drugs. *Current pharmaceutical design* **2004**, *10* (17), 2041-62.
  29. Connor, R. I.; Sheridan, K. E.; Ceradini, D.; Choe, S.; Landau, N. R., Change in coreceptor use correlates with disease progression in HIV-1--infected individuals. *The Journal of experimental medicine* **1997**, *185* (4), 621-8.
  30. Raymond, S.; Delobel, P.; Mavigner, M.; Cazabat, M.; Encinas, S.; Souyris, C.; Bruel, P.; Sandres-Saune, K.; Marchou, B.; Massip, P.; Izopet, J., CXCR4-using viruses in plasma and peripheral blood mononuclear cells during primary HIV-1 infection and impact on disease progression. *Aids* **2010**, *24* (15), 2305-12.
  31. (a) Lapidot, T.; Petit, I., Current understanding of stem cell mobilization: the roles of chemokines, proteolytic enzymes, adhesion molecules, cytokines, and stromal cells. *Experimental hematology* **2002**, *30* (9), 973-81; (b) Pelus, L. M., Peripheral blood stem cell mobilization: new regimens, new cells, where do we stand. *Current opinion in hematology* **2008**, *15* (4), 285-92.
  32. Roberts, A. W.; DeLuca, E.; Begley, C. G.; Basser, R.; Grigg, A. P.; Metcalf, D., Broad inter-individual variations in circulating progenitor cell numbers induced by granulocyte colony-stimulating factor therapy. *Stem cells* **1995**, *13* (5), 512-6.
  33. Kim, C. H.; Broxmeyer, H. E., In vitro behavior of hematopoietic progenitor cells under the influence of chemoattractants: stromal cell-derived factor-1, steel factor, and the bone marrow environment. *Blood* **1998**, *91* (1), 100-10.
  34. (a) Broxmeyer, H. E.; Orschell, C. M.; Clapp, D. W.; Hangoc, G.; Cooper, S.; Plett, P. A.; Liles, W. C.; Li, X.; Graham-Evans, B.; Campbell, T. B.; Calandra, G.; Bridger, G.;

- Dale, D. C.; Srouf, E. F., Rapid mobilization of murine and human hematopoietic stem and progenitor cells with AMD3100, a CXCR4 antagonist. *The Journal of experimental medicine* **2005**, *201* (8), 1307-18; (b) Liles, W. C.; Broxmeyer, H. E.; Rodger, E.; Wood, B.; Hubel, K.; Cooper, S.; Hangoc, G.; Bridger, G. J.; Henson, G. W.; Calandra, G.; Dale, D. C., Mobilization of hematopoietic progenitor cells in healthy volunteers by AMD3100, a CXCR4 antagonist. *Blood* **2003**, *102* (8), 2728-30.
35. (a) Abraham, M.; Biyder, K.; Begin, M.; Wald, H.; Weiss, I. D.; Galun, E.; Nagler, A.; Peled, A., Enhanced unique pattern of hematopoietic cell mobilization induced by the CXCR4 antagonist 4F-benzoyl-TN14003. *Stem cells* **2007**, *25* (9), 2158-66; (b) Calandra, G.; McCarty, J.; McGuirk, J.; Tricot, G.; Crocker, S. A.; Badel, K.; Grove, B.; Dye, A.; Bridger, G., AMD3100 plus G-CSF can successfully mobilize CD34+ cells from non-Hodgkin's lymphoma, Hodgkin's disease and multiple myeloma patients previously failing mobilization with chemotherapy and/or cytokine treatment: compassionate use data. *Bone marrow transplantation* **2008**, *41* (4), 331-8; (c) Devine, S. M.; Vij, R.; Rettig, M.; Todt, L.; McGlauchlen, K.; Fisher, N.; Devine, H.; Link, D. C.; Calandra, G.; Bridger, G.; Westervelt, P.; Dipersio, J. F., Rapid mobilization of functional donor hematopoietic cells without G-CSF using AMD3100, an antagonist of the CXCR4/SDF-1 interaction. *Blood* **2008**, *112* (4), 990-8.

## 2 Design of Novel AMD3100 Analogs

### 2.1 Statement of Purpose

Our research group is interested in the development of CXCR4 receptor antagonists for the use as X4 HIV-1 entry inhibitors and for the mobilization of hematopoietic stem cells. Since the discovery elucidating CXCR4 as a co-receptor used along with CD4 by T-tropic (X4) HIV-1 strains for cellular entry, efforts have been made by our group and others to develop CXCR4 antagonists. Generally, these CXCR4 antagonists can be divided into three major classes: i) small modified CXCR4 peptide antagonists, ii) pseudo-peptide CXCR4 antagonists, and iii) small molecule CXCR4 antagonists (Figure 2.1).<sup>1</sup>

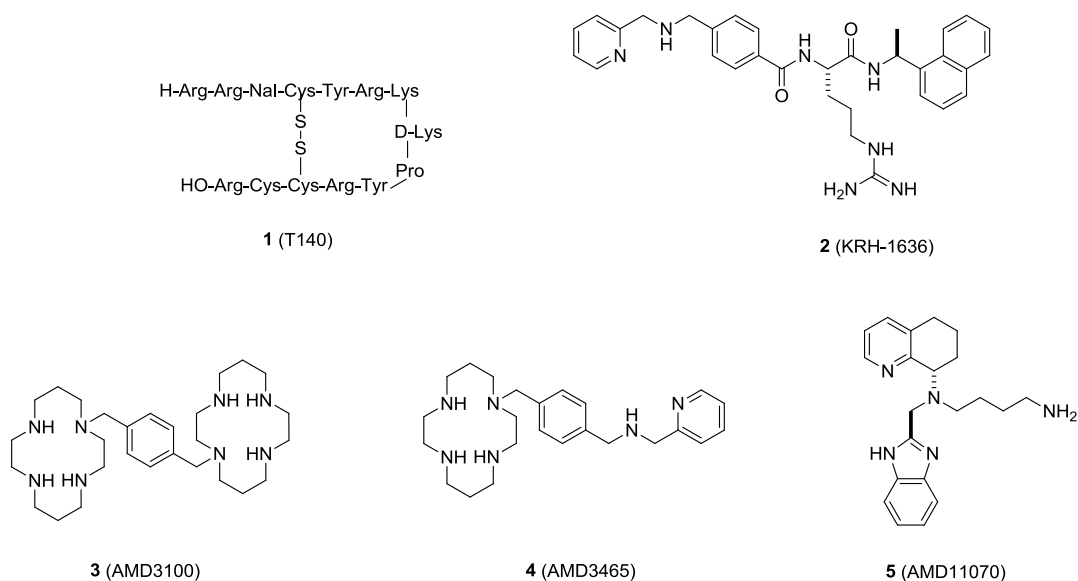


Figure 2.1: Structures of selected CXCR4 antagonists.

Peptide CXCR4 antagonists, such as T140 (**1**) were designed to mimic the action of CXCL12. However, due to the poor pharmacokinetic properties of peptides antagonists, pseudo-peptide antagonists, such as KRH-1686 (**2**), and small molecule antagonists, such as

AMD3100 (**3**), AMD3465 (**4**), and AMD11070 (**5**) were designed to improve the PK properties while maintaining the potency (SAR). AMD3100 (**3**) was the first CXCR4 antagonist to enter clinical trials as a X4 HIV-1 entry inhibitor, however it was subsequently withdrawn from Phase II clinical trials due to cardiotoxicity when administered at high doses.<sup>2</sup> Although AMD3100 exhibited this undesirable side-effect, we hypothesized it may represent a generalized scaffold which could be optimized to improve the potency as well as attenuate the unfavorable toxicity and pharmacokinetic characteristics. The projects goals were achieved using the following strategy:

- 1) Structure activity relationships were utilized to design analogues with CXCR4 potency, decreased toxicity, and increased bioavailability.
- 2) Novel AMD3100 analogues were synthesized.
- 3) The analogues were tested for *in vitro* CXCR4 receptor activity in an HIV-1 infectivity assay. All *in vitro* biological evaluation of synthesized analogues were carried out by Southern Research Institute.

## 2.2 Introduction and Background

Bicyclam-containing small molecule AMD3100 was the first CXCR4 antagonist to enter clinical trials for X4 HIV-1 infection.<sup>3</sup> At physiological pH it carries an overall charge of +2 and can adopt a stable *trans*-R,R,S,S type configuration with respect to the four nitrogen atoms.<sup>3</sup> In a putative model, the protonated cyclam has the propensity to form a direct, hydrogen-bonded complex with carboxylate groups in the CXCR4 receptor. Site directed mutagenesis studies demonstrated mutation of Asp<sup>171</sup> or Asp<sup>262</sup> (located in TM helices IV and VI of CXCR4) to alanine suggests the negatively charged aspartate residues at these positions may represent crucial sites for electrostatic interaction of the positively charged bicyclam rings.<sup>4</sup> Similarly,

molecular modeling studies proposed one of the cyclam rings of AMD3100 interacts with Asp<sup>171</sup> in the TM domain IV of CXCR4, whereas the other ring is sandwiched between the carboxylate groups of Asp<sup>262</sup> and Glu<sup>288</sup> (located in TM helices VI and VII of CXCR4) (Figure 2.2).<sup>5</sup>

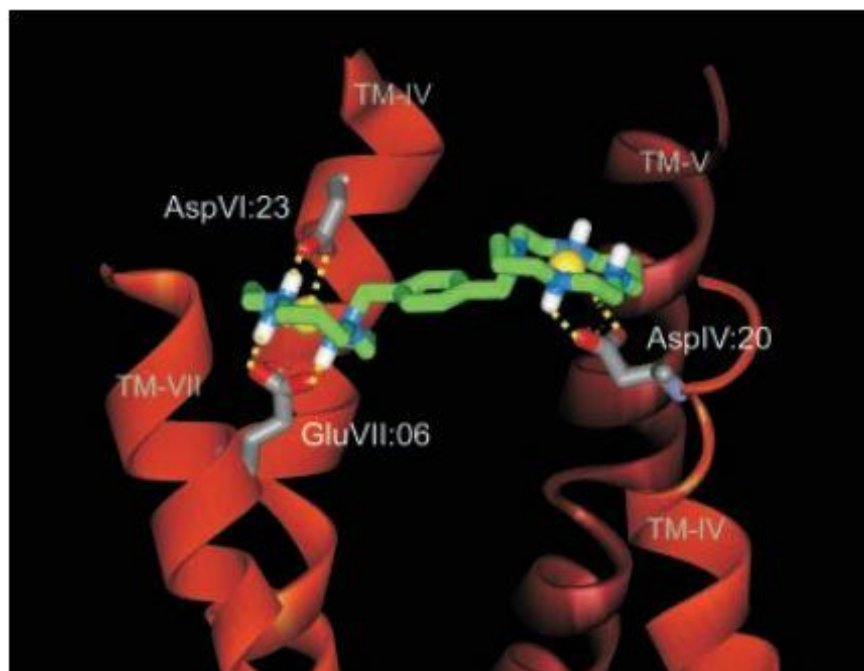


**Figure 2.2: Presumed binding mode of AMD3100 with CXCR4.** The receptor model is built over the X-ray crystal structure of rhodopsin (x) and shows the interaction of one of the cyclam rings of AMD3100 ( $Zn_2$ ) with AspIV:20 (Asp 171 in CXCR4), whereas the other cyclam is sandwiched between AspVI:23 (Asp262 in CXCR4).<sup>5</sup>

On the basis of this proposed molecular mechanism for AMD3100, and in an initial effort to discover compounds with similarly potent inhibition of X4 HIV-1 infection, decreased toxicity, and an improved pharmacokinetic profile, Weiqiang Zhan in the Liotta lab designed and synthesized a series of candidate compounds. Exemplary compounds replaced the cyclam moieties of AMD3100 with N-containing basic centers that could still bind to the hypothesized acidic residues in CXCR4, maintain a similar distribution of heteroatoms from the central 1,4-

biphenylene core of AMD3100, and eliminate toxicity from possible coordination of the cyclam rings with metal ions.

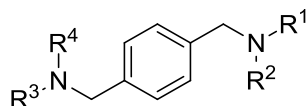
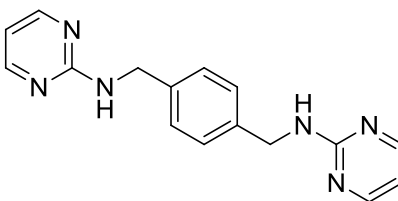


Figure 2.3: CXCR4 antagonist template used to generate AMD3100 analogues.

Of the over 150 analogs synthesized, WZ-41 (**6**) was the most promising showing IC<sub>50</sub> values close to 1 nM in a competitive binding assay, undetectable toxicity in mice, rats and monkeys at high doses (2000mg/kg for 5 days), a reasonable plasma exposure after oral dosing, and effectiveness in blocking bleomycin induced lung fibrosis.<sup>6</sup>



**6** (WZ-41)

Figure 2.4: WZ-41 structure.

While WZ-41 (**6**) abrogated toxicity, and dramatically improved the pharmacokinetic profile of AMD3100, it was not shown to effectively inhibit X4 HIV-1 and provided a foundation for our subsequent medicinal chemistry efforts in this arena.

## 2.3 Design Rationale

Given the structural similarity between AMD3100 (**3**) and WZ-41 (**6**), we were both surprised by and interested in the widely disparate efficacy against inhibiting X4 HIV-1 infection. In an effort to discover a novel and effective pharmacophore replacement for the pyrimidine rings in WZ-41, we turned our attention to the literature. During this search we observed the cyclic ether motif present in numerous bioactive natural products such as: the ionophore antibiotic monesim (**7**), and platelet activating factor antagonist, ginkgolide B (Figure 2.5).<sup>7</sup>

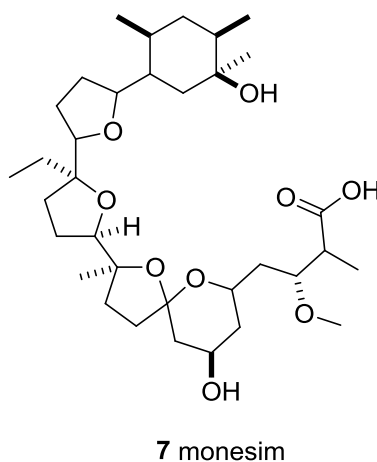


Figure 2.5: Structure of a select bioactive natural products that incorporates the bis-THF moiety.

Additionally, both of these compounds are not reported to suffer from oral bioavailability problems inherent to peptide based inhibitors, as well as AMD3100 (**3**). Most striking were the reports of potent new HIV-1 protease inhibitors Brecanavir (**9**) and Darunavir (**10**) (Figure 2.6). Notable in both structures is the presence of the fused bicyclic tetrahydrofuran or bis-tetrahydrofuran (bis-THF) moiety.<sup>8</sup>

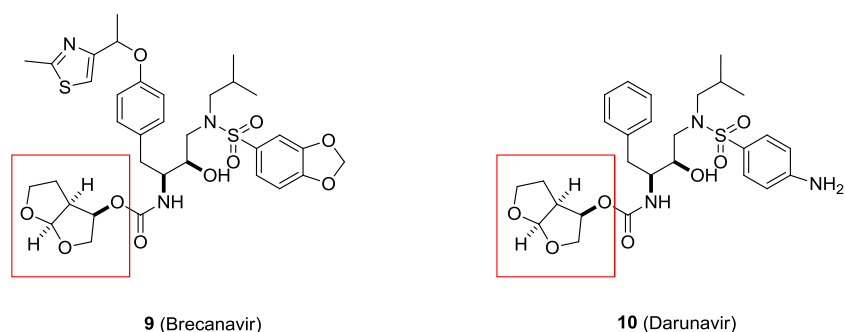


Figure 2.6:

Structures of BrecaNAVIR and DarunAVIR.

More specifically, a high resolution crystal structure of DarunAVIR (**10**) complexed with wild-type HIV-1 protease showed strong hydrogen bonding interactions of the bis-THF oxygens with the two Asp29 and Asp30 backbone amides.

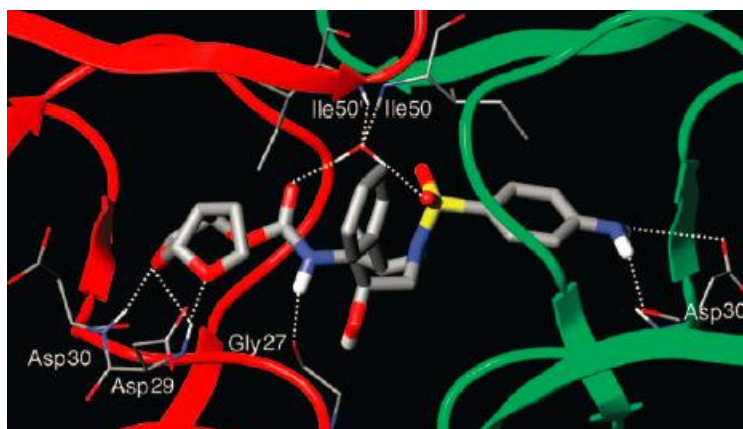


Figure 2.7: Interactions in X-ray crystal structure of DarunAVIR (**10**) bound HIV protease.<sup>8</sup>

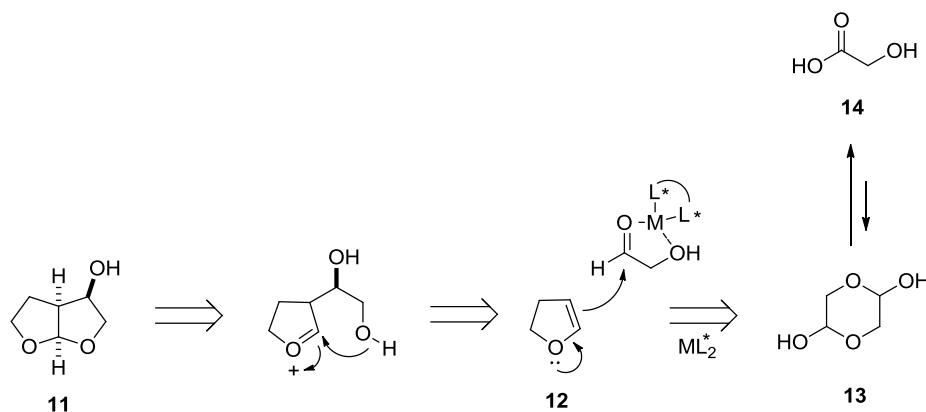
Based on this, we hypothesized the cyclic ether template could be an effective pharmacophore replacement for the cyclam(s) or pyrimidine(s) through the ability to maintain critical hydrogen bonding interactions with the CXCR4 receptor. Given this observation, we synthesized a select number of analogs that would replace the cyclam(s) or pyrimidine (s) with

the bis-THF moiety. Issues addressed throughout the course of the medicinal chemistry effort included:

- 1) How does the replacement of one or both of the pyrimidine rings with the bis-THF moiety affect potency against X4 HIV-1?
- 2) Can the nitrogen linker be replaced with an oxygen?
- 3) Is the optimal linker length 2 carbons between the central 1,4-biphenylene core and pyrimidines?

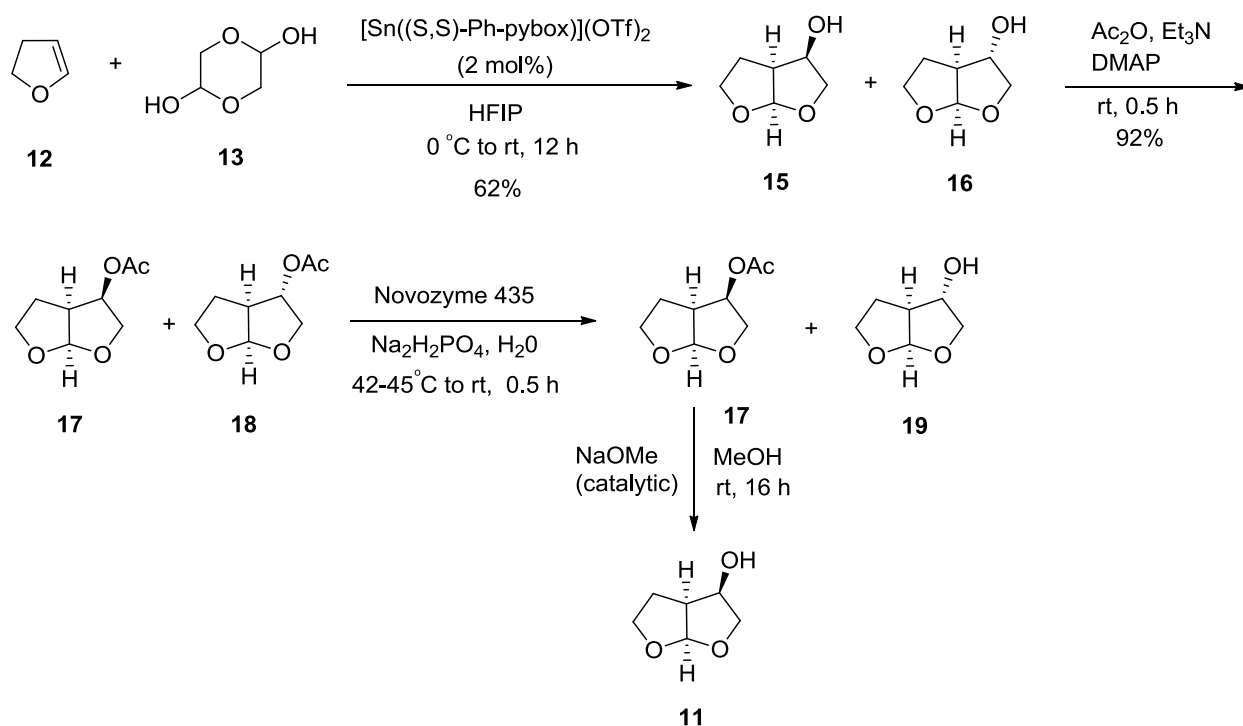
## 2.4 Synthesis

The importance of the bis-THF alcohol in drug discovery generated a significant interest in the synthesis. Although we considered a number of approaches precedent in the literature, we settled on the approach reported by Canoy and coworkers.<sup>9</sup> In this approach, the bis-THF alcohol moiety was achieved in high optical purity through a short and stereoselective synthesis that employed catalytic reagent control, as depicted retrosynthetically in Scheme 2.1. The bicyclic [2.2.0] ring structure of **11** means that only one of the two bridge-head stereocenters needs to be controlled, and the other stereocenter is formed in the cyclization.



Scheme 2.1: Strategy for asymmetric synthesis of bis-tetrahydrofuran alcohol (**11**).

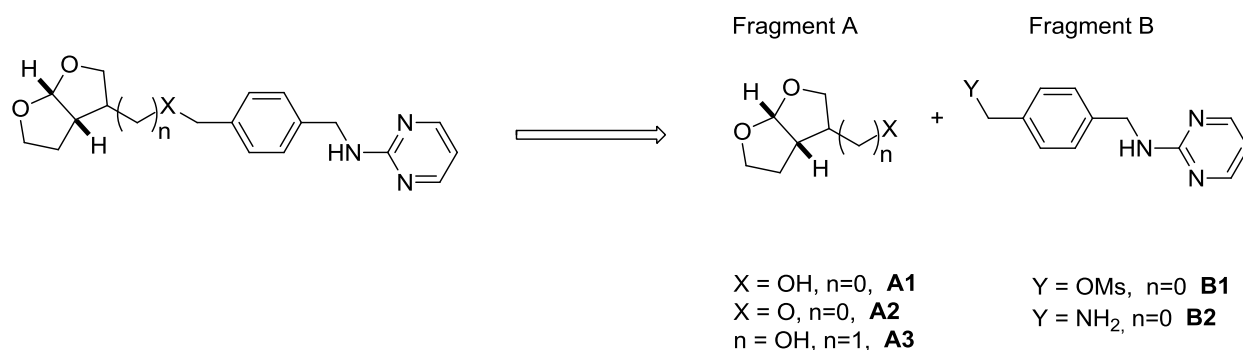
The commercially available glycoaldehyde dimer **13** served as the ultimate electrophile for the catalyzed reaction. The equilibrium of the glycoaldehyde **14** and its dimer **13** has been a subject of for several reports. As such, it was anticipated the cycloaddition would drive the equilibrium from **14** to **13**, and the desired product **11** obtained through the anti addition of **12**.



**Scheme 2.3: Synthesis of Fragment A1.** (3R,3aS,6aR)-Hexahydrofuro[2,3-b]furan-3-ol (**11**).

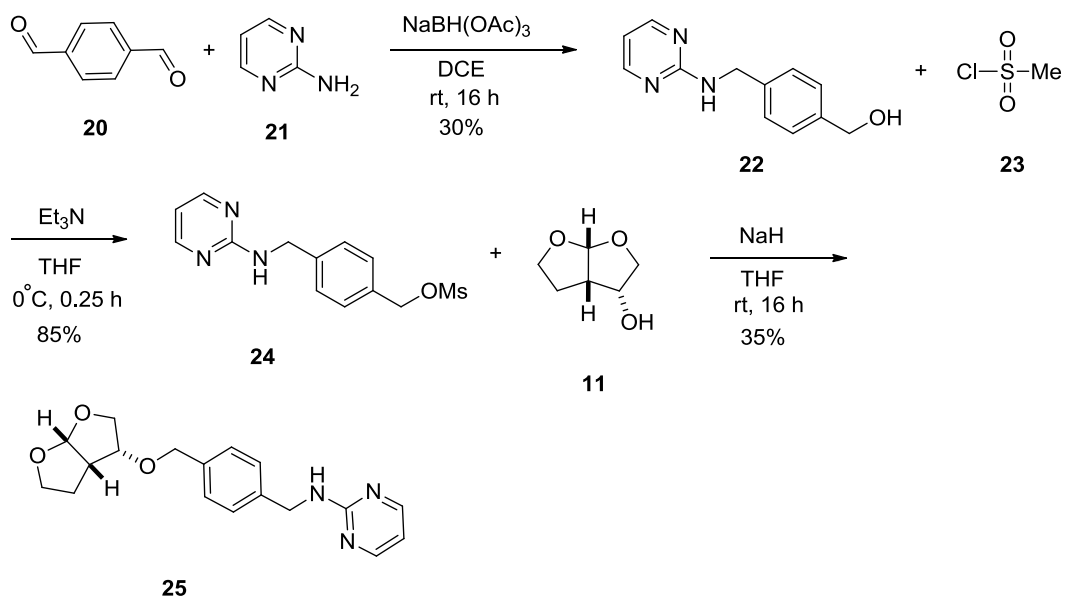
Synthesis of bis-THF **11** began with commercially available 2,3 DHF **12** and glycoaldehyde dimer **13** in the presence of 2 mol % of Evans pybox to give the desired cycloadduct products **15** and diastereomeric compound **16** (dr/er). Acetylation gave the corresponding acetates **17** and **18** in good yield, which were subjected to an enzymatic process with lipase Novozyme 435.  $\text{NaH}_2\text{PO}_4$  buffer at 40-45°C selectively hydrolyzed back the

undesired acetate **18** to the corresponding alcohol **19**. The highly soluble alcohol **19** was then removed from acetate **18** by aqueous wash of the DCM extract. Deacylation of acetate **18** with 2 mol % NaOMe in MeOH provided a 46% overall yield of the enantiomerically pure alcohol **11**.



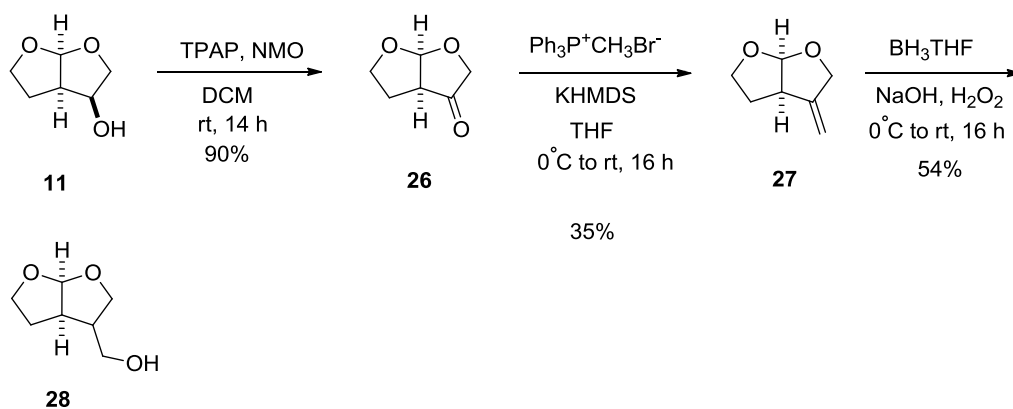
Scheme 2.4: Retrosynthesis of bis-THF compounds.

With compound **11** (fragment A1) in hand we sought to derivatize WZ-41, as illustrated in Scheme 2.5. Fragments A2 (**26**) and A3 (**28**) were synthesized as depicted in Scheme 2.6. Fragment B1 (**24**) was synthesized as illustrated in Scheme 2.7. Fragment B2 (**33**) was synthesized as illustrated in Scheme 2.8.



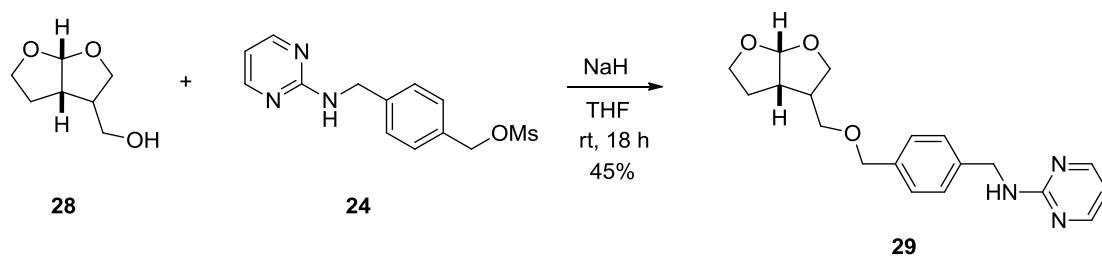
**Scheme 2.5:** Synthesis of Fragment B1 4-((pyrimidin-2-ylamino)methyl)benzyl methanesulfonate (24). Synthesis of analog 25 N-(4-(((3R,3aS,6aR)-hexahydrofuro[2,3-b]furan-3-yl)oxy)methyl)benzyl)pyrimidin-2-amine.

Replacement of the pyrimidine functionality with the hypothesized effective bis-THF pharmacophore was our first synthetic effort in this series, and synthesized as shown in Scheme 2.5. Reductive amination of commercially available **20** and **21** afforded secondary amine **22**, which was subsequently mesylated to afford compound **24**.<sup>10</sup> The bromine and iodine analogs of **22** were also synthesized, however it was found the mesyl leaving group was the most amenable to the subsequent nucleophilic substitution reaction that afforded final analog **25**.



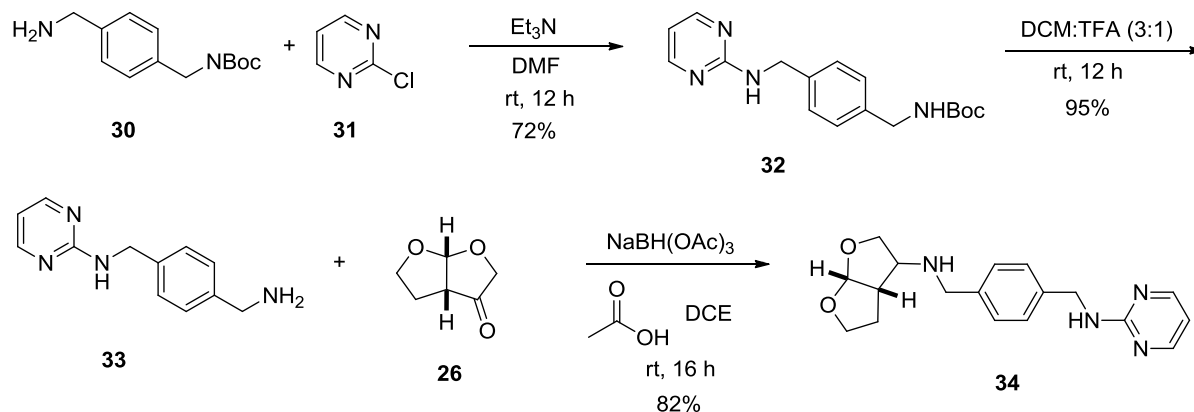
**Scheme 2.6:** Synthesis of Fragments A2 (**26**) and A3 (**28**). (3aR,6aR)-tetrahydrofuro[2,3-b]furan-3(2H)-one (**26**) and A3 ((3aS,6aR)-hexahydrofuro[2,3-b]furan-3-yl)methanol (**28**).

The effect of increasing flexibility in the linker region was probed through the addition of one carbon to the bis-THF moiety. To synthesize this compound, **11** was converted to a primary alcohol (fragment A3) as illustrated in Scheme 2.6. Ketone **26** was afforded from a TPAP mediated oxidation of **11**, and converted to terminal alkene **27** in a Wittig reaction.<sup>11</sup> Finally, hydroboration-oxidation of **27** afforded primary alcohol **28**. Significant optimization of the later two reactions was needed to obtain the products in an acceptable yield, and detailed *vide infra* (Section 2.7). Final compound **29** was then afforded from a nucleophilic substitution of the compound **24** (fragment B1) with **28**.



**Scheme 2.7:** Synthesis of **29** N-(4-(((3aR,6aS)-hexahydrofuro[2,3-b]furan-3-yl)methoxy)methyl)benzyl) pyrimidin-2-amine.

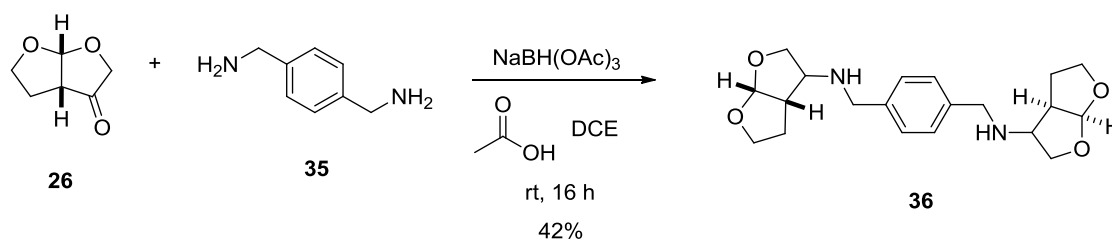
The effects of replacing the pyrimidine with the bis-THF moiety without changing the linker was probed through the synthesis of **34** as illustrated in Scheme 2.8.



**Scheme 2.8: Synthesis of fragment B2.** N-(4-(aminomethyl)benzyl)-5,6,7,8-tetrahydroquinolin-8-amine (**33**) **Synthesis of analog 34.** N-(4-(((3a*S*,6a*R*)-hexahydrofuro[2,3-*b*]furan-3-yl)amino)methyl)benzyl)pyrimidin-2-amine.

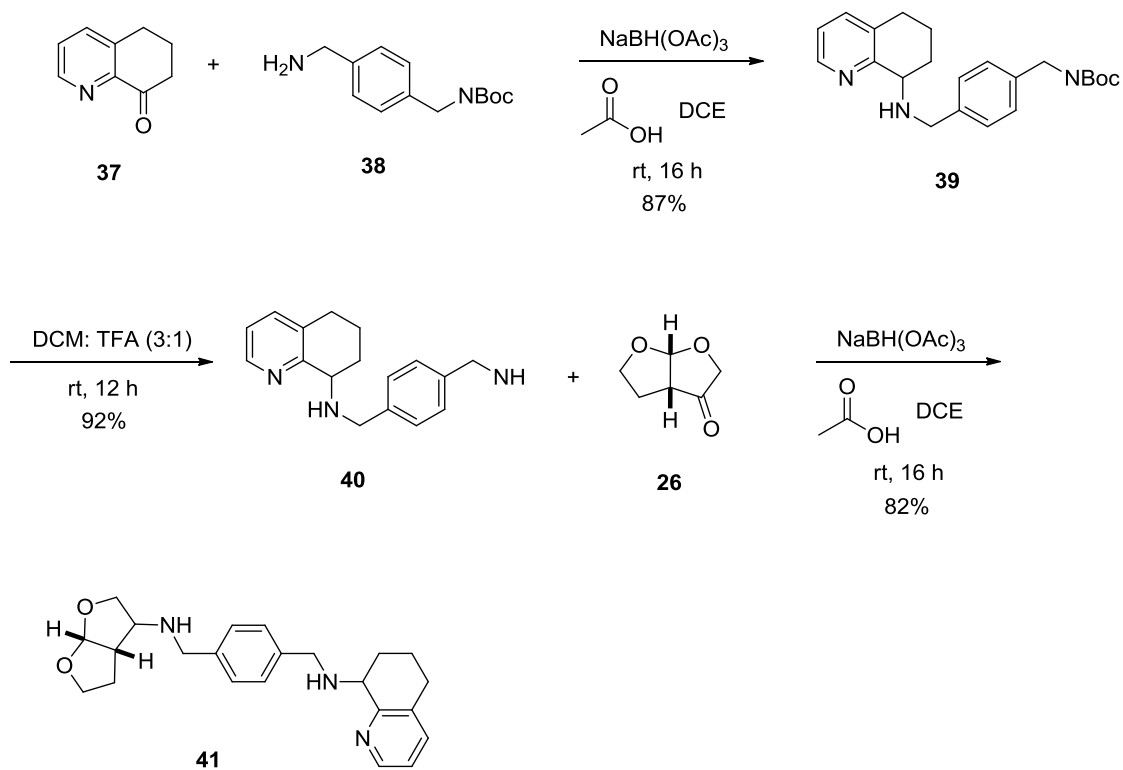
Nucleophilic displacement of 2-chloropyrimidine **31** with primary amine **30** afforded secondary amine **32**. The Boc protecting group was then removed through an acid-mediated deprotection with TFA to provide **33**. Finally, subjecting of ketone **26** and primary amine **33** to reductive amination conditions afforded analog **34**.

We next sought to probe the effect of replacing both pyrimidines with the bis-THF moiety. This was accomplished through the synthesis of **36** as illustrated in Scheme 2.9, where ketone **26** and commercially available 1,4-phenylenedimethanamine **35** were exposed to reductive amination conditions to afford final compound **36**.



**Scheme 2.9: Synthesis of analog 36.** (3aS,6aR)-N-(4-(((3aR,6aS)-hexahydrofuro[2,3-b]furan-3-yl)amino)methyl)benzyl)hexahydrofuro[2,3-b]furan-3-amine

In the course of our medicinal chemistry efforts to find an effective pharmacophore replacement for the cyclam(s) and pyrimidine (s), we were aware of another class of orally bioavailable compounds in the literature. In this class of compounds, an effective pharmacophore for the cyclam was at least in part, a tetrahydroquinoline, exemplified by 11070 (**5**).<sup>12</sup> To probe the importance of this moiety, we sought to maintain the bis-THF while incorporating the tetrahydroquinoline. Synthesis of this analog was synthesized according to the sequence shown in Scheme 2.10 from readily available **37** and **38**. Reductive amination of **37** and **38** provided secondary amine **39**. TFA deprotection afforded primary amine **40**, and reductive amination with **26** furnished final analog **41**.



**Scheme 2.10:** Synthesis of analog 41. (3aS,6aR)-N-(4-(((3aR,6aS)-hexahydrofuro[2,3-b]furan-3-yl)amino)methyl)benzyl)hexahydrofuro[2,3-b]furan-3-amine

## 2.5 Biological Evaluation of Analogs and Discussion

Initial evaluation of these compounds against CXCR4 mediated effects was performed in the viral attachment assay with HIV-1<sub>III-B</sub> in CCR5/CXCR4-expressing HeLa-CD4-LTR- $\beta$ -gal (MAGI) cells measuring each compound's ability to block potential viral entry as well as cellular toxicological properties.

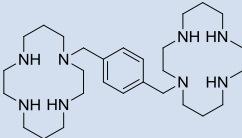
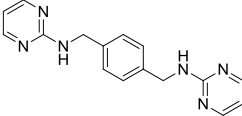
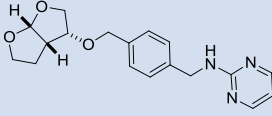
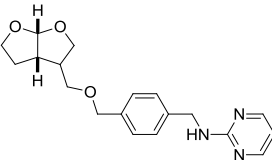
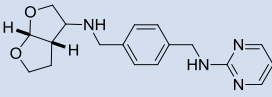
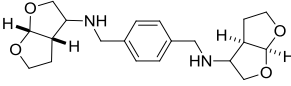
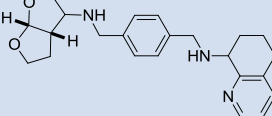
Compound ID	Structure	% Inhibition (at 10 $\mu$ M)
AMD3100		100%
WZ-41		3%
25		16%
29		0%
34		0%
36		3%
41		5%

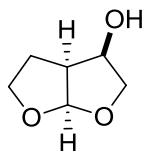
Table 2.1: Biological data for compounds 25, 29, 34, 36 & 41.

The SAR of bis-THF analogs (Table 2.1) indicated the bis-THF moiety was not an effective pharmacophore replacement for the cyclams in AMD3100. While compound **25**, and **41** showed a very minimal increase in potency, 16% and 5 % respectively when compared to WZ-41, the compounds overall lacked acceptable potency. Because our original hypothesis was at least in part based on a homology model of AMD3100 bound to the CXCR4 receptor, one potential reason for lack of efficacy of the bis-THF analogs could be due to the use of an incorrect homology model. After this work was conducted, the crystal structure of CXCR4 with a large cyclic peptide CVX15 and several with the small molecule antagonist (IT1t) was reported.<sup>13</sup> From the crystal structures two notable observations were made: 1) the existence of different ligand-binding sites for the peptide and small molecule, which makes structure based design for the CXCR4 receptor challenging, 2) the existence of different structural orientations in the transmembrane domains of CXCR4 comparison to the other previously resolved GPCRs.<sup>13-14</sup>

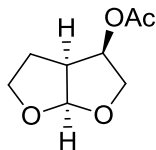
## 2.6 Conclusion

A novel series of AMD3100 and WZ-41 analogs were synthesized. This novel series made use of the bis-THF cyclic ether template that seemingly did not exploit unique and efficient contacts with amino acid residues in the receptor. The overall lack of efficacy of the analogs proved the bis-THF moiety was not an effective pharmacophore replacement for the cyclam rings in AMD3100 in their ability to block HIV-1.

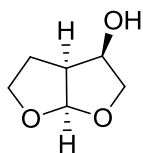
## 2.7 Chemistry Experimental



**(3R,3aS,6aR)-hexahydrofuro[2,3-b]furan-3-ol (15):** To a 15 mL round bottom flask was added 111 mg (0.300 mmol, 0.021 equiv) of 2,6-bis[(4S)-4-phenyl-2-oxazoliny]pyridine, 119 mg (0.286 mmol, 0.020 equiv) of tin (II) trifluoromethanesulfonate and 8.0 mL of 1,1,1,3,3,3-hexafluoro-2-propanol at ambient temperature. The heterogeneous mixture was stirred for 35 min and became a nearly clear solution. After stirring for an additional 20 min, the mixture was treated with 857 mg (7.13 mmol, 0.5 equiv) of glycolaldehyde dimer and stirred for 10 min. The solution was cooled with an ice bath, and 1.00 g (14.3 mmol, 1.0 equiv) of 2,3-dihydrofuran was added dropwise over 5 min, and the resulting mixture was allowed to gradually warm to ambient temperature and stir overnight (~20 h). The solvent was removed *in vacuo* and the crude product was then chromatographed on silica gel. Elution with 50-95% EtOAc in hexanes afforded 1.17 g (63%) of desired *anti* product **15** and 59 mg (3.2%) of the syn product **16**, both as a light yellow oil.  $[\alpha]_D^{25} -2.20$ ;  $^1\text{H NMR}$  ( $\text{CDCl}_3$ ):  $\delta$  1.89 (m, 1H), 2.04 (d,  $J = 6 \text{ Hz}$ , 1H), 2.31 (m, 1H), 2.87 (m, 1H), 3.65 (dd,  $J = 7.1, 9.2 \text{ Hz}$ , 1H), 3.89 (m, 1H), 3.99 (m, 2H), 4.46 (m, 1H), 5.70 (d,  $J = 5.2 \text{ Hz}$ , 1H);  $^{13}\text{C NMR}$  ( $\text{CDCl}_3$ ):  $\delta$  24.9, 46.5, 69.9, 70.6, 73.0, 109.5. Anal. Calc for  $\text{C}_6\text{H}_{10}\text{O}_3$ : C, 55.37%; H, 7.74%. Found: C, 54.05%; H, 8.03%. **16**:  $^1\text{H NMR}$  ( $\text{CDCl}_3$ ): 1.73 (m, 1H), 1.86 (bs, 1H), 2.20 (m, 1H), 2.83 (m, 1H), 3.87 (m, 3H), 4.01 (m, 1H), 4.24 (bs, 1H), 5.90 (d,  $J = 4.9 \text{ Hz}$ , 1H).

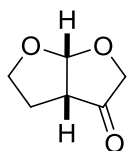


**(3R,3aS,6aR)-hexahydrofuro[2,3-b]furan-3-yl acetate (17):** To a 50 mL round bottom flask was successively added 1.00 g (7.68 mmol) of (3R,3aS,6aR)-hexahydrofuro[2,3-b]furan-3-ol (3, 15% ee), 10 mL of THF, 1.10 mL (7.68 mmol) of triethylamine and 15 mg (catalytic) of 4-(dimethylamino)pyridine. The mixture was cooled with an ice bath, and 0.73 mL (7.68 mmol) of acetic anhydride was added dropwise. The reaction was allowed to gradually warm to ambient temperature and stirred overnight (~20 h). The solvent was removed by rotary evaporation. The resultant oily residue was dissolved with 20 mL of dichloromethane, and washed successively with 8 mL of 1N HCl and 10 mL of saturated aqueous NaHCO<sub>3</sub>. The organic layer was evaporated by rotary evaporation and chromatographed on silica gel. Elution with 40-60% EtOAc in hexanes afforded 1.24 g (94%) of acetates **17** and **18** as a colorless oil. <sup>1</sup>H NMR (CDCl<sub>3</sub>): δ 1.92 (m, 1H), 2.01 (m, 1H), 2.11 (s, 3H), 3.07 (m, 1H), 3.77 (dd, *J* = 7.1, 9.2 Hz, 1H), 3.95 (m, 1H), 4.00 (m, 1H), 4.09 (m, 1H), 5.22 (m, 1H), 5.73 (d, *J* = 5.2 Hz, 1H); <sup>13</sup>C NMR (CDCl<sub>3</sub>): δ 20.9, 26.1, 44.9, 69.5, 70.7, 73.0, 109.2, 170.4. Anal. Calcd for C<sub>8</sub>H<sub>12</sub>O<sub>4</sub>: C, 55.81%; H, 7.02%. Found: C, 55.47%; H, 7.04%.

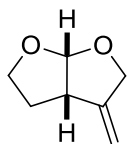


**(3R,3aS,6aR)-hexahydrofuro[2,3-b]furan-3-ol (11):** A solution of  $\text{NaH}_2\text{PO}_4$  buffer was prepared by dissolving 1.56 g of  $\text{NaH}_2\text{PO}_4$  in 10 mL of water (pH4.2). The pH was adjusted to 5.5 with 30% aqueous NaOH. To 1.10 g (6.39 mmol) of the acetates (10 and ent-10, 15% ee) in a 25 mL round bottom flask was added 5 mL of the buffer solution, followed by addition of 275 mg of Novozyme 435. The mixture was stirred for 5 min, and then moved to an oil bath of 42-45 °C. After about 35 min, the pH was at less than 4.0. About 0.5 mL of 5 N NaOH was added to adjust the reaction to pH 5.5, and the pH of the reaction remained about the same thereafter. . After being stirred for an additional 40 min, the reaction mixture was cooled to ambient temperature, and filtered through a glass frit funnel. The polymer bound enzyme was washed with a 15:85 mixture of *i*-PrOH/ $\text{H}_2\text{O}$  three times (about 10 mL) to make sure that none of acetate **10** was retained by the polymer. The filtrate was diluted with 5 mL of water and extracted with 30 mL of DCM. The organic layer was successively washed with 2 x 4 mL of water and 1x10 mL of saturated brine to remove the hydrolyzed alcohol products. The organic layer was concentrated *in vacuo* to give 751 mg (3.67 mmol, theoretical maximum based on 15% ee going into enzymatic reaction) of acetate 17 as a yellow oil. The crude oil from the enzymatic reaction was dissolved in 3 mL of MeOH, treated with 17  $\mu\text{L}$  (0.073 mmol) of 25 wt.% NaOMe in MeOH. After stirring at ambient temperature for 2 h, the mixture was treated with 6.3  $\mu\text{L}$  (0.11 mmol) of acetic acid. The solvent was removed *in vacuo* and the resultant thick oil was chromatographed on a short silica gel column. Elution with 80-90% EtOAc in hexanes provided 432 mg (52% for overall enzymatic process and deacetylation) of bis-furan alcohol **3** as a light yellow oil.  $[\alpha]^{25}_{\text{D}} -13.7$

(c 1.31 , MeOH); Anal. Cald for C<sub>6</sub>H<sub>10</sub>O<sub>3</sub>: C, 55.37%; H, 7.74%. Found: C, 55.29%;  
H, 7.98.

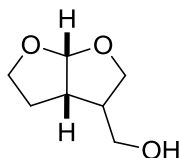


**(3aR,6aR)-tetrahydrofuro[2,3-b]furan-3(2H)-one (26):** Solid TPAP (5 mol %) was added in one portion to a stirring mixture of (3R,3aS,6aR)-hexahydrofuro[2,3-b]furan-3-ol (**11**). NMO (1.5 eq) 4A° molecule sieves (500mg/mmol) in DCM at ambient temperature under argon and allowed to proceed overnight. The reaction mixture was filtered through a silica pad, and eluted with EtOAc. <sup>1</sup>H NMR (CDCl<sub>3</sub>): 1.94 (m, 1H), 2.19 (m, 1H), 3.03 (dd, *J* = 7.0, 9.3 Hz, 1 H), 3.75 (m, 2H), 4.48 (m, 1H), 4.53 (m, 1H), 5.37 (d, *J* = 10 Hz, 1H) <sup>13</sup>C NMR (CDCl<sub>3</sub>): 23.5, 56.9, 64.5, 68.1, 107.2, 210.2 HRMS (ESI) [M+H]<sup>+</sup>, calc'd for C<sub>6</sub>H<sub>9</sub>O<sub>3</sub>; 128.13586, found 128.13572.



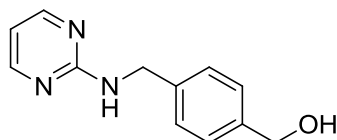
**(3aS,6aR)-3-methylenehexahydrofuro[2,3-b]furan (27):** To a suspension of methyltriphenylphosphonium bromide (7.0 g, 20 mmol) was added potassium bis(trimethyl)amide 1M solution (27 ml, 27 mmol) in 20 mL dry THF and allowed to stir for 2 hours. To this yellow ylide was added a solution of (3aS,6aS)-dihydrofuro[2,3-b]furan-3(2H,3aH,6aH)-one (1.00 g, 7.8 mmol) in dry 2mL dry THF dropwise at 0° C. The reaction mixture was allowed to proceed overnight under argon. The reaction mixture was quenched with saturated aqueous NH<sub>4</sub>Cl

solution and transferred to a separatory funnel. 200 mL was added with 20 mL pentane (and Rochelle's salt added because of emulsion formation). 20mL pentane was added to the organic layer followed by 100 mL water. The organic layer was extracted 2 x 50 mL pentane. The combined organic layers were washed with brine and dried over anhydrous  $\text{MgSO}_4$ , and filtered. A 40g silica column was then flushed with 100% pentane, and the entire reaction mixture loaded and ran in 8:1 pentane:ether.  $^1\text{H}$  NMR ( $\text{CDCl}_3$ ): 1.96 (m, 1H), 2.21 (m, 1H), 3.03 (m, 1H), 3.75 (dd,  $J = 7.0, 9.3$  Hz, 1H), 3.95 (m, 1H), 4.42 (m, 1H), 4.53 (m, 1H), 5.05 (q,  $J = 1.6$  Hz, 1H), 5.07 (q,  $J = 1.6$  Hz, 1H) 5.81 (d,  $J = 4.4$  Hz, 1H);  $^{13}\text{C}$  NMR ( $\text{CDCl}_3$ ): 20.9, 26.1, 44.9, 69.5, 70.7, 73.0, 109.2, 170.4.; HRMS (ESI)  $[\text{M}+\text{H}]^+$ , calc'd for  $\text{C}_7\text{H}_{11}\text{O}_2$ ; 127.07536, found 127.07520.

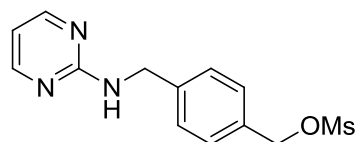


**((3a*S*,6a*R*)-hexahydrofuro[2,3-*b*]furan-3-yl)methanol (28):** To a stirring solution of **27** in dry THF (35 mL) cooled to 0° C, was added a solution of (1.0 M) of  $\text{BH}_3$ -THF solution. The reaction mixture was allowed to proceed at ambient temperature overnight. A mixture of NaOH (3N, 2.5 mL), and  $\text{H}_2\text{O}_2$  (30% wt, 2.5 mL) was then added and stirred for 4h. TLC 100% ether showed new spot at  $R_f = 0.2$ . The reaction mixture was diluted with ether, washed with brine and solvents evaporated under reduced pressure. To the product was added 2x the amount of pentane to final solvent volume. To a 12 g column was then added 100% pentane, and the entire reaction volume ran through the column with 2:1 Pentane:Ether for 200 mL, at which point the column was then run with 100% ether to yield a clear oil.  $^1\text{H}$  NMR ( $\text{CDCl}_3$ ): 1.96 (m, 1H), 2.21

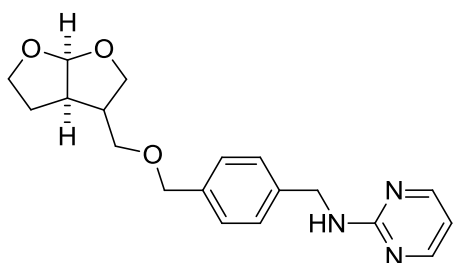
(m, 1H), 3.03 (m, 1H), 3.75 (dd,  $J = 7.0, 9.3$  Hz, 1H), 3.95 (m, 1H), 4.42 (m, 1H), 4.53 (m, 1H), 5.05 (q,  $J = 1.6$  Hz, 1H), 5.07 (q,  $J = 1.6$  Hz, 1H) 5.81 (d,  $J = 4.4$  Hz, 1H);  $^{13}\text{C}$  NMR ( $\text{CDCl}_3$ ): 20.9, 26.1, 44.9, 69.5, 70.7, 73.0, 109.2, 170.4.; HRMS (ESI)  $[\text{M}+\text{H}]^+$ , calc'd for  $\text{C}_7\text{H}_{11}\text{O}_2$ ; 127.07536, found 127.07520.



**(4-((pyrimidin-2-ylamino)methyl)phenyl)methanol (22):** Terephthalaldehyde (10 g, 74.6 mmol) and pyrimidin-2-amine (7.44 g, 78 mmol) were added to 600mL of stirring anhydrous DCE. Acetic acid (4.39 ml, 74.6 mmol) was added in one portion and allowed to stir until dissolved. 20g of activated molecular sieves was then added, followed by sodium triacetoxyborohydride in one portion (39.5 g, 186 mmol). The reaction mixture allowed to stir overnight. The molecular sieves were filtered off and reaction mixture concentrated under reduced pressure. The resultant oil was then partitioned between water and EtOAc, and the water layer washed 3 x 100 mL EtOAc. The organic fractions were combined, dried over  $\text{MgSO}_4$ , and concentrated under rotary evaporation to give a yellow oil. The material was purified via column chromatography 80g silica 40-100% EtOAc over 30 minutes  $R_f = (1:1$  of EtOAc:Hex).  $^1\text{H}$  NMR ( $\text{CDCl}_3$ , 400 MHz) 8.28 (d, 2H,  $J = 4.80$  Hz), 7.31 (m, 4H), 6.56 (t, 1H,  $J = 4.80$  Hz), 5.64 (bs, 1H), 4.63 (d, 2H,  $J = 600$  Hz), 4.45 (s, 2H), 2.98 (s, 3H);  $^{13}\text{C}$  NMR ( $\text{CDCl}_3$ , 100 MHz) 162.5, 158.3, 138.7, 137.4, 128.2, 127.8, 110.0, 70.7, 45.6, 38.2.

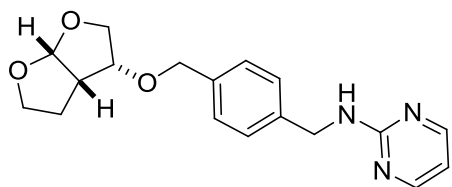


**4-((pyrimidin-2-ylamino)methyl)benzyl methanesulfonate (24):** 4-((pyrimidin-2-ylamino)methyl)phenyl)methanol **22** (5.06g, 23.5 mmol) was dissolved in THF (50 mL) and cooled to 0 °C. Methanesulfonyl chloride (2.73 mL, 35.3 mmol) was then added followed by Et<sub>3</sub>N (9.80 mL, 70.5 mmol) dropwise under continuous stirring. The reaction was stirred for 15 minutes at which time TLC showed complete conversion to the mesylate. The reaction was quenched with cold saturated NaHCO<sub>3</sub>, then extracted with DCM. The organic layer was dried over MgSO<sub>4</sub> and evaporated to give the crude product (7.24g, 94%). R<sub>f</sub> = (1:1 of EtOAc:Hex). <sup>1</sup>H NMR (CDCl<sub>3</sub>, 400 MHz) 8.28 (d, 2H, J = 4.80 Hz), 7.31 (m, 4H), 6.56 (t, 1H, J = 4.80 Hz), 5.64 (bs, 1H), 4.63 (d, 2H, J = 600 Hz), 4.45 (s, 2H), 2.98 (s, 3H); <sup>13</sup>C NMR (CDCl<sub>3</sub>, 100 MHz) 162.5, 158.3, 138.7, 137.4, 128.2, 127.8, 110.0, 70.7, 45.6, 38.2.



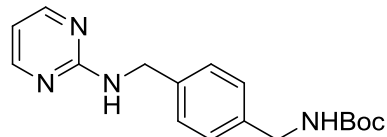
**N-(4-(((3aR,6aS)-hexahydrofuro[2,3-b]furan-3-yl)methoxy)methyl)benzyl)pyrimidin-2-amine (29):** (3S,3aR,6aS)-hexahydrofuro[2,3-b]furan-3-ol (.150 g, 1 mmol) was added to a dry 25ml rbf and dissolved in 4 mL dry THF. Sodium hydride (0.02g, 1 mmol) was then added in

one portion and the reaction was allowed to stir at room temperature for 45 minutes. To the reaction mixture was then added (via canula), 4-((pyrimidin-2-ylamino)methyl)benzyl methanesulfonate (0.5 g, 2 mmol) that was stirring in a separate 25ml rbf with 4 mL of dry THF and allowed to proceed overnight under argon. The reaction was purified on a 12g ISCO column, 10-100% EtOAc to yield an off-white foam (0.029 g, 4.97%).  $^1\text{H}$  NMR ( $\text{CDCl}_3$ , 400 MHz) 8.45 (m, 2H), 7.11 (m, 4H), 6.49 (m, 1H), 5.09 (m, 1H), 4.63 (m, 2H), 3.70 (m, 4H), 3.24 (m, 2H), 2.16 (m, 2H), 1.91 (m, 1H) NMR ( $\text{CDCl}_3$ , 100 MHz) 164.2, 158.2, 139.4, 135.5, 127.3, 115.7, 114.3, 81.3, 73.8, 71.5, 68.2, 47.5, 46.1, 34.8; HRMS (ESI)  $[\text{M}+\text{H}]^+$ , calc'd for  $\text{C}_{18}\text{H}_{23}\text{N}_4\text{O}_2$ ; 328.17557, found 328.17548; HPLC/MS purity (> 95%)  $r_t = 1.862$  at 254nM, 50-95% MeOH, hold for 5 minutes; HPLC/MS purity (> 95%)  $r_t = 2.896$  at 254nM, 50-95% MeOH over 6 minutes.



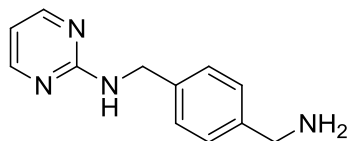
**N-(4-(((3R,3aS,6aR)-hexahydrofuro[2,3-b]furan-3-yl)oxy)methyl)benzyl)pyrimidin-2-amine (25):** (3S,3aR,6aS)-hexahydrofuro[2,3-b]furan-3-ol (.100 g, 0.8 mmol) was added to a dry 25 mL rbf and dissolved in 4 mL dry THF followed by the addition of Sodium Hydride (0.02 g, 0.9 mmol) in one portion. The reaction was allowed to stir at ambient for 45 minutes. The reaction mixture was then added (via canula) to 4-((pyrimidin-2-ylamino)methyl)benzyl methanesulfonate (0.3 g, 0.9 mmol) that was stirring in a separate 25 mL rbf with 4 mL of dry

THF). The reaction was allowed to proceed at ambient temperature under argon overnight. Purification via ISCO column: 12g column, 10%EtOAc to 100%EtOAc to yield a light yellow oil product (0.047 g, 19%).  $^1\text{H}$  NMR ( $\text{CDCl}_3$ , 400 MHz) 8.57 (d,  $J = 3.6$  Hz, 1H), 7.25 (m, 4H), 7.14 (m 5H), 6.49 (t,  $J = 2.8$  Hz, 1H), 5.06 (m, 1H), 4.33 (m, 1H), 4.11 (m, 1H), 3.86 (m, 2H), 3.54 (m, 2H), 2.85 (m, 1H), 2.55 (m, 1H), 2.37 (m, 1H); NMR ( $\text{CDCl}_3$ , 100 MHz) 161.2, 157.4, 139.4, 135.5, 127.3, 115.7, 114.3, 81.3, 73.8, 68.2, 47.5, 46.1, 34.8; HRMS (ESI)  $[\text{M}+\text{H}]^+$ , calc'd for  $\text{C}_{18}\text{H}_{23}\text{N}_3\text{O}_2$ ; 328.16557, found 328.16548; HPLC/MS purity ( $> 95\%$ )  $r_t = 1.862$  at 254nm, 50-95% MeOH, hold for 5 minutes.

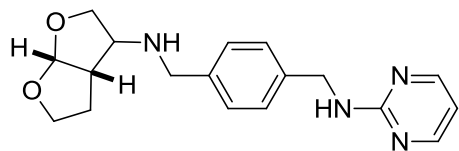


**Tert-butyl 4-((pyrimidin-2-ylamino)methyl)benzylcarbamate (32):** To a solution of 21 mL DCM was added tert-butyl 4-(aminomethyl)benzylcarbamate (.500 g, 2.116 mmol) and picolinaldehyde (0.202 ml, 2.116 mmol). The reaction was allowed to proceed overnight at ambient temperature. The reaction mixture was extracted diluted with saturated sodium carbonate and extracted 2 x 50 mL DCM. The organic layers were combined, dried over  $\text{MgSO}_4$  and evaporated to give the crude product. The reaction was purified on a 40 g column and ran in 90:10:1 DCM:MeOH: $\text{NH}_4\text{OH}$  to yield a yellow foam (0.467 g, 67 %).  $^1\text{H}$  NMR ( $\text{CDCl}_3$ , 400 MHz) 8.45 (d, 2H,  $J = 12$  Hz), 8.03 (bs, 1H), 6.93 (m, 1H), 4.31 (m, 2H), 4.00 (bs, 1H), 1.32 (s,

9H);  $^{13}\text{C}$  NMR ( $\text{CDCl}_3$ , 100 MHz) 161.1, 157.8, 154.3, 137.8, 128.0, 115.2, 77.4, 44.2, 42.9, 24.3; HRMS (ESI)  $[\text{M}+\text{H}]^+$ , calc'd for  $\text{C}_{17}\text{H}_{23}\text{O}_2$ ; 314.17024, found 314.17062.

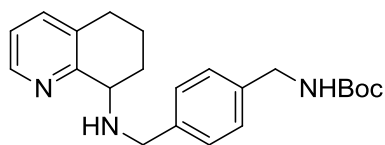


**N-(4-(aminomethyl)benzyl)pyrimidin-2-amine (33):** tert-butyl 4-((pyrimidin-2-ylamino)methyl)benzylcarbamate (.250 g, 0.764 mmol) was added to a dry 15ml rbf with DCM (4.44 ml). TFA (1.480 ml) was then added dropwise. The reaction was allowed to stir at ambient temperature for 2 hours. The reaction was diluted with saturated sodium bicarbonate until pH 11. The aqueous layer was extracted 3 x 10 mL DCM, the organic layers combined, dried with magnesium sulfate and solvent evaporated under reduced pressure. Purification: 6g silica loaded with 95:5:0.5 (DCM:MeOH: $\text{NH}_4\text{OH}$ ) and eluted with 100 mL of the same solvent, followed by 100 mL 90:10:0.5 (DCM:MeOH: $\text{NH}_4\text{OH}$ ), followed by 100 mL 85:15:0.5 (DCM:MeOH: $\text{NH}_4\text{OH}$ ), followed by 80:20:0.5 (DCM:MeOH: $\text{NH}_4\text{OH}$ ) to yield a yellow oil (0.528 g, 70%).  $^1\text{H}$  NMR ( $\text{CDCl}_3$ , 400 MHz) 8.42 (d, 2H,  $J = 12$  Hz), 6.91 (m, 1H), 4.40 (m, 4H), 4.00 (bs, 1H);  $^{13}\text{C}$  NMR ( $\text{CDCl}_3$ , 100 MHz) 163.5, 155.2, 150.2, 137.6, 43.1; HRMS (ESI)  $[\text{M}+\text{H}]^+$ , calc'd for  $\text{C}_{12}\text{H}_{23}\text{N}_4\text{O}_2$ ; 214.18135, found 214.18113.



**N-(4-(((3aS,6aR)-hexahydrofuro[2,3-b]furan-3-yl)amino)methyl)benzyl)pyrimidin-2-amine (34):** To a solution of 6 mL DCM was added **26** (.070 g, 0.546 mmol) and **33** (0.124g,

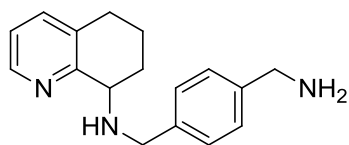
0.546 mmol). Sodium triacetoxyborohydride was then added in one portion. The reaction was allowed to proceed overnight at ambient temperature. The reaction mixture was extracted diluted with saturated sodium carbonate and extracted 2 x 50 mL DCM. The organic layers were combined, dried over  $\text{MgSO}_4$  and evaporated to give the crude product. The reaction was purified on a 40 g column and ran in 90:10:1 DCM:MeOH: $\text{NH}_4\text{OH}$  to yield a yellow foam (0.295 g, 54 %).  $^1\text{H}$  NMR ( $\text{CDCl}_3$ , 400 MHz) 8.45 (d,  $J = 3.6$  Hz, 1H), 7.15 (m, 4H), 6.49 (m, 1H), 5.06 (m, 1H), 4.33 (m, 2H), 3.86 (m, 24), 3.74 (m, 3H), 2.95 (m, 4H), 2.93 (m, 1H), 1.94 (m, 2H); NMR ( $\text{CDCl}_3$ , 100 MHz) 160.5, 152.2, 138.7, 132.5, 127.7, 117.9, 115.3, 80.9, 72.8, 65.4, 42.3, 46.1, 32.2; HRMS (ESI)  $[\text{M}+\text{H}]^+$ , calc'd for  $\text{C}_{18}\text{H}_{23}\text{N}_4\text{O}_2$ ; 328.16557, found 328.16548; HPLC/MS purity (> 95%)  $r_t = 1.732$  at 254nM, 50-95% MeOH, hold for 5 minutes.



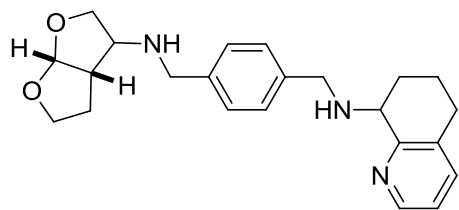
**tert-butyl 4-(((5,6,7,8-tetrahydroquinolin-8-yl)amino)methyl)benzylcarbamate (39)**

tert-butyl 4-((pyrimidin-2-ylamino)methyl)benzylcarbamate (**32**) To a solution of 21 mL DCM was added tert-butyl 4-(aminomethyl)benzylcarbamate (.500 g, 2.116 mmol) and picolinaldehyde (0.202 ml, 2.116 mmol). Sodium triacetoxyborohydride was then added in one portion. The reaction was allowed to proceed overnight at ambient temperature. The reaction mixture was extracted diluted with saturated sodium carbonate and extracted 2 x 50 mL DCM. The organic layers were combined, dried over  $\text{MgSO}_4$  and evaporated to give the crude product. The reaction was purified on a 40 g column and ran in 90:10:1 DCM:MeOH: $\text{NH}_4\text{OH}$  to yield a yellow foam (0.467 g, 67 %).  $^1\text{H}$  NMR ( $\text{CDCl}_3$ , 400 MHz) 8.82 (m,1H), 8.61 (m, 1H), 8.32 (m

1H), 8.01 (bs, 1H), 7.56 (m, 2H), 7.10 (m, 4H), 4.43 (m, 2H), 1.21 (m, 9H);  $^{13}\text{C}$  NMR ( $\text{CDCl}_3$ , 100 MHz) 155.2, 148.6, 143.7, 136.2, 135.7, 134.2, 129.4, 128.8, 121.3, 119.1, 113.5, 80.9, 48.2, 45.7, 29.1; HRMS (ESI)  $[\text{M}+\text{H}]^+$ , calc'd for  $\text{C}_{22}\text{H}_{25}\text{N}_3\text{O}_2$ ; 363.19723, found 363.19751.



**N-(4-(aminomethyl)benzyl)-5,6,7,8-tetrahydroquinolin-8-amine (40):** To a stirring solution of **39** (.500 g, 1.301 mmol) was added DCM (10 mL). TFA (3.40 mL) was then added dropwise. The reaction was allowed to stir at ambient temperature for 2 hours. The reaction was diluted with saturated sodium bicarbonate until pH 11. The aqueous layer was extracted 3 x 10 mL DCM, the organic layers combined, dried with magnesium sulfate and solvent evaporated under reduced pressure. Purification: 40 g silica loaded with 95:5:0.5 (DCM:MeOH: $\text{NH}_4\text{OH}$ ) and eluted with 100 mL of the same solvent, followed by 100 mL 90:10:0.5 (DCM:MeOH: $\text{NH}_4\text{OH}$ ), followed by 100 mL 85:15:0.5 (DCM:MeOH: $\text{NH}_4\text{OH}$ ), followed by 80:20:0.5 (DCM:MeOH: $\text{NH}_4\text{OH}$ ) to yield a yellow oil (0.300 g, 82%).  $^1\text{H}$  NMR ( $\text{CDCl}_3$ , 400 MHz) 143.7, 141.2, 137.2, 136.8, 128.2, 127.4, 121.1, 118.9, 112.1, 48.7, 45.8; HRMS (ESI)  $[\text{M}+\text{H}]^+$ , calc'd for  $\text{C}_{17}\text{H}_{17}\text{N}_3$ ; 263.14581, found 263.14541.



**N-(4-(((3aS,6aR)-hexahydrofuro[2,3-b]furan-3-yl)amino)methyl)benzyl)-5,6,7,8-**

**tetrahydroquinolin-8-amine (41):** To a stirring solution of DCE (7.80 ml) was added **26** and **40**. The reaction was allowed to proceed at ambient temperature under argon overnight. The reaction was quenched with saturated NaHCO<sub>3</sub>, and allowed to stir for 20 minutes. The organic layer was extracted with DCM, combined and dried over magnesium sulfate. The solvent was removed under reduced pressure. Purification: 12g ISCO column, 20 minutes 5-100% MeOH - 90:10:1 (DCM: MeOH: NH<sub>4</sub>OH); <sup>1</sup>H NMR (CDCl<sub>3</sub>, 400 MHz) 8.41 (d, J = 4.2 Hz, 1H), 7.65 (d, J = 4.2, 1H), 7.14 (m 5H), 6.89 (m, 1H), 5.09 (m, 1H), 3.81 (m, 9H), 3.00 (m, 1H), 2.82 (m, 2H), 2.39 (m, 2H), 1.98 (m, 8H); NMR (CDCl<sub>3</sub>, 100 MHz) 162.3, 147.8, 139.2, 136.2, 131.1, 194.8, 121.5, 116.9, 70.2, 68.4, 58.4, 60.2, 36.0, 52.1, 51.3, 30.4, 28.9, 25.7, 20.1; HRMS (ESI) [M+H]<sup>+</sup>, calc'd for C<sub>23</sub>H<sub>30</sub>N<sub>3</sub>O<sub>2</sub>; 379.23174, found 379.23152; HPLC/MS purity (> 95%) r<sub>t</sub> = 1.862 at 254nm, 50-95% MeOH, hold for 5 minutes.

## 2.6 Biological Experimental

### Evaluation in MAGI-CCR5/CXCR4 Cells with T-tropic virus.

Experiments performed at Southern Research Institute, Frederick MD.

#### MAGI Antiviral Assay with HIV-1IIIB

Cell Preparation: MAGI-CCR5/CXCR4 cells (obtained from the NIH AIDS Research and Reference Reagent Program) are passaged in T-75 flasks prior to use in the antiviral assay.

MAGI-CCR5/CXCR4 cells are derived from HeLa-CD4-LTR- $\beta$ -gal cells. The cells have been engineered to express high levels of CD4 and CXCR4 and contain one copy of the HIV-1 LTR promoter driving expression of the  $\beta$ -galactosidase gene upon HIV-1 Tat transactivation. On the day preceding the assay, the cells are plated at  $1 \times 10^4$  well and incubated at 37° C overnight. Total cell and viability quantification is performed using a hemacytometer and trypan blue exclusion. Cell viability is greater than 95% for the cells to be utilized in the assay.

Virus Preparation: The virus used for these tests is the CXCR4-tropic strains HIV-1IIIB. This virus was obtained from the NIH AIDS Research and Reference Reagent Program and was grown in Ghost Hi5/MAGI-CCR5/CXCR4 co-cultures for the production of stock virus pools. For each assay, a pre-titered aliquot of virus is removed from the freezer (-80°C) and allowed to thaw slowly to room temperature in a biological safety cabinet. The virus is re-suspended and diluted into tissue culture medium such that the amount of virus added to each well in a volume of 50  $\mu$ L is approximately ten TCID<sub>50</sub>/well (~0.001 TCID<sub>50</sub>/cell).

Assay Setup – Compounds are evaluated at one or two concentrations (e.g., for initial screening) or in dose-response at six concentrations (triplicate wells/concentration). On the day of assay setup, compound dilutions are prepared at two-times (2X) the final required concentrations. Media used for plating the cells the day before assay setup is aspirated from the plates and

replaced with 50  $\mu$ L of the 2X compounds, followed by the addition of 50  $\mu$ L of virus, which dilutes the compounds to the final 1X concentrations. Cell control wells (cells only) and virus control wells (cells plus virus) are included on each assay plate. Identical uninfected assay plates (virus replaced with media) are prepared for parallel cytotoxicity testing. The cultures are incubated for 48 hours or 6 days (depending on compound or client requirements) after which antiviral efficacy is measured as the inhibition of  $\beta$ -galactosidase reporter expression and cytotoxicity is monitored by MTS staining.

**$\beta$ -galactosidase Chemiluminescent Endpoint Analysis:** A chemiluminescent endpoint is used to determine the extent of  $\beta$ -galactosidase expression as a measure of HIV-1 infection of the cells. Once HIV-1 has attached and entered the MAGI-CXCR4 cells, HIV-1 Tat transactivates the LTR dependent  $\beta$ -galactosidase enzyme to express higher than normal levels of  $\beta$ -galactosidase. Thus there is a direct relationship between the level of HIV-1 infection and the level of  $\beta$ -galactosidase detected in the cells. At 48 hours or 6 days post infection, plates are aspirated and PBS is added to each well. Gal-screen reagent (Tropix, Bedford, MA) is then added per the manufacturer's instructions for chemiluminescent detection of  $\beta$ -galactosidase activity and incubated at room temperature for 90 minutes. The resulting chemiluminescence signal is then read using a Microbeta Trilux luminescence reader (PerkinElmer/Wallace).

**MTS Staining for Cell Viability:** At assay termination, the cytotoxicity assay plates are stained with the soluble tetrazolium-based dye MTS (CellTiter Reagent, Promega) to determine cell viability and quantify compound toxicity. MTS is metabolized by the mitochondrial enzymes of metabolically active cells to yield a soluble formazan product, allowing the rapid quantitative analysis of cell viability and compound cytotoxicity. The MTS is a stable solution that does not require preparation before use. At termination of the assay, 15  $\mu$ L of MTS reagent is added per well. The

microtiter plates are then incubated 1.5-2 hrs at 37°C; the incubation interval was chosen based on empirically determined time times for optimal dye reduction. The plates are read spectrophotometrically at 490/650nm with a Molecular Devices Vmax plate reader. Data Analysis: Percent inhibition of virus replication and percent cell viability at each concentration are calculated using an in-house computer program. For dose-response testing, IC<sub>50</sub> (50% inhibition of virus replication), IC<sub>90</sub> (90% inhibition of virus replication), TC<sub>50</sub> (50% cytotoxicity), and therapeutic index values (TI = TC<sub>50</sub>/IC<sub>50</sub>; also referred to as Antiviral Index or AI) are provided.

## References

1. Debnath, B.; Xu, S.; Grande, F.; Garofalo, A.; Neamati, N., Small molecule inhibitors of CXCR4. *Theranostics* **2013**, *3* (1), 47-75.
2. (a) Hendrix, C. W.; Collier, A. C.; Lederman, M. M.; Schols, D.; Pollard, R. B.; Brown, S.; Jackson, J. B.; Coombs, R. W.; Glesby, M. J.; Flexner, C. W.; Bridger, G. J.; Badel, K.; MacFarland, R. T.; Henson, G. W.; Calandra, G.; Group, A. H. S., Safety, pharmacokinetics, and antiviral activity of AMD3100, a selective CXCR4 receptor inhibitor, in HIV-1 infection. *Journal of acquired immune deficiency syndromes* **2004**, *37* (2), 1253-62; (b) Hendrix, C. W.; Flexner, C.; MacFarland, R. T.; Giandomenico, C.; Fuchs, E. J.; Redpath, E.; Bridger, G.; Henson, G. W., Pharmacokinetics and safety of AMD-3100, a novel antagonist of the CXCR-4 chemokine receptor, in human volunteers. *Antimicrobial agents and chemotherapy* **2000**, *44* (6), 1667-73.
3. De Clercq, E., The bicyclam AMD3100 story. *Nature reviews. Drug discovery* **2003**, *2* (7), 581-7.
4. Donzella, G. A.; Schols, D.; Lin, S. W.; Este, J. A.; Nagashima, K. A.; Maddon, P. J.; Allaway, G. P.; Sakmar, T. P.; Henson, G.; De Clercq, E.; Moore, J. P., AMD3100, a small molecule inhibitor of HIV-1 entry via the CXCR4 co-receptor. *Nature medicine* **1998**, *4* (1), 72-7.
5. Gerlach, L. O.; Skerlj, R. T.; Bridger, G. J.; Schwartz, T. W., Molecular interactions of cyclam and bicyclam non-peptide antagonists with the CXCR4 chemokine receptor. *The Journal of biological chemistry* **2001**, *276* (17), 14153-60.
6. Zhan, W.; Liang, Z.; Zhu, A.; Kurtkaya, S.; Shim, H.; Snyder, J. P.; Liotta, D. C., Discovery of small molecule CXCR4 antagonists. *Journal of medicinal chemistry* **2007**, *50* (23), 5655-64.
7. Ghosh, A. K.; Dawson, Z. L.; Mitsuya, H., Darunavir, a conceptually new HIV-1 protease inhibitor for the treatment of drug-resistant HIV. *Bioorganic & medicinal chemistry* **2007**, *15* (24), 7576-80.
8. Ghosh, A. K.; Martyr, C. D.; Steffey, M.; Wang, Y. F.; Agniswamy, J.; Amano, M.; Weber, I. T.; Mitsuya, H., Design of substituted bis-Tetrahydrofuran (bis-THF)- derived Potent HIV-1 Protease Inhibitors, Protein-ligand X-ray Structure, and Convenient Syntheses of bis-THF and Substituted bis-THF Ligands. *ACS medicinal chemistry letters* **2011**, *2* (4), 298-302.
9. Canoy, W. L.; Cooley, B. E.; Corona, J. A.; Lovelace, T. C.; Millar, A.; Weber, A. M.; Xie, S.; Zhang, Y., Efficient synthesis of (3R,3aS,6aR)- hexahydrofuro[2,3-b]furan-3-ol from glycolaldehyde. *Organic letters* **2008**, *10* (6), 1103-6.
10. Abdel-Magid, A. F.; Carson, K. G.; Harris, B. D.; Maryanoff, C. A.; Shah, R. D., Reductive Amination of Aldehydes and Ketones with Sodium Triacetoxyborohydride. Studies on Direct and Indirect Reductive Amination Procedures(1). *The Journal of organic chemistry* **1996**, *61* (11), 3849-3862.
11. Ley, S. V.; Baxendale, I. R., New tools and concepts for modern organic synthesis. *Nature reviews. Drug discovery* **2002**, *1* (8), 573-86.
12. Skerlj, R. T.; Bridger, G. J.; Kaller, A.; McEachern, E. J.; Crawford, J. B.; Zhou, Y.; Atsma, B.; Langille, J.; Nan, S.; Veale, D.; Wilson, T.; Harwig, C.; Hatse, S.; Princen, K.; De Clercq, E.; Schols, D., Discovery of novel small molecule orally bioavailable C-X-C chemokine receptor 4 antagonists that are potent inhibitors of T-

- tropic (X4) HIV-1 replication. *Journal of medicinal chemistry* **2010**, *53* (8), 3376-88.
13. Wu, B.; Chien, E. Y.; Mol, C. D.; Fenalti, G.; Liu, W.; Katritch, V.; Abagyan, R.; Brooun, A.; Wells, P.; Bi, F. C.; Hamel, D. J.; Kuhn, P.; Handel, T. M.; Cherezov, V.; Stevens, R. C., Structures of the CXCR4 chemokine GPCR with small-molecule and cyclic peptide antagonists. *Science* **2010**, *330* (6007), 1066-71.
  14. Kufareva, I.; Rueda, M.; Katritch, V.; Stevens, R. C.; Abagyan, R.; participants, G. D., Status of GPCR modeling and docking as reflected by community-wide GPCR Dock 2010 assessment. *Structure* **2011**, *19* (8), 1108-26.

### 3 Discovery of 1,2,3,4-tetrahydroisoquinoline-based CXCR4 Antagonists

#### 3.1 Statement of Purpose

In our continued interest in the development of novel and effective CXCR4 antagonists, we were intrigued by a series of reported orally bioavailable CXCR4 antagonists, exemplified by AMD11070 **5** (Figure 3.1).<sup>1</sup> As AMD11070 was the first orally available CXCR4 antagonist to enter the clinic and advance to phase II clinical trials, it paved the way for other efforts which produced preclinical leads, such as the hybrid-piperazine **1** and isothioureia series **2**.<sup>2</sup>

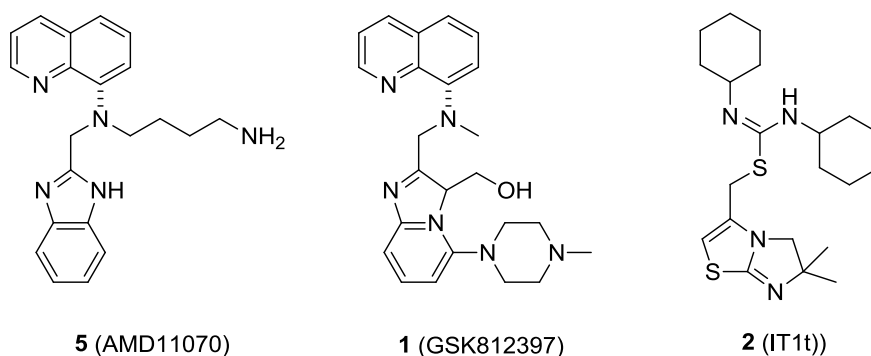


Figure 3.1: Selected orally bioavailable small-molecule CXCR4 antagonists.

Although AMD11070 was withdrawn from phase II clinical trials due to CYP450 isozyme (3A4, 2D6) inhibition activities, we hypothesized this class of molecules may represent a generalized scaffold which could be optimized based on its reported HIV-1 potency, and oral bioavailability.<sup>3</sup> Exemplary compounds would potentially exhibit two important properties:

1. Potency in blocking X4 HIV-1 entry.

2. Potency in blocking CXCR4 induced  $\text{Ca}^{2+}$  flux.

In addition, drug-like characteristics in terms of absorption, distribution, metabolism, and excretion (ADME) parameters is required. These project goals were achieved using the following strategy:

1. A series of novel antagonists based on AMD11070 were synthesized.
2. The analogues were tested for *in vitro* CXCR4 receptor activity in an HIV-1 infectivity assay. All *in vitro* biological evaluation of synthesized analogues were carried out by Southern Research Institute.
3. The analogues were tested in an *in vitro* Calcium flux assay by Millipore.
4. Molecular modeling and reported mutagenesis studies were utilized to guide the medicinal chemistry efforts.

### 3.2 Introduction and Background

The unique biological properties of the CXCR4/CXCL12 axis prompted a surge in activity around small-molecule CXCR4 antagonists (*vide supra*, Chapter 1). Systematic efforts to replace the cyclam rings of AMD3100 with moieties that retain basic character, while also reducing molecular weight and overall charge, resulted in the disclosure of a series of compounds exemplified AMD11070. Specific to the AMD11070 series of CXCR4 antagonists are three intriguing structural modifications shown to be effective as cyclam pharmacophore replacements: (i) a chiral tetrahydroquinoline (THQ) (ii) a basic heterocycle; and (iii) a butyl amine side chain.<sup>1</sup> In light of the development of AMD11070 as an oral HIV treatment, we

initially focused on replacement of the benzimidazole, as we hypothesized this subunit to be the likely source of CYP450 isozyme (3A4, 2D6) inhibition activities observed with this compound.<sup>3</sup> To test this hypothesis, Dr. Larry Wilson a senior scientist in the Liotta lab synthesized compounds where the benzimidazole was replaced with prolines, fused piperidines, piperazines, and/or derivatives thereof. (Figure 3.2).

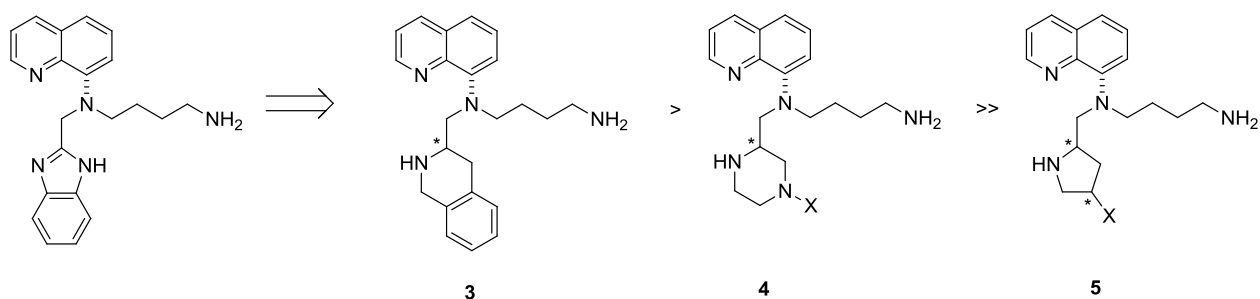


**Figure 3.2: Initial hit-to-lead efforts and general conclusions (\* stereochemical preference unknown).**

In general, the fused piperidines **3** and piperazines **4** showed *in vitro* antagonist effects at the CXCR4 receptor, with similar potencies to the 11070 series in an HIV infectivity assay. Initial modifications made to the prolines resulted in inactivity, and could indicate the importance of having a larger heterocycle at this position. More specifically, the (*R*)- isomer was more potent than the (*S*)- isomer, and in both bases the fused piperdines **6** and **7** were more potent than the piperazines **8** and **9** (Figure 3.3).

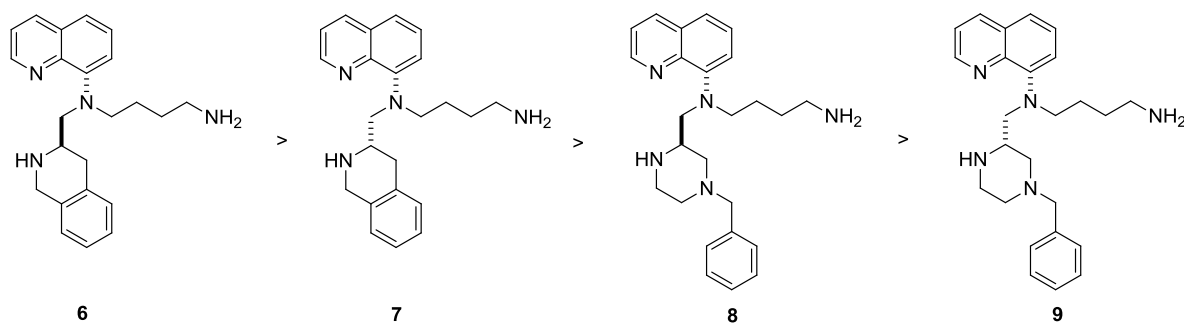
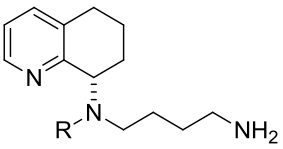
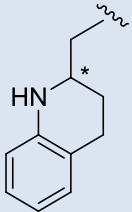
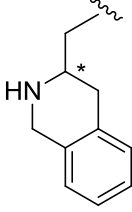
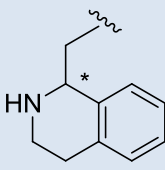
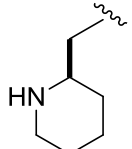


Figure 3.3: General conclusions on initial hit-to-lead efforts.

Given these results Huanyu Zhao, Ph.D. in the Liotta group synthesized a group of piperidine compounds in which the isomeric heterocycle and additional stereogenic center were variable. We settled on using isomeric fused phenyl piperidines because they are sub-structures found in many drug-like compounds and GPCR ligands, as well as synthetically accessible starting from amino acids or suitable derivatives via the Pictet-Splenger reaction. The (*S*)-tetrahydroquinoline headpiece previously disclosed was retained due to observed benefits for CXCR4 potency (Figure 3.4).<sup>1</sup> Initial evaluation of these compounds against CXCR4 mediated effects was performed in the viral attachment assay with HIV-1<sub>III-B</sub> in CCR5/CXCR4-expressing HeLa-CD4-LTR- $\beta$ -gal (MAGI) cells measuring each compound's ability to block potential viral entry as well as cellular toxicological properties. The stereochemistry, inclusion, and point of fusion of the aromatic ring all affected potency. Unlike previous quinoline and isoquinoline heterocyclic replacements, the action of the tetrahydroquinoline and the tetrahydroisoquinoline moieties indicate that both the placement of the phenyl ring and the need for the nitrogen atom basicity are important.

Compound #	 Product	MAGI-HIV-1 <sub>III</sub> B IC <sub>50</sub> (μM) <sup>a</sup>	MAGI-HIV-1 <sub>III</sub> B TC <sub>50</sub> (μM) <sup>a</sup>
10-(R) 11-(S)		>30 >30	>30 >30
6-(R) 7-(S)		0.005 1.36	>10 >10
12-(R) 13-(S)		0.25 0.45	>30 >30
14-(R)		0.42	>30 >30

<sup>a</sup> All assays were performed in duplicate.

\* Stereocenter.

**Figure 3.4: Conclusions on hit-to-lead efforts.**

Surprisingly, in the case of the tetrahydroisoquinolines **10** and **11**, the compounds showed no effect against viral entry in the MAGI assay at concentrations as high as 30 μM suggesting the basicity of the nitrogen heterocycle may be important. In comparison, tetrahydroisoquinolines **6,7, and 12-14** showed a range of antiviral potencies with therapeutic selectivity and two important features of note. First, the site of the phenyl ring fusion to the

piperidine ring had dramatic effects on potency, with the distal ring (*R*)-isomer **6** being 50-500 fold more potent than the isomeric compounds **12** and **13** with the phenyl ring adjacent to the extending carbon. The second important activity relationship was evident in the dramatic effect on potency that the stereochemistry on the tetrahydroisoquinoline demonstrated. The respective isomers with the (*R*) configuration at the TIQ ring stereocenter (**6** and **12**) are the most potent analogues, and in the case of **6**, 100-fold or more potent than the compounds bearing the alternative stereochemistry (**7** and **13**). As compound **6** was identified as the most potent in both assays, we decided to examine other in vitro CXCR4 based properties. As a confirmation of antiviral properties, screening in peripheral blood mononuclear cells (PBMCs), resulted in IC<sub>50</sub> and IC<sub>90</sub> values of 35 and 240 nM, respectively, for the blockade of infection of HIV-1<sub>IIIB</sub>. Similar to the TC<sub>50</sub> result observed in the MAGI assay, at these concentrations cytotoxicity was not observed in PBMCs, resulting in a therapeutic index of > 1000 (TC<sub>50</sub> = 47 μM). Concerning anti-HIV activity, the potencies of **6** and 11070 is comparable and equal to both the literature and in-house assays (30-40 nM for both compounds). Further validation of CXCR4-antagonist behavior was provided by a competitive binding assay and other functional assays. Competitive binding studies with radiolabeled <sup>125</sup>I-SDF-1 showed displacement of the chemokine with an IC<sub>50</sub> value of 112 nM for **6**. In the forskolin/CXCL12 stimulated cAMP production assay, a measure of Gα<sub>i</sub> signaling, **6** inhibited cAMP production with an IC<sub>50</sub> value of 19 nM. Compound **6** also inhibited β-arrestin recruitment with an IC<sub>50</sub> value of 15 nM. Finally, to measure chemokine family and type selectivity, compound **6** was screened in a panel of chemokine receptor assays in both CXCR and CCR types with no observed cross-activity up to 10 μM indicating high selectivity towards CXCR4.

In an effort to assess the drug potential of compound **6**, several ADME based tests were performed. In terms of physical parameters, the aqueous solubility of the free base was investigated by nephelometry and found to be  $> 100 \mu\text{g/mL}$  at physiological pH (7.4). The metabolic stability of compound **6** was assessed in mouse, rat, and human liver microsomes, where it exhibited species-dependent stability behavior. Given these results, compound **6** was chosen for further medicinal chemistry and biological studies.

### 3.2 Design Rational

Given the structural similarity between the two scaffolds 11070 and **6**, the Liotta group sought to further explore the subtleties between the benzimidazole and tetrahydroisoquinoline series. This included an investigation into making conservative independent modifications on the N-tetrahydroisoquinoline (N-THIQ) and butyl amine side chain atoms. The structure activity relationship of CXCR4 potency was explored to determine if, and to what extent lessons gleaned from published work on the 11070 scaffold and preliminary work on scaffold **6** could be used in the optimization of a more potent tetrahydroisoquinoline series. Issues to be addressed throughout the course of the medicinal chemistry around tetrahydroisoquinoline (THIQ) **6** included the following and illustrated in Figure 3.5.

- 1) Can the tetrahydroisoquinoline nitrogen and butyl amine nitrogen be substituted with alkyl, acyl, aromatic, and heteroaromatic compounds and still retain potency?
- 2) Will decreasing the flexibility in the butyl amine side chain increase potency?
- 3) Is the position of the butyl amine nitrogen important for potency?

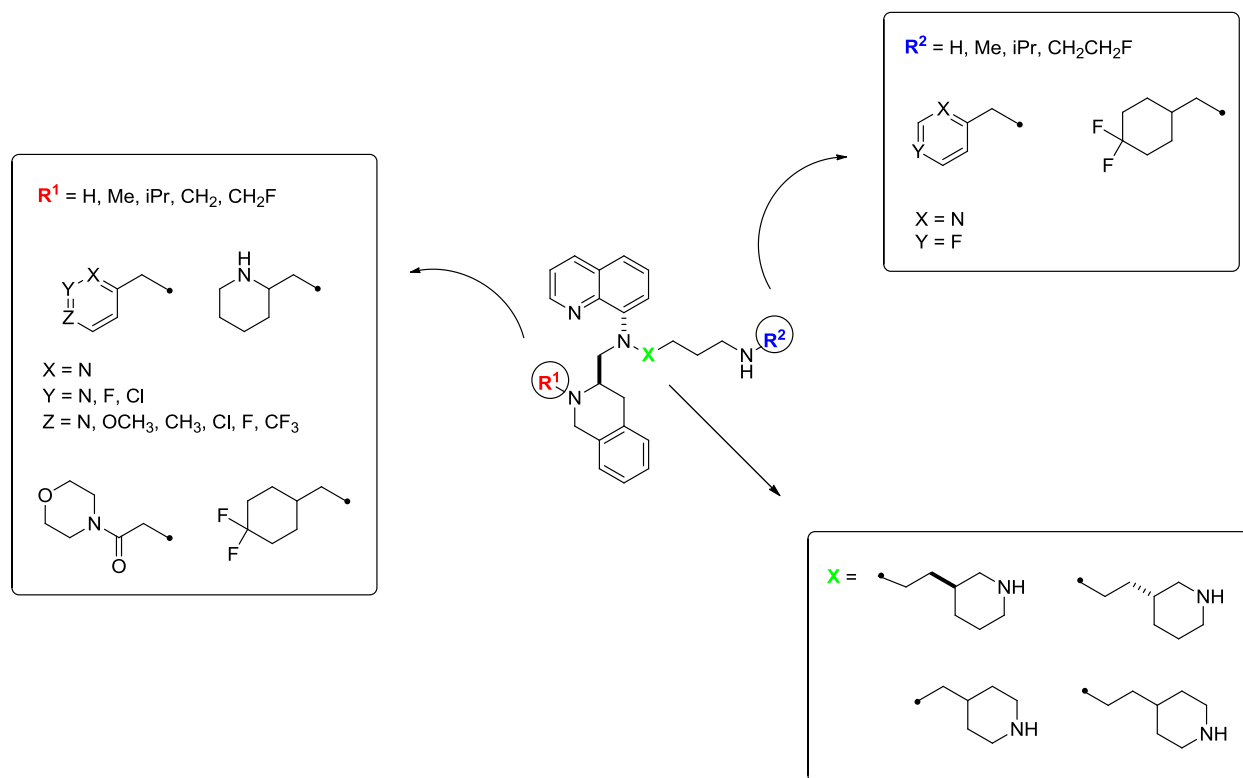


Figure 3.5: Overview of proposed N-THIQ and butyl amine analogs.

Generally, initial modifications were chosen to explore the lipophilic, electronic, and steric effects of introducing conservative and independent modifications at the tetrahydroisoquinoline nitrogen and butyl amine side chain on the potency and ADME properties of compound **6** (Figure 3.5).

### 3.3 Synthesis

To access the desired compounds we orthogonally protected **6** such that conservative independent modifications would be accessible; whereby the N-THIQ was protected with the acid sensitive boc group, and the butyl amine nitrogen was protected with the base sensitive phthalimide group (Figure 3.6).

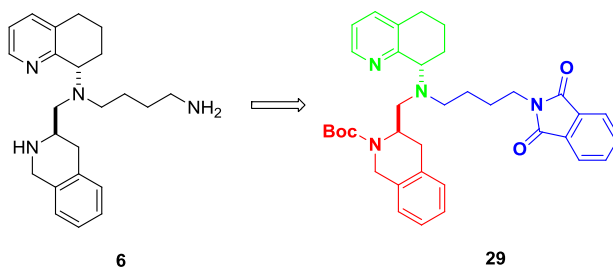
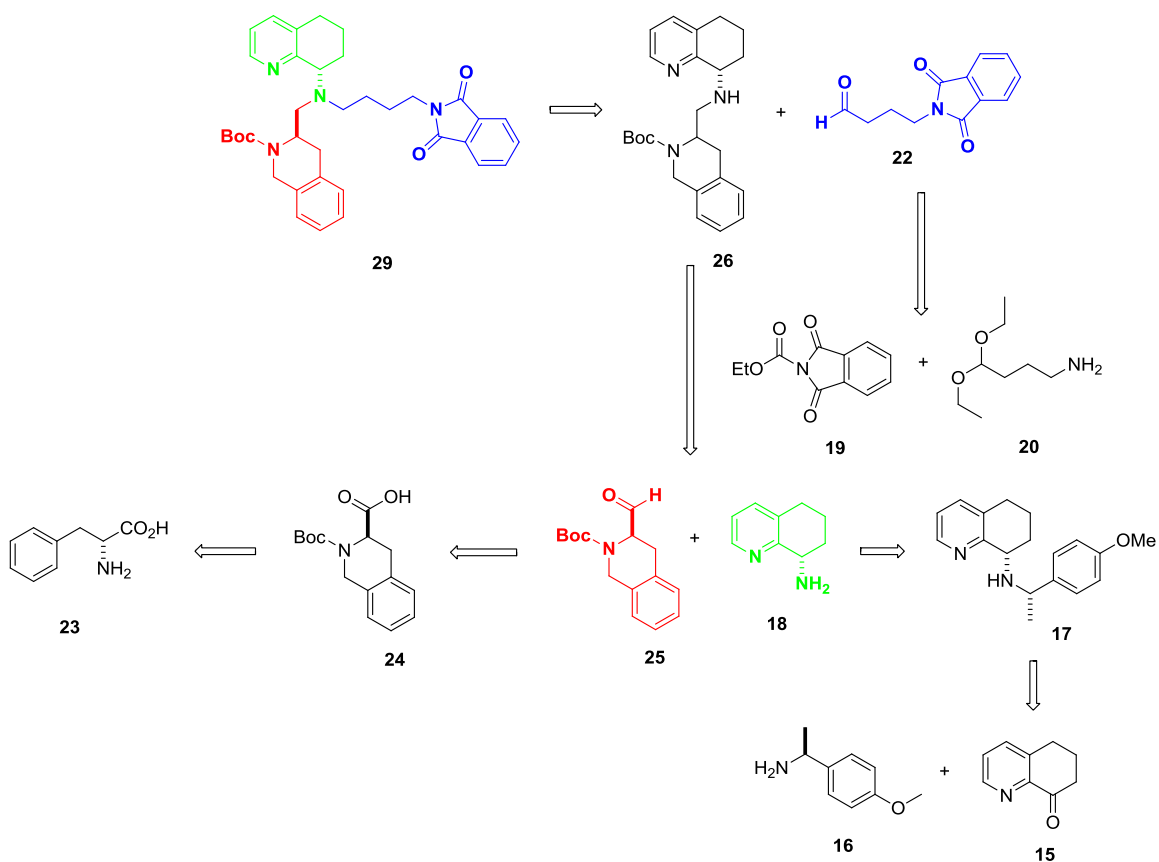


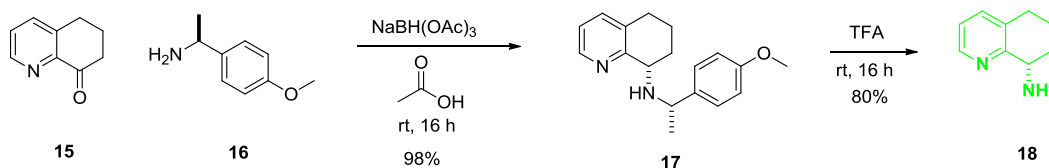
Figure 3.6: Advanced intermediate scaffold.

Retrosynthetically, it was envisaged that **29** would come from a reductive amination between Boc protected half scaffold **26** and phthalimide protected butyl amine side chain **22** (Figure 3.7).<sup>4</sup> The half scaffold **26** was envisaged to come from tetrahydroisoquinoline **25**, accessed via the Pictet-Spengler reaction with D-phenylalanine.<sup>5</sup> Chiral amine **18** could be generated via a reductive amination with commercially available ketone **15** and chiral protecting group **16**.<sup>4</sup>



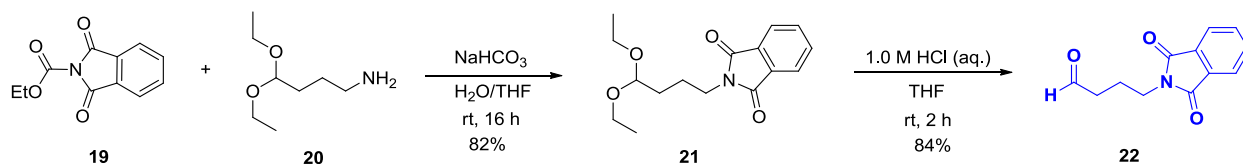
**Figure 3.7: Retrosynthesis of N-THIQ analogs.**

The synthesis of the three main components of the scaffold: **18**, **25**, and **22** are illustrated in Schemes 3.1, 3.2, and 3.3.



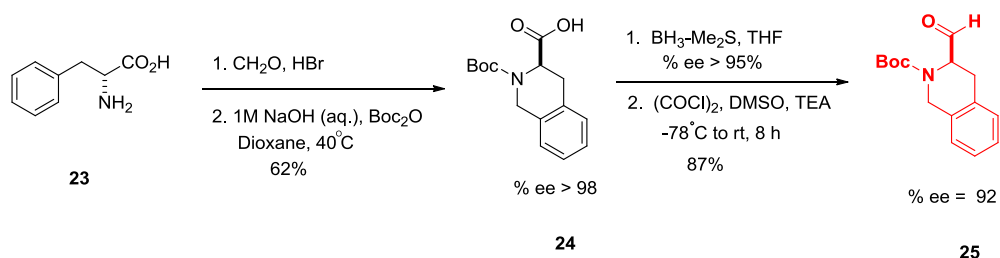
**Scheme 3.1: Synthesis of (S)-5,6,7,8-tetrahydroquinolin-8-amine (**18**).**

Reductive amination with commercially available ketone **15** and chiral amine **16** furnished the protected secondary amine **17**. This was followed by a Boc deprotection to afford chiral primary amine **18**.<sup>6</sup>



Scheme 3.2: Synthesis 4-(1,3-dioxoisindolin-2-yl)butanol (**22**).

Compound **22** was generated through a base mediated coupling of **19** and **20**. Hydrolysis of **21** afforded butylaldehyde **22**.

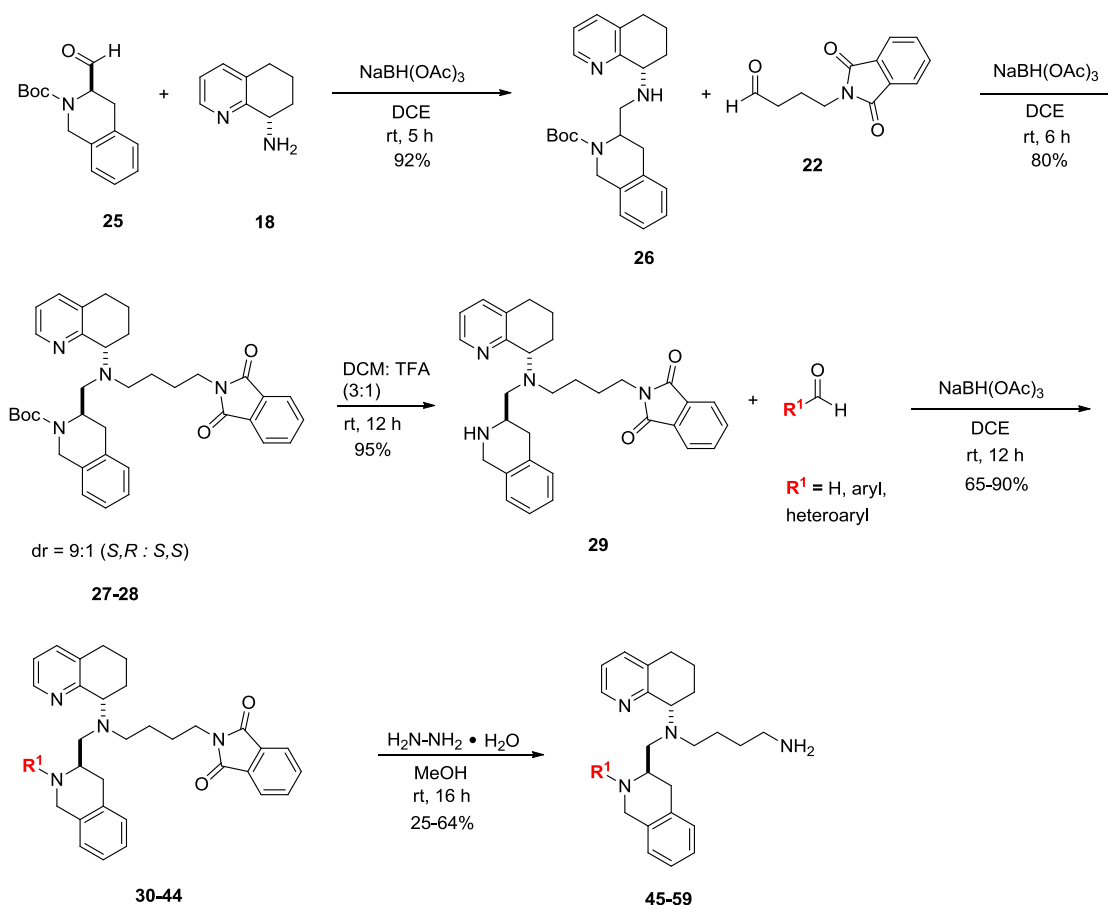


Scheme 3.3: Synthesis of (*R*)-*tert*-butyl 3-formyl-3,4-dihydroisoquinoline-2(*1H*)-carboxylate (**25**).

Employing the Pictet Spengler method in the reaction of commercially available D-phenylalanine **23** provided the chiral carboxylic tetrahydroisoquinoline (Scheme 3.3). Boc-protection followed by reduction using borane dimethyl sulfide provided the corresponding alcohol. Finally, Swern oxidation of **24** afforded the chirally enriched aldehyde **25**.

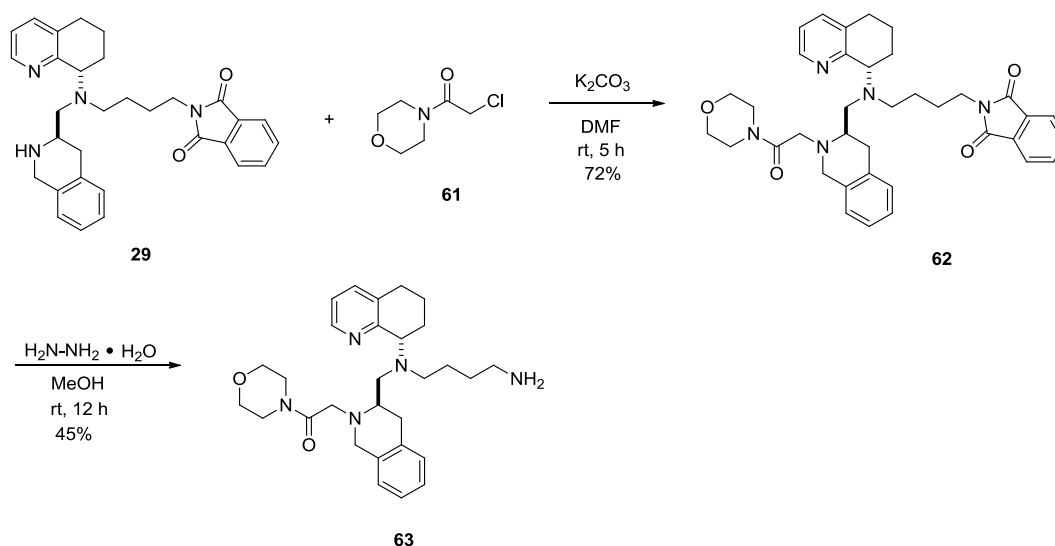
### 3.3.1 Tetrahydroisoquinoline Modifications

The effect of modifying the tetrahydroisoquinoline was initially probed through the addition of aryl-, and heteroaryl groups with different regio- and chemo- properties. The group of compounds **45-60** can be synthesized according to Scheme 3.4. Reductive amination with aldehyde **25** and chiral amine **18** furnished secondary amine **26**. Subsequent reductive amination of **26** with butylaldehyde **22** and separation of the diastereomers provided the desired advanced intermediate **27** (*S, R*). Boc deprotection followed by reductive amination with commercially available aldehydes provided THIQ modified compounds 30-44.



Scheme 3.4: Synthesis of N-TIC analogs 45-59.

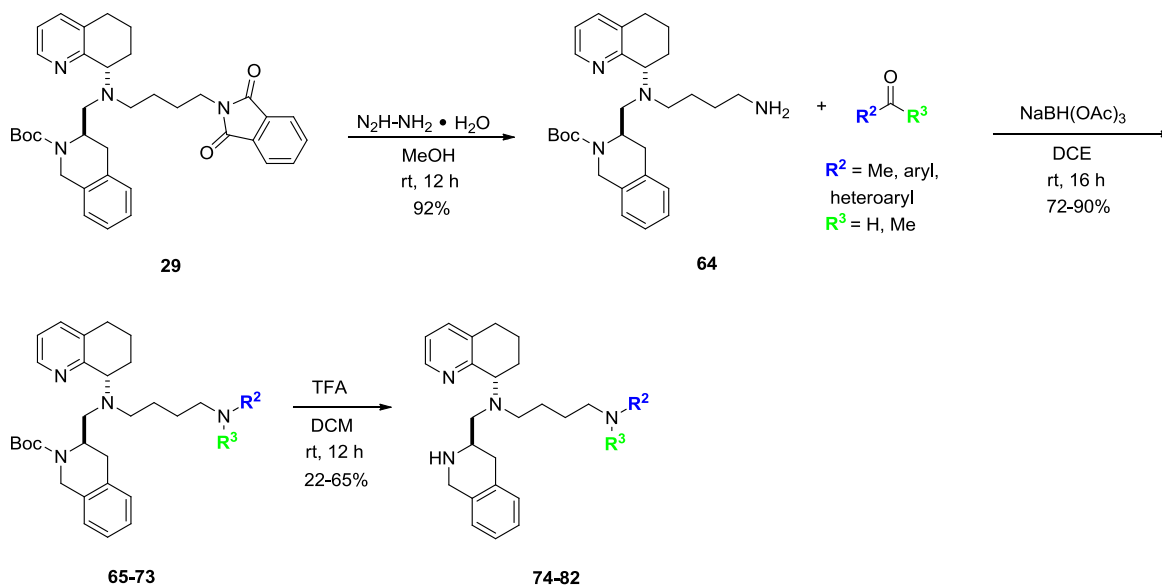
Phthalimide deprotection with hydrated hydrazine furnished final analogs **45-59**. Nucleophilic displacement of **61** generated acyl intermediate **62**. Phthalimide deprotection furnished final analog **63**.



Scheme 3.5: Synthesis of N-TIC morpholine analog **63**.

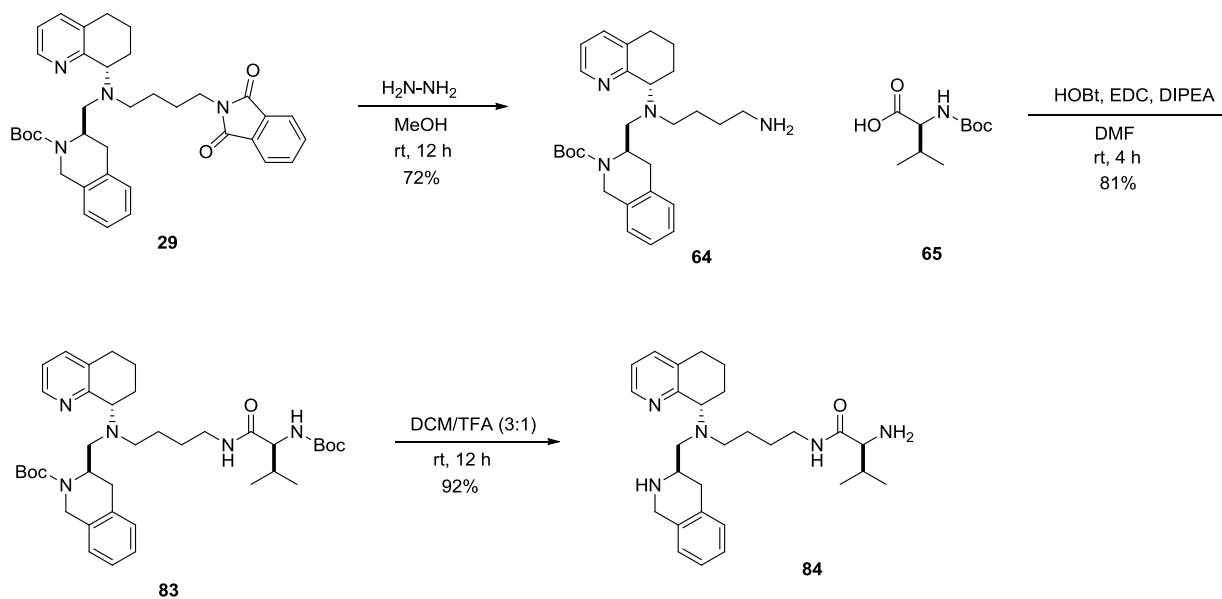
### 3.3.2 Butyl Amine Side Chain Modifications

The effect of modifying the butylamine nitrogen was initially probed with the addition of simple N-alkyl moieties, bulkier aromatic and non-aromatic N-alkyl moieties, and carbamides. Final analogs **74-82** were synthesized according to Scheme 3.6. The synthesis commenced with previously synthesized advanced intermediate **29**. Phthalimide removal of **29** followed by reductive amination with commercially available aldehydes and/or ketones furnished compounds **65-73**. Boc-deprotection of the tetrahydroisoquinoline nitrogen afforded final butyl amine analogs **74-82**.



Scheme 3.6: Synthesis of butyl amine analogs 74-82.

Final analog **84** was synthesized according to Scheme 3.7. The synthesis commenced with previously synthesized advanced intermediate **29**, followed by a peptide coupling with **65**. Subsequent global deprotection afforded final compound **84**.



Scheme 3.7: Synthesis of butyl amine analog 84.

To probe the effect of modifying the position of the basic amine on the butylamine side chain, analogs **92-95** were synthesized. It was envisaged that these compounds would come from a reductive amination between previously synthesized **26** (Fragment A) and readily available aldehydes (Fragment B), illustrated in Figure 3.8.

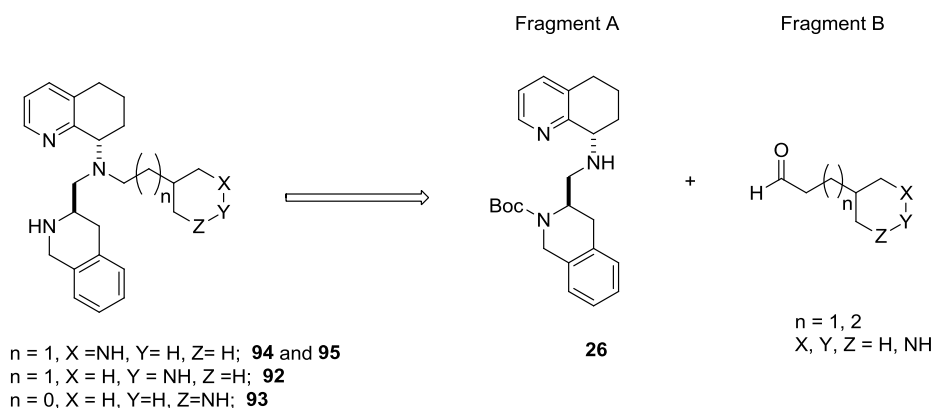
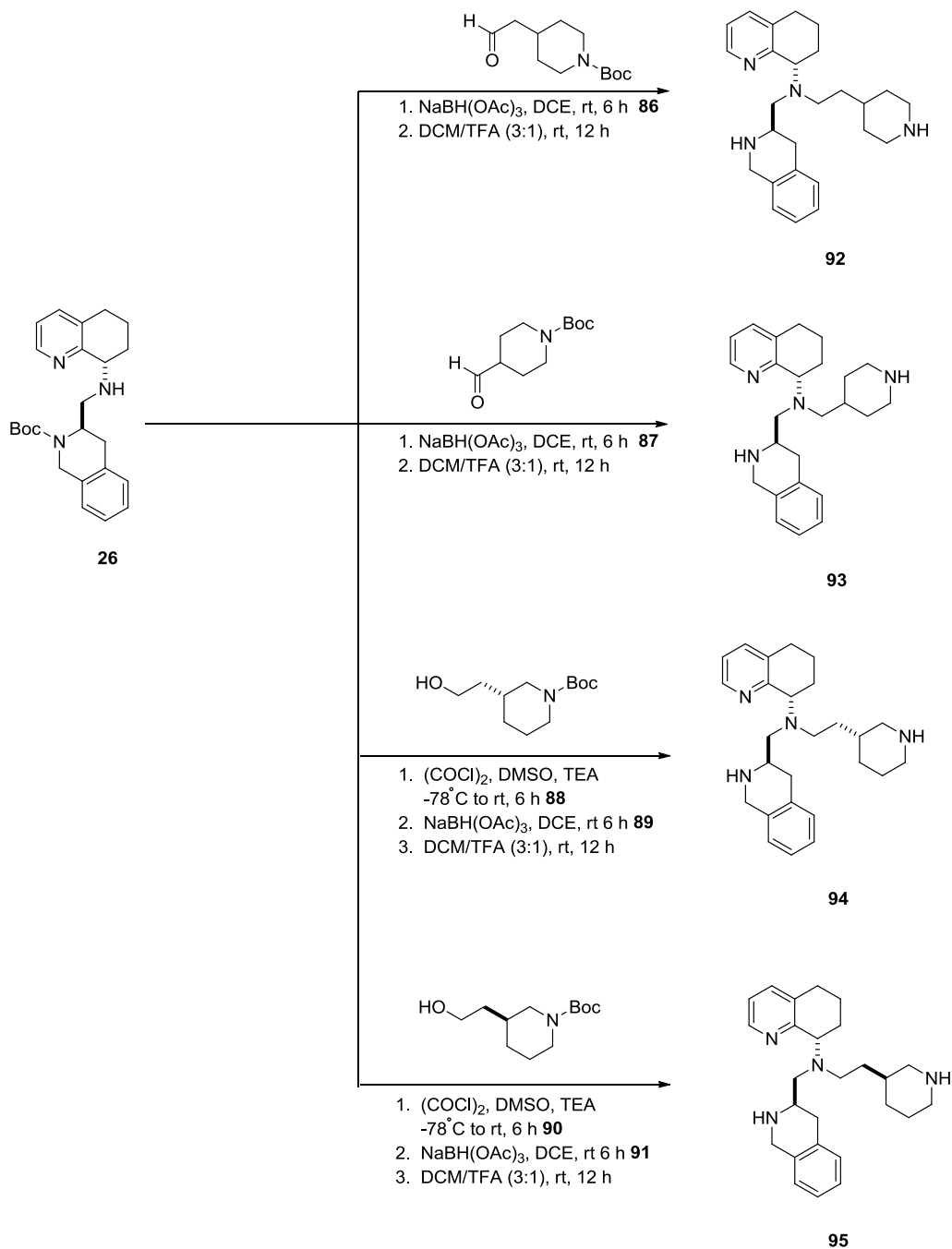


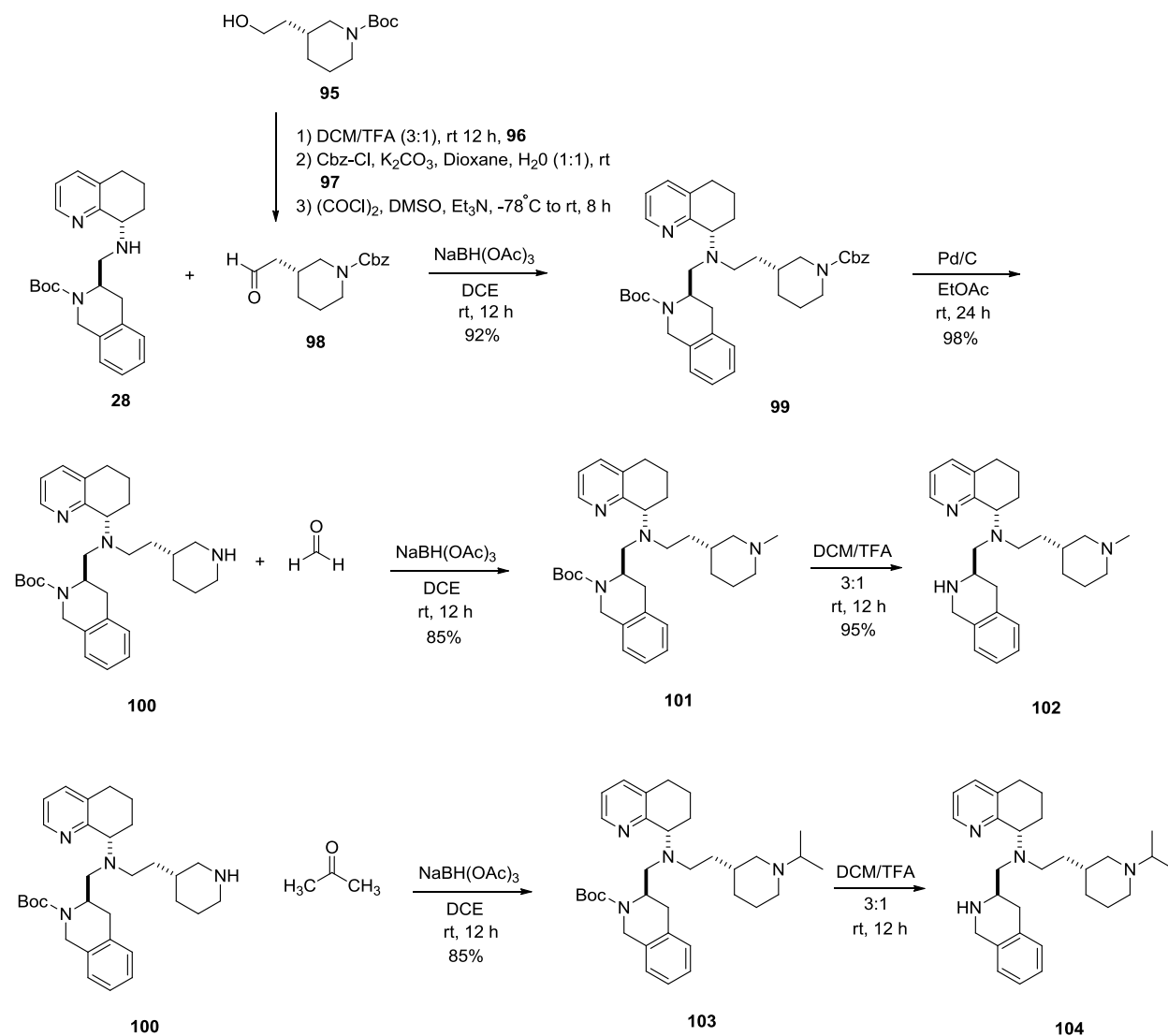
Figure 3.8: Retrosynthesis of butyl amine analogs 92-95.

To access compounds **92-95**, reductive amination of commercially available aldehydes provided advanced intermediates **86-90** (Scheme 3.8). Subsequent Boc deprotection provided the final compounds.



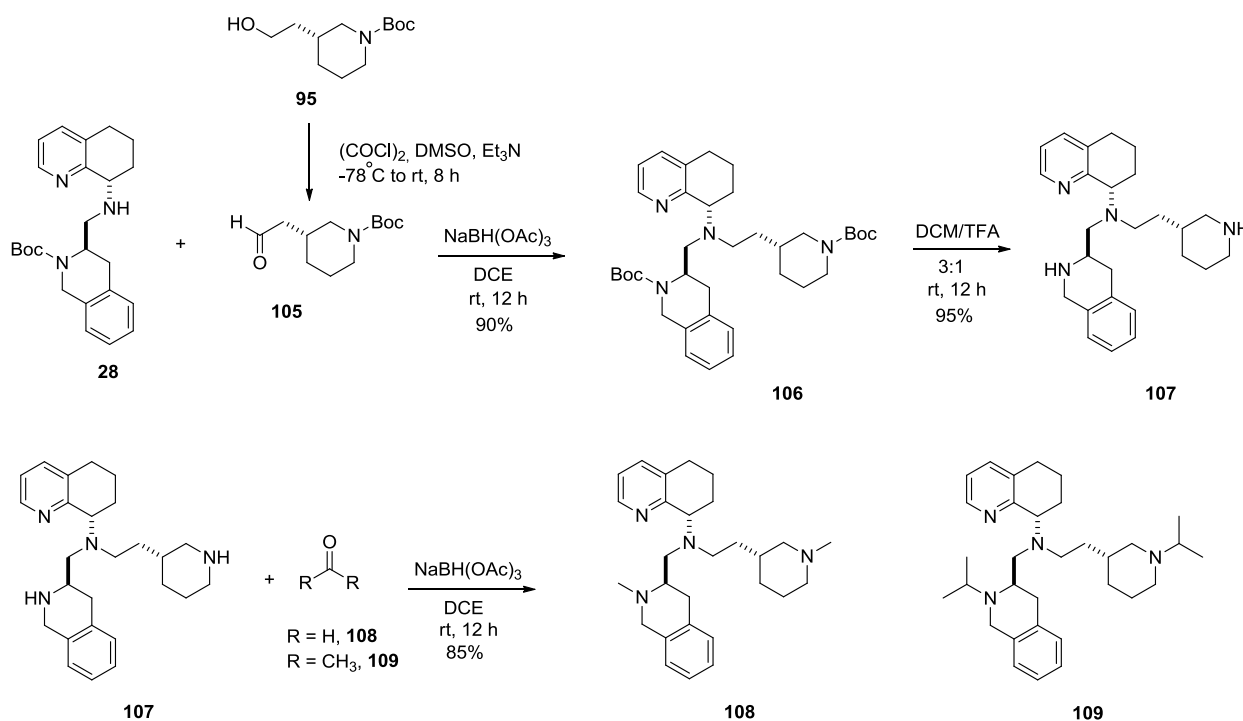
Scheme 3.8: Synthesis of butyl amine analogs **92-95**.

To probe the importance of having at least one hydrogen bond donor either the tetrahydroisoquinoline nitrogen or butyl amine nitrogen compounds **102** and **104**, and **108-109** were synthesized as illustrated in Schemes 3.9 and 3.10.



Scheme 3.9: Synthesis of butyl amine analogs **102** & **104**.

Acid mediated Boc deprotection of commercially available (R)-tert-butyl 3-(2-hydroxyethyl)piperidine-1-carboxylate **28**, followed by protection with carboxybenzyl chloride provided intermediate **29**. Swern oxidation of **29** followed by reductive amination with previously synthesized **28**, afforded orthogonally protected scaffold **99**. Cbz deprotection and reductive amination with compound **100** and either formaldehyde or acetone furnished tertiary amines **101** and **103**. Finally, Boc deprotection provided final compounds **102** and **104**.



Scheme 3.10: Synthesis of butyl amine analogs **108** & **109**.

Acid mediated deprotection of commercially available (R)-tert-butyl 3-(2-hydroxyethyl)piperidine-1-carboxylate **95**, followed by a reductive amination with **28** afforded

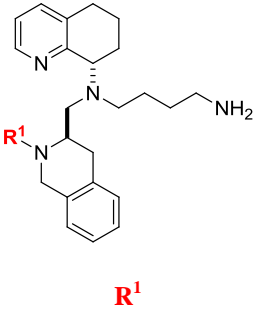
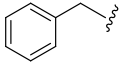
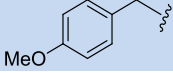
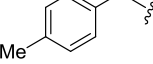
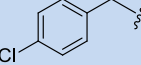
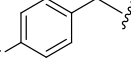
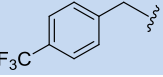
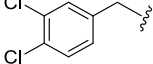
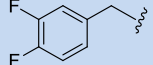
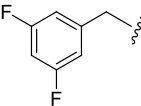
di-Boc intermediate **106**. Reductive amination followed by a global deprotection afforded final compounds **108** and **109**.

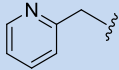
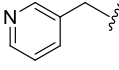
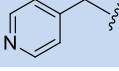
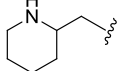
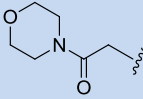
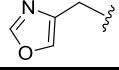
### 3.4 Results and Discussion

The data used to elucidate the structure activity relationships (SAR) of these series was generated by a combination of two assays: 1) blockade of HIV-1<sub>IIIB</sub> attachment via the CXCR4 receptor in MAGI cells, and 2) the inhibition of CXCL12 induced calcium ( $\text{Ca}^{2+}$ ) flux/release in Chem-1 cells. The compounds revealed a range of potencies and divergent SAR. All compounds were put in both agonist and antagonist modes in the calcium flux, and none showed any agonist activity, while showing complete blockade of SDF-1 induced calcium flux at various potencies (Tables 3.1-3.4).

Substitution on the tetrahydroisoquinoline nitrogen with H-bond acceptors, H-bond donors, aromatic moieties with either electron withdrawing or donating substituents and well as aliphatic moieties all resulted in a slight loss of potency (**44-59**, 2-10 fold) in the MAGI attachment assay when compared to **6** (Table 3.1). As a trend, bulkier heterocycles (compounds **47-59**, **63**) decreased potency more than the smaller groups (**45-46**, **64**). A similar trend was exhibited for CXCL12 induced  $\text{Ca}^{2+}$  flux, however the effect was much more dramatic. While there was generally a 2 to 10 fold decrease in anti-HIV potency compared to **6**, there was a 10 to 100-fold decrease in the compounds ability to block CXCL12  $\text{Ca}^{2+}$ . For example, the most bulky heterocycle **63** was approximately 100 fold less active in the MAGI, while the pyridyl groups (**56-58**) and the methyl and isopropyl alkyl groups (**45-46**), less of a difference was observed. Noteworthy in the data are compounds with various regio-chemical substitutions containing electron withdrawing substituents (**50-51**, **54-55**); where the addition of either

chlorine(s) or fluorine(s) resulted in noted solubility issues during the testing of these compounds. Therefore, it is hard to assign meaning to the data generated in the context of this SAR exploration. The exception to this trend is trifluoromethyl compound **52**, and implications there of discussed further *vide infra* (Conclusions).

Compound #		Magi-HIV-1 <sub>III</sub> B IC <sub>50</sub> (μM) <sup>a</sup>	Ca <sup>2+</sup> Flux IC <sub>50</sub> (μM) <sup>a</sup>
<b>6</b>	H	0.005	0.003
<b>45</b>	Me	0.02	0.039
<b>46</b>	<i>i</i> Pr	0.03	0.14
<b>47</b>		0.06 (TC <sub>50</sub> = 3.39)	0.1
<b>48</b>		0.01 (TC <sub>50</sub> = 5.35)	0.197
<b>49</b>		0.06	0.019
<b>50</b>		0.04	0.002 (sol.)
<b>51</b>		0.07	0.590
<b>52</b>		0.07 (TC <sub>50</sub> = 4.46)	0.654
<b>53</b>		0.05	0.16 (sol.)
<b>54</b>		0.1	0.2 (sol.)
<b>55</b>		0.19	0.29 (sol)

<b>56</b>		0.06	0.056
* <b>57</b>		0.07	0.35
* <b>58</b>		0.06	0.66
<b>59</b>		0.02	0.091
<b>63</b>		0.08	0.57
<b>64</b>		0.04	0.49

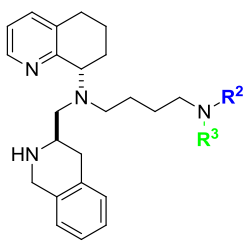
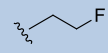
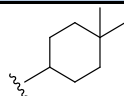
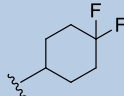
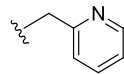
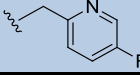
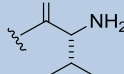
TC<sub>50</sub> > 10 μM for all compounds unless noted.

<sup>a</sup> Assay run in triplicate.

\* Compounds synthesized by Tony Prosser

**Table 3.1: Tetrahydroisoquinoline analogs 45-64.**

Regarding the preliminary SAR of the carbamides and N-alkyl moieties (**74-84**, Table 2), the simple N-alkylated compounds **74** and **75** retained both potent HIV activity and CXCL12 induced Ca<sup>2+</sup>, although were slightly less potent in the MAGI assay (2-5 fold). Surprisingly, the 2-pyridyl and carbamide based derivatives (**79-84**) were 40-80 fold less potent than **6** in the MAGI assay, but retained potency in blocking CXCL12 induced Ca<sup>2+</sup> flux. These results potentially signify the basicity and steric environment may be more important for anti-HIV activity, but not for normal CXCL12 mediated receptor signaling, since nearly all substitutions (**74-82**) resulted in potent Ca<sup>2+</sup> flux inhibition, with the exception being the dimethyl urea **83**.

Compound #			Magi-HIV-1 <sub>IMB</sub> IC <sub>50</sub> (μM) <sup>a</sup>	Ca <sup>2+</sup> Flux IC <sub>50</sub> (μM) <sup>a</sup>
	R <sup>2</sup>	R <sup>3</sup>		
6	H	H	0.005	0.003
74	Me	Me	0.03	0.008
75	H	<i>i</i> Pr	0.04	0.007
76	H		0.10	0.24
77	H		0.21 (TC <sub>50</sub> = 5.35)	0.012
78	H		0.01 (TC <sub>50</sub> = 4.1)	0.007
** 79	H		0.12	0.001
80	H		0.13 (TC <sub>50</sub> = 6.94)	0.24
* 81	H		0.29	0.004
* 82	H		0.21	0.003
* 83	H		0.42	0.18
84	H		0.06	0.016

TC<sub>50</sub> > 10 μM for all compounds unless noted.

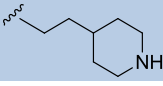
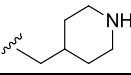
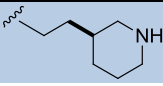
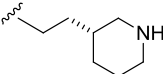
<sup>a</sup> Assay run in triplicate

\* Compounds synthesized by Brooke Katzman

\*\* Compound synthesized by Larry Wilson, Ph.D.

Table 3.2: Butyl amine analogs 74-84.

The SAR of the butyl amine analogs **92-95** (Table 3.3) indicated both the location and orientation of the nitrogen was important for both anti-HIV activity and CXCL12 induced  $\text{Ca}^{2+}$  flux. Moving the nitrogen around the piperidine ring resulted in a significant loss of HIV activity (100-200 fold), with a less pronounced loss of activity for CXCL12 induced  $\text{Ca}^{2+}$ .

Compound #		Magi-HIV-1 <sub>III</sub> B IC <sub>50</sub> (μM)	Ca <sup>2+</sup> Flux IC <sub>50</sub> (μM)
<b>92</b>		0.12	0.22
<b>93</b>		.44	0.052
<b>94</b>		0.11	0.028
<b>95</b>		0.02	0.006

TC<sub>50</sub> > 10 μM for all compounds unless noted.

**Table 3.3: Butyl amine analogs 92-95.**

Moving the nitrogen around the piperidine ring (**92-93**) resulted in a significant loss of HIV activity (100-200 fold), with a less pronounced loss of activity for CXCL12 induced  $\text{Ca}^{2+}$ . Restricting the flexibility of the side chain and the orientation resulted in (**94-85**, Table 3) the retention of both potent HIV activity and CXCL12 induced  $\text{Ca}^{2+}$ . These results potentially signify the location and orientation of the butyl amine nitrogen is more important for anti-HIV activity, than for normal CXCL12 mediated receptor signaling.

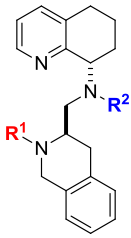
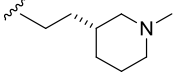
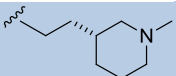
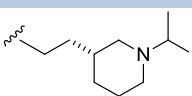
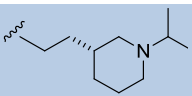
Compound #		Magi-HIV-1 <sub>MB</sub> IC <sub>50</sub> (μM)	Ca <sup>2+</sup> Flux IC <sub>50</sub> (μM)	
	R <sup>1</sup>	R <sup>2</sup>		
102	H		0.20	0.016
108	Me		4.27	0.032
104	H		0.07	0.013
109	<i>i</i> Pr		1.33	0.045

Table 3.4: Butyl amine analogs **102**, **104**, **108**, & **109**.

The SAR of the butyl amine analogs illustrated in Table 3.4 indicated the piperidine methyl and isopropyl analogs **102** and **104** were less potent in the MAGI assay (2-5 fold). Surprisingly, analogs **108** and **109** were 200-400 fold less potent than **6** in the MAGI assay, but retained potency in blocking CXCL12 induced Ca<sup>2+</sup> flux. These results potentially signify the importance of having at least one hydrogen bond donor may be more important for anti-HIV activity, but not for normal CXCL12 mediated receptor signaling, since nearly all substitutions in Table 3.4 resulted in potent Ca<sup>2+</sup> flux inhibition.

Several important observations can be gleaned from the structure activity relationship of the tetrahydroisoquinoline-based analogs, summarized in Figure 3.9 and Table 3.5. As indicated,

the presence of aliphatic or aryl ( $R^1$ , Figure 3.9) did not dramatically effect potency. Bulkier heterocycles exhibited a 2-10 fold decrease in the ability to block HIV entry, but also a 10 - 100 fold decrease in the ability to block  $Ca^{2+}$ .

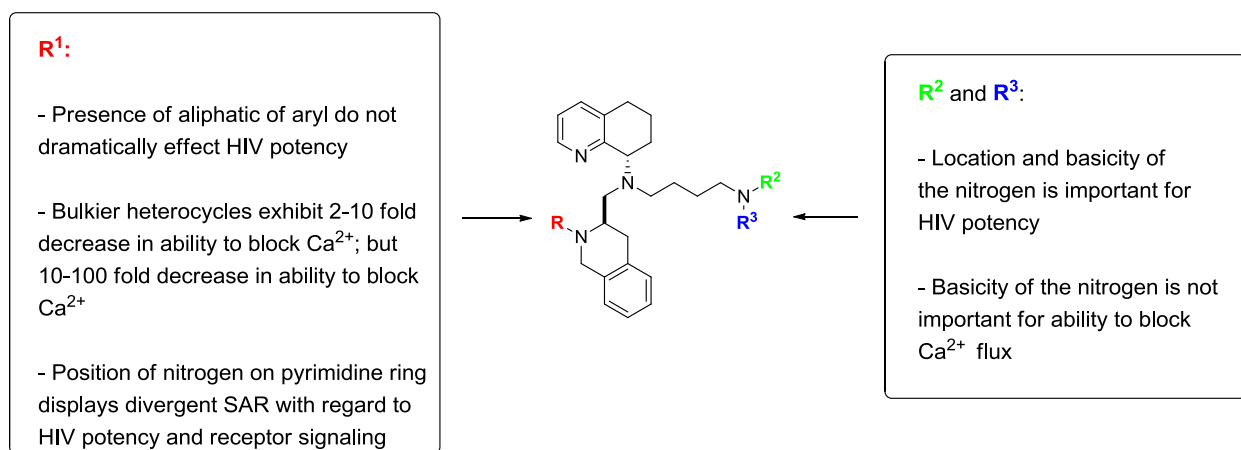
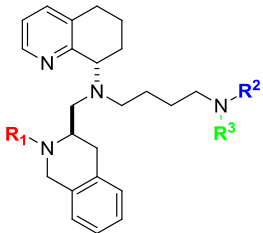
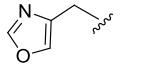
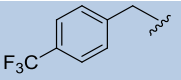
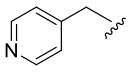
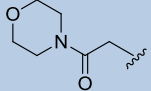
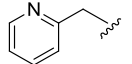
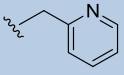
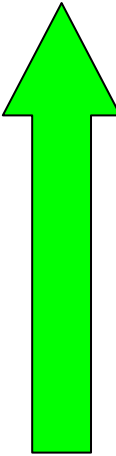


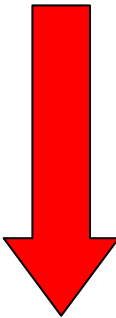
Figure 3.9: SAR summary of analogs.

Additionally, both the location and basicity of the butyl amine nitrogen was shown important for HIV potency, but not for the ability to block CXCL12 induced  $Ca^{2+}$ . Most interestingly, was the trend illustrated in Table 3.5 where the oxazole (**64**), electron deficient heterocycle (**52**), 3-pyridyl (**57**) and 4-pyridyl (**56**) compounds lead to a group of compounds highly potent against HIV entry, while showing decreased potency in the ability to block CXCL12 induced  $Ca^{2+}$  flux. This interesting and unique trend was the subject of further investigation in Chapter 4 (*vide infra*).

Cmpd. #				Magi- HIV-1 <sub>MB</sub> IC <sub>50</sub> ( $\mu$ M)	Ca <sup>2+</sup> Flux IC <sub>50</sub> ( $\mu$ M)	Selectivity Index Ca <sup>2+</sup> /HIV Ratio
	R <sup>1</sup>	R <sup>2</sup>	R <sup>3</sup>			
64		H	H	0.04	0.49	12
52		H	H	0.07	0.65	10
56		H	H	0.06	0.66	10
63		H	H	0.06	0.56	10
58		H	H	0.06	0.06	1
6	H	H	H	0.005	0.003	1
74	H	Me	Me	0.13 (TC <sub>50</sub> = 6.94)	0.24	.027
* 79	H	H		0.07	0.001	.010
* 81	H	H		0.29	0.004	.008
* 82	H	H		0.21	0.003	.013



> 1



< 1

Table 3.5: SAR trends.

Based on these results, we undertook a computational docking study in order to better understand the SAR observed in this study and develop a working hypothesis on how our compounds interact with the CXCR4 receptor. Using the recently reported CXCR4 receptor small molecule co-crystal structure (Figure 3.6), we developed a computational model of **6**

bound to CXCR4. Because of the importance of the interaction of IT1t with Asp97 and Glu288 in the crystal structure, we hypothesized that **6** would interact with the same residues (Figure 3.10). Thus, we flexibly docked compound **6** into the IT1t subsite of CXCR4 (PDB ID 30DU). In the best pose, the positively charged butyl amine of **6** interacts with the Glu288 carboxylate via a salt bridge and forms a hydrogen bond with the Tyr116 side chain phenol oxygen at the bottom of the pocket, while the protonated THIQ ring forms a salt bridge with Asp97 carboxylate (Figure 3.11) The THIQ moiety is situated in a hydrophobic pi-stacking pocket comprising mainly indole of Trp94 and the imidazole of His113.

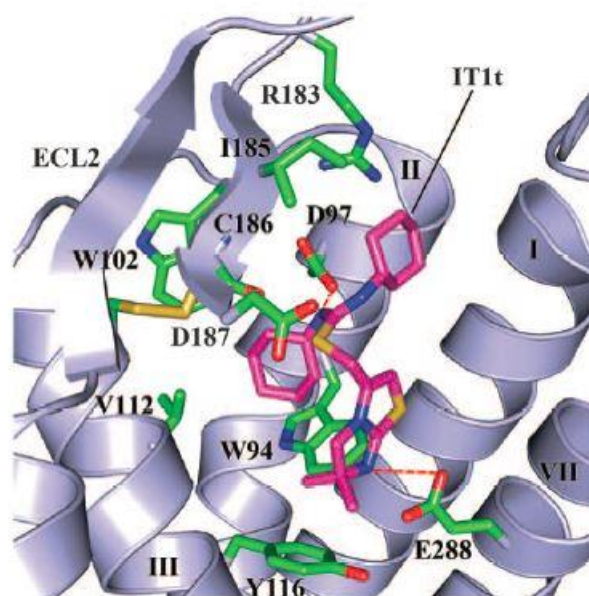


Figure 3.10: Crystal structure of small molecule IT1t.<sup>7</sup>

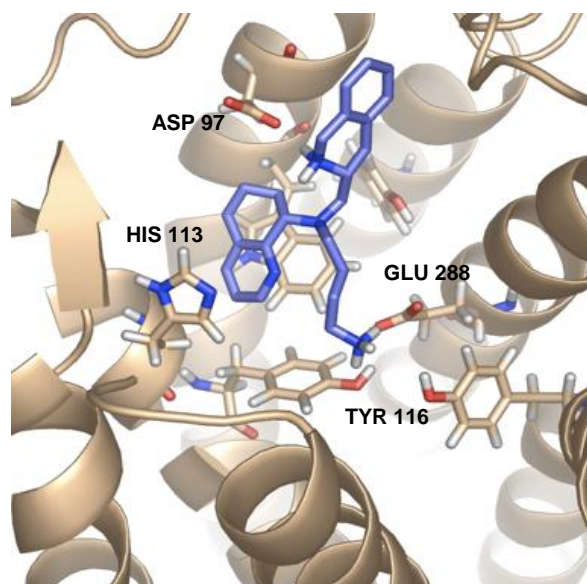


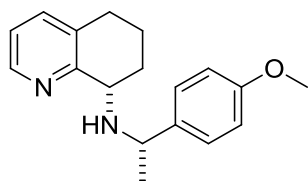
Figure 3.11: Docking pose of compound **6** in the IT1t/3ODU crystal structure showing hydrogen bonding interactions and key amino acids.

The key role of the THIQ nitrogen in salt bridge formation is consistent with the SAR of the compounds in Table 1, where activity drops off significantly for the non-basic tetrahydroisoquinolines. Additionally, the SAR from the alteration of substitution on both nitrogen atoms of **6** (Table 3.4) provides some support for this model. Since Glu288 is a key residue for HIV interaction with Asp97 is more important for CXCL12 function, the modifications of the THIQ (Table 3.1), which reduce calcium flux potency more than HIV activity, are consistent with altering the Asp97-THIQ interaction, while maintaining the integrity of the Glu288-butyl amine interaction. The modifications of the butyl amine side chain that alter basicity (**81-83**), which reduce HIV blocking effects while maintaining calcium flux potency, are consistent with maintaining the THIQ nitrogen-Asp97 interaction and altering the butyl amine-Glu288 interaction.

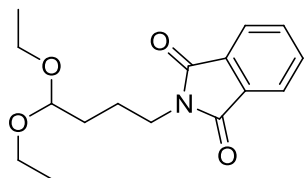
### 3.5 Conclusions

A novel series of highly potent and selective CXCR4 antagonists based on a chiral tetrahydroisoquinolone ((*R*)-THIQ) scaffold was identified through a hit-to-lead effort focused on benzamidazole, and butyl amine replacements. This novel series made use of a GPCR chemotype with a chiral linkage that may exploit unique and efficient contacts with amino acid residues in the receptor. The motif may also provide compounds with unique biological selectivity and initial modifications to the THIQ nitrogen and butyl amine side chain provided exciting insights for the potential design of T-tropic HIV select antagonists that do not interfere with CXCL12 based receptor signaling, while also more providing more potent antagonists of the CXCR4/CXCL12 axis. These intriguing trends became the foundation for further investigation and exemplified in Chapter 4 (*vide infra*).

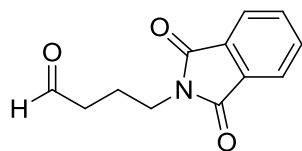
### 3.6 Chemistry Experimental



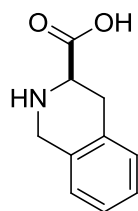
**(S)-N-((S)-1-(4-methoxyphenyl)ethyl)-5,6,7,8-tetrahydroquinolin-8-amine (17):** To a solution of (S)-1-(4-methoxyphenyl)ethanamine (24.41 ml, 165 mmol) and 6,7-dihydroquinolin-8(5H)-one (22.12 g, 150 mmol) in DCM (400 mL) was added acetic acid (12.91 ml, 225 mmol) followed by sodium triacetoxyborohydride (44.6 g, 210 mmol) in one portion under argon atm. A very mild exotherm is observed after adding sodium triacetoxyborohydride (2-3 °C). The reaction mixture was stirred at ambient temperature overnight (15 hours). The mixture was diluted with water 100 mL and stirred for an additional 30 min. The organic layers were separated, and the aqueous extracted with DCM (2 x 100 mL). The organic layers were combined, dried over MgSO<sub>4</sub>, and concentrated under reduced pressure to give an oil. The oil was then triturated with cold hexanes and the off-white solid was filtered, washed with cold hexanes and dried under vacuum filtration to yield 24.5g (77 % yield) of the product as an off-white solid. TLC 5% MeOH in DCM R<sub>f</sub> = .55



**2-(4,4-diethoxybutyl)isoindoline-1,3-dione (21):** Water (68.0 ml) and THF (68.0 ml) were added to a 500 mL round bottom flask. Sodium hydrogen carbonate (7.67 g, 91 mmol) and 4,4-diethoxybutan-1-amine (18.40 ml, 96 mmol) were suspended in a solution of Water (68.0 mL) and THF (68.0 mL). To the mixture was then added ethyl 1,3-dioxoisoindoline-2-carboxylate (20 g, 91 mmol). The reaction was kept at room temperature for 4 hours and was diluted with ethyl acetate (EtOAc) (150 mL) and water (15 mL) to dissolve the salt precipitation. The organic phase was separated, washed with brine (2 x 75 mL), dried over MgSO<sub>4</sub>, and concentrated to give 5.2 g of a yellow oil. The oil was purified by flash column chromatography (ISCO, 120 g silica gel column, 0-25% EtOAc over 15 minutes) to give 18 g (94%) of the product as white solid. <sup>1</sup>H NMR [400 MHz, CDCl<sub>3</sub>] δ 7.80 - 7.75 (m, 2H), 7.68 - 7.63 (m, 2H), 4.46 (t, *J* = 5.6 Hz, 1H), 3.66 (t, *J* = 7.1 Hz, 2H), 3.58 (dq, *J* = 9.4, 7.0 Hz, 2H), 3.43 (dq, *J* = 9.4, 7.1 Hz, 2H), 1.76 - 1.66 (m, 2H), 1.66 - 1.56 (m, 2H), 1.13 (t, *J* = 7.1 Hz, 6H); <sup>13</sup>C NMR [100 MHz, CDCl<sub>3</sub>] δ 168.39, 133.94, 132.19, 123.21, 102.48, 102.45, 77.55, 77.23, 76.91, 61.29, 37.79, 31.03, 24.06, 15.39.

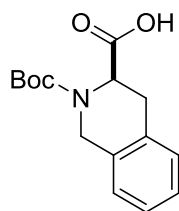


**4-(1,3-dioxoisindolin-2-yl)butanal (22):** In a 100 mL RBF was dissolved VT-03-045 (5.00 g, 17.16 mmol) in THF (19.07 mL). To the solution was added 1N HCl (4.82 mL, 4.82 mmol). Suspension was monitored by TLC. After 72 hours, reaction was quenched with careful addition of saturated NaHCO<sub>3</sub>. Solvent was removed, and the mixture was diluted with 50 mL EtOAc. The organic phase was washed with brine and dried over MgSO<sub>4</sub> resulting in a colorless oil (2.13 g). Material was purified by flash column chromatography (ISCO, 40 g silica gel column, 0-40% EtOAc-Hexanes over 22 minutes). The resulting oil recrystallized upon standing to give a white solid (1.73 g). <sup>1</sup>H NMR [400 MHz, CDCl<sub>3</sub>] δ 9.76 (d, *J* = 1.2 Hz, 1H), 7.83 (dd, *J* = 5.4, 3.1 Hz, 2H), 7.71 (dd, *J* = 5.5, 3.0 Hz, 2H), 3.73 (t, *J* = 6.8 Hz, 2H), 2.53 (td, *J* = 7.3, 1.1 Hz, 2H), 2.01 (p, *J* = 7.0 Hz, 2H); <sup>13</sup>C NMR [100 MHz, CDCl<sub>3</sub>] δ 201.06, 168.54, 134.21, 132.15, 123.45, 77.55, 77.23, 76.91, 41.25, 37.29, 21.33; HRMS calc'd for C<sub>12</sub>H<sub>12</sub>NO<sub>3</sub> 218.08117; found 218.08144 [M+H].

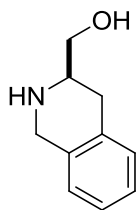


**(R)-1,2,3,4-tetrahydroisoquinoline-3-carboxylic acid (24):** A slurry containing D-phenylalanine (5 g, 30.3 mmol) in 48% HBr (24.00 mL, 212 mmol) was heated to 40 °C and 37% formaldehyde (4.60 mL, 61.8 mmol) was added to the slurry at 1 mL/min. The reaction was then heated to 85 °C. Heating was continued at 85 °C for 8 hours, then cooled for 48 hours after a

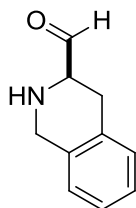
precipitate was formed. The precipitate was collected by filtration and washed 20 mL EtOH. The wet cake was then dried under vacuum. The white solid (3.32 g) was carried forward without purification. HRMS calc'd for C<sub>10</sub>H<sub>12</sub>NO<sub>2</sub> 178.08626; found 178.08650 [M+H].



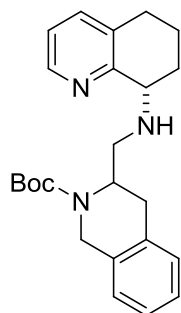
**(R)-2-(tert-butoxycarbonyl)-1,2,3,4-tetrahydroisoquinoline-3-carboxylic acid (24):** To a suspension of (3R)-2-bromo-3-carboxy-1,2,3,4-tetrahydroquinolin-2-ium (1.5 g, 8.47 mmol) in dioxane (36.0 ml) was added 1N NaOH (aq.) (36.6 ml, 36.6 mmol) and BOC-Anhydride (3.93 ml, 16.93 mmol). The resulting reaction mixture was stirred at room temperature for 16 hours before being heated at 40 °C overnight. The mixture was then concentrated to remove solvent and dissolved in 200 mL EtOAc. To the solution was added 1N HCl (aq.) to neutralize the reaction mixture to about pH 2.0. The organic phase was washed with brine, water, and over anhydrous MgSO<sub>4</sub>. Solvent was removed over reduced pressure resulting in a white solid (2.2 g). <sup>1</sup>H NMR [400 MHz, CDCl<sub>3</sub>] δ 9.78 (s, 1H), 7.06-7.25 (m, 4H), 5.13 (d, *J* = 2.9 Hz, 0.5 H), 4.78 - 4.64 (m, 1.5 H), 4.48 (t, *J* = 16.7 Hz, 1H), 3.36 - 3.03 (m, 2H), 1.52 (s, 4.5H), 1.41 (s, 4.5H); <sup>13</sup>C NMR [100 MHz, CDCl<sub>3</sub>] δ 178.00, 177.16, 155.89, 154.95, 134.00, 132.90, 132.07, 131.82, 128.71, 127.97, 127.18, 127.14, 126.98, 126.93, 126.56, 126.40, 81.20, 77.54, 77.22, 76.91, 54.32, 52.54, 44.69, 44.06, 31.51, 31.02, 28.58, 28.41. HRMS calc'd for C<sub>16</sub>H<sub>18</sub>NO<sub>4</sub> 276.12413 ; found 276.12394 [M-H].

**(R)-(1,2,3,4-tetrahydroisoquinolin-3-yl)methanol:**

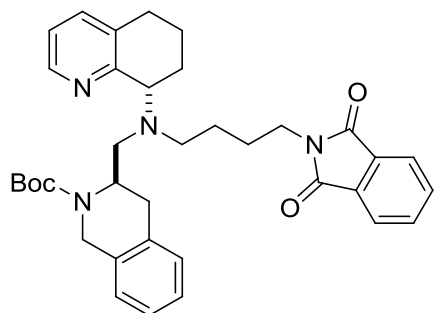
A stirred solution of 2.25 g (8.1 mmoles) of (*R*)-2-(*tert*-butoxycarbonyl)-1,2,3,4-tetrahydroisoquinoline-3-carboxylic acid in 40 mL of THF was cooled to 0 °C. Next, 12 mL of a 2M solution of BH<sub>3</sub>-SMe<sub>2</sub> complex in THF (0.24 moles) was added slowly in 1 mL aliquots over a twenty-minute period. The reaction was allowed to warm to room temperature and allowed to stir overnight. The reaction was then quenched with MeOH (5 mL), followed by the addition of 50 mL of 1N NaOH (aq.) solution. The reaction was then extracted with Et<sub>2</sub>O (200 mL) and washed with 1N NaOH (aq.) and saturated NaCl (aq.) solutions. The aqueous layers were re-extracted with Et<sub>2</sub>O and the organic layers were combined and dried over anhydrous MgSO<sub>4</sub>(s). The compound was then purified by flash column chromatography with a Hexanes/EtOAc gradient. Solvent removal gave 2.04 g (63% yield) of a clear, viscous oil. R<sub>f</sub>: 0.45 (1% MeOH in DCM UV/PMA); <sup>1</sup>H NMR (400Hz, CDCl<sub>3</sub>) δ 1.52 (s, 9H), 1.91 (m, 1H), 2.24 (m, 1H), 2.69 (m, 2H), 4.64 (m, 1H), 7.01 (m, 1H), 7.07 (m, 1H), 7.20 (m, 1H), 7.73 (s, 1H), 9.53 (s, 1H); HRMS calc'd for C<sub>15</sub>H<sub>21</sub>NNaO<sub>3</sub> 286.14137; found 286.14156 [M+H].

**(R)-tert-butyl 3-formyl-3,4-dihydroisoquinoline-2(1H)-carboxylate (25):**

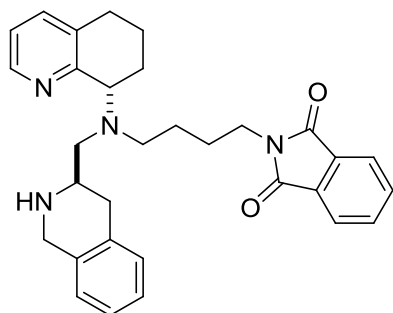
A solution of oxalyl dichloride (3.54 ml, 40.6 mmol) in DCM (100 ml) was cooled to -78 °C (dry-ice acetone) under argon atm. Methylsulfinylmethane (5.72 ml, 81 mmol) was then added over a 30-45 minute period. The temperature was maintained above -60 °C during the addition. After the addition was complete the mixture stirred for 30 min. (R)-tert-butyl 3-(hydroxymethyl)-3,4-dihydroisoquinoline-2(1H)-carboxylate (4.75 g, 18.04 mmol) was then added in portion while maintaining the temperature above -70 °C over 15 minutes. After the addition was complete reaction stirred for 1h. Triethylamine (11.34 ml, 81 mmol) was then added dropwise over 30 minutes while maintaining the temp. above -70 °C. After the addition was complete the mixture was stirred at -78 °C for 1 hour. The reaction was then allowed to warm to 0 °C (ice-bath) and stirred for 2h. The reaction was then quenched with 10 mL sat. aq. NaHCO<sub>3</sub>. The organic layer was separated and the aq. layer extracted with 40 mL DCM. The combined organic layers were washed with brine and water and dried over MgSO<sub>4</sub>. The solvent was removed under reduced pressure. Material was purified by column chromatography: 80g SiO<sub>2</sub> column, eluted with 25% EtOAc:Hexanes to yield a colorless oil in 80% yield. <sup>1</sup>H NMR 400 Hz, CDCl<sub>3</sub> (mixture of 1:1 rotamers): 1.48 (s, 4.5 H), 1.53 (s, 4.5 H), 3.1 (m, 1.5 H), 3.24 (dd, 0.5 H, *J*=3 Hz, *J*=16 Hz), 4.53 (t, 0.5 H, *J*=4 Hz), 4.57 (d, 1H, *J*=18 Hz), 4.69 (d, 1H, *J*=16 Hz), 4.83 (t, 0.5 H, *J*=4 Hz), 7.1 (m, 0.5 H), 7.18 (m, 3.5 H), 9.47 (s, 0.5 H), 9.52 (s, 0.5 H); HRMS (m/z): 262 (M+H), 261 (M), 260 (M-H).



**tert-butyl 3-((((S)-5,6,7,8-tetrahydroquinolin-8-yl)amino)methyl)-3,4-dihydroisoquinoline-2(1H)-carboxylate (26):** To a solution of 0.87 g (2.21 mmoles) of (*S*)-*N*-((((*R*)-1,2,3,4-tetrahydroisoquinolin-3-yl)methyl)-5,6,7,8-tetrahydroquinolin-8-amine in 15 mL of DCM was added 0.8 g (2.79 mmoles) of 4-(*tert*-butylcarbonylamino)-butyraldehyde. The mixture was stirred at room temperature for 30 minutes and then 0.83 g of NaBH(OAc)<sub>3</sub> was added. The reaction was stirred overnight and then extracted with DCM and washed with NaHCO<sub>3</sub>(aq.) and NaCl(aq.) solutions. The organics were separated and dried over Na<sub>2</sub>SO<sub>4</sub>(s). Filtration and solvent removal gave a brown oil, which was subjected to column chromatography (silica gel, Hexanes/EtOAc gradient) to give 0.89 g of a pale yellow viscous oil. <sup>1</sup>H NMR [600 MHz, CDCl<sub>3</sub>] δ 8.36 (d, 1H, *J* = 16.2 Hz), 7.28-7.24 (m, 1H), 7.11-7.09 (m, 2H), 7.02-6.97 (m, 3H), 4.68-4.63 (m, 2H), 4.15-4.12 (d, 1H, *J* = 16.8 Hz), 3.90-3.85 (m, 1H), 3.10-3.01 (m, 1H), 2.94-2.92 (m, 1H), 2.79-2.68 (m, 3H), 2.65-2.60 (m, 6H), 2.45-2.29 (m, 5H), 2.01-1.93 (m, 3H), 1.73-1.52 (m, 3H), 1.49-1.34 (m, 9H); <sup>13</sup>C NMR [100 MHz, CDCl<sub>3</sub>] δ 156.51, 154.97, 147.50, 136.82, 136.44, 134.24, 132.68, 129.44, 126.23, 125.83, 125.48, 121.80, 80.14, 59.28, 53.73, 50.83, 48.51, 43.27, 39.09, 30.46, 29.13, 28.97, 27.15, 24.03, 21.46.



**(R)-tert-butyl 3-(((4-(1,3-dioxoisindolin-2-yl)butyl)((S)-5,6,7,8-tetrahydroquinolin-8-yl)amino)methyl)-3,4-dihydroisoquinoline-2(1H)-carboxylate (27):** To a solution of **26** (4.1 g, 10.42 mmol) in DCE (75 mL) was added **22** (2.3 g, 10.42 mmol). Sodium triacetoxyborohydride (3.31g, 15.63 mmol) was then added to the mixture in one portion. The reaction was kept at ambient temperature and allowed to stir overnight. The reaction mixture was quenched with saturated NaHCO<sub>3</sub> and the aqueous phase extracted with DCM (2 x 200 mL). The organic extracts were combined, washed with brine, and dried over MgSO<sub>4</sub>. The solvent was removed *in vacuo* yielding a light yellow oil. Crude material was purified by gravity chromatography (120 g silica gel, 1% MeOH in DCM, containing 0.5% NH<sub>4</sub>OH) to afford a light yellow foam (4.9 g, 79.1%). <sup>1</sup>H NMR [600 MHz, CDCl<sub>3</sub>] δ 8.32 (d, 1H, *J* = 16.2 Hz), 7.84-7.81 (m, 2H), 7.71-7.68 (m, 2H), 7.21 (d, 1H, *J* = 7.8 Hz), 7.09-7.06 (m, 3H), 7.01-6.98 (m, 1H), 6.95-6.92 (m, 1H), 4.64 (d, 1H, *J* = 16.8 Hz), 4.12 (d, 1H, *J* = 16.8 Hz), 3.59-3.53 (m, 2H), 2.98-2.91 (m, 2H), 2.78-2.53 (m, 5H), 2.42-2.40 (m, 1H), 2.05-2.01 (m, 2H), 1.93 (bs, 1H), 1.74-1.63 (m, 5H), 1.49 (s, 9H), 1.37-1.33 (m, 2H); <sup>13</sup>C NMR [150 MHz, CDCl<sub>3</sub>] δ 168.36, 158.15, 155.09, 146.83, 136.24, 134.04, 133.82, 133.25, 132.17, 129.42, 128.96, 126.29, 126.09, 125.90, 123.10, 121.29, 79.67, 61.64, 55.31, 51.11, 49.64, 43.16, 37.95, 30.52, 29.12, 28.58, 27.12, 26.35, 21.26; HRMS (ESI) [M+H]<sup>+</sup>, calc'd for C<sub>36</sub>H<sub>43</sub>N<sub>4</sub>O<sub>4</sub> 595.32788, found 595.32697; HPLC/MS purity (> 95%) *r*<sub>t</sub> = 0.633 at 254nm, 75-95% MeOH over 5 minutes.



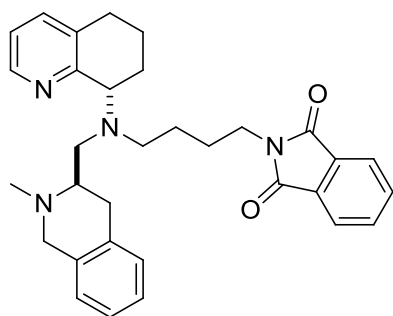
**2-(4-(((R)-1,2,3,4-tetrahydroisoquinolin-3-yl)methyl)((S)-5,6,7,8-tetrahydroquinolin-8-yl)amino)butyl)isoindoline-1,3-dione (29a):** To a solution of (*R*)-*tert*-butyl 3-(((4-(1,3-dioxisoindolin-2-yl)butyl)((*S*)-5,6,7,8-tetrahydroquinolin-8-yl)amino)methyl)-3,4-dihydroisoquinoline-2(1*H*)-carboxylate (1.10 g, 1.85 mmol) (**27**) in DCM (14 mL) was added trifluoroacetic acid TFA (4 mL). The dark purple reaction mixture was kept at ambient temperature and allowed to stir overnight. The reaction mixture was concentrated under reduced pressure and diluted with DCM (20 mL). Saturated NaHCO<sub>3</sub> was added until the reaction mixture pH was adjusted to 11-12. The aqueous phase was extracted with DCM (2 x 20 mL). The organic extracts were combined, washed with brine, and dried over MgSO<sub>4</sub>. The solvent was removed *in vacuo* yield to a yellow oil. Crude material was purified by gravity chromatography (30 g silica, 1% MeOH in DCM to 5% MeOH in DCM) to afford a light yellow amorphous solid (0.870 mg, 95%). <sup>1</sup>H NMR [600 MHz, CDCl<sub>3</sub>] δ 8.35 (d, 1H, *J* = 4.8 Hz), 7.76-7.73 (m, 2H), 7.69-7.67 (m, 2H), 7.37 (d, 1H, *J* = 7.2 Hz) 7.20-7.18 (m, 2H), 7.12-7.06 (m, 3H), 4.51 (d, 1H, *J* = 15.6 Hz), 4.27 (d, 1H, *J* = 15.6 Hz), 4.15 (dd, 1H, *J* = 9.6, 6.0 Hz), 3.56 (dt, 2H, *J* = 7.2, 3.4 Hz), 3.24 (m, 3H), 3.05-3.01 (m, 1H), 2.81-2.71 (m, 4H), 2.69-2.66 (m, 1H), 2.52 (dd, 1H, *J* = 13.8, 7.2), 2.11-2.09 (m, 1H), 1.97-1.94 (m, 1H), 1.82 (dq, 1H, *J* = 12.6, 2.4

Hz), 1.72 (dq, 1H,  $J = 12.6, 2.4$  Hz), 1.61-1.53 (m, 2H), 1.40-1.31 (m, 2H);  $^{13}\text{C}$  NMR [100 MHz,  $\text{CDCl}_3$ ]  $\delta$  168.58, 158.36, 146.36, 137.95, 134.52, 134.15, 123.20, 132.10, 129.35, 127.63, 126.96, 126.73, 123.33, 122.34, 63.68, 56.03, 54.01, 44.56, 37.68, 30.06, 29.28, 27.08, 26.48, 26.18, 21.96; HRMS (ESI)  $[\text{M}+\text{H}]^+$ , calc'd for  $\text{C}_{31}\text{H}_{35}\text{N}_4\text{O}_2$  495.27562, found 495.27545; HPLC/MS purity ( $> 95\%$ )  $r_t = 0.451$  at 254nm, 85% MeOH Isocratic over 3 minutes.

### General procedure of compounds 30-44:

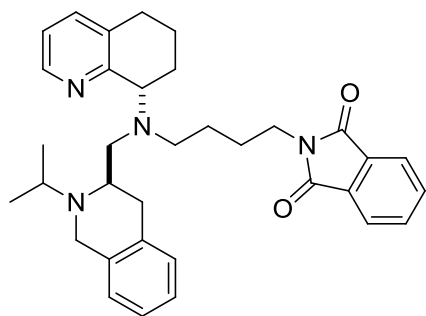
To a solution of 2-(4-(((R-1,2,3,4-tetrahydroisoquinoline-3-yl)methyl((S)-5,6,7,8-tetrahydroquinolin-8-yl)amino)butyl)isoindoline-1,3-dione (**29**) (.300 g, 0.607 mmol) in dichloroethane (DCE) (6.0 mL) was added pyrimidine-5-carbaldehyde (.076 g, 0.708 mmol). To this mixture was added sodium triacetoxyborohydride (0.193 g, 0.910 mmol) in one portion. The reaction was kept at ambient temperature and allowed to stir overnight. The reaction mixture was quenched with  $\text{NaHCO}_3$  and the aqueous phase extracted with DCM (2 x 20.0 mL). The organic layers were combined, washed with brine, and dried over  $\text{MgSO}_4$ . The solvent was removed *in vacuo* yielding a yellow oil. Crude material was purified by gravity chromatography (10 g silica gel, 2% MeOH/DCM) to afford a light yellow foam.

### Physical Data for 30-44:



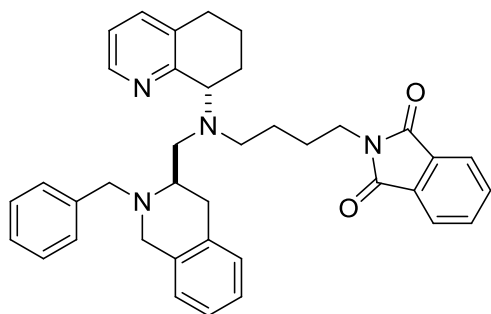
**2-(4-((((R)-2-methyl-1,2,3,4-tetrahydroisoquinolin-3-yl)methyl)((S)-5,6,7,8-tetrahydroquinolin-8-yl)amino)butyl)isoindoline-1,3-dione (30):**

$^1\text{H}$  NMR [600 MHz,  $\text{CDCl}_3$ ]  $\delta$  8.49 (d, 1H,  $J = 4.2$  Hz), 7.28 (d, 1H,  $J = 7.6$  Hz), 7.08-7.06 (m, 2H), 7.01-6.99 (m, 3H), 4.00 (1H, dd,  $J = 7.2, 4.8$  Hz), 3.75 (d, 1H,  $J = 15.6$  Hz), 3.68 (d, 1H,  $J = 15.6$  Hz), 3.09-3.07 (m, 1H), 2.98-2.92 (m, 3H), 2.77-2.70 (m, 3H), 2.65-2.63 (m, 3H), 2.57-2.54 (m, 2H), 2.39 (dd, 1H,  $J = 12, 10.2$  Hz), 2.00-1.99 (m, 2H), 1.87-1.81 (m, 1H), 1.67-1.63 (m, 1H), 1.49-1.38 (m, 5H), 1.15 (d, 3H,  $J = 7.2$  Hz), 1.07 (d, 3H,  $J = 6.0$  Hz);  $^{13}\text{C}$  NMR [150 MHz,  $\text{CDCl}_3$ ]  $\delta$  158.35, 147.51, 136.72, 136.37, 135.70, 134.71, 129.11, 126.39, 126.34, 125.73, 121.80, 61.88, 54.88, 53.56, 52.63, 51.08, 46.72, 42.39, 31.91, 31.18, 29.60, 26.56, 25.12, 21.77, 21.51, 19.57; HRMS (ESI)  $[\text{M}+\text{H}]^+$ , calc'd for  $\text{C}_{32}\text{H}_{36}\text{N}_4\text{O}_2$  508.31772, found 407.31861

**2-(4-((((R)-2-isopropyl-1,2,3,4-tetrahydroisoquinolin-3-yl)methyl)((S)-5,6,7,8-tetrahydroquinolin-8-yl)amino)butyl)isoindoline-1,3-dione (31):**

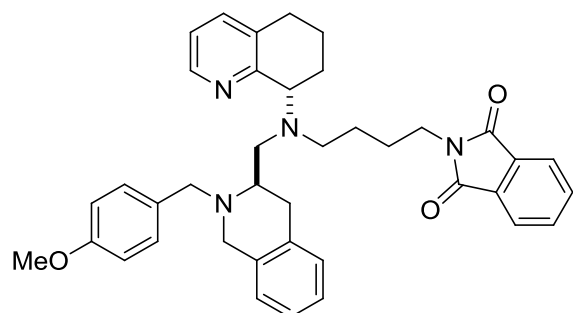
$^1\text{H}$  NMR [600 MHz,  $\text{CDCl}_3$ ]  $\delta$  8.49 (d, 1H,  $J = 4.2$  Hz), 7.28 (d, 1H,  $J = 7.6$  Hz), 7.08-7.06 (m, 2H), 7.01-6.99 (m, 3H), 4.00 (1H, dd,  $J = 7.2, 4.8$  Hz), 3.75 (d, 1H,  $J = 15.6$  Hz), 3.68 (d, 1H,  $J = 15.6$  Hz), 3.09-3.07 (m, 1H), 2.98-2.92 (m, 3H), 2.77-2.70 (m, 3H), 2.65-2.63 (m, 3H), 2.57-2.54 (m, 2H), 2.39 (dd, 1H,  $J = 12, 10.2$  Hz), 2.00-1.99 (m, 2H), 1.87-1.81 (m, 1H), 1.67-1.63 (m, 1H), 1.49-1.38 (m, 5H), 1.15 (d, 3H,  $J = 7.2$  Hz), 1.07 (d, 3H,  $J = 6.0$  Hz);  $^{13}\text{C}$  NMR [150 MHz,  $\text{CDCl}_3$ ]  $\delta$  158.35, 147.51, 136.72, 136.37, 135.70, 134.71, 129.11, 126.39, 126.34, 125.73,

121.80, 61.88, 54.88, 53.56, 52.63, 51.08, 46.72, 42.39, 31.91, 31.18, 29.60, 26.56, 25.12, 21.77, 21.51, 19.57; HRMS (ESI)  $[M+H]^+$ , calc'd for  $C_{34}H_{40}N_4O_2$  536.32692, found 407.31772



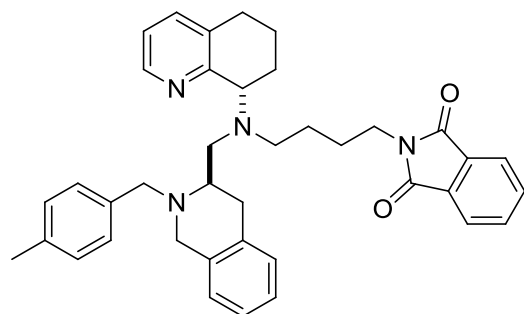
**2-(4-(((R)-2-benzyl-1,2,3,4-tetrahydroisoquinolin-3-yl)methyl)((S)-5,6,7,8-tetrahydroquinolin-8-yl)amino)butylisoindoline-1,3-dione (32):**

$^1H$  NMR [600 MHz,  $CDCl_3$ ]  $\delta$  8.45 (d, 1H,  $J = 4.2$  Hz), 7.84-7.82 (m, 2H), 7.72-7.70 (m, 2H), 7.29-7.24 (m, 3H), 7.16-7.11 (m, 5H), 6.99-6.97 (m, 1H), 6.92-6.90 (d, 1H,  $J = 7.2$  Hz), 4.00-3.98 (m, 1H), 3.73-3.61 (m, 6H), 3.09-3.01 (m, 2H), 2.91-2.88 (m, 2H), 2.77-2.73 (m, 1H), 2.67-2.57 (m, 4H), 2.37 (s, 3H), 2.08-1.99 (m, 2H), 1.85-1.81 (m, 1H), 1.70-1.61 (m, 3H), 1.45-1.42 (m, 2H);  $^{13}C$  NMR [600 MHz,  $CDCl_3$ ]  $\delta$  168.48, 158.17, 147.05, 136.58, 136.45, 136.20, 134.73, 134.63, 134.26, 132.26, 129.40, 129.28, 129.18, 126.48, 126.18, 125.87, 123.39, 121.53, 121.36, 61.67, 57.18, 55.91, 52.54, 51.94, 50.75, 38.02, 29.87, 29.10, 26.31, 25.99, 21.31; HRMS (ESI)  $[M+H]^+$ , calc'd for  $C_{39}H_{43}N_4O_2$ ; 599.33805, found 599.33872



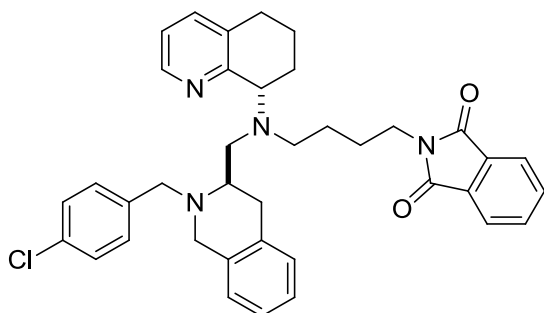
**2-(4-(((R)-2-(4-methoxybenzyl)-1,2,3,4-tetrahydroisoquinolin-3-yl)methyl)((S)-5,6,7,8-tetrahydroquinolin-8-yl)amino)butylisoindoline-1,3-dione (33):**

$^1\text{H NMR}$  [600 MHz,  $\text{CDCl}_3$ ]  $\delta$  8.41 (m, 2H), 8.37 (d, 1H,  $J = 3.6$  Hz), 7.78-7.75 (m, 2H), 7.66-7.64 (m, 2H), 7.21-7.29 (d, 1H,  $J = 7.2$  Hz), 7.07-7.01 (m, 3H), 6.93-6.84 (m, 1H), 6.84-6.83 (m, 1H), 5.25 (s, 2H), 3.97-3.92 (m, 4H), 3.54-3.51 (m, 4H), 3.04-3.01 (m, 1H), 2.93 (dd, 1H,  $J = 11$ , 5.4 Hz), 2.83 (dt, 2H,  $J = 8.4$ , 4.8 Hz), 2.72-2.67 (m, 2H), 2.64-2.61 (m, 2H), 2.59-2.48 (m, 2H), 1.98-1.93 (m, 2H), 1.80-1.75 (m, 1H), 1.65-1.58 (m, 3H), 1.42-1.36 (m, 2H);  $^{13}\text{C NMR}$  [600 MHz,  $\text{CDCl}_3$ ]  $\delta$  168.43, 165.19, 159.71, 158.13, 146.95, 136.58, 134.35, 134.12, 133.82, 132.18, 129.53, 126.51, 126.10, 125.77, 125.50, 121.53, 61.59, 61.59, 56.59, 54.92, 52.96, 52.15, 51.43, 50.14, 37.95, 29.90, 29.19, 26.75, 26.23, 21.11; HRMS (ESI)  $[\text{M}+\text{H}]^+$ , calc'd for  $\text{C}_{34}\text{H}_{41}\text{N}_6$ ; 617.32347, found 617.32231.



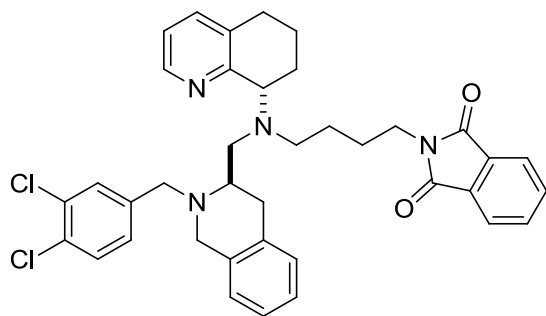
**2-(4-(((R)-2-(4-methylbenzyl)-1,2,3,4-tetrahydroisoquinolin-3-yl)methyl)((S)-5,6,7,8-tetrahydroquinolin-8-yl)amino)butyl)isoindoline-1,3-dione (34):**

$^1\text{H}$  NMR [600 MHz,  $\text{CDCl}_3$ ]  $\delta$  8.45 (d, 1H,  $J = 4.2$  Hz), 7.84-7.82 (m, 2H), 7.72-7.70 (m, 2H), 7.29-7.24 (m, 3H), 7.16-7.11 (m, 5H), 6.99-6.97 (m, 1H), 6.92-6.90 (d, 1H,  $J = 7.2$  Hz), 4.00-3.98 (m, 1H), 3.73-3.61 (m, 6H), 3.09-3.01 (m, 2H), 2.91-2.88 (m, 2H), 2.77-2.73 (m, 1H), 2.67-2.57 (m, 4H), 2.37 (s, 3H), 2.08-1.99 (m, 2H), 1.85-1.81 (m, 1H), 1.70-1.61 (m, 3H), 1.45-1.42 (m, 2H);  $^{13}\text{C}$  NMR [600 MHz,  $\text{CDCl}_3$ ]  $\delta$  168.48, 158.17, 147.05, 136.58, 136.45, 136.20, 134.73, 134.63, 134.26, 132.26, 129.40, 129.28, 129.18, 126.48, 126.18, 125.87, 123.39, 121.53, 121.36, 61.67, 57.18, 55.91, 52.54, 51.94, 50.75, 38.02, 29.87, 29.10, 26.31, 25.99, 21.31; HRMS (ESI)  $[\text{M}+\text{H}]^+$ , calc'd for  $\text{C}_{39}\text{H}_{43}\text{N}_4\text{O}_2$ ; 599.33805, found 599.33872

**2-(4-(((R)-2-(4-chlorobenzyl)-1,2,3,4-tetrahydroisoquinolin-3-yl)methyl)((S)-5,6,7,8-tetrahydroquinolin-8-yl)amino)butyl)isoindoline-1,3-dione (35):**

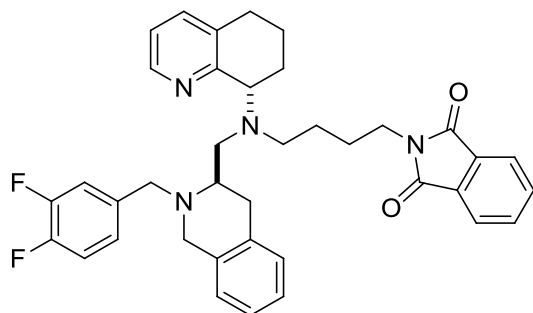
$^1\text{H}$  NMR [600 MHz,  $\text{CDCl}_3$ ]  $\delta$  8.37-8.36 (m, 1H), 7.76-7.73 (m, 2H), 7.67-7.64 (m, 2H), 7.29-7.21 (m, 5H), 7.08-7.03 (m, 3H), 7.02-6.94 (m, 1H), 6.84 (d, 1H, 7.6 Hz), 4.01-3.98 (m, 1H), 3.69-3.63 (m, 4H), 3.57-3.54 (m, 2H), 3.21 (m, 1H), 3.00 (m, 1H), 2.84 (dd, 2H, 12, 4.4 Hz), 2.73-2.58 (m, 4H), 2.01-1.94 (m, 2H), 1.80-1.77 (m, 1H), 1.63-1.55 (m, 3H), 1.43-1.37 (m, 2H);  $^{13}\text{C}$  NMR [600 MHz,  $\text{CDCl}_3$ ]  $\delta$  168.48, 146.99, 136.80, 134.32, 133.99, 132.11, 130.71, 129.50, 128.57, 126.67, 125.86, 123.25, 121.90, 56.44, 56.07, 53.36, 51.93, 50.95, 37.84, 29.07,

26.48, 26.03, 25.58, 21.17; HRMS (ESI)  $[M+H]^+$ , calc'd for  $C_{38}H_{40}N_4O_2Cl$ ; 619.28343, found 619.28301



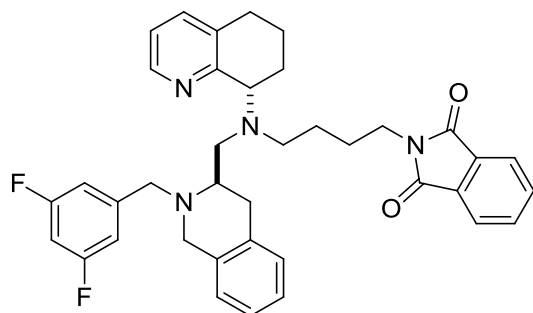
**2-(4-(((R)-2-(3,4-dichlorobenzyl)-1,2,3,4-tetrahydroisoquinolin-3-yl)methyl)((S)-5,6,7,8-tetrahydroquinolin-8-yl)amino)butyl)isoindoline-1,3-dione (38):**

$^1H$  NMR [400 MHz,  $CDCl_3$ ]  $\delta$  8.42-8.44 (m, 1H,  $J = 3.6$  Hz), 7.84-7.81 (m, 2H), 7.31-7.70 (m, 2H), 7.47 (d, 1H,  $J = 1.2$  Hz), 7.37 (d, 1H,  $J = 7.2$  Hz), 7.23 (d, 1H,  $J = 7.2$  Hz), 7.18-7.13 (m, 1H), 7.12-7.09 (m, 3H), 6.99-6.97 (m, 1H), 6.90-6.89 (m, 1H), 3.98-3.97 (m, 1H), 3.68-3.59 (m, 5H), 3.05-2.98 (m, 2H), 2.88-2.85 (m, 2H), 2.77-2.72 (m, 1H), 2.01-1.99 (m, 2H), 1.83-1.79 (m, 1H), 1.70-1.64 (m, 3H), 1.46-1.44 (m, 2H);  $^{13}C$  NMR [400 MHz,  $CDCl_3$ ]  $\delta$  168.58, 147.08, 140.67, 136.71, 136.31, 134.31, 134.82, 134.44, 132.39, 128.23, 126.58, 125.55, 123.13, 121.49, 66.05, 61.77, 56.37, 53.14, 51.92, 50.87, 38.08, 30.04, 29.15, 26.65, 21.35, 15.63 HRMS (ESI)  $[M+H]^+$ , calc'd for  $C_{38}H_{39}N_4O_2$ ; 653.24446, found 653.24375



**2-(4-(((R)-2-(3,4-difluorobenzyl)-1,2,3,4-tetrahydroisoquinolin-3-yl)methyl)((S)-5,6,7,8-tetrahydroquinolin-8-yl)amino)butyl)isoindoline-1,3-dione (39):**

$^1\text{H}$  NMR [400 MHz,  $\text{CDCl}_3$ ]  $\delta$  8.41-8.39 (m, 1H), 7.81-7.87 (m, 2H), 7.71-7.67 (m, 2H), 7.22-7.16 (m, 2H), 7.09-7.03 (m, 5H), 6.97-6.94 (m, 1H), 6.88-6.86 (d, 1H,  $J = 6.8$  Hz), 3.97-3.93 (m, 1H), 3.68-3.55 (m, 6H), 3.03-2.91 (m, 2H), 2.86-2.82 (m, 2H), 2.72-2.52 (m, 5H), 1.99-1.95 (m, 2H), 1.80-1.78 (m, 1H), 1.66-1.59 (m, 3H), 1.42-1.39 (m, 2H);  $^{13}\text{C}$  NMR [400 MHz,  $\text{CDCl}_3$ ]  $\delta$  169.65, 162.51, 159.11, 147.01, 137.22, 134.46, 134.11, 133.58, 132.23, 129.60, 126.82, 126.16, 123.36, 122.29, 120.93, 61.59, 55.81, 53.84, 51.96, 51.65, 50.73, 49.59, 37.81, 28.99, 28.56, 26.51, 25.91, 25.17, 21.14; HRMS (ESI)  $[\text{M}+\text{H}]^+$ , calc'd for  $\text{C}_{38}\text{H}_{39}\text{N}_4\text{O}_2\text{F}_2$ ; 621.30356, found 621.30371.

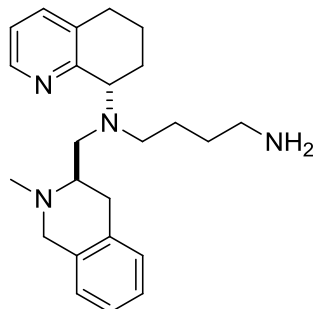


**2-(4-(((R)-2-(3,5-difluorobenzyl)-1,2,3,4-tetrahydroisoquinolin-3-yl)methyl)((S)-5,6,7,8-tetrahydroquinolin-8-yl)amino)butyl)isoindoline-1,3-dione (40):**

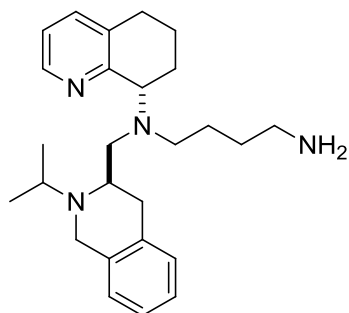
$^1\text{H}$  NMR [600 MHz,  $\text{CDCl}_3$ ]  $\delta$  8.43-8.42 (m, 1H), 7.84-7.81 (m, 2H), 7.30-7.00 (m, 2H), 7.29-7.24 (m, 1H), 7.12-7.07 (m, 3H), 6.99-6.89 (m, 1H), 6.93-6.89, 6.67 (tt, 1H,  $J = 2.8, 2.4$  Hz) 3.99-3.96 (m, 1H), 3.74-3.59 (m, 6H), 3.06-2.98 (m, 2H), 2.88-2.85 (m, 2H), 2.74-2.55 (m, 5H), 2.07-2.98 (m, 2H), 1.83-1.82 (m, 1H), 1.70-1.62 (m, 3H), 1.47-1.41 (m, 2H);  $^{13}\text{C}$  NMR [400 MHz,  $\text{CDCl}_3$ ]  $\delta$  168.57, 164.47, 162.00, 158.19, 147.05, 144.68, 136.52, 134.50, 134.00, 132.30, 129.54, 126.54, 126.58, 126.27, 125.65, 123.30, 121.57, 111.16, 102.26, 61.74, 56.87, 56.55, 53.05, 52.10, 50.91, 38.06, 30.06, 29.28, 26.63, 26.32, 21.21 HRMS (ESI)  $[\text{M}+\text{H}]^+$ , calc'd for  $\text{C}_{38}\text{H}_{39}\text{N}_4\text{O}_2\text{F}_2$ ; 621.30356, found 621.30337

#### General procedure of compounds 45-59:

To a solution of 2-(4-(((*R*)-2-(pyridin-2-ylmethyl)-1,2,3,4-tetrahydroisoquinolin-3-yl)methyl)((*S*)-5,6,7,8-tetrahydroquinolin-8-yl)amino)butyl)isoindoline-1,3-dione (1.2 g, 2.02 mmol) in methanol (20 mL) was added hydrazine (2.11 mL, 16.14 mmol) 24% in water. The reaction was allowed to proceed at ambient temperature overnight. The methanol was removed under rotary evaporation. To the oily residue was added  $\text{H}_2\text{O}$  (50 mL) and extracted with DCM (3 x 25 mL). The organic layer was washed once with 1N NaOH (50 mL) and the aqueous layer discarded. The organic layer was extracted with 1N HCl (2 x 50 mL) and the aqueous layers combined. The organic layer was discarded. The aqueous layer was made basic in cold with excess 1N NaOH (pH 13-14). The above solution was extracted with DCM (3 x 50 mL). The organic extracts were combined, dried over  $\text{MgSO}_4$  and concentrated under reduced pressure to yield a yellow oil. Crude material was purified by gravity chromatography (5% DCM/MeOH; 7% DCM/MeOH; 10% DCM/MeOH with 1%  $\text{NH}_4\text{OH}$ ) to afford a yellow amorphous foam (1.2 g, 77% yield).

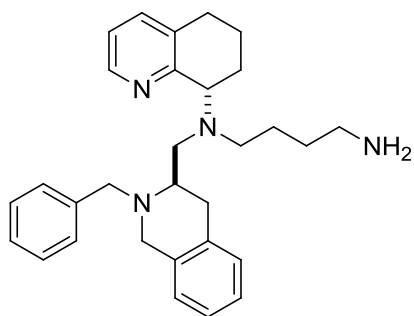
**Physical Data for 45-59:****N1-(((R)-2-methyl-1,2,3,4-tetrahydroisoquinolin-3-yl)methyl)-N1-((S)-5,6,7,8-tetrahydroquinolin-8-yl)butane-1,4-diamine (45):**

$^1\text{H}$  NMR [600 MHz,  $\text{CDCl}_3$ ]  $\delta$  8.46 (dd, 1H,  $J = 4.2$  Hz), 7.28-7.26 (m, 1H), 7.08-7.04 (m, 3H), 7.00-6.98 (m, 1H), 6.95-6.94 (m, 1H), 4.02 (dd, 1H,  $J = 8.7, 5.1$  Hz), 3.71 (d, 1H,  $J = 16.2$  Hz), 3.63 (d, 1H,  $J = 16.2$  Hz), 2.99 -2.96 (1H, m), 2.88 (1H, dd,  $J = 13.2, 3.6$  Hz), 2.77-2.68 (m, 4H), 2.66-2.60 (m, 3H), 2.58-2.50 (m, 2H), 2.46-2.42 (dd, 1H  $J = 12.6, 9.2$  Hz), 2.37-2.5 (m, 3H), 2.00-1.99 (m, 2H), 1.87-1.81 (m, 1H), 1.67-1.63 (m, 1H), 1.49-1.38 (m, 5H);  $^{13}\text{C}$  NMR [150 MHz,  $\text{CDCl}_3$ ]  $\delta$  157.97, 146.98, 136.32, 134.34, 134.22, 134.17, 129.00, 126.12, 125.93, 125.36, 121.40, 61.56, 57.84, 55.65, 53.49, 52.53, 42.14, 40.92, 31.71, 30.73, 29.15, 26.15, 25.27, 20.98; HRMS (ESI)  $[\text{M}+\text{H}]^+$ , calc'd for  $\text{C}_{24}\text{H}_{35}\text{N}_4$  379.28562, found 379.28576; HPLC/MS purity (> 95%)  $r_t = 0.606$  at 254nm, 85% MeOH Isocratic over 3 minutes.



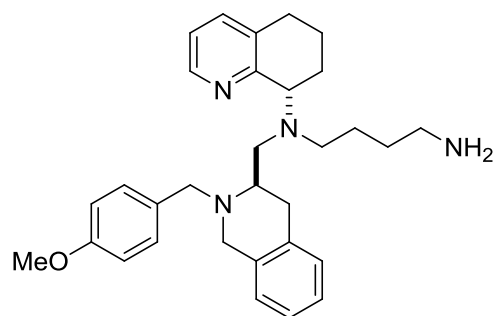
**N1-(((R)-2-isopropyl-1,2,3,4-tetrahydroisoquinolin-3-yl)methyl)-N1-((S)-5,6,7,8-tetrahydroquinolin-8-yl)butane-1,4-diamine (46):**

$^1\text{H}$  NMR [600 MHz,  $\text{CDCl}_3$ ]  $\delta$  8.49 (d, 1H,  $J = 4.2$  Hz), 7.28 (d, 1H,  $J = 7.6$  Hz), 7.08-7.06 (m, 2H), 7.01-6.99 (m, 3H), 4.00 (1H, dd,  $J = 7.2, 4.8$  Hz), 3.75 (d, 1H,  $J = 15.6$  Hz), 3.68 (d, 1H,  $J = 15.6$  Hz), 3.09-3.07 (m, 1H), 2.98-2.92 (m, 3H), 2.77-2.70 (m, 3H), 2.65-2.63 (m, 3H), 2.57-2.54 (m, 2H), 2.39 (dd, 1H,  $J = 12, 10.2$  Hz), 2.00-1.99 (m, 2H), 1.87-1.81 (m, 1H), 1.67-1.63 (m, 1H), 1.49-1.38 (m, 5H), 1.15 (d, 3H,  $J = 7.2$  Hz), 1.07 (d, 3H,  $J = 6.0$  Hz);  $^{13}\text{C}$  NMR [150 MHz,  $\text{CDCl}_3$ ]  $\delta$  158.35, 147.51, 136.72, 136.37, 135.70, 134.71, 129.11, 126.39, 126.34, 125.73, 121.80, 61.88, 54.88, 53.56, 52.63, 51.08, 46.72, 42.39, 31.91, 31.18, 29.60, 26.56, 25.12, 21.77, 21.51, 19.57; HRMS (ESI)  $[\text{M}+\text{H}]^+$ , calc'd for  $\text{C}_{26}\text{H}_{39}\text{N}_4$  407.31692, found 407.31772; HPLC/MS purity ( $> 95\%$ )  $r_t = 0.405$  at 254nm, 75-95% MeOH over 3 minutes.



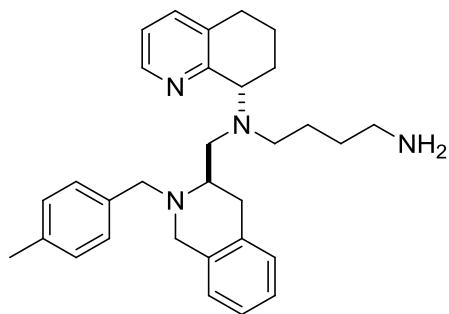
**N1-(((R)-2-benzyl-1,2,3,4-tetrahydroisoquinolin-3-yl)methyl)-N1-((S)-5,6,7,8-tetrahydroquinolin-8-yl)butane-1,4-diamine (47):**

$^1\text{H}$  NMR [600 MHz,  $\text{CDCl}_3$ ]  $\delta$  8.46 (d, 1H,  $J = 3.6$  Hz), 7.29-7.25 (m, 5H), 7.10-7.05 (m, 3H), 6.99-6.97 (m, 1H), 6.84 (d, 1H, 7.2 Hz), 4.01-3.97 (m, 1H), 3.69-3.63 (m, 4H), 3.70-3.60 (m, 5H), 3.04-2.96 (m, 2H), 2.86-2.81 (m, 2H), 2.74-2.69 (m, 1H), 2.65-2.59 (m, 3H), 2.54-2.50 (m, 2H), 2.21-2.12 (m, 2H), 2.00-1.95 (m, 2H), 1.81-1.77 (m, 1H), 1.65-1.61 (m, 1H) 1.42-1.34 (m, 4H);  $^{13}\text{C}$  NMR [600 MHz,  $\text{CDCl}_3$ ]  $\delta$  158.37, 147.35, 138.62, 136.92, 136.54, 134.79, 132.78, 130.71, 129.58, 128.48, 126.73, 125.94, 121.90, 61.82, 57.14, 56.12, 53.07, 51.15, 50.95, 42.35, 31.81, 29.07, 26.48, 25.58, 21.36; HRMS (ESI)  $[\text{M}+\text{H}]^+$ , calc'd for  $\text{C}_{30}\text{H}_{39}\text{N}_4$ ; 489.27795, found 489.27772; HPLC/MS purity ( $> 95\%$ )  $r_t = 0.425$  at 254nM, 75-95% MeOH over 3 minutes.



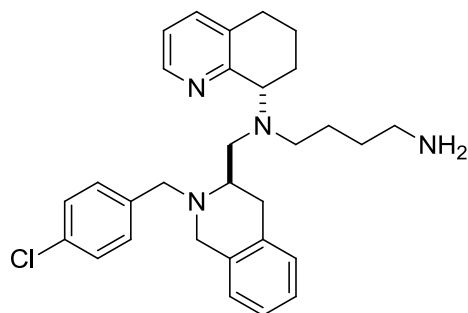
**N1-(((R)-2-(4-methoxybenzyl)-1,2,3,4-tetrahydroisoquinolin-3-yl)methyl)-N1-((S)-5,6,7,8-tetrahydroquinolin-8-yl)butane-1,4-diamine (48):**

$^1\text{H}$  NMR [400 MHz,  $\text{CDCl}_3$ ]  $\delta$  8.44-8.42 (m, 3H), 7.28-7.25 (m, 1H), 7.11-7.06 (m, 3H), 7.04-6.98 (m, 1H), 6.96-6.87 (m, 1H), 3.98-3.97 (m, 4H), 3.67-3.57 (m, 4H), 3.05-2.92 (m, 2H), 2.86-2.80 (m, 2H) 2.72-2.66 (m, 2H), 2.66-2.65 (m, 2H), 2.61-2.60 (m, 2H), 2.58-2.51 (m, 2H), 2.03-1.94 (m, 2H), 1.85-1.77 (m, 3H), 1.66-1.61 (m, 1H), 1.44-1.33 (m, 4H); NMR [400 MHz,  $\text{CDCl}_3$ ]  $\delta$  165.27, 159.79, 158.16, 147.08, 136.52, 134.36, 133.82, 129.46, 126.58, 126.31, 125.95, 125.73, 121.55, 61.51, 56.19, 55.01, 54.98, 52.84, 52.49, 52.55, 50.59, 42.21, 31.73, 29.65, 29.26, 26.31, 26.01, 21.19; HRMS (ESI)  $[\text{M}+\text{H}]^+$ , calc'd for  $\text{C}_{34}\text{H}_{41}\text{N}_6$ ; 484.33534, found 484.33565; HPLC/MS purity ( $> 95\%$ )  $r_t = 0.529$  at 254nM, 75-95% MeOH over 3 minutes.



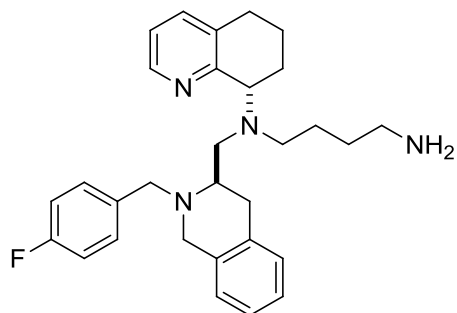
**N1-(((R)-2-(4-methylbenzyl)-1,2,3,4-tetrahydroisoquinolin-3-yl)methyl)-N1-((S)-5,6,7,8-tetrahydroquinolin-8-yl)butane-1,4-diamine (49):**

$^1\text{H}$  NMR [400 MHz,  $\text{CDCl}_3$ ]  $\delta$  8.49-8.48 (m, 1H), 7.29-7.24 (m, 3H), 7.14-7.07 (m, 5H), 7.06-7.00 (m, 1H), 6.92-6.90 (d, 1H,  $J = 7.2$  Hz), 4.03-3.99 (m, 1H), 3.73-3.63 (m, 5H), 3.09-3.03 (m, 2H), 2.89-2.84 (m, 2H), 2.75-2.67 (m, 2H), 2.62-2.59 (m, 2H), 2.57-2.51 (m, 3H), 2.35 (s, 3H), 2.04-1.96 (m, 2H), 1.87-1.78 (m, 2H), 1.67-1.63 (m, 1H), 1.45-1.36 (m, 4H);  $^{13}\text{C}$  NMR [400 MHz,  $\text{CDCl}_3$ ]  $\delta$  158.26, 147.99, 136.64, 136.53, 136.48, 1134.78, 134.66, 134.37, 129.49, 129.06, 128.89, 126.60, 126.05, 125.51, 121.52, 61.60, 57.14, 55.82, 55.56, 52.44, 50.89, 42.24, 31.79, 29.81, 29.36, 26.33, 25.42, 21.28; HRMS (ESI)  $[\text{M}+\text{H}]^+$ , calc'd for  $\text{C}_{31}\text{H}_{41}\text{N}_4$ ; 469.33257, found 469.33323



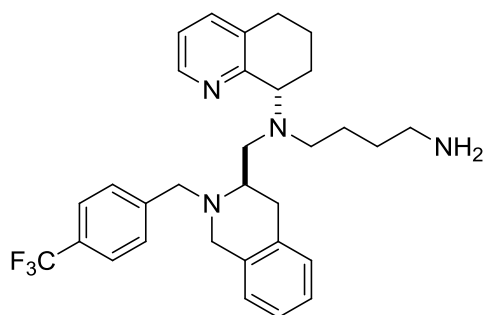
**N1-(((R)-2-(4-chlorobenzyl)-1,2,3,4-tetrahydroisoquinolin-3-yl)methyl)-N1-((S)-5,6,7,8-tetrahydroquinolin-8-yl)butane-1,4-diamine (50):**

$^1\text{H}$  NMR [600 MHz,  $\text{CDCl}_3$ ]  $\delta$  8.46 (d, 1H,  $J = 3.6$  Hz), 7.29-7.25 (m, 5H), 7.10-7.05 (m, 3H), 6.99-6.97 (m, 1H), 6.84 (d, 1H, 7.2 Hz), 4.01-3.97 (m, 1H), 3.69-3.63 (m, 4H), 3.70-3.60 (m, 5H), 3.04-2.96 (m, 2H), 2.86-2.81 (m, 2H), 2.74-2.69 (m, 1H), 2.65-2.59 (m, 3H), 2.54-2.50 (m, 2H), 2.21-2.12 (m, 2H), 2.00-1.95 (m, 2H), 1.81-1.77 (m, 1H), 1.65-1.61 (m, 1H), 1.42-1.34 (m, 4H);  $^{13}\text{C}$  NMR [600 MHz,  $\text{CDCl}_3$ ]  $\delta$  158.37, 147.35, 138.62, 136.92, 136.54, 134.79, 132.78, 130.71, 129.58, 128.48, 126.73, 125.94, 121.90, 61.82, 57.14, 56.12, 53.07, 51.15, 50.95, 42.35, 31.81, 29.07, 26.48, 25.58, 21.36; HRMS (ESI)  $[\text{M}+\text{H}]^+$ , calc'd for  $\text{C}_{30}\text{H}_{38}\text{N}_4\text{Cl}$ ; 489.27795, found 489.27772; HPLC/MS purity ( $> 95\%$ )  $r_t = 0.872$  at 254nM, 75-95% MeOH over 3 minutes.



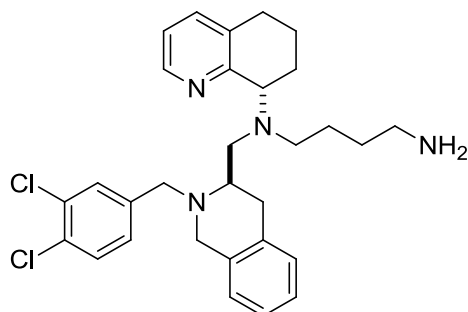
**N1-(((R)-2-(4-fluorobenzyl)-1,2,3,4-tetrahydroisoquinolin-3-yl)methyl)-N1-((S)-5,6,7,8-tetrahydroquinolin-8-yl)butane-1,4-diamine (51):**

$^1\text{H}$  NMR [400 MHz,  $\text{CDCl}_3$ ]  $\delta$  8.44 (d, 1H,  $J = 4.8$  Hz), 7.64-7.62 (m, 1H), 7.50-7.41 (m, 4H), 7.21-7.15 (m, 4H), 6.98-6.96 (m, 1H), 4.01-3.99 (m, 1H), 3.84 (q, 2H,  $J = 14$  Hz), 3.64 (q, 2H,  $J = 14$  Hz), 3.08-3.06 (m, 1H), 2.96-2.94 (m, 1H), 2.87-2.81 (m, 2H), 2.71-2.61 (m, 5H), 2.60-2.54 (m, 2H), 1.98-1.95 (m, 2H), 1.82-1.79 (m, 1H), 1.71-1.79 (m, 1H), 1.43-1.39 (m, 4H);  $^{13}\text{C}$  NMR [100 MHz,  $\text{CDCl}_3$ ]  $\delta$  158.13, 158.00, 155.79, 155.43, 146.99, 136.54, 135.85, 134.26, 134.21, 134.06, 133.29, 129.44, 126.55, 126.41, 125.85, 121.58, 121/16, 118.43, 61.41, 56.56, 53.22, 52.43, 51.77, 51.00, 41.99, 31.42, 29.70, 29.15, 26.13, 21.21 ; HRMS (ESI)  $[\text{M}+\text{H}]^+$ , calc'd for  $\text{C}_{31}\text{H}_{38}\text{N}_3\text{F}$  522.28761, found 522.28753; HPLC/MS purity ( $> 95\%$ )  $r_t = 0.586$  at 254nM, 75-95% MeOH over 3 minutes.



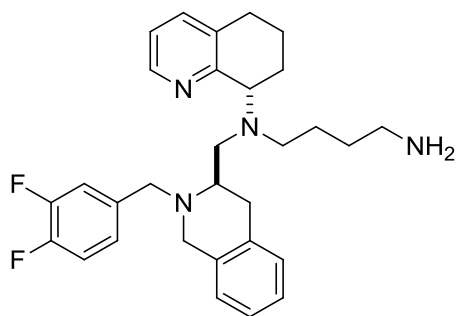
**N1-((S)-5,6,7,8-tetrahydroquinolin-8-yl)-N1-(((R)-2-(4-(trifluoromethyl)benzyl)-1,2,3,4-tetrahydroisoquinolin-3-yl)methyl)butane-1,4-diamine (52):**

$^1\text{H}$  NMR [400 MHz,  $\text{CDCl}_3$ ]  $\delta$  8.44 (d, 1H,  $J = 4.8$  Hz), 7.64-7.62 (m, 1H), 7.50-7.41 (m, 4H), 7.21-7.15 (m, 4H), 6.98-6.96 (m, 1H), 4.01-3.99 (m, 1H), 3.84 (q, 2H,  $J = 14$  Hz), 3.64 (q, 2H,  $J = 14$  Hz), 3.08-3.06 (m, 1H), 2.96-2.94 (m, 1H), 2.87-2.81 (m, 2H), 2.71-2.61 (m, 5H), 2.60-2.54 (m, 2H), 1.98-1.95 (m, 2H), 1.82-1.79 (m, 1H), 1.71-1.79 (m, 1H), 1.43-1.39 (m, 4H);  $^{13}\text{C}$  NMR [100 MHz,  $\text{CDCl}_3$ ]  $\delta$  158.13, 158.00, 155.79, 155.43, 146.99, 136.54, 135.85, 134.26, 134.21, 134.06, 133.29, 129.44, 126.55, 126.41, 125.85, 121.58, 121/16, 118.43, 61.41, 56.56, 53.22, 52.43, 51.77, 51.00, 41.99, 31.42, 29.70, 29.15, 26.13, 21.21 ; HRMS (ESI)  $[\text{M}+\text{H}]^+$ , calc'd for  $\text{C}_{31}\text{H}_{38}\text{N}_3\text{F}_4$  524.29134, found 529.30135; HPLC/MS purity ( $> 95\%$ )  $r_t = 0.586$  at 254nM, 75-95% MeOH over 3 minutes.

**N1-(((R)-2-(3,4-dichlorobenzyl)-1,2,3,4-tetrahydroisoquinolin-3-yl)methyl)-N1-((S)-5,6,7,8-tetrahydroquinolin-8-yl)butane-1,4-diamine (53):**

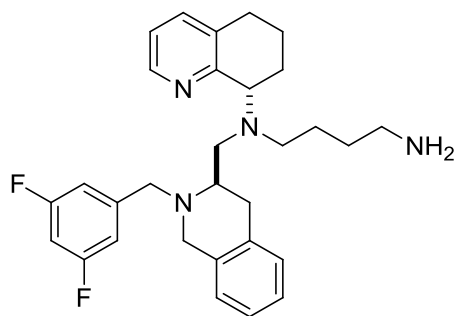
$^1\text{H}$  NMR [400 MHz,  $\text{CDCl}_3$ ]  $\delta$  8.65 (d, 1H,  $J = 4.2$  Hz), 6.67 (s, 1H), 7.55 (d, 1H,  $J = 7.8$  Hz), 7.46 (d, 1H,  $J = 7.8$  Hz), 7.46 (d, 1H,  $J = 7.8$  Hz), 7.36 (d, 1H,  $J = 7.37$  Hz), 7.31-7.25 (m, 3H), 7.19 (t, 1H,  $J = 6.6$  Hz), 7.10 (d, 1H,  $J = 6.6$  Hz), 4.20-4.18 (m, 1H), 3.83 (q, 5H,  $J = 21, 15$  Hz), 3.21-3.16 (m, 2H), 3.06-3.01 (m, 2H), 2.95-2.90 (m, 1H), 2.85-2.79 (m, 3H), 2.76-2.72 (m, 3H), 2.18 (m, 2H), 2.03-1.98 (m, 3H), 1.87-1.83 (m, 1H), 1.61-1.57 (m, 4H); NMR [600 MHz,

$\text{CDCl}_3$ ]  $\delta$  158.45, 147.35, 140.82, 136.94, 136.61, 132.64, 130.92, 130.59, 129.88, 128.42, 126.62, 126.03, 121.89, 61.81, 56.46, 52.84, 51.28, 42.49, 32.01, 30.10, 29.54, 21.18, 15.61; HRMS (ESI)  $[\text{M}+\text{H}]^+$ , calc'd for  $\text{C}_{30}\text{H}_{37}\text{N}_4\text{Cl}_2$ ; 523.23996, found 523.23996; HPLC/MS purity ( $> 95\%$ )  $r_t = 0.768$  at 254nM, 75-95% MeOH over 3 minutes



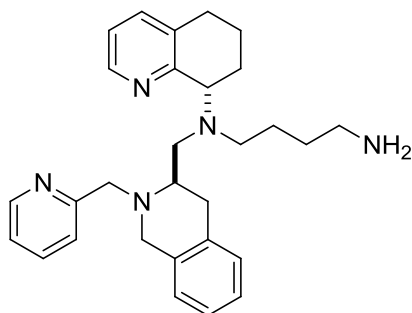
**N1-(((R)-2-(3,4-difluorobenzyl)-1,2,3,4-tetrahydroisoquinolin-3-yl)methyl)-N1-((S)-5,6,7,8-tetrahydroquinolin-8-yl)butane-1,4-diamine (54):**

$^1\text{H}$  NMR [400 MHz,  $\text{CDCl}_3$ ]  $\delta$  8.45-8.44 (m, 1H), 7.23-7.18 (m, 2H), 7.11-7.00 (m, 5H), 6.98-6.97 (m, 1H), 6.89-6.87 (m, 1H), 4.00-3.96 (m, 1H), 3.68-3.57 (m, 4H), 3.03-2.94 (m, 2H), 2.86-2.80 (m, 2H), 2.75-2.65 (m, 2H), 2.61-2.58 (m, 3H), 2.54-2.50 (m, 2H), 2.01-1.94 (m, 2H), 1.84-1.75 (m, 1H), 1.68-1.59 (m, 3H), 1.43-1.33 (m, 4H);  $^{13}\text{C}$  NMR [400 MHz,  $\text{CDCl}_3$ ]  $\delta$  169.65, 162.51, 159.11, 147.01, 137.22, 134.46, 134.11, 133.58, 132.23, 129.60, 126.82, 126.16, 123.36, 122.29, 120.93, 61.59, 55.81, 53.84, 51.96, 51.65, 50.73, 49.59, 37.81, 28.99, 28.56, 26.51, 25.91, 25.17, 21.14; HRMS (ESI)  $[\text{M}+\text{H}]^+$ , calc'd for  $\text{C}_{30}\text{H}_{37}\text{N}_4\text{F}_2$ ; 491.29808, found 491.29847; HPLC/MS purity ( $> 95\%$ )  $r_t = 0.752$  at 254nM, 75% MeOH over 3 minutes.



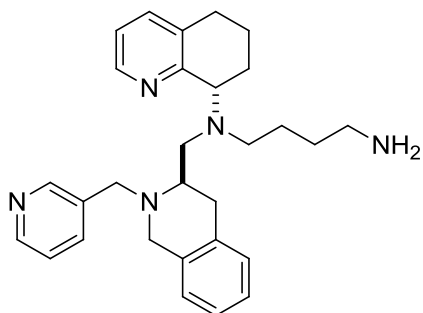
**N1-(((R)-2-(3,5-difluorobenzyl)-1,2,3,4-tetrahydroisoquinolin-3-yl)methyl)-N1-((S)-5,6,7,8-tetrahydroquinolin-8-yl)butane-1,4-diamine (55):**

$^1\text{H}$  NMR [600 MHz,  $\text{CDCl}_3$ ]  $\delta$  8.43 (d, 1H), 7.25-7.18 (m, 2H), 7.11-7.07 (m, 3H), 7.00-6.97 (m, 1H), 6.98-6.88 (m, 3H), 6.61 (tt, 1H,  $J = 2.8, 2.4$  Hz), 4.00-3.97 (m, 1H), 3.72-3.59 (m, 4H), 3.04-2.94 (m, 2H), 2.85-2.78 (m, 2H), 2.71-2.68 (m, 1H), 2.66-2.59 (m, 3H), 2.55-2.50 (m, 3H), 2.16-2.04 (m, 2H), 2.01-1.94 (m, 2H), 1.84-1.76 (m, 1H), 1.66-1.61 (m, 1H), 1.44-1.35 (m, 4H);  $^{13}\text{C}$  NMR [400 MHz,  $\text{CDCl}_3$ ]  $\delta$  164.50, 162.03, 158.15, 147.15, 144.63, 136.60, 134.41, 129.57, 126.60, 126.27, 125.69, 121.62, 111.07, 102.30, 61.45, 56.74, 56.17, 52.68, 52.44, 51.05, 42.14, 31.63, 29.91, 29.31, 26.24, 25.67, 21.21; HRMS (ESI)  $[\text{M}+\text{H}]^+$ , calc'd for  $\text{C}_{30}\text{H}_{36}\text{N}_4\text{F}_2$ ; 491.29808, found 491.29849; HPLC/MS purity ( $> 95\%$ )  $r_t = 0.652$  at 254nM, 75% MeOH over 3 minutes.



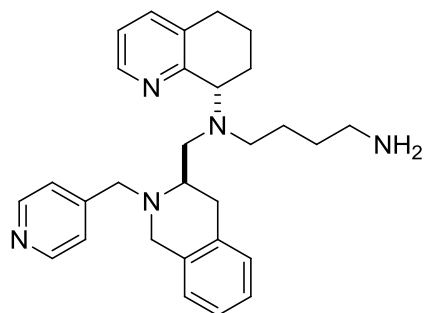
**N1-(((R)-2-(pyridin-2-ylmethyl)-1,2,3,4-tetrahydroisoquinolin-3-yl)methyl)-N1-((S)-5,6,7,8-tetrahydroquinolin-8-yl)butane-1,4-diamine (56):**

Physical data for **23**:  $^1\text{H}$  NMR [400 MHz,  $\text{CDCl}_3$ ]  $\delta$  8.48 (d, 1H,  $J = 4.2$  Hz), 8.28 (d, 1H,  $J = 4.2$  Hz), 7.64-7.62 (m, 1H), 7.51-7.49 (m, 1H), 7.29 (d, 1H,  $J = 6.6$  Hz), 7.17-7.08 (m, 4H), 6.99 (q, 1H, 4.8 Hz), 6.92 (d, 1H,  $J = 7.2$  Hz), 3.99 (dd, 1H,  $J = 9.6, 6.0$ ), 3.84-3.82 (m, 2H), 3.73 (d, 1H,  $J = 16.4$  Hz), 3.64 (d, 1H,  $J = 16.4$  Hz), 2.98 (dd, 1H,  $J = 16.8, 4.8$ ), 2.85-2.77 (m, 2H), 2.74-2.60 (m, 5H), 2.49 (t, 1H,  $J = 6.6$  Hz), 2.38 (dd, 1H,  $J = 13.6, 9.6$  Hz), 2.01 (t, 2H,  $J = 6.6$  Hz), 1.93-1.90 (m, 1H), 1.72-1.61 (m, 3H), 1.50-1.36 (m, 5H);  $^{13}\text{C}$  NMR [150 MHz,  $\text{CDCl}_3$ ]  $\delta$  168.67, 157.14, 149.06, 146.65, 136.47, 136.3, 133.87, 129.29, 126.52, 126.02, 125.15, 122.87, 121.88, 121.32, 60.95, 55.95, 52.96, 52.51, 51.41, 41.95, 31.81, 29.21, 26.82, 26.56, 25.82, 21.65; HRMS (ESI)  $[\text{M}+\text{H}]^+$ , calc'd for  $\text{C}_{29}\text{H}_{38}\text{N}_5$  456.31217, found 456.31272; HPLC/MS purity (> 95%)  $r_t = 0.475$  at 254nm, 50-95% MeOH over 3 minutes.



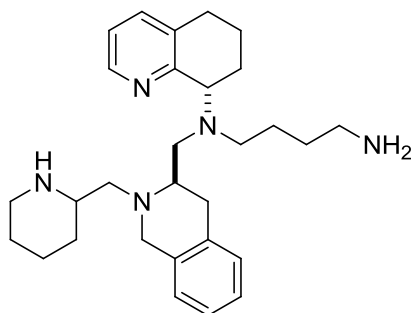
**N1-(((R)-2-(pyridin-3-ylmethyl)-1,2,3,4-tetrahydroisoquinolin-3-yl)methyl)-N1-((S)-5,6,7,8-tetrahydroquinolin-8-yl)butane-1,4-diamine (57):**

$^1\text{H}$  NMR (400 MHz,  $\text{CDCl}_3$ )  $\delta$  8.55-8.39 (m, 3H), 7.66 (dt, 1H,  $J = 7.9, 2.0$  Hz), 7.19 (dd, 2H,  $J = 7.7, 5.0$  Hz), 7.05-6.91 (m, 4H), 6.84 – 6.79 (m, 1H), 3.99 (dd, 1H,  $J = 8.8, 5.6$  Hz), 3.73-3.52 (m, 5H), 3.08-2.89 (m, 2H), 2.77-2.42 (m, 8H), 2.00-1.85 (m, 2H), 1.76-1.50 (m, 2H), 1.49-1.33 (m, 5H);  $^{13}\text{C}$  NMR (100 MHz,  $\text{CDCl}_3$ )  $\delta$  157.79, 150.33, 148.64, 147.33, 136.68, 136.66, 135.24, 134.40, 134.28, 134.03, 129.61, 126.56, 126.27, 125.70, 123.57, 121.70, 61.20, 56.03, 54.77, 52.79, 52.30, 50.68, 41.46, 30.63, 29.79, 29.31, 25.92, 24.77, 21.37; HRMS (ESI)  $[\text{M}+\text{H}]^+$ , calc'd for  $\text{C}_{29}\text{H}_{38}\text{N}_5$  456.31217; found 415.31161  $[\text{M}+\text{H}]$ ; HPLC/MS purity (>95%)  $r_t = 0.894$  at 254 nm, 75% MeOH Isocratic over 3 minutes.



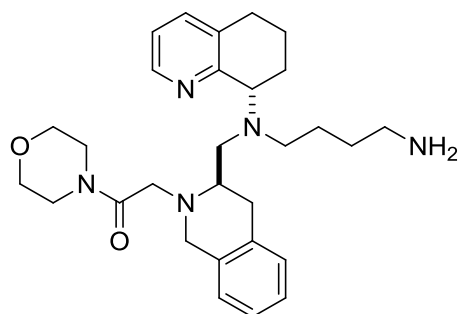
**N1-(((R)-2-(pyridin-4-ylmethyl)-1,2,3,4-tetrahydroisoquinolin-3-yl)methyl)-N1-((S)-5,6,7,8-tetrahydroquinolin-8-yl)butane-1,4-diamine (58):**

$^1\text{H}$  NMR (400 MHz,  $\text{CDCl}_3$ )  $\delta$  8.50-8.47 (m, 2H), 8.43 (dd, 1H,  $J = 4.7, 1.7$  Hz), 7.28-7.25 (m, 2H), 7.23 (dd, 1H,  $J = 7.4, 1.5$  Hz), 7.09-7.01 (m, 3H), 6.96 (dd, 1H,  $J = 7.6, 4.7$  Hz), 6.86 (dd, 1H,  $J = 7.5, 1.7$  Hz), 3.97 (dd, 1H,  $J = 8.8, 5.2$  Hz), 3.78-3.56 (m, 5H), 3.02-2.91 (m, 2H), 2.82 (ddd, 2H,  $J = 16.9, 8.7, 3.9$  Hz), 2.71-2.48 (m, 6H), 1.99-1.87 (m, 2H), 1.83-1.71 (m, 1H), 1.66-1.56 (m, 1H), 1.47-1.14 (m, 5H);  $^{13}\text{C}$  NMR (100 MHz,  $\text{CDCl}_3$ )  $\delta$  158.18, 149.90, 149.50, 147.18, 136.58, 134.46, 134.38, 134.16, 129.57, 126.59, 126.31, 125.71, 123.71, 121.63, 61.56, 56.40, 52.91, 52.55, 51.27, 42.18, 31.66, 29.99, 29.32, 26.31, 25.82, 21.24; HRMS (ESI)  $[\text{M}+\text{H}]^+$ , calc'd for  $\text{C}_{29}\text{H}_{38}\text{N}_5$  456.31217; found 456.31174; HPLC/MS purity (>95%)  $r_t = 0.861$  at 254 nm, 75% MeOH Isocratic.



**N1-(((3R)-2-(piperidin-2-ylmethyl)-1,2,3,4-tetrahydroisoquinolin-3-yl)methyl)-N1-((S)-5,6,7,8-tetrahydroquinolin-8-yl)butane-1,4-diamine (59):**

Reported as a mixture of diastereomers (1:1)  $^1\text{H}$  NMR (600 MHz,  $\text{CDCl}_3$ )  $\delta$  8.48 (d, 0.5H,  $J = 4.5$  Hz), 8.41 (d, 0.5H,  $J = 4.7$  Hz), 7.34-7.26 (m, 1H), 7.10-7.04 (m, 2H), 7.04-7.00 (m, 1H), 7.00-6.92 (m, 2H), 5.79 (bs, 2H), 4.15-4.08 (m, 1H), 3.84 (d, 0.5H,  $J = 16.9$  Hz), 3.66 (d, 0.5H,  $J = 16.2$  Hz), 3.58 (d, 0.5H, 16.8 Hz), 3.52 (d, 0.5H, 16.4 Hz), 3.37 (d, 0.5H,  $J = 12.4$  Hz), 3.24 (d, 0.5H, 12.2 Hz), 3.10-2.99 (m, 1H), 2.90-2.74 (m, 4H), 2.74-2.60 (m, 6H), 2.51-2.37 (m, 3H), 2.16-2.06 (m, 1H), 2.03-1.92 (m, 1H), 1.88-1.79 (m, 1H), 1.77-1.48 (m, 10H), 1.47-1.32 (m, 2H), 1.32-1.22 (m, 1H)



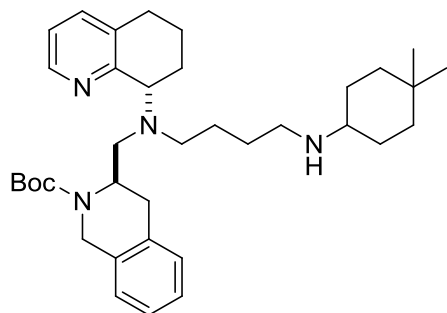
**2-(((R)-3-(((4-aminobutyl)((S)-5,6,7,8-tetrahydroquinolin-8-yl)amino)methyl)-3,4-dihydroisoquinolin-2(1H)-yl)-1-morpholinoethanone (63):**

$^1\text{H}$  NMR [400 MHz,  $\text{CDCl}_3$ ]  $\delta$  8.45 (d, 1H,  $J = 3.6$  Hz), 7.25 (d, 1H,  $J = 7.2$  Hz), 7.10-7.02 (m, 2H), 7.01-6.93 (m, 3H), 3.98 (dd, 1H,  $J = 12, 5.2$  Hz), 3.79-3.57 (m, 10H), 3.50-3.39 (m, 3H),

3.00-2.98 (m, 1H), 2.95-2.87 (m, 1H), 2.83-2.76 (m, 2H), 2.72-2.52 (m, 5H), 2.50-2.44 (m, 1H), 2.01-1.96 (m, 3H), 1.79-1.77 (m, 1H), 1.65-1.64 (m, 1H), 1.48-1.37 (m, 5H);  $^{13}\text{C}$  NMR [100 MHz,  $\text{CDCl}_3$ ]  $\delta$ 169.35, 147.28, 147.26, 136.62, 134.38, 133.73, 129.53, 126.59, 126.34, 125.78, 121.69, 67.13, 66.24, 61.64, 57.08, 56.22, 52.68, 50.94, 46.26, 42.43, 29.35, 27.54, 26.39, 25.54, 21.39; HRMS (ESI)  $[\text{M}+\text{H}]^+$ , calc'd for  $\text{C}_{29}\text{H}_{42}\text{N}_5\text{O}_2$  492.3330, found 492.33250; HPLC/MS purity (> 95%)  $r_t = 0.460$  at 254nm, 50-95% MeOH over 3 minutes.

### General procedure of compounds 65-73:

To a solution of dichloromethane (DCM) (6 mL) was added (R)-*tert*-butyl-3-(((4-aminobutyl)((S)-5,6,7,8-tetrahydroquinolin-8-yl)amino)methyl)-3,4-dihydroisoquinoline-2(1H)-carboxylate (.300 g, 0.646 mmol) and formaldehyde (0.078 g, 2.58 mmol). The reaction was allowed to stir at ambient temperature for 1 hour. STAB-H (0.547 g, 2.58 mmol) was then added in one portion and the reaction mixture allowed to stir overnight. The reaction mixture was quenched with  $\text{NaHCO}_3$  and the aqueous phase extracted with DCM (2 x 20 mL). The organic layers were combined, washed with brine, and dried over  $\text{MgSO}_4$ . The crude material was purified by gravity chromatography (10 g silica gel, 2% MeOH/DCM) to afford a light yellow foam.

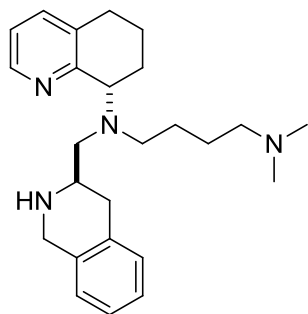


**(3R)-tert-butyl 3-(((4-(((3,3-dimethylcyclohexyl)methyl)amino)butyl)((S)-5,6,7,8-tetrahydroquinolin-8-yl)amino)methyl)-3,4-dihydroisoquinoline-2(1H)-carboxylate (67):**

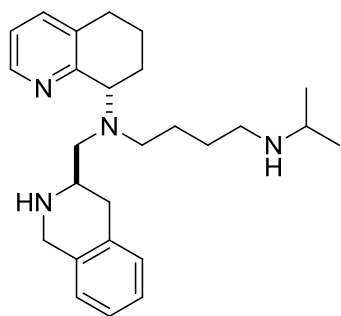
$^1\text{H}$  NMR [400 MHz,  $\text{CDCl}_3$ ]  $\delta$  8.43 (d, 1H,  $J=16$  Hz), 7.32 (d, 1H,  $J=6.2$  Hz), 7.09-6.94 (m, 5H), 4.66-4.61 (m, 1H), 4.14 (d, 1H,  $J=5.4$  Hz), 3.89 (m, 1H), 2.99 (m, 1H), 2.67 (m, 1H), 2.57 (m, 1H), 2.39 (m, 3H), 2.00 (bs, 1H), 1.91 (bs, 1H), 1.60 (m, 5H), 1.41 (m, 16H), 1.17 (m, 2H), 0.88 (m, 4H);  $^{13}\text{C}$  NMR [100 MHz,  $\text{CDCl}_3$ ]  $\delta$  147.06, 136.40, 134.22, 133.35, 129.59, 126.40, 126.21, 121.45, 79.78, 61.66, 57.28, 55.26, 51.88, 51.55, 49.75, 48.07, 47.18, 43.23, 32.47, 30.06, 30.23, 29.45, 28.75, 28.17, 27.84, 27.25, 27.03, 27.78, 21.49; HRMS (ESI)  $[\text{M}+\text{H}]^+$ , calc'd for  $\text{C}_{36}\text{H}_{55}\text{N}_4\text{O}_2$  575.43195

**General procedure of compounds 74-82:**

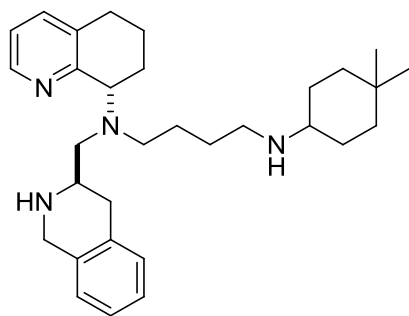
To a solution of DCM (4 mL) was added (R)-tert-butyl 3-(((4-(isopropylamino)butyl)((S)-5,6,7,8-tetrahydroquinolin-8-yl)amino)methyl)-3,4-dihydroisoquinoline-2(1H)-carboxylate (.300 g, 0.592 mmol). TFA (1.480 ml) was then added dropwise to the reaction mixture. The resulting solution was allowed to stir under argon for 2 hours. The reaction was diluted with saturated sodium bicarbonate and the aqueous layer was extracted with DCM (3 x 10 mL). The organic layers were combined, dried with magnesium sulfate and solvent evaporated under reduced pressure. Purification: 6g silica loaded with 95:5:0.5 (DCM:MeOH: $\text{NH}_4\text{OH}$ ) and eluted with 100 mL of the same solvent, followed by 100 mL 90:10:0.5 (DCM:MeOH: $\text{NH}_4\text{OH}$ ), followed by 100 mL 85:15:0.5 (DCM:MeOH: $\text{NH}_4\text{OH}$ ), followed by 80:20:0.5.

**Physical Data for 74-82:****N1,N1-dimethyl-N4-(((R)-1,2,3,4-tetrahydroisoquinolin-3-yl)methyl)-N4-((S)-5,6,7,8-tetrahydroquinolin-8-yl)butane-1,4-diamine (74):**

$^1\text{H}$  NMR [600 MHz,  $\text{CDCl}_3$ ]  $\delta$  8.40 (d, 1H,  $J = 3.6$  Hz), 7.38 (d, 1H,  $J = 7.2$  Hz), 7.16-7.13 (m, 2H), 7.11-7.04 (m, 3H), 4.38 (d, 1H,  $J = 15.6$  Hz), 4.09-4.29 (m, 2H), 3.20 (dd, 1H,  $J = 4.2, 2.4$  Hz), 3.08-3.06 (m, 1H), 2.96-2.87 (m, 2H), 2.81-2.65 (m, 4H), 2.58-2.49 (m, 3H), 2.48-2.41 (m, 6H), 2.11-2.08 (m, 1H), 2.00-1.97 (m, 1H), 1.84 (dq, 1H,  $J = 10.2, 2.4$  Hz), 1.74-1.67 (m, 1H), 1.69-1.39 (m, 5H);  $^{13}\text{C}$  NMR [150 MHz,  $\text{CDCl}_3$ ]  $\delta$  162.21, 158.17, 146.68, 137.78, 134.44, 132.44, 132.27, 130.56, 129.24, 127.46, 126.72, 122.33, 63.07, 58.81, 56.09, 53.13, 52.22, 45.29, 44.34, 30.90, 29.38, 26.87, 26.41, 23.99, 22.03; HRMS (ESI)  $[\text{M}+\text{H}]^+$ , calc'd for  $\text{C}_{25}\text{H}_{37}\text{N}_4$  393.30127, found 393.30161; HPLC/MS purity ( $> 95\%$ )  $r_t = 0.426$  at 254nm, 85% MeOH over 3 minutes.

**N1-isopropyl-N4-(((R)-1,2,3,4-tetrahydroisoquinolin-3-yl)methyl)-N4-((S)-5,6,7,8-tetrahydroquinolin-8-yl)butane-1,4-diamine (75):**

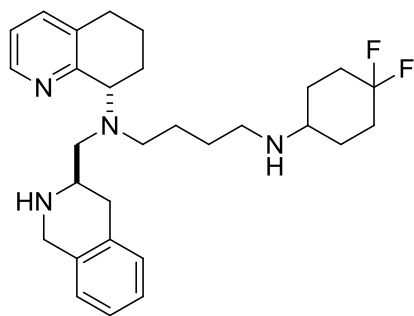
$^1\text{H}$  NMR [600 MHz,  $\text{CDCl}_3$ ]  $\delta$  8.41 (d, 1H,  $J = 3.6$  Hz), 7.36 (d, 1H,  $J = 7.8$  Hz), 7.22-7.14 (m, 2H), 7.13-7.07 (m, 3H), 4.44 (d, 1H,  $J = 16.2$  Hz), 4.25 (d, 1H,  $J = 16.2$  Hz), 3.94 (dd, 1H,  $J = 10.2, 6.6$  Hz), 3.28 (quintet, 2H,  $J = 6.6$  Hz), 3.05-2.97 (m, 2H), 2.92-2.80 (m, 4H), 2.76-2.65 (m, 4H), 2.30-2.28 (m, 1H), 2.18-2.16 (m, 1H), 2.11(bs, 1H), 2.00-1.97 (m, 1H), 1.75-1.64 (m, 5H), 1.46-1.42 (m, 1H), 1.35-1.32 (m, 6H);  $^{13}\text{C}$  NMR [150 MHz,  $\text{CDCl}_3$ ]  $\delta$  162.20, 158.21, 146.84, 137.37, 134.23, 132.04, 129.14, 127.71, 127.05, 126.58, 122.21, 61.87, 56.40, 52.71, 52.40, 51.01, 45.51, 45.42, 30.64, 29.42, 27.71, 26.36, 24.93, 22.20, 19.40, 18.98; HRMS (ESI)  $[\text{M}+\text{H}]^+$ , calc'd for  $\text{C}_{26}\text{H}_{39}\text{N}_4$  407.31692, found 407.31745; HPLC/MS purity ( $> 95\%$ )  $r_t = 0.409$  at 254nm, 75-95% MeOH over 3 minutes.



**N1-(4,4-dimethylcyclohexyl)-N4-(((R)-1,2,3,4-tetrahydroisoquinolin-3-yl)methyl)-N4-((S)-5,6,7,8-tetrahydroquinolin-8-yl)butane-1,4-diamine (77):**

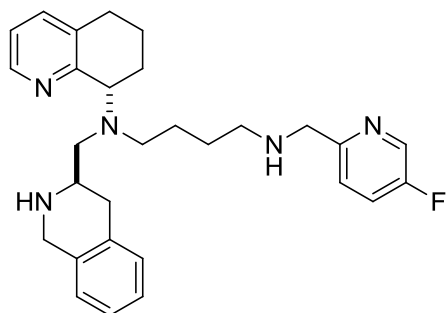
$^1\text{H}$  NMR [400 MHz,  $\text{CDCl}_3$ ]  $\delta$  8.43 (dd, 1H,  $J = 1.4, 4.7$  Hz), 7.32 (d, 1H,  $J = 6.7$  Hz), 6.96-7.08 (m, 5H), 6.69 (bs, 1H), 4.05 (dd, 1H,  $J = 6.4, 9.5$  Hz), 3.97 (d, 1H,  $J = 15.0$  Hz), 3.68 (d, 1H,  $J = 15.0$  Hz), 3.19-3.33 (m, 2H), 3.01 (dd, 1H,  $J = 2.7, 13.1$  Hz), 2.93 (bs, 1H), 2.84-2.88 (m, 1H), 2.73-2.87 (m, 1H), 2.69 (bs, 1H), 2.57-2.65 (m, 3H), 2.37-2.43 (m, 2H), 1.92-2.10 (m, 3H), 1.88 (s, 3H), 1.52-1.76 (m, 5H);  $^{13}\text{C}$  NMR [100 MHz,  $\text{CDCl}_3$ ]  $\delta$  170.55, 158.67, 146.88, 136.90, 135.59, 134.63, 134.16, 129.21, 126.59, 126.12, 125.71, 121.75, 61.50, 57.63, 54.23, 52.23, 48.62, 39.72, 34.04, 29.70, 27.27, 26.98, 26.65, 23.30, 22.19; HRMS (ESI)  $[\text{M}+\text{H}]^+$ , calc'd for

C<sub>31</sub>H<sub>47</sub>N<sub>4</sub> 474.37104 found 474.37112; HPLC/MS purity (> 95%)  $r_t = 0.1.409$  at 254nm, 75-95% MeOH over 3 minutes.



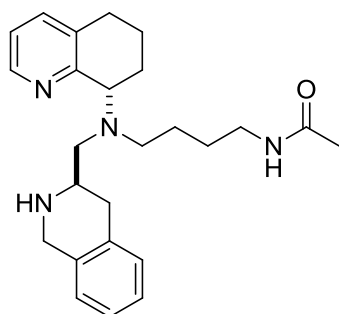
**N1-(4,4-difluorocyclohexyl)-N4-(((R)-1,2,3,4-tetrahydroisoquinolin-3-yl)methyl)-N4-((S)-5,6,7,8-tetrahydroquinolin-8-yl)butane-1,4-diamine (78):**

<sup>1</sup>H NMR [400 MHz, CDCl<sub>3</sub>]  $\delta$  8.43 (dd, 1H,  $J = 1.4, 4.7$  Hz), 7.32 (d, 1H,  $J = 6.7$  Hz), 6.96-7.08 (m, 5H), 6.69 (bs, 1H), 4.05 (dd, 1H,  $J = 6.4, 9.5$  Hz), 3.97 (d, 1H,  $J = 15.0$  Hz), 3.68 (d, 1H,  $J = 15.0$  Hz), 3.19-3.33 (m, 2H), 3.01 (dd, 1H,  $J = 2.7, 13.1$  Hz), 2.93 (bs, 1H), 2.84-2.88 (m, 1H), 2.73-2.87 (m, 1H), 2.69 (bs, 1H), 2.57-2.65 (m, 3H), 2.37-2.43 (m, 2H), 1.92-2.10 (m, 3H), 1.88 (s, 3H), 1.52-1.76 (m, 5H); <sup>13</sup>C NMR [100 MHz, CDCl<sub>3</sub>]  $\delta$  170.55, 158.67, 146.88, 136.90, 135.59, 134.63, 134.16, 129.21, 126.59, 126.12, 125.71, 121.75, 61.50, 57.63, 54.23, 52.23, 48.62, 39.72, 34.04, 29.70, 27.27, 26.98, 26.65, 23.30, 22.19; HRMS (ESI) [M+H]<sup>+</sup>, calc'd for C<sub>31</sub>H<sub>47</sub>N<sub>4</sub>F<sub>2</sub> 482.32107 found 474.32118; HPLC/MS purity (> 95%)  $r_t = 0.1.319$  at 254nm, 75-95% MeOH over 3 minutes.



**N1-((5-fluoropyridin-2-yl)methyl)-N4-(((R)-1,2,3,4-tetrahydroisoquinolin-3-yl)methyl)-N4-((S)-5,6,7,8-tetrahydroquinolin-8-yl)butane-1,4-diamine (80):**

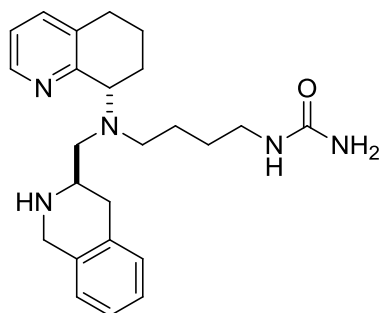
$^1\text{H}$  NMR [600 MHz,  $\text{CDCl}_3$ ]  $\delta$  8.39 (d, 1H,  $J = 4.8$  Hz), 7.32 (m, 3H), 7.13 (m, 2H), 7.05 (m, 3H), 4.30 (d, 1H,  $J = 15.6$  Hz), 4.07 (m, 2H), 3.93 (m, 2H), 3.12 (d, 1H,  $J = 16$  Hz), 3.06 (m, 1H), 2.85 (m, 1H), 2.76 (m, 5H), 2.66 (m, 4H), 2.51 (quin., 1H,  $J = 7.2$  Hz), 2.00 (m, 1H), 1.97 (m, 1H), 1.84 ( $^{13}\text{C}$  NMR [100 MHz,  $\text{CDCl}_3$ ]  $\delta$  159.94, 158.36, 146.86, 137.10, 135.26, 134.35, 134.19, 129.15, 126.58, 126.17, 125.76, 121.91, 61.55, 57.31, 53.89, 52.02, 48.22, 40.29, 33.82, 29.69, 26.94, 26.70, 25.81, 22.09; HRMS (ESI)  $[\text{M}+\text{H}]^+$ , calc'd for  $\text{C}_{24}\text{H}_{34}\text{N}_5\text{O}$  408.27579, found 408.27590; HPLC/MS purity (> 95%)  $r_t = 1.166$  at 254nm, 25-95% MeOH over 3 minutes.



**N-4-(((R)-1,2,3,4-tetrahydroisoquinolin-3-yl)methyl)((S)-5,6,7,8-tetrahydroquinolin-8-yl)amino)butyl)acetamide (81):**

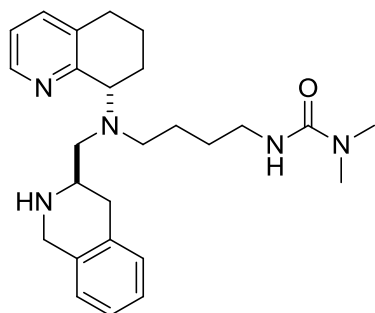
$^1\text{H}$  NMR [400 MHz,  $\text{CDCl}_3$ ]  $\delta$  8.43 (dd, 1H,  $J = 1.2, 4.9$  Hz), 7.32 (d, 1H,  $J = 6.7$  Hz), 6.94-7.08 (m, 5H), 6.32 (bs, 1H), 4.93 (s, 2H), 4.03 (dd, 1H,  $J = 6.7, 9.2$  Hz), 3.91 (d, 1H,  $J = 15.3$  Hz),

3.52 (d, 1H,  $J = 14.6$  Hz), 3.12-3.23 (m, 4H), 3.01 (d, 1H,  $J = 10.4$  Hz), 2.55-2.80 (m, 5H), 2.35-2.51 (m, 3H), 1.86-2.07 (m, 3H), 1.48-1.75 (m, 4H);  $^{13}\text{C}$  NMR [100 MHz,  $\text{CDCl}_3$ ]  $\delta$  159.94, 158.36, 146.86, 137.10, 135.26, 134.35, 134.19, 129.15, 126.58, 126.17, 125.76, 121.91, 61.55, 57.31, 53.89, 52.02, 48.22, 40.29, 33.82, 29.69, 26.94, 26.70, 25.81, 22.09; HRMS (ESI)  $[\text{M}+\text{H}]^+$ , calc'd for  $\text{C}_{24}\text{H}_{34}\text{N}_5\text{O}$  408.27579, found 408.27590; HPLC/MS purity ( $> 95\%$ )  $r_t = 1.166$  at 254nm, 25-95% MeOH over 3 minutes.



**1-(4-(((R)-1,2,3,4-tetrahydroisoquinolin-3-yl)methyl)((S)-5,6,7,8-tetrahydroquinolin-8-yl)amino)butyl)urea (82):**

$^1\text{H}$  NMR [400 MHz,  $\text{CDCl}_3$ ]  $\delta$  8.43 (dd, 1H,  $J = 1.4, 4.7$  Hz), 7.32 (d, 1H,  $J = 6.7$  Hz), 6.96-7.08 (m, 5H), 6.69 (bs, 1H), 4.05 (dd, 1H,  $J = 6.4, 9.5$  Hz), 3.97 (d, 1H,  $J = 15.0$  Hz), 3.68 (d, 1H,  $J = 15.0$  Hz), 3.19-3.33 (m, 2H), 3.01 (dd, 1H,  $J = 2.7, 13.1$  Hz), 2.93 (bs, 1H), 2.84-2.88 (m, 1H), 2.73-2.87 (m, 1H), 2.69 (bs, 1H), 2.57-2.65 (m, 3H), 2.37-2.43 (m, 2H), 1.92-2.10 (m, 3H), 1.88 (s, 3H), 1.52-1.76 (m, 5H);  $^{13}\text{C}$  NMR [100 MHz,  $\text{CDCl}_3$ ]  $\delta$  170.55, 158.67, 146.88, 136.90, 135.59, 134.63, 134.16, 129.21, 126.59, 126.12, 125.71, 121.75, 61.50, 57.63, 54.23, 52.23, 48.62, 39.72, 34.04, 29.70, 27.27, 26.98, 26.65, 23.30, 22.19; HRMS (ESI)  $[\text{M}+\text{H}]^+$ , calc'd for  $\text{C}_{25}\text{H}_{35}\text{N}_4\text{O}$  407.28054, found 407.28162; HPLC/MS purity ( $> 95\%$ )  $r_t = 0.596$  at 254nm, 50-95% MeOH over 3 minutes.

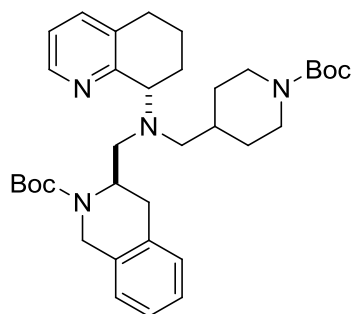


**1,1-dimethyl-3-(4-(((R)-1,2,3,4-tetrahydroisoquinolin-3-yl)methyl)((S)-5,6,7,8-tetrahydroquinolin-8-yl)amino)butylurea (83):**

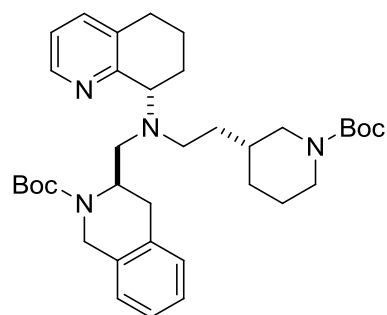
$^1\text{H}$  NMR [400 MHz,  $\text{CDCl}_3$ ]  $\delta$  8.43 (d, 1H,  $J = 4.3$  Hz), 7.32 (d, 1H,  $J = 7.0$  Hz), 6.99-7.09 (m, 5H), 4.54 (bs, 1H), 4.02-4.09 (m, 2H), 3.88 (d, 1H,  $J = 15.0$  Hz), 3.22-3.24 (m, 2H), 2.97-3.03 (m, 2H), 2.86 (s, 6H), 2.59-2.81 (m, 6H), 2.41 (q, 2H,  $J = 12.7$  Hz), 2.05-2.08 (m, 1H), 1.94-2.00 (m, 1H), 1.85-1.91 (m, 1H), 1.65-1.74 (m, 1H), 1.54-1.56 (m, 4H);  $^{13}\text{C}$  NMR [100 MHz,  $\text{CDCl}_3$ ]  $\delta$  158.87, 158.74, 146.89, 136.71, 135.61, 134.76, 134.14, 129.24, 126.60, 126.10, 125.67, 121.59, 61.56, 57.83, 54.23, 52.48, 48.70, 41.07, 36.36, 36.33, 33.89, 29.62, 28.85, 28.26, 27.16, 22.15; HRMS (ESI)  $[\text{M}+\text{H}]^+$ , calc'd for  $\text{C}_{26}\text{H}_{38}\text{N}_5\text{O}$  436.30709, found 436.30740; HPLC/MS purity (> 95%)  $r_t = 1.385$  at 254nm, 25-95% MeOH over 3 minutes. .

**General Procedure for Compounds 86-87, 89 & 91:**

To a solution of DCE (13 mL) was added (R)-*tert*-butyl-3-(((S)-5,6,7,8-tetrahydroquinolin-8-yl)amino)methyl)-3,4-dihydroisoquinoline-2(1H)-carboxylate (.540 g, 1.372 mmol) and (S)-*tert*-butyl 3-(2-oxoethyl)piperidine-1-carboxylate (0.343 g, 1.509 mmol). The resulting mixture was reaction was allowed to stir under argon overnight. The reaction was quenched with aqueous  $\text{NaHCO}_3$ , extracted with DCM (2 x 100 mL), dried over magnesium sulfate, and evaporated under reduced pressure. The diastereomers were separated on a 20g silica column (1% MeOH, 0.5%  $\text{Et}_3\text{N}$ ) in DCM.

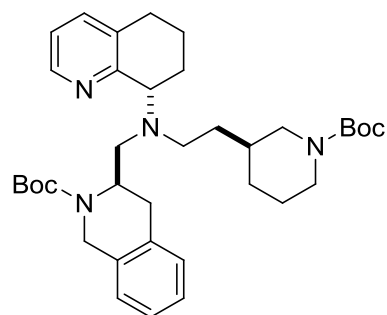
**Physical Data for 87, 89 & 91:****(R)-tert-butyl-3-(((1-(tert-butoxycarbonyl)piperidin-4-yl)methyl)((S)-5,6,7,8-tetrahydroquinolin-8-yl)amino)methyl)-3,4-dihydroisoquinoline-2(1H)-carboxylate (87):**

$^1\text{H}$  NMR [600 MHz,  $\text{CDCl}_3$ ]  $\delta$  8.42 (d, 1H,  $J = 4.2$  Hz), 7.33 (d, 1H,  $J = 4.2$  Hz), 7.06-7.02 (m, 5H), 4.08-4.05 (m, 2H), 4.03-3.95 (m, 1H), 3.11 (m, 3H), 2.96 (d, 1H,  $J = 11.4$  Hz), 2.80- 2.75 (m, 5H), 2.61-2.56 (m, 4H), 2.44-2.41 (m, 2H), 2.32-2.83 (m, 1H), 4.03-4.02 (m, 2H), 3.99-3.97 (m, 1H), 3.13-3.08 (m, 3H), 2.96 (d, 1H,  $J = 11.4$  Hz), 2.89-2.65 (m, 5H), 2.66-2.56 (m, 4H), 2.44-2.42 (m, 2H), 2.32-2.28 (m, 1H), 2.10-1.06 (m, 1H), 1.98-1.85 (m, 3H), 1.79 (d, 1H,  $J = 11.4$  Hz), 1.73-1.69 (m, 1H), 1.58-1.57 (m, 1H), 1.27-1.05 (m, 2H);  $^{13}\text{C}$  NMR [100 MHz,  $\text{CDCl}_3$ ]  $\delta$  159.31, 147.09, 136.80, 136.03, 135.42, 134.58, 129.53, 126.91, 126.32, 125.91, 121.77, 62.19, 58.74, 52.92, 49.24, 46.90, 36.69, 34.19, 31.14, 30.67, 29.87, 22.63; HRMS (ESI)  $[\text{M}+\text{H}]^+$ , calc'd for  $\text{C}_{25}\text{H}_{35}\text{N}_4$  390.56173, found 390.56284; HPLC/MS purity (> 95%)  $r_t = 1.301$  at 254nm, 50-95% MeOH over 3 minutes.



**(R)-tert-butyl-3-(((2-((R)-1-(tert-butoxycarbonyl)piperidin-3-yl)ethyl)((S)-5,6,7,8-tetrahydroquinolin-8-yl)amino)methyl)-3,4-dihydroisoquinoline-2(1H)-carboxylate (89):**

$^1\text{H}$  NMR [600 MHz,  $\text{CDCl}_3$ ]  $\delta$  8.41 (d, 1H,  $J = 4.6$  Hz), 7.12-7.11 (m, 1H), 7.12-7.00 (m, 3H), 6.99-6.98 (m, 1H), 4.69-4.66 (m, 1H), 4.38 (bs, 1H), 4.15 (d, 1H,  $J = 16$  Hz), 3.90-3.84 (m, 4H), 2.97-2.93 (m, 2H), 2.86-2.70 (m, 3H), 2.63-2.60 (m, 4H), 2.43-2.40 (m, 2H), 2.02-1.99 (m, 2H), 1.71-1.53 (m, 5H), 1.50-1.36 (m, 12H), 1.33-1.27 (m, 2H), 1.20-1.17 (m, 1H);  $^{13}\text{C}$  NMR [100 MHz,  $\text{CDCl}_3$ ]  $\delta$  158.71, 147.06, 136.99, 134.88, 134.35, 134.08, 129.29, 126.69, 126.40, 125.96, 121.87, 62.05, 58.01, 52.74, 51.29, 47.88, 45.92, 34.05, 33.77, 33.35, 30.85, 29.60, 27.69, 24.49, 22.04; HRMS (ESI)  $[\text{M}+\text{H}]^+$ , calc'd for  $\text{C}_{36}\text{H}_{53}\text{N}_4\text{O}_4$  604.40167, found 604.40178



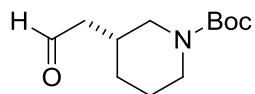
**(R)-tert-butyl-3-(((2-((S)-1-(tert-butoxycarbonyl)piperidin-3-yl)ethyl)((S)-5,6,7,8-tetrahydroquinolin-8-yl)amino)methyl)-3,4-dihydroisoquinoline-2(1H)-carboxylate (91):**

$^1\text{H}$  NMR [600 MHz,  $\text{CDCl}_3$ ]  $\delta$  8.41 (d, 1H,  $J = 4.6$  Hz), 7.12-7.11 (m, 1H), 7.12-7.00 (m, 3H), 6.99-6.98 (m, 1H), 4.69-4.66 (m, 1H), 4.38 (bs, 1H), 4.15 (d, 1H,  $J = 16$  Hz), 3.90-3.84 (m, 4H), 2.97-2.93 (m, 2H), 2.86-2.70 (m, 3H), 2.63-2.60 (m, 4H), 2.43-2.40 (m, 2H), 2.02-1.99 (m, 2H),

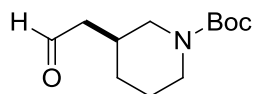
1.71-1.53 (m, 5H), 1.50-1.36 (m, 12H), 1.33-1.27 (m, 2H), 1.20-1.17 (m, 1H);  $^{13}\text{C}$  NMR [100 MHz,  $\text{CDCl}_3$ ]  $\delta$  158.71, 147.06, 136.99, 134.88, 134.35, 134.08, 129.29, 126.69, 126.40, 125.96, 121.87, 62.05, 58.01, 52.74, 51.29, 47.88, 45.92, 34.05, 33.77, 33.35, 30.85, 29.60, 27.69, 24.49, 22.04; HRMS (ESI)  $[\text{M}+\text{H}]^+$ , calc'd for  $\text{C}_{36}\text{H}_{53}\text{N}_4\text{O}_4$  604.40167, found 604.40178

### General Procedure for Compounds 88 & 90:

A solution of oxalyl dichloride (1.229 ml, 14.10 mmol) in DCM (30.9 ml) was cooled to  $-78^\circ\text{C}$  (dry-ice acetone) under argon. (methylsulfinyl)methane (1.766 ml, 25.06 mmol) was then added over a period of 35-45 minutes. After the addition was complete, the reaction was stirred for 30 minutes. (R)-benzyl 3-(2-hydroxyethyl)piperidine-1-carboxylate (1.65 g, 6.27 mmol) was then added in one portion while maintaining the temperature below  $-70^\circ\text{C}$  and allowed to stir for 1 hour. Triethylamine (3.50 ml, 25.06 mmol) was then added dropwise over a period of 30 minutes. After the addition was completed the mixture was stirred at  $-78^\circ\text{C}$  for 1 hour and then warmed to  $0^\circ\text{C}$  and stirred for 2 hours. The reaction was quenched with 10 mL saturated  $\text{NaHCO}_3$ . The organic layer was separated and aqueous layer extracted with DCM (2 x 40 mL). The combined organic layers were washed with brine, dried over magnesium sulfate and solvent was removed under reduced pressure to yield a light yellow oil (1.60 g, 95%).

**Physical Data for 88 & 90:****(R)-tert-butyl 3-(2-oxoethyl)piperidine-1-carboxylate (88):**

$^1\text{H}$  NMR [400 MHz,  $\text{CDCl}_3$ ]  $\delta$  9.59 (s, 1H,  $J = 4.3$  Hz), 3.63-3.61 (m, 2H), 2.71 (bs, 1H), 2.27 (dd,  $J = 3.2$  Hz, 2H), 1.88-1.86 (m, 1H), 1.67-1.64 (m, 1H), 1.44-1.42 (m, 1H), 1.26-1.24 (m, 1H), 1.06-1.04 (m, 2H);  $^{13}\text{C}$  NMR [100 MHz,  $\text{CDCl}_3$ ]  $\delta$  ; 200.78, 154.50, 79.15, 49.05, 47.01, 30.41, 28.21, 24.26

**(S)-tert-butyl 3-(2-oxoethyl)piperidine-1-carboxylate (90):**

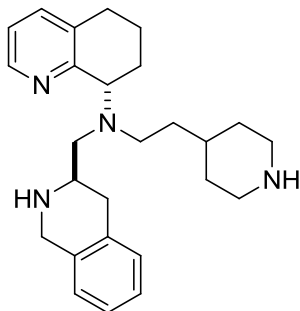
$^1\text{H}$  NMR [400 MHz,  $\text{CDCl}_3$ ]  $\delta$  9.59 (s, 1H,  $J = 4.3$  Hz), 3.63-3.61 (m, 2H), 2.71 (bs, 1H), 2.27 (dd,  $J = 3.2$  Hz, 2H), 1.88-1.75 (m, 1H), 1.68-1.65 (m, 1H), 1.43-1.41 (m, 1H), 1.25-1.23 (m, 1H), 1.04-1.02 (m, 2H);  $^{13}\text{C}$  NMR [100 MHz,  $\text{CDCl}_3$ ]  $\delta$  ; 200.78, 154.50, 79.15, 49.05, 47.01, 30.41, 28.21, 24.26

**General Procedure for Compounds 92-95:**

(R)-tert-butyl-3-(((S)-5,6,7,8-tetrahydroquinolin-8-ylamino)methyl)-3,4-dihydroisoquinoline-2(1H)-carboxylate (.500 g, 1.271 mmol) and *tert*-butyl 4-formylpiperidine-1-carboxylate (0.298 g, 1.398 mmol) were added to DCM (12.71 ml). STAB-H (0.404 g, 1.906 mmol) was then added in one portion, followed by the addition of acetic acid (0.073 ml, 1.271 mmol). The

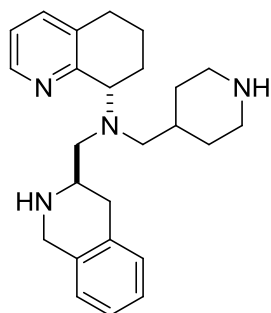
reaction was allowed to stir under argon overnight. The reaction was quenched with aqueous NaHCO<sub>3</sub>, extracted with DCM (2 x 100 mL), dried over magnesium sulfate and evaporated under reduced pressure. The resulting yellow oil was purified by column chromatography

### Physical Data for 92-95:



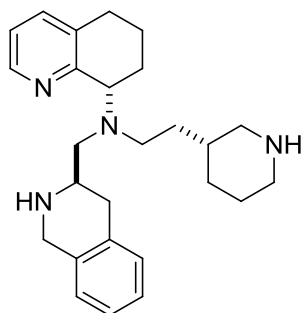
### (S)-N-(2-(piperidin-4-yl)ethyl)-N-(((R)-1,2,3,4-tetrahydroisoquinolin-3-yl)methyl)-5,6,7,8-tetrahydroquinolin-8-amine (92):

<sup>1</sup>H NMR [600 MHz, CDCl<sub>3</sub>] δ 8.42 (d, 1H, *J* = 4.2 Hz), 7.33 (d, 1H, *J* = 4.2 Hz), 7.06-7.02 (m, 5H), 4.08-4.05 (m, 2H), 4.03-3.95 (m, 1H), 3.11 (m, 3H), 2.96 (d, 1H, *J* = 11.4 Hz), 2.80- 2.75 (m, 5H), 2.61-2.56 (m, 4H), 2.44-2.41 (m, 2H), 2.32-2.83 (m, 1H), 4.03-4.02 (m, 2H), 3.99-3.97 (m, 1H), 3.13-3.08 (m, 3H), 2.96 (d, 1H, *J* = 11.4 Hz), 2.89-2.65 (m, 5H), 2.66-2.56 (m, 4H), 2.44-2.42 (m, 2H), 2.32-2.28 (m, 1H), 2.10-1.06 (m, 1H), 1.98-1.85 (m, 3H), 1.79 (d, 1H, *J* = 11.4 Hz), 1.73-1.69 (m, 1H), 1.58-1.57 (m, 1H), 1.27-1.05 (m, 2H); <sup>13</sup>C NMR [100 MHz, CDCl<sub>3</sub>] δ 159.31, 147.09, 136.80, 136.03, 135.42, 134.58, 129.53, 126.91, 126.32, 125.91, 121.77, 62.19, 58.74, 52.92, 49.24, 46.90, 36.69, 34.19, 31.14, 30.67, 29.87, 22.63; HRMS (ESI) [M+H]<sup>+</sup>, calc'd for C<sub>25</sub>H<sub>35</sub>N<sub>4</sub> 404.29754, found 404.29736; HPLC/MS purity (> 95%) *r*<sub>t</sub> = 1.324 at 254nm, 50-95% MeOH over 3 minutes.



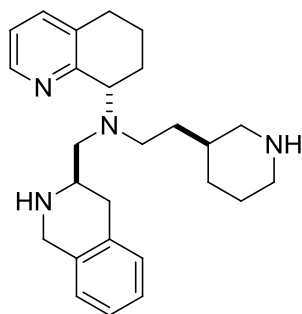
**(S)-N-(piperidin-4-ylmethyl)-N-(((R)-1,2,3,4-tetrahydroisoquinolin-3-yl)methyl)-5,6,7,8-tetrahydroquinolin-8-amine (93):**

$^1\text{H}$  NMR [600 MHz,  $\text{CDCl}_3$ ]  $\delta$  8.42 (d, 1H,  $J = 4.2$  Hz), 7.33 (d, 1H,  $J = 4.2$  Hz), 7.06-7.02 (m, 5H), 4.08-4.05 (m, 2H), 4.03-3.95 (m, 1H), 3.11 (m, 3H), 2.96 (d, 1H,  $J = 11.4$  Hz), 2.80- 2.75 (m, 5H), 2.61-2.56 (m, 4H), 2.44-2.41 (m, 2H), 2.32-2.83 (m, 1H), 4.03-4.02 (m, 2H), 3.99-3.97 (m, 1H), 3.13-3.08 (m, 3H), 2.96 (d, 1H,  $J = 11.4$  Hz), 2.89-2.65 (m, 5H), 2.66-2.56 (m, 4H), 2.44-2.42 (m, 2H), 2.32-2.28 (m, 1H), 2.10-1.06 (m, 1H), 1.98-1.85 (m, 3H), 1.79 (d, 1H,  $J = 11.4$  Hz), 1.73-1.69 (m, 1H), 1.58-1.57 (m, 1H), 1.27-1.05 (m, 2H);  $^{13}\text{C}$  NMR [100 MHz,  $\text{CDCl}_3$ ]  $\delta$  159.31, 147.09, 136.80, 136.03, 135.42, 134.58, 129.53, 126.91, 126.32, 125.91, 121.77, 62.19, 58.74, 52.92, 49.24, 46.90, 36.69, 34.19, 31.14, 30.67, 29.87, 22.63; HRMS (ESI)  $[\text{M}+\text{H}]^+$ , calc'd for  $\text{C}_{25}\text{H}_{35}\text{N}_4$  390.56173, found 390.56284; HPLC/MS purity ( $> 95\%$ )  $r_t = 1.301$  at 254nm, 50-95% MeOH over 3 minutes.



**(S)-N-(2-((R)-piperidin-3-yl)ethyl)-N-(((R)-1,2,3,4-tetrahydroisoquinolin-3-yl)methyl)-5,6,7,8-tetrahydroquinolin-8-amine (94):**

$^1\text{H}$  NMR [600 MHz,  $\text{CDCl}_3$ ]  $\delta$  8.47 (d, 1H,  $J = 4.2$  Hz), 7.33 (d, 1H,  $J = 4.2$  Hz), 7.06-7.02 (m, 5H), 4.05 (m, 3H), 3.83 (d, 1H,  $J = 16$  Hz), 3.10-3.07 (m, 2H), 2.96 (dd, 1H,  $J = 6.8, 2$  Hz), 2.88 (quin., 1H, 11.4 Hz), 2.77 (quin., 1H, 11.4 Hz), 2.65-2.61 (m, 5H), 2.60-2.56 (m, 3H), 2.07-2.04 (m, 1H), 1.98-1.97 (m, 1H), 1.88-1.82 (m, 1H), 1.69-1.61 (m, 4H), 1.56-1.52 (m, 1H), 1.48 (sex., 1H,  $J = 7.2$  Hz), 1.33 (sex., 1H,  $J = 7.2$  Hz);  $^{13}\text{C}$  NMR [100 MHz,  $\text{CDCl}_3$ ]  $\delta$  158.71, 147.06, 136.99, 134.88, 134.35, 134.08, 129.29, 126.69, 126.40, 125.96, 121.87, 62.05, 58.01, 52.74, 51.29, 47.88, 45.92, 34.05, 33.77, 33.35, 30.85, 29.60, 27.69, 24.49, 22.04; HRMS (ESI)  $[\text{M}+\text{H}]^+$ , calc'd for  $\text{C}_{26}\text{H}_{37}\text{N}_4$  404.30709, found 404.30740; HPLC/MS purity (> 95%)  $r_t = 1.419$  at 254nm, 50-95% MeOH over 3 minutes.

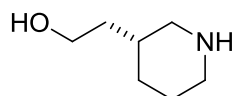


**(S)-N-(2-((S)-piperidin-3-yl)ethyl)-N-(((R)-1,2,3,4-tetrahydroisoquinolin-3-yl)methyl)-5,6,7,8-tetrahydroquinolin-8-amine (95):**

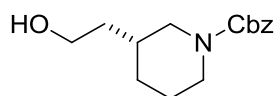
$^1\text{H}$  NMR [600 MHz,  $\text{CDCl}_3$ ]  $\delta$  8.43 (d, 1H,  $J = 4.2$  Hz), 7.30 (d, 1H,  $J = 4.2$  Hz), 7.04 (m, 5H), 4.05 (m, 3H), 3.91 (d, 1H,  $J = 16$  Hz), 3.07 (m, 2H), 2.96 (dd, 1H,  $J = 6.8, 2$  Hz), 2.88 (quin.,

1H, 11.4 Hz), 2.77 (quin., 1H, 11.4 Hz), 2.65-2.61 (m, 5H), 2.60-2.56 (m, 3H), 2.07-2.04 (m, 1H), 1.98-1.97 (m, 1H), 1.88-1.82 (m, 1H), 1.69-1.61 (m, 4H), 1.56-1.52 (m, 1H), 1.48 (sex., 1H,  $J = 7.2$  Hz), 1.33 (sex, 1H,  $J = 7.2$  Hz);  $^{13}\text{C}$  NMR [100 MHz,  $\text{CDCl}_3$ ]  $\delta$  158.96, 146.94, 136.58, 134.08, 134.35, 134.08, 129.25, 126.38, 126.40, 125.96, 121.49, 62.73, 58.09, 52.57, 50.17, 48.99, 45.92, 34.05, 33.77, 33.35, 30.85, 29.60, 27.69, 24.49, 22.04; HRMS (ESI)  $[\text{M}+\text{H}]^+$ , calc'd for  $\text{C}_{26}\text{H}_{37}\text{N}_4$  404.30709, found 404.31620; HPLC/MS purity ( $> 95\%$ )  $r_t = 1.405$  at 254nm, 50-95% MeOH over 3 minutes.

#### Procedures and Physical Data for 96-104:

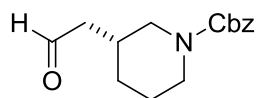


(R)-2-(piperidin-3-yl)ethanol (**96**): To a solution of DCM (21.80 ml) and TFA (7.27 ml) was added (R)-tert-butyl 3-(2-hydroxyethyl)piperidine-1-carboxylate (1 g, 4.36 mmol). The reaction mixture stirred overnight under argon. The solvent was removed under reduced pressure and pH adjusted to 10 with aqueous  $\text{NaHCO}_3$ . The aqueous phase was extracted with DCM (2x100ml), dried over anhydrous magnesium sulfate and solvent removed under reduced pressure. LC/MS, TLC shows complete conversion of starting material to product. The yellow oil was carried forward without purification (0.550g, 98%).



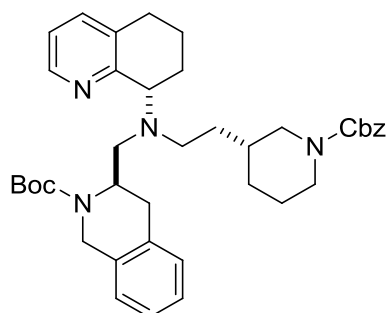
(R)-benzyl 3-(2-hydroxyethyl)piperidine-1-carboxylate (**97**): To a solution of (R)-2-(piperidin-3-yl)ethanol (.560 g, 4.33 mmol) and potassium carbonate (1.557 g, 11.27 mmol) in dioxane

(21.67 ml) and water (21.67 ml) was added benzyl carbonochloridate (0.681 ml, 4.77 mmol) dropwise at 0 C. After addition, the reaction mixture was stirred at ambient temperature for 18 h, at which time TLC analysis showed complete consumption of the reaction. The reaction mixture was then concentrated under reduced pressure, and the residue was extracted with EtOAc (3x10 ml). The combined organic layers were dried with anhydrous magnesium sulfate and evaporated to give (R)-benzyl 3-(2-hydroxyethyl)piperidine-1-carboxylate (1.2g, 96%).  $^1\text{H}$  NMR [400 MHz,  $\text{CDCl}_3$ ] 7.29 (m, 2H), 7.21 (m, 3H), 3.63 (m, 2H), 5.09 (s, 1H), 3.87 (m, 4H), 2.89 (bs, 2H), 2.47 (bs, 1H), 1.79 (bs, 1H), 1.56 (bs, 2H), 1.46 (bs, 2H)  $^{13}\text{C}$  NMR [100 MHz,  $\text{CDCl}_3$ ]  $\delta$  ; 155.37, 137.02, 128.65, 127.97, 67.17, 60.50, 49.31, 44.58, 30.56, 21,17



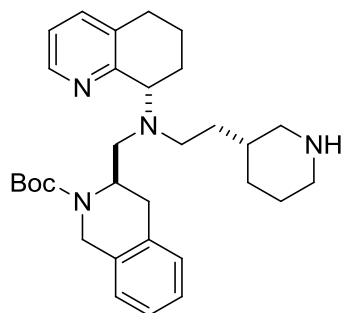
(R)-benzyl 3-(2-hydroxyethyl)piperidine-1-carboxylate (**98**): A solution of oxalyl dichloride (1.229 ml, 14.10 mmol) in DCM (30.9 ml) was cooled to  $-78^\circ\text{C}$  (dry-ice acetone) under argon. (methylsulfinyl) methane (1.766 ml, 25.06 mmol) was then added over a period of 35-45 minutes (temperature kept below  $-60^\circ\text{C}$ ). After the addition was complete, the reaction was stirred for 30 minutes. (R)-benzyl 3-(2-hydroxyethyl)piperidine-1-carboxylate (1.65 g, 6.27 mmol) was then added in one portion while maintaining the temperature below  $-70^\circ\text{C}$  and allowed to stir for 1 hour. triethylamine (3.50 ml, 25.06 mmol) was then added drop-wise over a period of 30 minutes. After the addition was completed the mixture was stirred at  $-78^\circ\text{C}$  for 1 hour and then warmed to 0 C and stirred for 2 hours. The reaction was quenched with 10 ml sat.  $\text{NaHCO}_3$ . The organic layer was separated and aq. layer extracted with 40ml DCM. The combined organic layers were washed with brine and water and dried over magnesium sulfate. The solvent was

removed under reduced pressure.  $^1\text{H}$  NMR [400 MHz,  $\text{CDCl}_3$ ]  $\delta$  9.67 (s, 1H), 7.29 (m, 2H), 7.21 (m, 3H), 3.63 (m, 2H), 5.09 (s, 1H), 3.87 (m, 4H), 2.89 (bs, 2H), 2.47 (bs, 1H), 1.79 (bs, 1H), 1.56 (bs, 2H), 1.46 (bs, 2H)  $^{13}\text{C}$  NMR [100 MHz,  $\text{CDCl}_3$ ]  $\delta$  ; 201.07, 155.37, 137.02, 128.65, 127.97, 67.17, 60.50, 49.31, 44.58, 30.56, 21.11



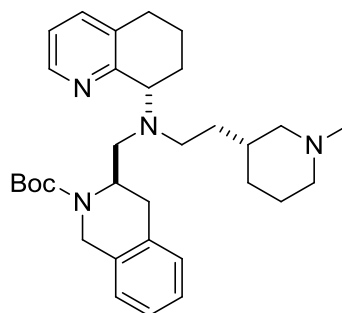
**(R)-tert-butyl-3-(((2-((R)-1-((benzyloxy)carbonyl)piperidin-3-yl)ethyl)((S)-5,6,7,8-tetrahydroquinolin-8-yl)amino)methyl)-3,4-dihydroisoquinoline-2(1H)-carboxylate (99):**

To a solution of **26** (1.30 g, 3.30 mmol) in DCE (35 mL) was added **98** (0.863 g, 3.30 mmol). To this mixture was added sodium triacetoxyborohydride (1.05 g, 4.96 mmol) in one portion. The reaction was kept at ambient temperature and allowed to stir overnight. The reaction mixture was quenched with saturated  $\text{NaHCO}_3$  and the aqueous phase extracted with DCM (2 x 200 mL). The organic extracts were combined, washed with brine, and dried over  $\text{MgSO}_4$ . The solvent was removed *in vacuo* yielding a light yellow oil. Crude material was purified by gravity chromatography (120 g silica gel, 2% MeOH in DCM, containing 0.5%  $\text{Et}_3\text{N}$ ) to afford a light yellow foam (1.78g, 84%).



**(R)-tert-butyl-3-(((2-((R)-piperidin-3-yl)ethyl)((S)-5,6,7,8-tetrahydroquinolin-8-yl)amino)methyl)-3,4-dihydroisoquinoline-2(1H)-carboxylate (100):**

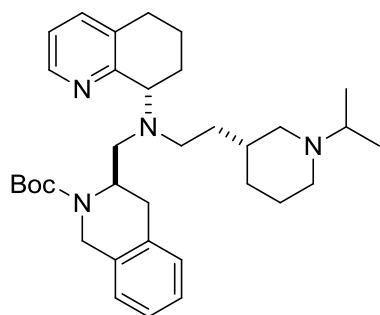
To a solution of 25 mL EtOAc was added **26**. Pd/C (10% by weight, 0.300 mg) was then added in one portion. The reaction was allowed to proceed in the Parr hydrogenator overnight. The reaction was filtered over celite and washed with EtOAc. The yellow foam was carried on without further purification (0.630 g, 80%).



**(R)-tert-butyl-3-(((2-((R)-1-methylpiperidin-3-yl)ethyl)((S)-5,6,7,8-tetrahydroquinolin-8-yl)amino)methyl)-3,4-dihydroisoquinoline-2(1H)-carboxylate (101):**

To a solution of **100** (0.330 g, 6.54 mmol) in DCE (35 mL) was added formaldehyde (0.079 g, 2.62 mmol). To this mixture was added sodium triacetoxyborohydride (0.346 g, 1.63 mmol) in one portion. The reaction was kept at ambient temperature and allowed to stir overnight. The reaction mixture was quenched with saturated NaHCO<sub>3</sub> and the aqueous phase extracted with DCM (2 x 200 mL). The organic extracts were combined, washed with brine, and dried over

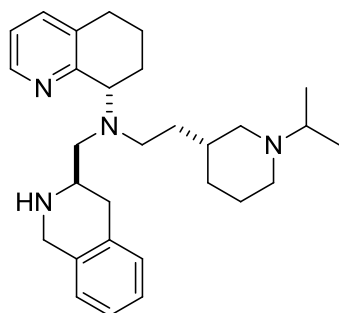
MgSO<sub>4</sub>. The solvent was removed *in vacuo* yielding a light yellow oil. The solvent was removed *in vacuo* yielding a light yellow oil. Crude material was purified by gravity chromatography (120 g silica gel, 2% MeOH in DCM, containing 0.5% Et<sub>3</sub>N) to afford a light yellow foam. <sup>1</sup>H NMR [600 MHz, CDCl<sub>3</sub>] δ 8.37 (d, *J* = 24 Hz, 1H), 7.24 (d, *J* = 7.8 Hz, 1H), 7.09-7.04 (m, 3H), 6.99-6.96 (m, 2H), 4.63 (m, 2H), 4.12 (d, *J* = 17.4 Hz, 1H), 3.89 (d, *J* = 24 Hz, 1H), 3.11-3.09 (m, 1H), 2.28 (d, *J* = 16 Hz, 1H), 2.79 (d, *J* = 16 Hz, 1H), 2.72-2.68 (m, 2H), 2.67-2.57 (m, 4H), 2.52-2.51 (m, 1H), 2.46-2.42 (m, 1H), 2.02-1.98 (m, 1H), 1.82-1.81 (m, 1H), 1.75-1.70 (m, 1H), 1.61-1.52 (m, 5H), 1.48 (s, 9H), 1.31-1.27 (m, 1H), 1.23-1.19 (m, 1H), 1.112-1.088 (m, 3H) ; <sup>13</sup>C NMR [100 MHz, CDCl<sub>3</sub>] δ 158.10, 155.06, 146.96, 136.24, 134.06, 133.03, 129.10, 126.24, 126.02, 125.81, 121.30, 62.47, 61.39, 56.20, 54.82, 53.87, 49.50, 49.15, 47.86, 46.53, 46.12, 43.06, 34.34, 30.45, 30.45, 29.13, 28.59, 26.49, 25.36, 21.18, 10.91



**(R)-tert-butyl 3-(((2-((R)-1-isopropylpiperidin-3-yl)ethyl)((S)-5,6,7,8-tetrahydroquinolin-8-yl)amino)methyl)-3,4-dihydroisoquinoline-2(1H)-carboxylate (103):**

To a solution of **100** (0.330 g, 6.54 mmol) in DCE (35 mL) was added formaldehyde (0.079 g, 2.62 mmol). To this mixture was added sodium triacetoxyborohydride (0.346 g, 1.63 mmol) in one portion. The reaction was kept at ambient temperature and allowed to stir overnight. The reaction mixture was quenched with saturated NaHCO<sub>3</sub> and the aqueous phase extracted with DCM (2 x 200 mL). The organic extracts were combined, washed with brine, and dried over

MgSO<sub>4</sub>. The solvent was removed *in vacuo* yielding a light yellow oil. Crude material was purified by gravity chromatography (20 g silica gel, 2% MeOH in DCM, containing 0.5% Et<sub>3</sub>N) to afford a light yellow foam <sup>1</sup>H NMR [600 MHz, CDCl<sub>3</sub>] δ 8.37 (d, *J* = 24 Hz, 1H), 7.24 (d, *J* = 7.8 Hz, 1H), 7.10-7.08 (m, 3H), 6.99-6.96 (m, 2H), 4.66-4.64 (m, 2H), 4.12 (d, *J* = 16 Hz, 1H), 3.89 (d, *J* = 24 Hz, 1H), 2.05-1.93 (m, 3H), 1.74-1.72 (m, 2H), 1.62-1.54 (m, 6H), 1.49-1.46 (m, 12H); <sup>13</sup>C NMR [100 MHz, CDCl<sub>3</sub>] δ 158.64, 155.53, 147.38, 136.68, 134.50, 133.53, 129.90, 129.51, 126.67, 126.41, 126.23, 80.06, 66.28, 62.03, 55.89, 55.38, 50.04, 49.83, 46.64, 43.49, 34.67, 31.95, 30.86, 29.57, 29.05, 27.22, 26.04, 21.62, 18.46, 15.71, 11.82



**(S)-N-(2-((R)-1-isopropylpiperidin-3-yl)ethyl)-N-(((R)-1,2,3,4-tetrahydroisoquinolin-3-yl)methyl)-5,6,7,8-tetrahydroquinolin-8-amine (104):**

Compound **103** was dissolved in a 3:1 mixture of DCM and TFA and the solution stirred for 3h at ambient temperature. The solvent was removed under reduced pressure and pH adjusted to 8-10 with aqueous NaHCO<sub>3</sub>. The aqueous phase was extracted with DCM (2 x 100 mL), dried over anhydrous magnesium sulfate and solvent removed under reduced pressure. The solvent was removed *in vacuo* yielding a light yellow oil. Crude material was purified by gravity chromatography (20 g silica gel, 2% MeOH in DCM, containing 0.5% Et<sub>3</sub>N) to afford a light yellow foam. <sup>1</sup>H NMR [600 MHz, CDCl<sub>3</sub>] δ 8.37 (d, *J* = 24 Hz, 1H), 7.24 (d, *J* = 7.8 Hz, 1H), 7.09-7.04 (m, 3H), 6.99-6.96 (m, 2H), 4.63 (m, 2H), 4.12 (d, *J* = 17.4 Hz, 1H), 3.89 (d, *J* = 24 Hz, 1H), 3.11-3.09 (m, 1H), 2.28 (d, *J* = 16 Hz, 1H), 2.79 (d, *J* = 16 Hz, 1H), 2.72-2.68 (m, 2H),

2.67-2.57 (m, 4H), 2.52-2.51 (m, 1H), 2.46-2.42 (m, 1H), 2.02-1.98 (m, 1H), 1.82-1.81 (m, 1H), 1.75-1.70 (m, 1H), 1.61-1.52 (m, 5H), 1.48 (s, 9H), 1.31-1.27 (m, 1H), 1.23-1.19 (m, 1H), 1.112-1.088 (m, 3H) ;  $^{13}\text{C}$  NMR [100 MHz,  $\text{CDCl}_3$ ]  $\delta$  158.10, 155.06, 146.96, 136.24, 134.06, 133.03, 129.10, 126.24, 126.02, 125.81, 121.30, 62.47, 61.39, 56.20, 54.82, 53.87, 49.50, 49.15, 47.86, 46.53, 46.12, 43.06, 34.34, 30.45, 30.45, 29.13, 28.59, 26.49, 25.36, 21.18, 10.91; HPLC/MS purity (> 95%)  $r_t = 1.517$  at 254nm, 50-95% MeOH over 3 minutes.

### Methods for Computational Docking

The protein structures 3ODU and 3OE01 were downloaded from the PDB1 prepared and refined with the Maestro Protein Preparation tool, adding hydrogen atoms and optimizing the side chain positions to avoid vdW contacts. Grids were then generated for each structure, centered on the small molecule ligand IT1t in 3ODU and residues Arg2 and Aln3 of the peptide CVX15 in 3OE0. Compound **6** was then flexibly docked into each using standard precision (SP) flexible docking in Glide with default settings and keeping the top 25 poses for each ligand, followed by MM-GBSA optimization and rescoring. Using the mutation data available for AMD11070 as a guide, each pose was manually examined to determine which makes more contacts with residues deemed important for ligand binding, specifically Asp97, Asp171 and Glu288. Other possible important residues are Tyr45, Trp94 and Asp262. The poses that make interactions with any of these residues were kept and ranked by both the number of interactions to the six residues and MM-GBSA  $\Delta G$  binding scores. Each protein resulted in a different pose for ligand **6**. In 3ODU (IT1t structure) **6** forms salt bridges with Asp97 and Glu288 and a  $\pi$ -stacking interaction between the tetrahydroquinoline head group and Trp94. For 3OE0 (CVX15 peptide) the salt bridges occur with Asp171 and Glu288 instead. The comparison of these poses to the elucidated

SAR exhibited on derivatives of compound **6** is the topic of further study, and addressed in *vide infra* (Chapter 4).

### 3.7 Biological Experimental

#### 3.6.1 Evaluation in MAGI-CCR5/CXCR4 Cells with T-tropic virus.

Experiments performed at Southern Research Institute, Frederick MD.

##### MAGI Antiviral Assay with HIV-1IIIIB

Cell Preparation: MAGI-CCR5/CXCR4 cells (obtained from the NIH AIDS Research and Reference Reagent Program) are passaged in T-75 flasks prior to use in the antiviral assay. MAGI-CCR5/CXCR4 cells are derived from HeLa-CD4-LTR- $\beta$ -gal cells. The cells have been engineered to express high levels of CD4 and CXCR4 and contain one copy of the HIV-1 LTR promoter driving expression of the  $\beta$ -galactosidase gene upon HIV-1 Tat transactivation. On the day preceding the assay, the cells are plated at  $1 \times 10^4$  well and incubated at 37° C overnight. Total cell and viability quantification is performed using a hemacytometer and trypan blue exclusion. Cell viability is greater than 95% for the cells to be utilized in the assay.

Virus Preparation: The virus used for these tests is the CXCR4-tropic strains HIV-1IIIIB. This virus was obtained from the NIH AIDS Research and Reference Reagent Program and was grown in Ghost Hi5/MAGI-CCR5/CXCR4 co-cultures for the production of stock virus pools. For each assay, a pre-titered aliquot of virus is removed from the freezer (-80°C) and allowed to thaw slowly to room temperature in a biological safety cabinet. The virus is re-suspended and diluted into tissue culture medium such that the amount of virus added to each well in a volume of 50  $\mu$ L is approximately ten TCID<sub>50</sub>/well (~0.001 TCID<sub>50</sub>/cell).

Assay Setup – Compounds are evaluated at one or two concentrations (e.g., for initial screening) or in dose-response at six concentrations (triplicate wells/concentration). On the day of assay

setup, compound dilutions are prepared at two-times (2X) the final required concentrations. Media used for plating the cells the day before assay setup is aspirated from the plates and replaced with 50  $\mu$ L of the 2X compounds, followed by the addition of 50  $\mu$ L of virus, which dilutes the compounds to the final 1X concentrations. Cell control wells (cells only) and virus control wells (cells plus virus) are included on each assay plate. Identical uninfected assay plates (virus replaced with media) are prepared for parallel cytotoxicity testing. The cultures are incubated for 48 hours or 6 days (depending on compound or client requirements) after which antiviral efficacy is measured as the inhibition of  $\beta$ -galactosidase reporter expression and cytotoxicity is monitored by MTS staining.

**$\beta$ -galactosidase Chemiluminescent Endpoint Analysis:** A chemiluminescent endpoint is used to determine the extent of  $\beta$ -galactosidase expression as a measure of HIV-1 infection of the cells. Once HIV-1 has attached and entered the MAGI-CXCR4 cells, HIV-1 Tat transactivates the LTR dependent  $\beta$ -galactosidase enzyme to express higher than normal levels of  $\beta$ -galactosidase. Thus there is a direct relationship between the level of HIV-1 infection and the level of  $\beta$ -galactosidase detected in the cells. At 48 hours or 6 days post infection, plates are aspirated and PBS is added to each well. Gal-screen reagent (Tropix, Bedford, MA) is then added per the manufacturer's instructions for chemiluminescent detection of  $\beta$ -galactosidase activity and incubated at room temperature for 90 minutes. The resulting chemiluminescence signal is then read using a Microbeta Trilux luminescence reader (PerkinElmer/Wallace).

**MTS Staining for Cell Viability:** At assay termination, the cytotoxicity assay plates are stained with the soluble tetrazolium-based dye MTS (CellTiter Reagent, Promega) to determine cell viability and quantify compound toxicity. MTS is metabolized by the mitochondrial enzymes of metabolically active cells to yield a soluble formazan product, allowing the rapid quantitative analysis of cell

viability and compound cytotoxicity. The MTS is a stable solution that does not require preparation before use. At termination of the assay, 15  $\mu$ L of MTS reagent is added per well. The microtiter plates are then incubated 1.5-2 hrs at 37°C; the incubation interval was chosen based on empirically determined time times for optimal dye reduction. The plates are read spectrophotometrically at 490/650nm with a Molecular Devices Vmax plate reader. Data Analysis: Percent inhibition of virus replication and percent cell viability at each concentration are calculated using an in-house computer program. For dose-response testing, IC<sub>50</sub> (50% inhibition of virus replication), IC<sub>90</sub> (90% inhibition of virus replication), TC<sub>50</sub> (50% cytotoxicity), and therapeutic index values (TI = TC<sub>50</sub>/IC<sub>50</sub>; also referred to as Antiviral Index or AI) are provided. Raw data for both antiviral activity and cytotoxicity with analyzed/tabulated data are provided in a printout summarizing the individual compound activity

### 3.6.2 Calcium Flux Assay

Experiments performed at Millipore, Inc. St. Charles, MO.

Calcium flux in human CXCR4-expressing (full length cDNA) Chem-1 cell line induced by SDF-1 $\alpha$ . CXCR4 -expressing Chem-1 cells were loaded with Fluo-4 and calcium flux in response to recombinant human SDF-1 $\alpha$  (10<sup>-5</sup> to 10<sup>-9</sup> M) was determined in triplicate on a Molecular Devices FLIPR-TETRA™ Flex Station. Inhibition of SDF-1 $\alpha$ -mediated calcium flux in CXCR4-expressing Chem-1 cells by test compounds. CXCR4 expressing Chem-1 cells were loaded with Fluo-4, washed, and pre incubated with the indicated concentrations of test compounds for 10 min. Calcium flux in response to 5 nM recombinant human SDF-1 $\alpha$  was determined on a Molecular Devices Flex Station. An EC<sub>50</sub> for calcium mobilization by SDF-1 $\alpha$  of ~ 4 nM with Signal/noise at ligand E<sub>max</sub>=542 and Z' = 0.82 with SDF-1 $\alpha$  at the EC<sub>50</sub>. An IC<sub>50</sub> of 57 nM was obtained for AMD3100.

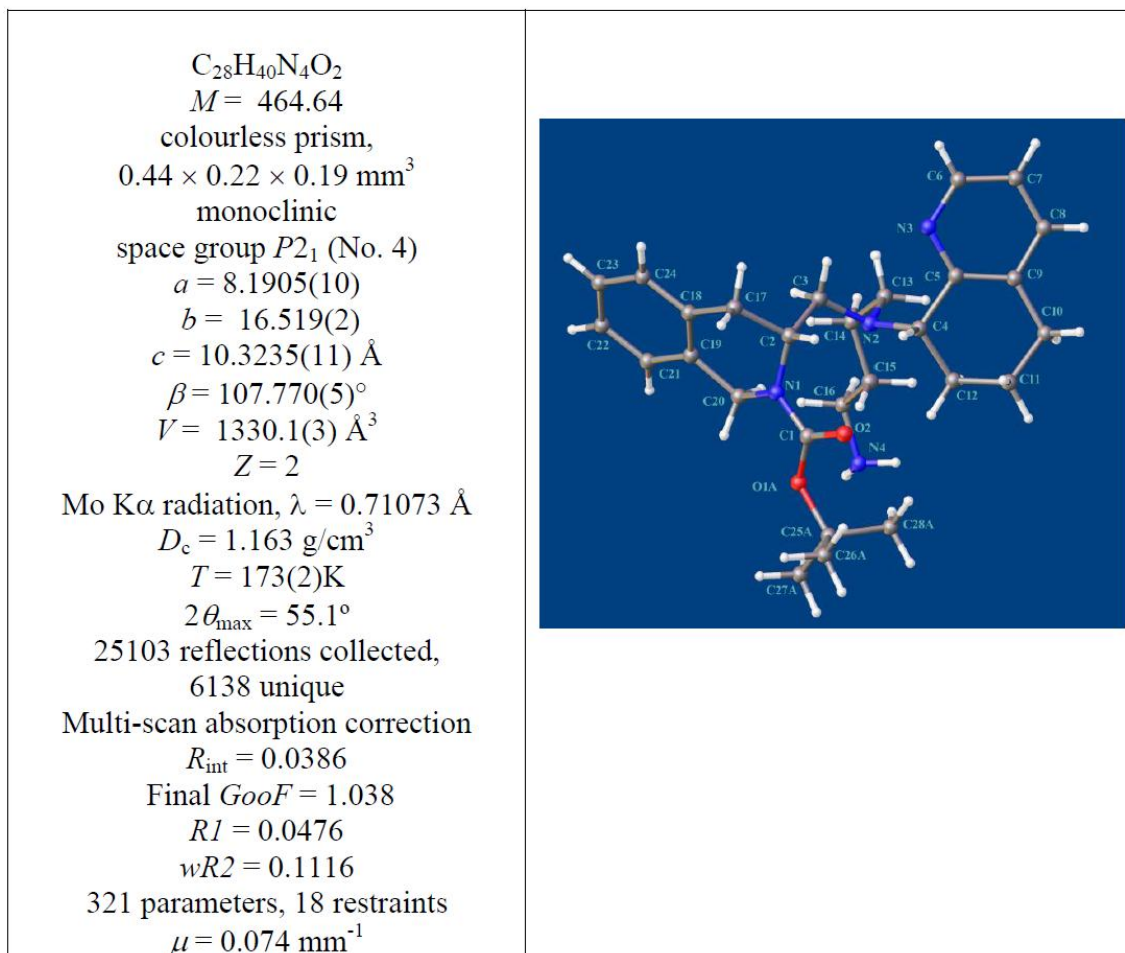
**Compound and Plate Preparation :**Compounds were prepared in DMSO, and ultimately prepared in EMD Millipore's GPCR Profiler Assay Buffer<sup>®</sup> to concentrations that were three fold higher than the final assay concentration. Similarly, vehicle controls and positive controls were prepared to ensure all assays were properly controlled. The GPCR Profiler Assay Buffer was a modified Hanks Balanced Salt Solution (HBSS) where HBSS was supplemented to contain 20mM HEPES and 2.5mM Probencid at pH 7.4.

**Agonist Assay :**Compounds were plated in duplicate for each concentration assayed. During the agonist assay, the concentrations reflect accommodation for the dilution of compound during the Antagonist Assay. Reference agonist for each GPCR assayed was prepared in a similar manner to serve as assay control. The reference agonist for each GPCR was included at  $E_{max}$  (the concentration where the reference agonist elicited a maximal response). The agonist assay was conducted on a FLIPR<sup>TETRA</sup> instrument where the test compounds, vehicle controls, and reference agonist were added to the assay plate after a fluorescence/luminescence baseline was established. The agonist assay was a total of 180 seconds and was used to assess each compounds ability to activate each GPCR assayed. Upon completion of the three minute agonist assay, the assay plate was incubated at 25 C for further seven or two minutes. After the incubation period the antagonist assay was initiated.

**Antagonist Assay :** Using  $EC_{80}$  potency values determined during the agonist assay, all pre-incubated sample compound wells were challenged with  $EC_{80}$  concentration of reference agonist after establishment of a fluorescence/luminescence baseline. The antagonist assay was conducted using the same assay plate that was used for the agonist assay. The antagonist assay was conducted on a FLIPR<sup>TETRA</sup> instrument where vehicle controls and  $EC_{80}$  concentration of

reference agonist were added to appropriate wells. The antagonist assay was a total of 180 seconds and was used to assess each compound's ability to inhibit each GPCR assayed.

### Crystal Structure of 64



### Data collection, structure solution and refinement (John Basco, Ph.D.)

The crystals grew as large, intergrown prisms. A single crystal was cut into a suitable size for the analysis and mounted onto a nylon fibre with paratone oil and placed under a cold stream at 173K. Single crystal X-ray data were collected on a Bruker APEX2 diffractometer with 1.6 kW graphite monochromated Mo radiation. The detector to crystal distance was 5.1 cm. Exposure times of 20 s and scan widths of  $0.5^\circ$  were used throughout the data collection. The data

collection was performed using a combination of  $\omega$  scans and  $\phi$  scans yielding data in the range 2.07 to 27.57° with an average completeness of 99.7%. The frames were integrated with the SAINT v7.68a (Bruker, 2009). The structure was solved and refined with Olex22 and SHELX (Sheldrick, 2008). The hydrogen atoms were located from difference electron density maps but were refined with constraints. In the final cycles of refinement all non-hydrogen atoms were refined anisotropically. The crystal structure is a chiral. However, the uncertainties in the Flack and Hooft parameters were too large to determine its absolute structure. Under normal circumstances for light atom structures the absolute structure cannot be determined with Mo K $\alpha$  radiation. The TBOC group is disordered. The disorder was modeled using two components with similarity restraints for the atom 1,2 and 1,3 distances and constraints on thermal parameters for individual split atoms. The populations of the components refined to 53% and 43%. Plots of the structure with and without disorder are shown in Figures 3.9

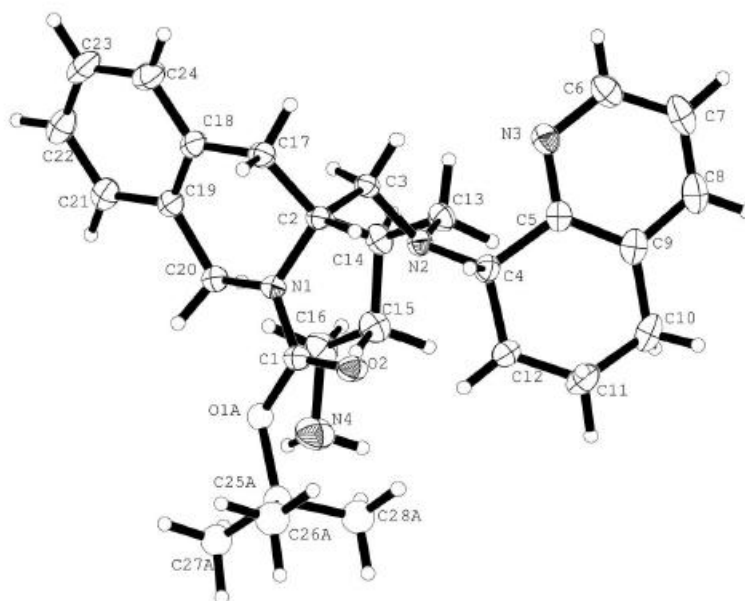


Figure 3.9: Thermal ellipsoid plot of the molecular structure.

### 3.6.2 Caco-2

Cell monolayers were grown to confluence on collagen-coated, microporous, polycarbonate membranes in 12-well Costar Transwell plates. The permeability assay buffer was Hanks Balanced Salt Solution containing 10 mM HERPES and 15 mM glucose at pH of 7.4. The buffer in the receiver chamber also contained 1 bovine serum albumin. The dosing solution concentration was 5  $\mu$ M test compound in the assay buffer. Cell monolayers were dosed on the apical side (A-to-B) or basolateral side (B-to-A) and incubated at 37° C with 5% CO<sub>2</sub> in a humidified incubator. Samples were taken from the donor and receiver chambers at 120 minutes. Each determination was performed in duplicate. The co-dosed lucifer yellow flux was also measured for each monolayer to ensure no damage was inflicted to the cell monolayers during the flux period. All samples were assayed by LC-MS/MS using electrospray ionization. The apparent permeability,  $P_{app}$ , and percent recovery were calculated as follows:

$$P_{app} = (dC_r/dt) \times V_r / (A \times C_A)$$

$$\text{Percent Recovery} = 100 \times (V_r \times C_r^{\text{final}}) + (V_d \times C_d^{\text{final}}) / (V^d \times C_N)$$

## References

1. Skerlj, R. T.; Bridger, G. J.; Kaller, A.; McEachern, E. J.; Crawford, J. B.; Zhou, Y.; Atsma, B.; Langille, J.; Nan, S.; Veale, D.; Wilson, T.; Harwig, C.; Hatse, S.; Princen, K.; De Clercq, E.; Schols, D., Discovery of novel small molecule orally bioavailable C-X-C chemokine receptor 4 antagonists that are potent inhibitors of T-tropic (X4) HIV-1 replication. *Journal of medicinal chemistry* **2010**, *53* (8), 3376-88.
2. (a) Jenkinson, S.; Thomson, M.; McCoy, D.; Edelstein, M.; Danehower, S.; Lawrence, W.; Wheelan, P.; Spaltenstein, A.; Gudmundsson, K., Blockade of X4-tropic HIV-1 cellular entry by GSK812397, a potent noncompetitive CXCR4 receptor antagonist. *Antimicrobial agents and chemotherapy* **2010**, *54* (2), 817-24; (b) Miller, J. F.; Turner, E. M.; Gudmundsson, K. S.; Jenkinson, S.; Spaltenstein, A.; Thomson, M.; Wheelan, P., Novel N-substituted benzimidazole CXCR4 antagonists as potential anti-HIV agents. *Bioorganic & medicinal chemistry letters* **2010**, *20* (7), 2125-8.
3. Nyunt, M. M.; Becker, S.; MacFarland, R. T.; Chee, P.; Scarborough, R.; Everts, S.; Calandra, G. B.; Hendrix, C. W., Pharmacokinetic effect of AMD070, an Oral CXCR4 antagonist, on CYP3A4 and CYP2D6 substrates midazolam and dextromethorphan in healthy volunteers. *Journal of acquired immune deficiency syndromes* **2008**, *47* (5), 559-65.
4. Abdel-Magid, A. F.; Carson, K. G.; Harris, B. D.; Maryanoff, C. A.; Shah, R. D., Reductive Amination of Aldehydes and Ketones with Sodium Triacetoxyborohydride. Studies on Direct and Indirect Reductive Amination Procedures(1). *The Journal of organic chemistry* **1996**, *61* (11), 3849-3862.
5. Campiglia, P.; Gomez-Monterrey, I.; Lama, T.; Novellino, E.; Grieco, P., A new efficient synthetic methodology for tetrahydroisoquinoline and tetrahydro-beta-carboline derivatives using the Pictet-Spengler reaction. *Molecular diversity* **2004**, *8* (4), 427-30.
6. Neelapapu, R.; Petukhov, P. A., A One-Pot Selective Synthesis of N-Boc Protected Secondary Amines: Tandem Direct Reductive Amination/N-Boc Protection. *Tetrahedron* **2012**, *68* (35), 7056-7062.
7. Wu, B.; Chien, E. Y.; Mol, C. D.; Fenalti, G.; Liu, W.; Katritch, V.; Abagyan, R.; Brooun, A.; Wells, P.; Bi, F. C.; Hamel, D. J.; Kuhn, P.; Handel, T. M.; Cherezov, V.; Stevens, R. C., Structures of the CXCR4 chemokine GPCR with small-molecule and cyclic peptide antagonists. *Science* **2010**, *330* (6007), 1066-71.

## 4 Discovery of Novel CXCR4 Allosteric Modulators

### 4.1 Statement of Purpose

In our interest in the development of novel first in class CXCR4 allosteric modulators, we were intrigued by the trend observed (*vide supra*, Chapter 3) whereby oxazole (**64**), select electron-deficient heterocycles (**10**), and pyridine isomers (**56-57**) exhibited disparate inhibitory activity profiles in HIV-1 co-receptor function versus the normal function of CXCR4. Because the interaction between CXCR4 and its natural ligand CXCL12 is not only involved in HIV entry, but also synchronizes many essential physiological roles, such as homeostatic regulation of leukocyte trafficking, hematopoiesis, and embryonic development<sup>1</sup>; selective inhibition of X4-tropic HIV-1 entry without compromising the physiologically important signaling between CXCR4 and CXCL12 is both crucial and therapeutically relevant.

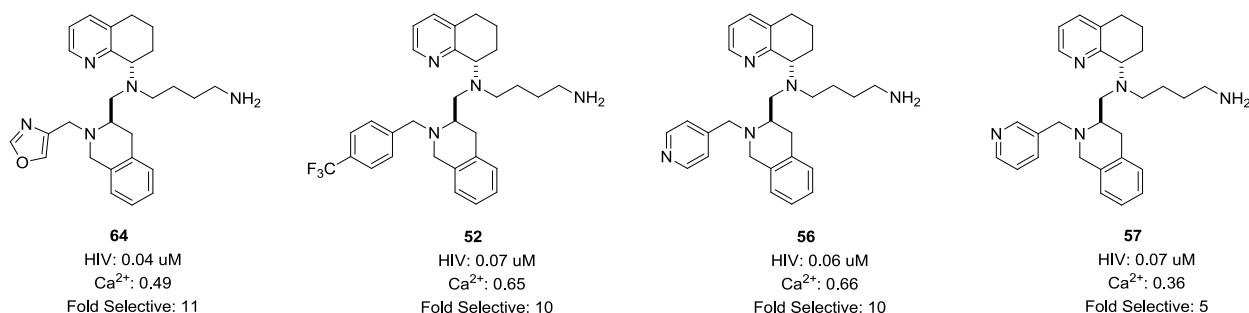


**Figure 4.1:** Tetrahydroisoquinoline-based selective HIV compounds.

Consequently, the development of CXCR4 allosteric modulators is urgently needed to: 1) block X4 HIV-1 entry, 2) reduce the occurrence of translational intermediate variants that can successfully switch to CXCR4-using variants (from CCR5, or R5-tropic), and 3) overcome

potential viral drug resistance against CCR5 inhibitors, such as Maraviroc.<sup>2</sup> The approval of the first CXCR4 antagonist, AMD3100 (Mozobil™) inspired the development of a plethora of AMD3100-type analogs, which were utilized as pre-clinical, and clinical candidates (*vide supra*, Chapters 1-3). Since AMD3100's discovery, greater than 1000 compounds have been disclosed in the development of novel CXCR4 antagonists for X4-tropic HIV-1 entry inhibition.<sup>3</sup> However, within this class, there are no small molecule CXCR4 allosteric modulators exemplified. As a result, there is still much to learn about the relationship between the CXCR4 receptor, its natural ligand CXCL12 and if, and to what extent the physiological and pathological pathways between can be dissected. In order to gain a greater understanding of this relationship, the Liotta group sought to identify and develop the first small molecule CXCR4 allosteric modulators. The goal was to lay the foundation for further expansion in the research community, and develop a vast knowledge base in this arena. The compounds disclosed herein represent the first reported novel small molecule allosteric CXCR4 modulators that mediate X4 HIV-1, while at the same time preserve the natural chemokine function between CXCR4/CXCL12. Exemplary compounds exhibit two important properties:

1. Highly potent CXCR4 allosteric modulators that block X4 HIV-1 entry.
2. Highly potent CXCR4 allosteric modulators that preserve the normal function of CXCR4 and do not inhibit CXCL12 induced  $\text{Ca}^{2+}$  flux.

In addition, drug-like characteristics in terms of absorption, distribution, metabolism, and excretion (ADME) parameters is required. These project goals were achieved using the following strategy:

1. A series of novel modulators based on knowledge gained from the chiral tetrahydroisoquinolines (*vide supra*, Chapter 3) series were synthesized.
2. The analogues were tested for *in vitro* CXCR4 receptor activity in an HIV-1 infectivity assay. All *in vitro* biological evaluation of synthesized analogues were carried out by Southern Research Institute.
3. The analogues were tested in an *in vitro* Calcium flux assay by Millipore.
4. Molecular modeling was utilized to guide the medicinal chemistry efforts.
5. Compound(s) that exhibited greater than 10 fold HIV selectivity were tested *in vitro* for CXCL12 binding displacement, and cytochrome p450 isozyme inhibition. All ADME *in vitro* biological evaluation of analogues were carried out by Eurofin PanLabs.

## 4.2 Introduction and Background

### Allosteric Modulation

Classical drugs, agonists, partial agonists, antagonists, or partial inverse agonists bind to the orthosteric site; the same site where the physiological agonist binds (Figure 4.1).<sup>4</sup> Proteins and receptors can also be allosterically regulated where a ligand binds to a site distinct from the orthosteric site, the allosteric site, changes the conformation of the protein and thereby modulates the protein's binding properties and/or functions.<sup>5</sup> Allosteric modulators as drugs are well known for ligand-gated ion channels. However, the concept of targeting an allosteric binding site at GPCRs is a relatively new concept in drug discovery and development.<sup>6</sup> Only recently have the first allosteric modulators for GPCRs been approved: Cincalet, a positive allosteric modulator (PAM) of the calcium-sensing receptor (Class C GPCR), and Maraviroc, a negative

allosteric modulator of the chemokine receptor CCR5 (Class A GPCR) used as a virus entry inhibitor for R-tropic HIV virus.<sup>2</sup> It is well known CXCR4 mediates entry for X4-tropic virus. It has additionally been shown AMD3100 blocks both CXCR4 receptor mediated HIV entry and signaling of the natural agonist CXCL12. Because CXCR4 also actively participates in the retention of hematopoietic cells in the bone marrow, and it is functionally expressed on many other cell types, the long term blockage of the CXCR4/CXCL12 axis, as required for long-term inhibition of X4 viral entry, may result in significant adverse effects.<sup>1,7</sup> Therefore, a modulator that blocks the function of this receptor as a mediator of X4 HIV virus (pathological effect) while preserving natural chemokine function (physiological effect) is therapeutically important in the treatment of AIDS.

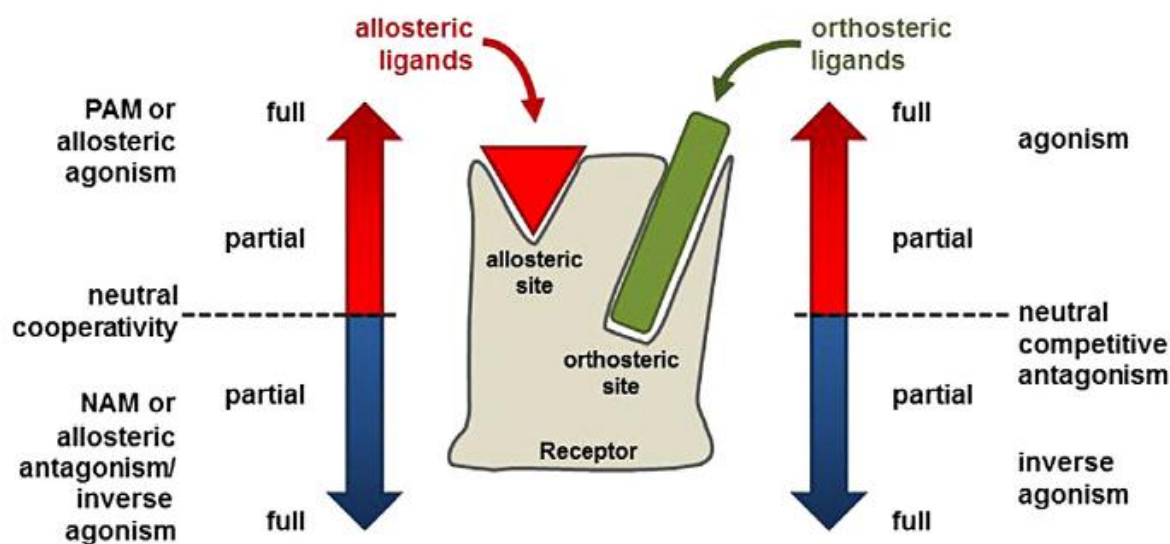
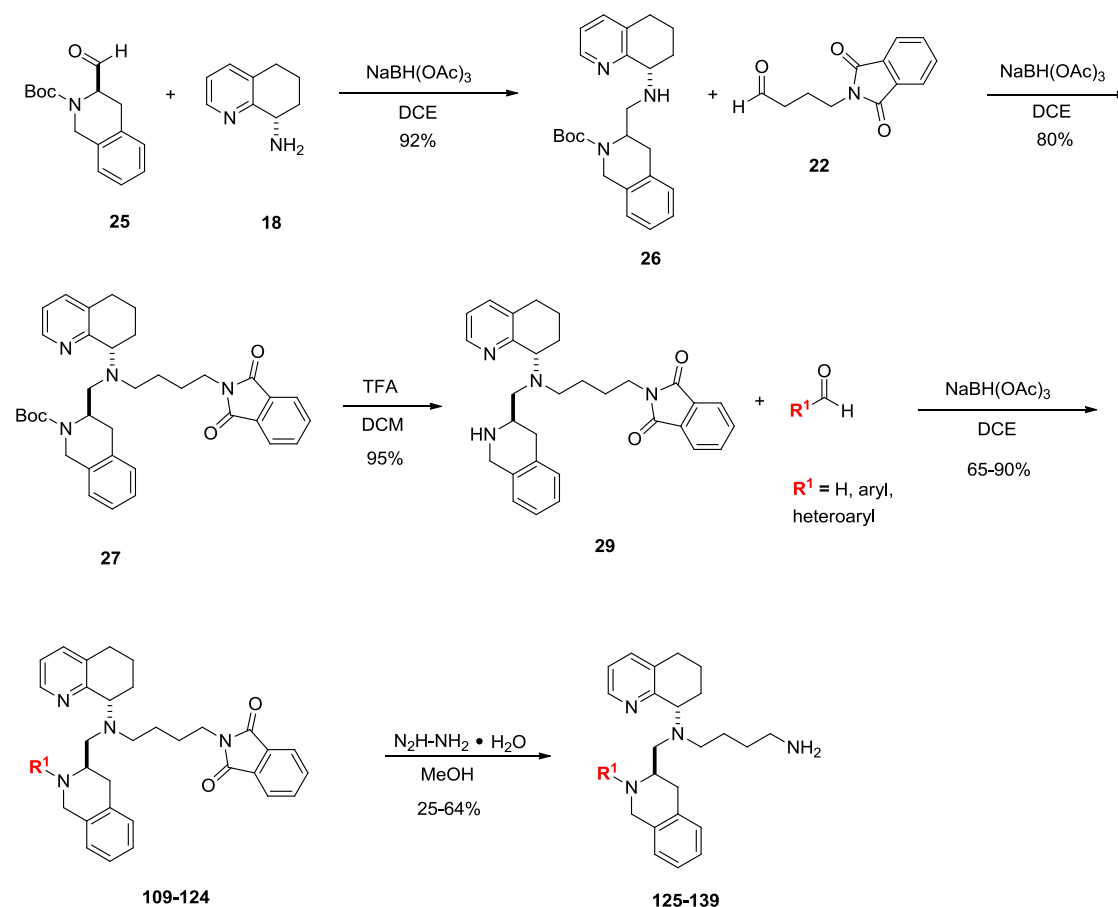


Figure 4.2: Allosteric and orthosteric ligands of G protein-coupled receptors; range of possible activities.<sup>8</sup>

### 4.3 Design Rational

Given the disparate activity profiles of compounds (**52**, **64**, **56-57**) in their ability to potently block HIV-1<sub>IIIB</sub> attachment via the CXCR4 receptor in MAGI cells, as well as their

reduced ability to inhibit CXCL12 induced calcium ( $\text{Ca}^{2+}$ ) flux/release in Chem-1 cells, the Liotta group sought to further investigate in this remarkable observation. This included an investigation into making conservative modifications on the N-TIQ. To accomplish this goal a variety of 5-membered heterocycles, bulkier heterocycles, diazines, and pyrimidines with both electron withdrawing and donating substituents were synthesized. The structure activity relationship of CXCR4 potency was explored to determine if, and to what extent lessons gleaned from the work on the chiral tetrahydroisoquinoline series (*vide supra*, Chapter 3) could be used in the discovery and optimization of a novel tetrahydroisoquinoline based CXCR4 allosteric modulator series. These compounds were synthesized as illustrated in Scheme 3.4. Reductive amination with aldehyde **26** and chiral amine **18** furnished secondary amine **26**. Subsequent reductive amination of **26** with butylaldehyde **22** followed by separation of the diastereomers provided the desired advanced intermediate **27**. Boc deprotection followed by reductive amination with commercially available aldehydes provided N-THIQ modified compounds **109-124**. Phthalimide deprotection with hydrated hydrazine furnished final analogs **125-139**.

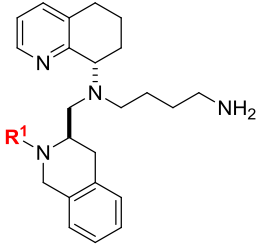
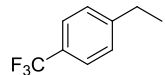
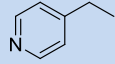
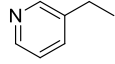
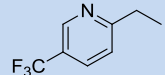
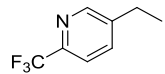
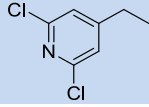
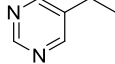
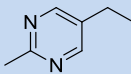
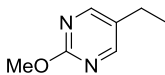
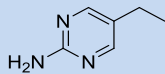
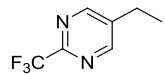


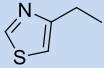
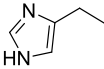
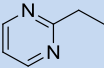
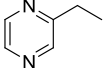
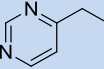
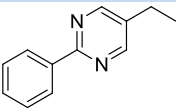
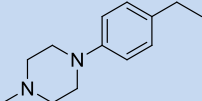
Scheme 4.1: Synthesis of N-TIC analogs 125-139.

### 4.3 Results and Discussion

The data used to elucidate the structure activity relationships (SAR) of these series was generated by a combination of two assays: 1) blockade of HIV-1<sub>III<sub>B</sub></sub> attachment via the CXCR4 receptor in MAGI cells, and 2) the inhibition of CXCL12 induced calcium (Ca<sup>2+</sup>) flux/release in Chem-1 cells. The compounds revealed a range of potencies and divergent SAR. All compounds were put in both agonist and antagonist modes in the calcium flux, and none showed any agonist activity, while showing blockade of SDF-1 induced calcium flux at various potencies (Table 1).

Substitution on the tetrahydroisoquinoline nitrogen with 5-membered heterocycles (**133-134**, Table 1) and bulkier heterocycles (**138-139**, Table 1) resulted in equipotent inhibition in the MAGI attachment assay. Thiazole **134**, a 5 fold loss in potency for imidazole **133**, and 4-10 fold loss in potency for bulkier heterocycles **138-139** when compared to **64**. Both of these groups exhibited similar potency for CXCL12 induced  $\text{Ca}^{2+}$  flux, where the HIV selectivity was 10 fold when compared to **64**. Substitution with electron donating or withdrawing groups on diazines **129-132** surprisingly did not result in divergent SAR with regard to either potency in the HIV infectivity assay or CXCL12 induced  $\text{Ca}^{2+}$ . Most interestingly was the divergent SAR observed for diazine analogs (**128**, **135-138**). While there was generally equal anti-HIV potency compared to **64**, there was a significant and poignant decrease in the ability of compound **137** to block CXCL12 induced  $\text{Ca}^{2+}$ , resulting in approximately a 2500 fold selectivity in the ability to mediate HIV entry.

Compound #	 $R^1$	Magi-HIV-1 <sub>III</sub> B IC <sub>50</sub> (μM) <sup>a</sup>	Ca <sup>2+</sup> Flux IC <sub>50</sub> (μM) <sup>a</sup>	Fold Selectivity Ca <sup>2+</sup> /HIV
64		0.04	0.49	12
52		0.07	0.05	10
56		0.06	0.66	10
57		0.07	0.36	5
125		0.03	0.21	7
126		0.08	0.599	7
127		0.1	1	10
128		0.01	3.00	300
129		0.03	0.03	-
130		0.04	0.16	4
131		0.04	0.16	4
132		0.28	.15	-

<b>133</b>		0.03	.033	-
<b>134</b>		0.27	0.076	-
<b>135</b>		0.02	0.12	10
<b>136</b>		0.22	0.011	-
<b>137</b>		0.003	7.7	2500
<b>138</b>		0.14	0.41	4
<b>139</b>		0.09	1.2	10

<sup>a</sup> Assays run in triplicate.

**Table 4.1:** Tetrahydroisoquinoline analogs 125-139; (64, 52, 56-57 *vide supra*, Chapter 3)

As compound **137** was identified as the most potent CXCR4 allosteric antagonist discovered in this series, we sought to examine other *in vitro* CXCR4 based properties. As a confirmation of antiviral properties, screening in peripheral blood mononuclear cells (PBMCs), resulted in IC<sub>50</sub> and IC<sub>90</sub> values of 60 and 220 nM, respectively, for the blockade of infection of HIV-1<sub>IIIB</sub>. Similar to the TC<sub>50</sub> result observed in the MAGI assay, at these concentrations cytotoxicity was not observed in PMBCs, resulting in a therapeutic index of > 1000. Further validation of CXCR4 allosteric modulator behavior was provided by a competitive binding assay. Competitive binding studies with radiolabeled <sup>125</sup>I-SDF-1 showed displacement of the chemokine with an IC<sub>50</sub> value of 1.7 μM for **137**, resulting in greater than 2000 fold selectivity for blockage of X4-HIV. In an initial effort to assess the drug potential of compound **137**, an

ADME based test was performed. In terms of human CYP450 inhibition studies for isozymes 2C19, 2D6, and 3A4 by compound **137**, the inhibition was minimal for isozymes 2C19, and 2D6 (*vide infra*, 4.6). Given these results, compound **137** was chosen for further medicinal chemistry and biological studies in this arena.

In an effort to understand the selectivity observed for **137**, we undertook a computational docking study in order to better understand the preliminary SAR study and develop a working hypothesis on how our compounds interact with the CXCR4 receptor. Using the recently reported CXCR4 receptor co-crystal structures we developed a computational model of both lead compounds **6** (*vide supra*, Chapter 3) and **137** bound to CXCR4 (Figure 4.3).

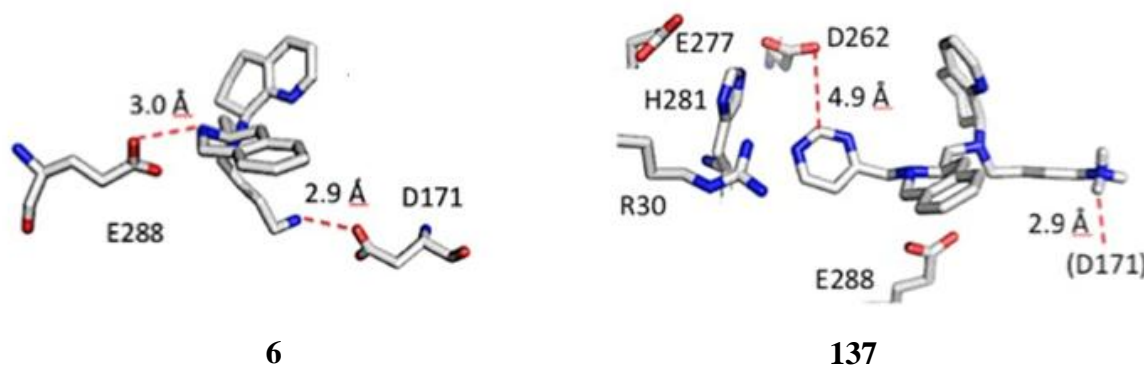


**Figure 4.3: Docking pose of compound 6 & 137 in the CVX15/30EU crystal structure.** Compound **6** (left). Compound **137** (right). Figures generated by James Snyder, Ph.D.

Because of the importance of the interaction of CVX15 with Asp171 and Glu288 in the peptide crystal structure, we hypothesized **6** would interact with the same residues.<sup>9</sup> Thus, we flexibly docked compound **6** into the CVX15 subsite of CXCR4 (PDB ID 30EU). In the best pose, the positively charged butyl amine of **6** interacts with the Asp171 carboxylate via a salt bridge and forms a while the protonated tetrahydroisoquinoline ring forms a salt bridge with Glu288 carboxylate. Based on this model, a regression analysis was performed for a congeneric series of

12 compounds resulting in a  $R^2=0.70$ . Using this model, we then docked we compound **137**. The compound conserves the charged interaction between the butylamine 171 seen in compound 6, but is unable to interact with Glu288, while the pyrimidine ring is surrounded by a cluster of charged amino acid side chains including Arg30, Asp262, Glu277, and His281. Notable is that both Glu288 and Asp262 residues are involved in the HIV gp120 interaction with CXCR4, while of the two only 288 is critical for SDF-1 based signaling.

## 4.5 Conclusions

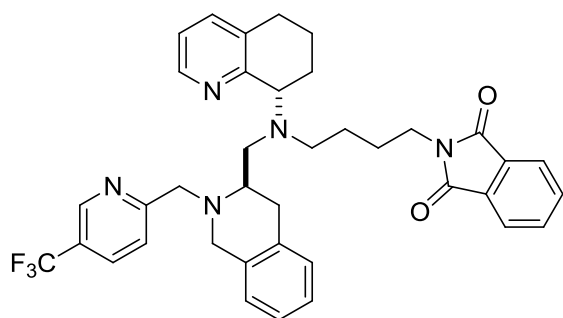
A novel series of highly potent and selective CXCR4 allosteric modulators based on a chiral tetrahydroisoquinolone ((*R*)-TIQ) scaffold was identified through a hit-to-lead effort focused on tetrahydroisoquinoline nitrogen substitution with 5-membered heterocycles, bulkier heterocycles, and a variety of diazines and pyrimidines. These modifications provided insight to the further development of novel compounds with unique biological selectivity and provided potent inhibition of T-tropic HIV select antagonists that do not interfere with CXCL12 based receptor signaling. These compounds represent a new class of CXCR4 allosteric modulators, and on the basis of the encouraging *in vivo* and *in vitro* properties of compound **137** has become the target for further lead optimization studies.

## 4.6 Chemistry Experimental

### General Procedure for Compounds 109-124:

To a solution of 2-(4-(((R-1,2,3,4-tetrahydroisoquinoline-3-yl)methyl((S)-5,6,7,8-tetrahydroquinolin-8-yl)amino)butyl)isoindoline-1,3-dione (**29**) (.300 g, 0.607 mmol) in DCE (6.0 mL) was added pyrimidine-5-carbaldehyde (.076 g, 0.708 mmol). To this mixture was added sodium triacetoxyborohydride (0.193 g, 0.910 mmol) in one portion. The reaction was kept at ambient temperature and allowed to stir overnight. The reaction mixture was quenched with  $\text{NaHCO}_3$  and the aqueous phase extracted with DCM (2 x 20 mL). The organic layers were combined, washed with brine, and dried over  $\text{MgSO}_4$ . The solvent was removed *in vacuo* yielding a yellow oil. Crude material was purified by gravity chromatography (10 g silica gel, 2% MeOH/DCM).

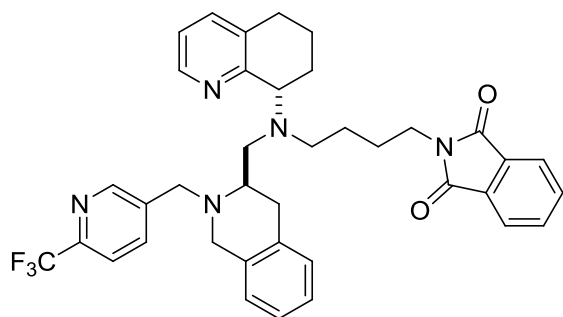
### Physical Data for Compounds 109-124:



### 2-(4-(((S)-5,6,7,8-tetrahydroquinolin-8-yl)amino)butyl)-1,2,3,4-tetrahydroisoquinolin-3-ylmethyl((R)-2-((5-(trifluoromethyl)pyridin-2-yl)methyl)amino)butyl)isoindoline-1,3-dione (**109**):

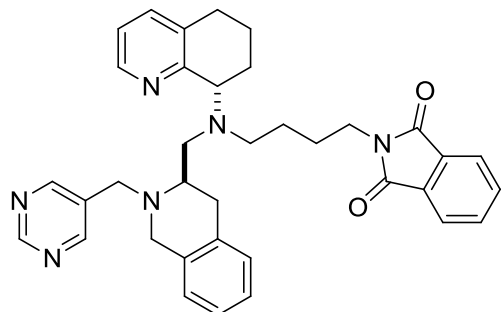
$^1\text{H}$  NMR [400 MHz,  $\text{CDCl}_3$ ]  $\delta$  8.44-8.40 (m, 2H), 7.78-7.69 (m, 2H), 7.67-7.65 (m, 2H), 7.24 (d, 1H,  $J = 6.8$  Hz), 7.09-7.08 (m, 3H), 6.98-6.96 (m, 1H), 6.89 (d, 1H,  $J = 6.8$  Hz), 4.01-3.99 (m, 1H), 3.84 (q, 2H,  $J = 14$  Hz), 3.64 (q, 2H,  $J = 14$  Hz), 3.06-3.04 (m, 1H), 2.95-2.94 (m, 1H),

2.86-2.82 (m, 2H), 2.71-2.61 (m, 5H), 2.60-2.54 (m, 2H), 1.98-1.95 (m, 2H), 1.82-1.79 (m, 1H), 1.71-1.79 (m, 1H), 1.43-1.39 (m, 4H);  $^{13}\text{C}$  NMR [100 MHz,  $\text{CDCl}_3$ ]  $\delta$ 158.13, 158.00, 155.79, 155.43, 146.99, 136.54, 135.85, 134.26, 134.21, 134.06, 133.29, 132.46, 129.44, 126.55, 126.41, 125.85, 123.24, 121.58, 121/16, 118.43, 61.41, 56.56, 53.22, 52.43, 51.77, 51.00, 41.99, 31.42, 29.70, 29.15, 26.13, 21.21 ; HRMS (ESI)  $[\text{M}+\text{H}]^+$ , calc'd for  $\text{C}_{38}\text{H}_{40}\text{N}_5\text{O}_2\text{F}_3$  653.29169, found 653.29157



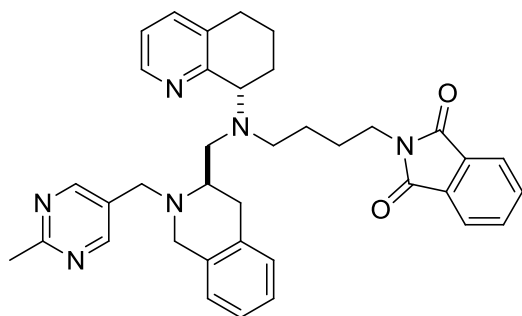
**2-(4-(((S)-5,6,7,8-tetrahydroquinolin-8-yl)(((R)-2-((6-(trifluoromethyl)pyridin-3-yl)methyl)-1,2,3,4-tetrahydroisoquinolin-3-yl)methyl)amino)butyl)isoindoline-1,3-dione (110):**

$^1\text{H}$  NMR [400 MHz,  $\text{CDCl}_3$ ]  $\delta$  8.42-8.40 (m, 2H) 7.77-7.72 (m, 2H), 7.65-7.64 (m, 2H), 7.24 (d, 1H,  $J = 6.8$  Hz), 7.31-7.29 (m, 1H) 7.08-7.07 (m, 3H), 6.98-6.96 (m, 1H), 6.89 (d, 1H,  $J = 6.8$  Hz), 4.01-3.99 (m, 1H), 3.84 (q, 2H,  $J = 14$  Hz), 3.64 (q, 2H,  $J = 14$  Hz), 3.06-3.04 (m, 1H), 2.95-2.94 (m, 1H), 2.86-2.82 (m, 2H), 2.71-2.61 (m, 5H), 2.60-2.54 (m, 2H), 1.98-1.95 (m, 2H), 1.82-1.79 (m, 1H), 1.71-1.79 (m, 1H), 1.43-1.39 (m, 4H);  $^{13}\text{C}$  NMR [100 MHz,  $\text{CDCl}_3$ ]  $\delta$ 161.13, 157.01, 154.76, 152.43, 142.89, 137.44, 134.86, 134.26, 134.20, 134.06, 133.28, 132.46, 129.35, 126.55, 126.41, 125.85, 123.24, 121.50, 121.16, 119.52, 62.32, 56.45, 52.23, 52.43, 51.68, 51.11, 41.89, 31.36, 29.71, 29.15, 26.13, 21.21 ; HRMS (ESI)  $[\text{M}+\text{H}]^+$ , calc'd for  $\text{C}_{38}\text{H}_{40}\text{N}_5\text{O}_2\text{F}_3$  653.29169, found 653.26742



**2-(4-(((R)-2-(pyrimidin-5-ylmethyl)-1,2,3,4-tetrahydroisoquinolin-3-yl)methyl)((S)-5,6,7,8-tetrahydroquinolin-8-yl)amino)butyl)isoindoline-1,3-dione (111):**

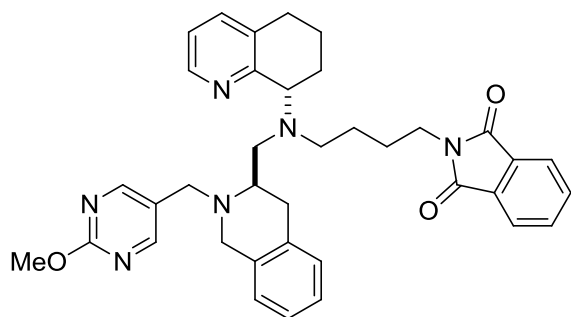
$^1\text{H}$  NMR [400 MHz,  $\text{CDCl}_3$ ]  $\delta$  9.14 (s, 1H), 8.73 (s, 2H,  $J = 3.6$  Hz), 8.44-8.42 (m, 1H), 7.85-7.83 (m, 2H), 7.35-7.71 (m, 2H), 7.28-7.27 (m, 1H), 7.13-7.07 (m, 3H), 7.01-6.98 (m, 1H), 6.91 (d, 1H, 7.2 Hz) 4.04-3.99 (m, 1H), 3.81-3.59 (m, 5H), 3.12-3.01 (m, 2H), 2.94-2.86 (m, 2H), 2.74-2.57 (m, 5H), 2.07-1.96 (m, 2H), 1.85-1.82 (m, 1H), 1.72-1.64 (m, 3H), 1.47-1.43 (m, 2H);  $^{13}\text{C}$  NMR [400 MHz,  $\text{CDCl}_3$ ]  $\delta$  168.51, 158.16, 157.74, 157.37, 146.99, 136.48, 134.30, 134.25, 133.98, 133.70, 133.18, 132.24, 129.46, 126.57, 126.39, 125.75, 123.26, 121.54, 61.68, 56.83, 53.33, 52.40, 52.04, 50.73, 38.00, 29.90, 29.23, 26.67, 26.57, 26.30, 21.22; HRMS (ESI)  $[\text{M}+\text{H}]^+$ , calc'd for  $\text{C}_{36}\text{H}_{39}\text{N}_6\text{O}_2$  587.31290, found 587.31499



**2-(4-(((R)-2-((2-methylpyrimidin-5-yl)methyl)-1,2,3,4-tetrahydroisoquinolin-3-yl)methyl)((S)-5,6,7,8-tetrahydroquinolin-8-yl)amino)butyl)isoindoline-1,3-dione (112):**

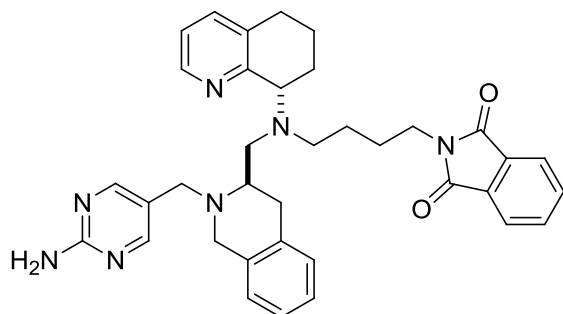
$^1\text{H}$  NMR [600 MHz,  $\text{CDCl}_3$ ]  $\delta$  8.45 (d, 1H,  $J = 4.2$  Hz), 7.84-7.82 (m, 2H), 7.72-7.70 (m, 2H), 7.29-7.24 (m, 3H), 7.16-7.11 (m, 5H), 6.99-6.97 (m, 1H), 6.92-6.90 (d, 1H,  $J = 7.2$  Hz), 4.00-

3.98 (m, 1H), 3.73-3.61 (m, 6H), 3.09-3.01 (m, 2H), 2.91-2.88 (m, 2H), 2.77-2.73 (m, 1H), 2.67-2.57 (m, 4H), 2.37 (s, 3H), 2.08-1.99 (m, 2H), 1.85-1.81 (m, 1H), 1.70-1.61 (m, 3H), 1.45-1.42 (m, 2H);  $^{13}\text{C}$  NMR [600 MHz,  $\text{CDCl}_3$ ]  $\delta$  168.48, 158.17, 147.05, 136.58, 136.45, 136.20, 134.73, 134.63, 134.26, 132.26, 129.40, 129.28, 129.18, 126.48, 126.18, 125.87, 123.39, 121.53, 121.36, 61.67, 57.18, 55.91, 52.54, 51.94, 50.75, 38.02, 29.87, 29.10, 26.31, 25.99, 21.31; HRMS (ESI)  $[\text{M}+\text{H}]^+$ , calc'd for  $\text{C}_{39}\text{H}_{43}\text{N}_4\text{O}_2$ ; 599.33805, found 599.3387.



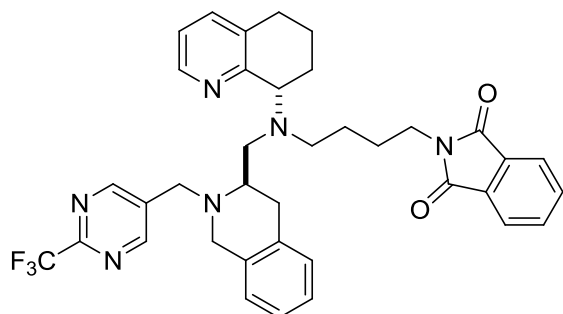
**2-(4-(((R)-2-((2-methoxypyrimidin-5-yl)methyl)-1,2,3,4-tetrahydroisoquinolin-3-yl)methyl)((S)-5,6,7,8-tetrahydroquinolin-8-yl)amino)butyl)isoindoline-1,3-dione (113):**

$^1\text{H}$  NMR [600 MHz,  $\text{CDCl}_3$ ]  $\delta$  8.45 (d, 1H,  $J = 4.2$  Hz), 7.84-7.82 (m, 2H), 7.72-7.70 (m, 2H), 7.29-7.24 (m, 3H), 7.16-7.11 (m, 5H), 6.99-6.97 (m, 1H), 6.92-6.90 (d, 1H,  $J = 7.2$  Hz), 4.00-3.98 (m, 1H), 3.73-3.61 (m, 6H), 3.09-3.01 (m, 2H), 2.91-2.88 (m, 2H), 2.77-2.73 (m, 1H), 2.67-2.57 (m, 4H), 2.37 (s, 3H), 2.08-1.99 (m, 2H), 1.85-1.81 (m, 1H), 1.70-1.61 (m, 3H), 1.45-1.42 (m, 2H);  $^{13}\text{C}$  NMR [600 MHz,  $\text{CDCl}_3$ ]  $\delta$  168.48, 158.17, 147.05, 136.58, 136.45, 136.20, 134.73, 134.63, 134.26, 132.26, 129.40, 129.28, 129.18, 126.48, 126.18, 125.87, 123.39, 121.53, 121.36, 61.67, 57.18, 55.91, 52.54, 51.94, 50.75, 38.02, 29.87, 29.10, 26.31, 25.99, 21.31



**2-(4-(((R)-2-((2-aminopyrimidin-5-yl)methyl)-1,2,3,4-tetrahydroisoquinolin-3-yl)methyl)((S)-5,6,7,8-tetrahydroquinolin-8-yl)amino)butyl)isoindoline-1,3-dione (114):**

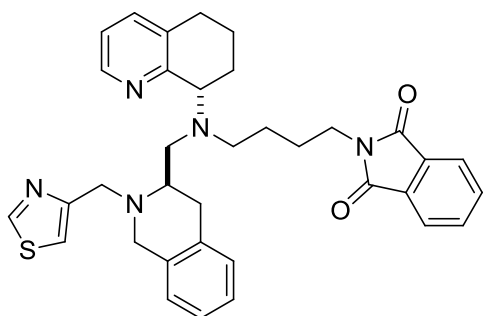
$^1\text{H}$  NMR [400 MHz,  $\text{CDCl}_3$ ]  $\delta$  8.41-8.23 (m, 1H), 8.23 (s, 1H), 7.79-7.77 (m, 2H), 7.70-7.67 (m, 2H), 7.31-7.29 (m, 1H), 7.11-7.06 (m, 3H), 7.03-7.00 (m, 1H), 6.89-6.88 (m, 1H), 5.59 (bs, 2H), 4.09-4.03 (m, 1H), 3.67-3.57 (m, 7H), 3.26-3.25 (m, 1H), 3.01-2.99 (m, 2H), 2.84-2.79 (m, 2H), 2.71-2.62 (m, 4H), 2.61-2.51 (m, 6H), 2.01 (bs, 2H), 1.99-1.94 (m, 2H), 1.66-1.58 (m, 3H), 1.43-1.38 (m, 2H);  $^{13}\text{C}$  NMR [400 MHz,  $\text{CDCl}_3$ ]  $\delta$  169.65, 162.51, 159.11, 147.01, 137.22, 134.46, 134.11, 133.58, 132.23, 129.60, 126.82, 126.16, 123.36, 122.29, 120.93, 61.59, 55.81, 53.84, 51.96, 51.65, 50.73, 49.59, 37.81, 28.99, 28.56, 26.51, 25.91, 25.17, 21.14; HRMS (ESI)  $[\text{M}+\text{H}]^+$ , calc'd for  $\text{C}_{36}\text{H}_{40}\text{N}_7\text{O}_2$ ; 602.32380, found 602.32286



**2-(4-(((S)-5,6,7,8-tetrahydroquinolin-8-yl)((R)-2-((2-(trifluoromethyl)pyrimidin-5-yl)methyl)-1,2,3,4-tetrahydroisoquinolin-3-yl)methyl)amino)butyl)isoindoline-1,3-dione (115):**

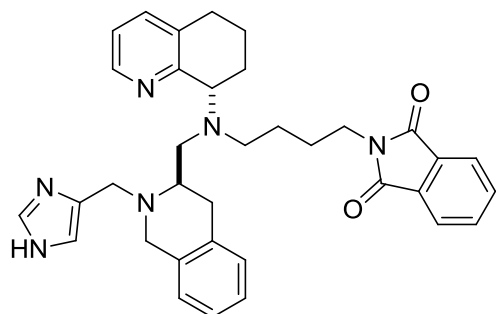
$^1\text{H}$  NMR [400 MHz,  $\text{CDCl}_3$ ]  $\delta$  8.85 (d, 1H,  $J = 4.8$  Hz), 7.78-7.69 (m, 2H), 7.77-7.67 (m, 2H), 8.43 (d, 1H,  $J = 4.8$  Hz), 7.24 (d, 1H,  $J = 6.8$  Hz), 7.09-7.08 (m, 3H), 6.98-6.96 (m, 1H), 6.89 (d, 1H,  $J = 6.8$  Hz), 4.01-3.99 (m, 1H), 3.84 (q, 2H,  $J = 14$  Hz), 3.64 (q, 2H,  $J = 14$  Hz), 3.06-3.04

(m, 1H), 2.95-2.94 (m, 1H), 2.86-2.82 (m, 2H), 2.71-2.61 (m, 5H), 2.60-2.54 (m, 2H), 1.98-1.95 (m, 2H), 1.82-1.79 (m, 1H), 1.71-1.79 (m, 1H), 1.43-1.39 (m, 4H);  $^{13}\text{C}$  NMR [100 MHz,  $\text{CDCl}_3$ ]  $\delta$  158.13, 158.00, 155.79, 155.43, 146.99, 136.54, 135.85, 134.26, 134.21, 134.06, 133.29, 132.46, 129.44, 126.55, 126.41, 125.85, 123.24, 121.58, 121/16, 118.43, 61.41, 56.56, 53.22, 52.43, 51.77, 51.00, 41.99, 31.42, 29.70, 29.15, 26.13, 21.21 ; HRMS (ESI)  $[\text{M}+\text{H}]^+$ , calc'd for  $\text{C}_{32}\text{H}_{38}\text{N}_6\text{O}_2\text{F}_3$  654.29146, found 654.29147



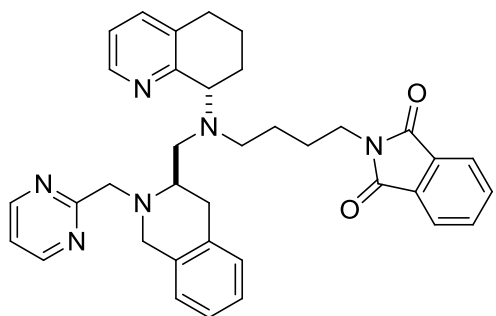
**2-(4-(((S)-5,6,7,8-tetrahydroquinolin-8-yl))((R)-2-(thiazol-4-ylmethyl)-1,2,3,4-tetrahydroisoquinolin-3-yl)methyl)amino)butyl)isoindoline-1,3-dione (116):**

$^1\text{H}$  NMR [400 MHz,  $\text{CDCl}_3$ ]  $\delta$  8.85 (s, 1H), 7.83 (m, 1H), 8.56 (d, 1H,  $J = 6$ ), 7.25-7.23 (m, 1H), 7.10-7.09 (m, 2H), 7.03-7.00 (m, 4H), 6.93-6.90 (m, 3H), 4.03 (m, 1H), 3.97-3.93 (m, 4H), 3.75-3.69 (m, 1H), 3.61-3.55 (m, 1H), 3.20-3.18 (m, 1H), 3.06-2.99 (m, 1H) 2.97-2.91 (m, 2H), 2.70-2.66 (m, 6H), 2.58-2.52 (m, 2H), 1.97-1.90 (m, 2H), 1.79-1.76 (m, 1H), 1.75-1.72 (m, 1H), 1.62-1.60 (m, 1H), 1.83-1.54 (m, 2H), 1.39-1.35 (m, 4H);  $^{13}\text{C}$  NMR [100 MHz,  $\text{CDCl}_3$ ]  $\delta$  165.44, 153.57, 152.74, 147.35, 136.91, 134.39, 133.83, 129.42, 126.96, 126.48, 121.90, 116.32, 62.29, 54.50, 55.34, 51.50, 41.02, 29.59, 29.06, 28.61, 26.18, 24.15, 21.30; HRMS (ESI)  $[\text{M}+\text{H}]^+$ , calc'd for  $\text{C}_{37}\text{H}_{40}\text{N}_5\text{O}_2\text{S}$  591.27340, found 591.2123.



**2-(4-(((R)-2-((1H-imidazol-4-yl)methyl)-1,2,3,4-tetrahydroisoquinolin-3-yl)methyl)((S)-5,6,7,8-tetrahydroquinolin-8-yl)amino)butyl)isoindoline-1,3-dione (117):**

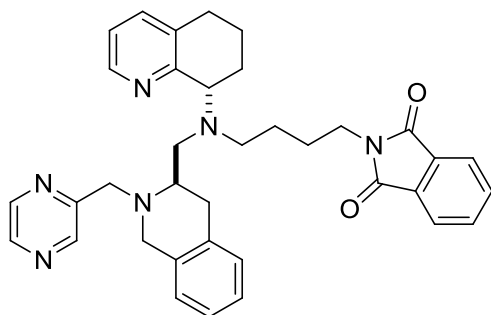
$^1\text{H}$  NMR [400 MHz,  $\text{CDCl}_3$ ]  $\delta$  8.41 (d, 1H,  $J = 4.8$  Hz), 7.55-7.73 (m, 1H), 7.66-7.64 (m, 1H), 7.33-7.32 (m, 1H), 7.12-7.05 (m, 4H), 6.98-6.94 (m, 1H), 6.86-6.80 (m, 1H), 4.13-4.09 (m, 1H), 3.82-3.65 (m, 4H), 3.49-3.46 (m, 1H), 3.46 (m, 1H), 3.15-3.12 (m, 1H), 2.99-2.93 (m, 1H), 2.86-2.53 (m, 6H), 2.44-2.40 (m, 2H), 2.14-1.95 (m, 2H), 1.82-1.76 (m, 1H), 1.64-1.61 (m, 1H), 1.49-1.40 (m, 2H), 1.33-1.30 (m, 1H);  $^{13}\text{C}$  NMR [100 MHz,  $\text{CDCl}_3$ ]  $\delta$  169.08, 157.07, 146.21, 136.94, 135.31, 134.11, 133.67, 133.62, 131.73, 129.21, 128.70, 126.50, 126.03, 125.64, 124.39, 122.88, 121.71, 64.02, 55.85, 55.34, 51.06, 46.00, 37.34, 29.59, 29.06, 26.18, 23.42, 21.28; HRMS (ESI)  $[\text{M}+\text{H}]^+$ , calc'd for  $\text{C}_{35}\text{H}_{39}\text{N}_6\text{O}_2$  574.31340, found 574.31239



**2-(4-(((R)-2-(pyrimidin-2-ylmethyl)-1,2,3,4-tetrahydroisoquinolin-3-yl)methyl)((S)-5,6,7,8-tetrahydroquinolin-8-yl)amino)butyl)isoindoline-1,3-dione (118):**

$^1\text{H}$  NMR [400 MHz,  $\text{CDCl}_3$ ]  $\delta$  8.71 (d, 1H,  $J = 4.8$  Hz), 8.40-8.39 (m, 1H,  $J = 3.6$  Hz), 7.79-7.78 (m, 2H), 7.69-7.65 (m, 2H), 7.20-7.14 (m, 2H), 7.03-7.00 (m, 3H), 6.93-6.87 (m, 2H), 4.04-3.99

(m, 1H), 3.83 (bs, 2H), 3.58 (t, 2H,  $J = 6.6$  Hz), 3.12-3.03 (m, 2H) 2.92-2.79 (m, 4H), 2.59-2.48 (m, 4H), 2.02-1.92 (m, 2H), 1.76-1.75 (m, 1H), 1.66-1.54 (m, 3H), 1.43-1.37 (m, 2H);  $^{13}\text{C}$  NMR [400 MHz,  $\text{CDCl}_3$ ]  $\delta$ 168.98, 168.54, 158.12, 157.37, 147.21, 136.38, 134.67, 134.33, 134.34, 133.96, 132.32, 129.43, 126.46, 126.11, 125.46, 123.27, 121.46, 119.34; HRMS (ESI)  $[\text{M}+\text{H}]^+$ , calc'd for  $\text{C}_{36}\text{H}_{39}\text{N}_6\text{O}_2$  587.31290, found 587.31233

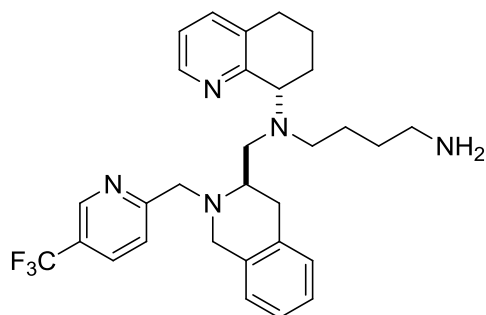


**2-(4-(((R)-2-(pyrazin-2-ylmethyl)-1,2,3,4-tetrahydroisoquinolin-3-yl)methyl)((S)-5,6,7,8-tetrahydroquinolin-8-yl)amino)butyl)isoindoline-1,3-dione (119):**

$^1\text{H}$  NMR [400 MHz,  $\text{CDCl}_3$ ]  $\delta$  8.71 (d, 1H,  $J = 4.8$  Hz), 8.40-8.39 (m, 1H,  $J = 3.6$  Hz), 7.79-7.78 (m, 2H), 7.69-7.65 (m, 2H), 7.20-7.14 (m, 2H), 7.03-7.00 (m, 3H), 6.93-6.87 (m, 2H), 4.04-3.99 (m, 1H), 3.83 (bs, 2H), 3.58 (t, 2H,  $J = 6.6$  Hz), 3.12-3.03 (m, 2H) 2.92-2.79 (m, 4H), 2.59-2.48 (m, 4H), 2.02-1.92 (m, 2H), 1.76-1.75 (m, 1H), 1.66-1.54 (m, 3H), 1.43-1.37 (m, 2H);  $^{13}\text{C}$  NMR [400 MHz,  $\text{CDCl}_3$ ]  $\delta$ 168.98, 168.54, 158.12, 157.37, 147.21, 136.38, 134.67, 134.33, 134.34, 133.96, 132.32, 129.43, 126.46, 126.11, 125.46, 123.27, 121.46, 119.34; HRMS (ESI)  $[\text{M}+\text{H}]^+$ , calc'd for  $\text{C}_{36}\text{H}_{39}\text{N}_6\text{O}_2$  587.31290, found 587.31233

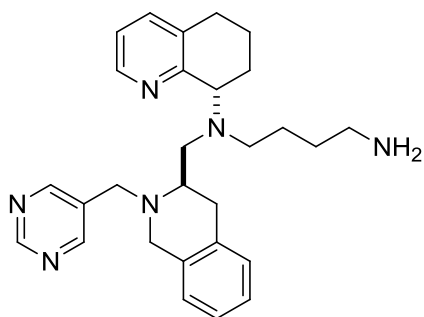
**General Procedure for Compounds 125-139:**

To a solution of MeOH (2 mL) was added 2-(4-(((R)-2-(pyrimidin-4-ylmethyl)-1,2,3,4-tetrahydroisoquinolin-3-yl)methyl)((S)-5,6,7,8-tetrahydroquinolin-yl)-amino)butyl) isoindoline-1,3-dione (.130 g, 0.222 mmol) in one portion. Hydrazine (0.232 ml, 1.773 mmol) 24% in water was then added dropwise, and the reaction was allowed to proceed at ambient temperature overnight. The methanol was then removed under vacuum. To the oily residue was added H<sub>2</sub>O (20 mL) and extracted with DCM (3 x 10 mL). The organic layer was washed once with 1N NaOH (20 mL) and the aqueous layer discarded. The organic layer was extracted with 1N HCl (2 x 20 mL) and the aqueous layers combined. The aqueous layer was made basic in cold with excess 1N NaOH (pH 13-14). The above solution was extracted with DCM (3 x 20 mL). The organic extracts were combined, dried over MgSO<sub>4</sub> and concentrated under reduced pressure to yield a yellow oil. Crude material was purified by gravity chromatography (5% DCM/MeOH; 7% DCM/MeOH; 10%DCM/MeOH with 1% NH<sub>4</sub>OH).

**N1-((S)-5,6,7,8-tetrahydroquinolin-8-yl)-N1-(((R)-2-((5-(trifluoromethyl)pyridin-2-yl)methyl)-1,2,3,4-tetrahydroisoquinolin-3-yl)methyl)butane-1,4-diamine (125):**

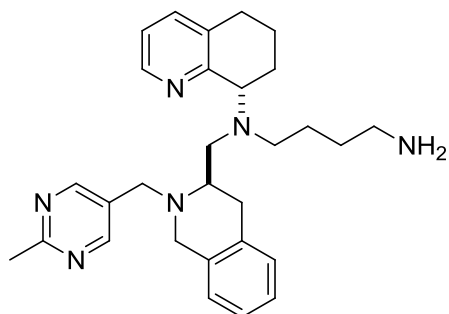
<sup>1</sup>H NMR [400 MHz, CDCl<sub>3</sub>] δ 8.44-8.40 (m, 2H) 7.24 (d, 1H, *J* = 6.8 Hz), 7.09-7.08 (m, 3H), 6.98-6.96 (m, 1H), 6.89 (d, 1H, *J* = 6.8 Hz), 4.01-3.99 (m, 1H), 3.84 (q, 2H, *J* = 14 Hz), 3.64 (q, 2H, *J* = 14 Hz), 3.06-3.04 (m, 1H), 2.95-2.94 (m, 1H), 2.86-2.82 (m, 2H), 2.71-2.61 (m, 5H),

2.60-2.54 (m, 2H), 1.98-1.95 (m, 2H), 1.82-1.79 (m, 1H), 1.71-1.79 (m, 1H), 1.43-1.39 (m, 4H);  $^{13}\text{C}$  NMR [100 MHz,  $\text{CDCl}_3$ ]  $\delta$  158.13, 158.00, 155.79, 155.43, 146.99, 136.54, 135.85, 134.26, 134.21, 134.06, 133.29, 132.46, 129.44, 126.55, 126.41, 125.85, 123.24, 121.58, 121/16, 118.43, 61.41, 56.56, 53.22, 52.43, 51.77, 51.00, 41.99, 31.42, 29.70, 29.15, 26.13, 21.21 ; HRMS (ESI)  $[\text{M}+\text{H}]^+$ , calc'd for  $\text{C}_{30}\text{H}_{38}\text{N}_5\text{F}_3$  523.29613, found 523.29535; ; HPLC/MS purity (> 95%)  $r_t = 0.589$  at 254nM, 75-95% MeOH over 3 minutes.



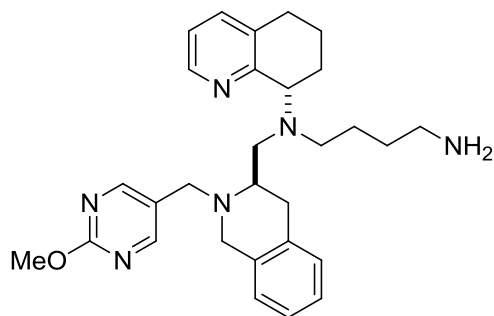
**N1-(((R)-2-(pyrimidin-5-ylmethyl)-1,2,3,4-tetrahydroisoquinolin-3-yl)methyl)-N1-((S)-5,6,7,8-tetrahydroquinolin-8-yl)butane-1,4-diamine (128):**

$^1\text{H}$  NMR [400 MHz,  $\text{CDCl}_3$ ]  $\delta$  9.11 (s, 1H), 8.69 (s, 2H), 8.43 (d, 1H,  $J = 4$  Hz), 7.24-7.23 (m, 1H), 7.12-7.06 (m, 3H), 6.99-6.96 (m, 1H), 6.89-6.87 (m, 1H), 4.00-3.98 (m, 1H), 3.76-3.57 (m, 4H), 3.06-2.94 (m, 2H) 2.86-2.80 (m, 2H), 2.72-2.66 (m, 1H), 2.65-2.60 (m, 4H), 2.58-2.52 (m, 2H), 1.99-1.90 (m, 4H), 1.84-1.76 (m, 1H), 1.65-1.61 (m, 1H), 1.44-1.32 (m, 4H);  $^{13}\text{C}$  NMR [600 MHz,  $\text{CDCl}_3$ ]  $\delta$  158.21, 157.84, 157.82, 157.42, 147.13, 136.59, 134.36, 134.33, 133.73, 133.21, 129.54, 126.64, 126.45, 125.84, 121.64, 61.55, 56.55, 53.05, 52.58, 52.29, 50.95, 42.23, 31.75, 29.81, 26.33, 26.18, 21.22; HRMS (ESI)  $[\text{M}+\text{H}]^+$ , calc'd for  $\text{C}_{28}\text{H}_{37}\text{N}_6$  457.30742, found 457.30713; HPLC/MS purity (> 95%)  $r_t = 0.572$  at 254nM, 75-95% MeOH over 3 minutes.



**N1-(((R)-2-((2-methylpyrimidin-5-yl)methyl)-1,2,3,4-tetrahydroisoquinolin-3-yl)methyl)-N1-((S)-5,6,7,8-tetrahydroquinolin-8-yl)butane-1,4-diamine (129):**

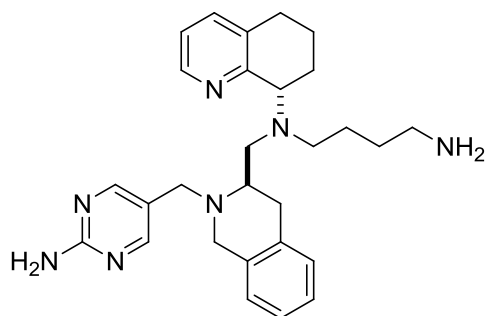
$^1\text{H}$  NMR [400 MHz,  $\text{CDCl}_3$ ]  $\delta$  8.57 (s, 2H), 8.44-8.43 (m, 1H), 7.26-7.24 (m, 1H), 7.09-7.03 (m, 3H), 6.99-6.96 (m, 1H), 6.88-6.86 (m, 1H), 4.01-3.97 (m, 1H), 3.69-3.56 (m, 4H), 3.06-3.02 (m, 1H), 2.97-2.93 (m, 2H), 2.83-2.78 (m, 2H), 2.71-2.62 (m, 4H), 2.61-2.51 (m, 6H), 2.17 (bs, 2H), 1.99-1.94 (m, 2H), 1.80-1.77 (m, 1H), 1.64-1.60 (m, 1H), 1.43-1.36 (m, 4H);  $^{13}\text{C}$  NMR [400 MHz,  $\text{CDCl}_3$ ]  $\delta$  167.05, 158.13, 157.60, 147.15, 136.60, 134.38, 134.32, 133.77, 129.51, 126.63, 126.39, 125.81, 121.63, 61.43, 56.35, 52.95, 52.48, 52.00, 50.77, 42.12, 31.57, 29.67, 29.30, 26.86, 25.90, 21.26; HRMS (ESI)  $[\text{M}+\text{H}]^+$ , calc'd for  $\text{C}_{29}\text{H}_{39}\text{N}_6$ ; 469.33257, found 469.33323; HPLC/MS purity (> 95%)  $r_t = 0.558$  at 254nM, 75% MeOH over 3 minutes.



**N1-(((R)-2-((2-methoxypyrimidin-5-yl)methyl)-1,2,3,4-tetrahydroisoquinolin-3-yl)methyl)-N1-((S)-5,6,7,8-tetrahydroquinolin-8-yl)butane-1,4-diamine (130):**

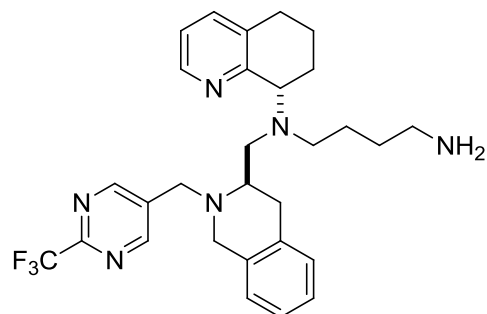
$^1\text{H}$  NMR [400 MHz,  $\text{CDCl}_3$ ]  $\delta$  8.43 (m, 3H), 7.28 (m, 1H), 7.08 (m, 3H), 6.99-6.96 (m, 1H), 6.88-6.86 (m, 1H), 4.01-3.97 (m, 1H), 3.69-3.56 (m, 4H), 3.06-3.02 (m, 1H), 2.97-2.93 (m, 2H),

2.83-2.78 (m, 2H), 2.71-2.62 (m, 4H), 2.61-2.51 (m, 6H), 2.17 (bs, 2H), 1.99-1.94 (m, 2H), 1.80-1.77 (m, 1H), 1.64-1.60 (m, 1H), 1.43-1.36 (m, 4H);  $^{13}\text{C}$  NMR [400 MHz,  $\text{CDCl}_3$ ]  $\delta$  167.05, 158.13, 157.60, 147.15, 136.60, 134.38, 134.32, 133.77, 129.51, 126.63, 126.39, 125.81, 121.63, 61.43, 56.35, 52.95, 52.48, 52.00, 50.77, 42.12, 31.57, 29.67, 29.30, 26.86, 25.90, 21.26; HRMS (ESI)  $[\text{M}+\text{H}]^+$ , calc'd for  $\text{C}_{28}\text{H}_{36}\text{N}_6\text{O}$ ; 472.63157, found 469.63412; HPLC/MS purity ( $> 95\%$ )  $r_t = 0.628$  at 254nM, 75% MeOH over 3 minutes.



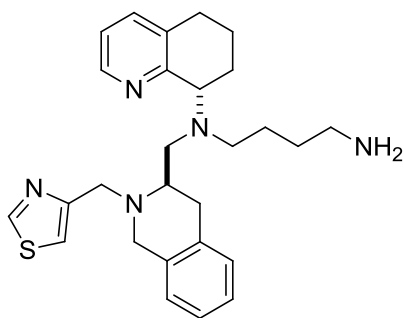
**N1-(((R)-2-((2-aminopyrimidin-5-yl)methyl)-1,2,3,4-tetrahydroisoquinolin-3-yl)methyl)-N1-((S)-5,6,7,8-tetrahydroquinolin-8-yl)butane-1,4-diamine (131):**

$^1\text{H}$  NMR [400 MHz,  $\text{CDCl}_3$ ]  $\delta$  8.41-8.23 (m, 1H), 8.23 (s, 1H), 7.79-7.77 (m, 2H), 7.70-7.67 (m, 2H), 7.31-7.29 (m, 1H), 7.11-7.06 (m, 3H), 7.03-7.00 (m, 1H), 6.89-6.88 (m, 1H), 5.59 (bs, 2H), 4.09-4.03 (m, 1H), 3.67-3.57 (m, 7H), 3.26-3.25 (m, 1H), 3.01-2.99 (m, 2H), 2.84-2.79 (m, 2H), 2.71-2.62 (m, 4H), 2.61-2.51 (m, 6H), 2.01 (bs, 2H), 1.99-1.94 (m, 2H), 1.66-1.58 (m, 3H), 1.43-1.38 (m, 2H);  $^{13}\text{C}$  NMR [400 MHz,  $\text{CDCl}_3$ ]  $\delta$  169.65, 162.51, 159.11, 147.01, 137.22, 134.46, 134.11, 133.58, 132.23, 129.60, 126.82, 126.16, 123.36, 122.29, 120.93, 61.59, 55.81, 53.84, 51.96, 51.65, 50.73, 49.59, 37.81, 28.99, 28.56, 26.51, 25.91, 25.17, 21.14; HRMS (ESI)  $[\text{M}+\text{H}]^+$ , calc'd for  $\text{C}_{36}\text{H}_{40}\text{N}_7\text{O}_2$ ; 602.32380, found 602.32286; HPLC/MS purity ( $> 95\%$ )  $r_t = 0.558$  at 254nM, 75% MeOH over 3 minutes.



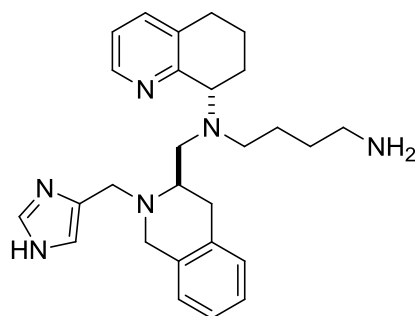
**N1-((S)-5,6,7,8-tetrahydroquinolin-8-yl)-N1-(((R)-2-((2-(trifluoromethyl)pyrimidin-5-yl)methyl)-1,2,3,4-tetrahydroisoquinolin-3-yl)methyl)butane-1,4-diamine (132):**

$^1\text{H}$  NMR [400 MHz,  $\text{CDCl}_3$ ]  $\delta$  8.85 (d, 1H,  $J = 4.8$  Hz), 8.43 (d, 1H,  $J = 4.8$  Hz), 7.26 (d, 1H,  $J = 6.8$  Hz), 7.08-7.06 (m, 3H), 6.99-6.96 (m, 1H), 6.89 (d, 1H,  $J = 6.8$  Hz), 4.01-3.99 (m, 1H), 3.84 (q, 2H,  $J = 14$  Hz), 3.64 (q, 2H,  $J = 14$  Hz), 3.08-3.06 (m, 1H), 2.96-2.94 (m, 1H), 2.87-2.81 (m, 2H), 2.71-2.61 (m, 5H), 2.60-2.54 (m, 2H), 1.98-1.95 (m, 2H), 1.82-1.79 (m, 1H), 1.71-1.79 (m, 1H), 1.43-1.39 (m, 4H);  $^{13}\text{C}$  NMR [100 MHz,  $\text{CDCl}_3$ ]  $\delta$  158.13, 158.00, 155.79, 155.43, 146.99, 136.54, 135.85, 134.26, 134.21, 134.06, 133.29, 129.44, 126.55, 126.41, 125.85, 121.58, 121/16, 118.43, 61.41, 56.56, 53.22, 52.43, 51.77, 51.00, 41.99, 31.42, 29.70, 29.15, 26.13, 21.21 ; HRMS (ESI)  $[\text{M}+\text{H}]^+$ , calc'd for  $\text{C}_{29}\text{H}_{36}\text{N}_6\text{F}_3$  524.29134, found 529.30135; HPLC/MS purity (> 95%)  $r_t = 0.586$  at 254nM, 75-95% MeOH over 3 minutes.



**N1-((S)-5,6,7,8-tetrahydroquinolin-8-yl)-N1-(((R)-2-(thiazol-4-ylmethyl)-1,2,3,4-tetrahydroisoquinolin-3-yl)methyl)butane-1,4-diamine (133):**

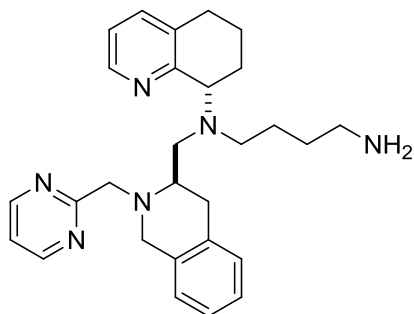
$^1\text{H}$  NMR [400 MHz,  $\text{CDCl}_3$ ]  $\delta$  8.85 (s, 1H), 7.83-7.80 (m, 1H), 8.56 (d, 1H,  $J = 6$ ), 7.23 (m, 1H), 7.09-7.06 (m, 1H), 7.03-7.00 (m, 3H), 6.93-6.94 (m, 2H), 4.03-4.00 (m, 1H), 3.91-3.89 (m, 4H), 3.47-3.45 (m, 1H), 3.46 (m, 1H), 3.14-3.01 (m, 1H), 2.84-2.70 (m, 1H), 2.69-2.50 (m, 6H), 2.41 (m, 2H), 2.07-2.04 (m, 2H), 1.79-1.76 (m, 1H), 1.76-1.73 (m, 1H), 1.62-1.55 (m, 1H), 1.44 (m, 2H), 1.38-1.24 (m, 1H);  $^{13}\text{C}$  NMR [100 MHz,  $\text{CDCl}_3$ ]  $\delta$  165.44, 153.57, 152.74, 147.35, 136.91, 134.39, 133.83, 129.42, 126.96, 126.48, 121.90, 116.32, 62.29, 54.50, 55.34, 51.50, 41.02, 29.59, 29.06, 28.61, 26.18, 24.15, 21.30; HRMS (ESI)  $[\text{M}+\text{H}]^+$ , calc'd for  $\text{C}_{27}\text{H}_{35}\text{N}_5\text{S}$  461.66514, found 461.65612.; HPLC/MS purity ( $> 95\%$ )  $r_t = 0.496$  at 254nM, 75-95% MeOH over 3 minutes.



**N1-(((R)-2-((1H-imidazol-4-yl)methyl)-1,2,3,4-tetrahydroisoquinolin-3-yl)methyl)-N1-((S)-5,6,7,8-tetrahydroquinolin-8-yl)butane-1,4-diamine (134):**

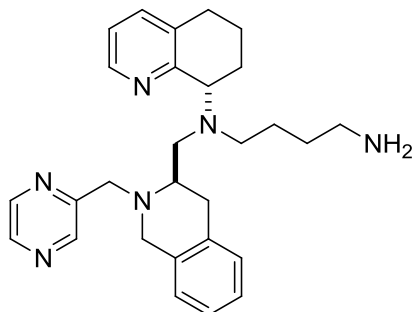
$^1\text{H}$  NMR [400 MHz,  $\text{CDCl}_3$ ]  $\delta$  8.44 (d, 1H,  $J = 4.8$  Hz), 7.83 (m, 1H), 7.07 (m, 4H), 7.00 (m, 1H), 6.98 (m, 2H), 4.12 (m, 1H), 3.73 (m, 4H), 3.47 (m, 1H), 3.46 (m, 1H), 3.14 (m, 1H), 2.95 (m, 1H), 2.68 (m, 6H), 2.41 (m, 2H), 2.05 (m, 2H), 1.79 (m, 1H), 1.62 (m, 1H), 1.62 (m, 1H), 1.45 (m, 2H), 1.31 (m, 1H);  $^{13}\text{C}$  NMR [100 MHz,  $\text{CDCl}_3$ ]  $\delta$  169.08, 157.07, 146.21, 136.94, 135.31, 134.11, 131.73, 129.21, 128.70, 126.50, 126.03, 125.64, 124.39, 121.71, 64.02, 55.85, 55.34, 51.06, 46.00, 37.34, 29.59, 29.06, 26.18, 23.42, 21.28; HRMS (ESI)  $[\text{M}+\text{H}]^+$ , calc'd for

C<sub>27</sub>H<sub>37</sub>N<sub>6</sub> 444.30169, found 444.32665; HPLC/MS purity (> 95%)  $r_t = 0.476$  at 254nM, 75-95% MeOH over 3 minutes.



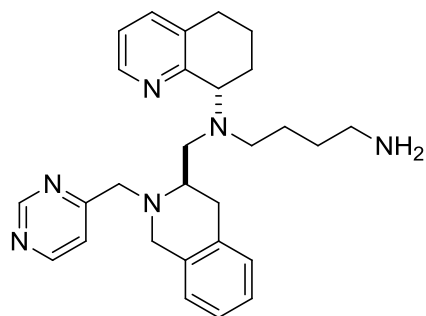
**N1-(((R)-2-(pyrimidin-2-ylmethyl)-1,2,3,4-tetrahydroisoquinolin-3-yl)methyl)-N1-((S)-5,6,7,8-tetrahydroquinolin-8-yl)butane-1,4-diamine (135):**

<sup>1</sup>H NMR [400 MHz, CDCl<sub>3</sub>]  $\delta$  8.71 (d, 1H,  $J = 4.8$  Hz), 8.49 (d, 1H,  $J = 3.6$  Hz), 7.25-7.23 (m, 1H), 7.17-7.14 (m, 1H), 7.05-6.95 (m, 4H), 6.89-6.87 (m, 1H), 4.00-3.96 (m, 1H), 3.82 (bs, 2H), 3.68 (s, 2H), 3.16-3.13 (m, 1H), 3.05-3.00 (m, 1H), 2.88-2.84 (m, 1H), 2.74-2.50 (m, 10H), 2.01-1.92 (m, 2H), 1.78-1.75 (m, 1H), 1.61-1.57 (m, 1H), 1.44-1.38 (m, 4H); <sup>13</sup>C NMR [400 MHz, CDCl<sub>3</sub>]  $\delta$  169.07, 158.11, 157.87, 157.72, 147.66, 137.07, 134.78, 134.57, 134.15, 129.76, 127.15, 126.61, 126.13, 122.10, 119.83; HRMS (ESI) [M+H]<sup>+</sup>, calc'd for C<sub>28</sub>H<sub>37</sub>N<sub>6</sub> 457.30742, found 457.30771; HPLC/MS purity (> 95%)  $r_t = 0.605$  at 254nM, 75-95% MeOH over 3 minutes.



**N1-(((R)-2-(pyrazin-2-ylmethyl)-1,2,3,4-tetrahydroisoquinolin-3-yl)methyl)-N1-((S)-5,6,7,8-tetrahydroquinolin-8-yl)butane-1,4-diamine (136):**

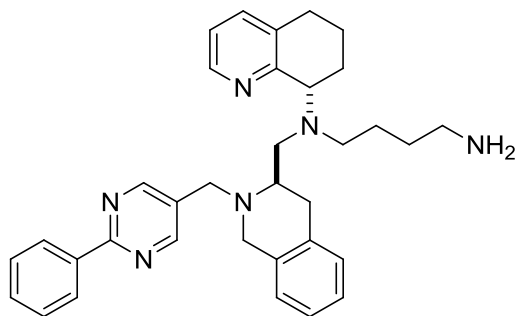
$^1\text{H}$  NMR [400 MHz,  $\text{CDCl}_3$ ]  $\delta$  8.70 (d, 1H,  $J = 1.2$  Hz), 8.48 (m, 1H), 8.44 (m, 2H), 7.22 (m, 1H), 7.03 (m, 3H), 6.97 (m, 1H), 6.88 (m, 1H), 3.98 (m, 1H), 3.90 (m, 2H), 3.72 (q, 1H,  $J = 11.2$ ), 3.05 (m, 1H), 2.84 (m, 1H), 2.66 (m, 1H), 2.57 (m, 6H), 1.96 (m, 1H), 1.76 (m, 1H), 1.61 (m, 1H), 1.37 (m, 1H)  $^{13}\text{C}$  NMR [100 MHz,  $\text{CDCl}_3$ ]  $\delta$  158.12, 155.78, 147.16, 145.35, 143.91, 143.10, 136.50, 136.50, 134.32, 133.89, 129.47, 126.55, 126.28, 125.68, 121.56, 61.50, 57.11, 56.61, 52.84, 52.57, 51.46, 42.15, 31.65, 30.00, 29.28, 26.33, 25.74, 21.24; HRMS (ESI)  $[\text{M}+\text{H}]^+$ , calc'd for  $\text{C}_{28}\text{H}_{37}\text{N}_6$  457.30742, found 457.301822; HPLC/MS purity ( $> 95\%$ )  $r_t = 0.576$  at 254nM, 75-95% MeOH over 3 minutes.



**N1-(((R)-2-(pyrimidin-4-ylmethyl)-1,2,3,4-tetrahydroisoquinolin-3-yl)methyl)-N1-((S)-5,6,7,8-tetrahydroquinolin-8-yl)butane-1,4-diamine (137):**

$^1\text{H}$  NMR [400 MHz,  $\text{CDCl}_3$ ]  $\delta$  9.11 (d, 1H,  $J = 1.2$  Hz), 8.64 (d, 1H,  $J = 4.8$  Hz), 8.43 (dd, 1H,  $J = 2.8, 1.6$  Hz), 7.57-7.56 (m, 1H), 7.24-7.23 (m, 1H), 7.11-7.06 (m, 3H), 6.89-6.95 (m, 1H),

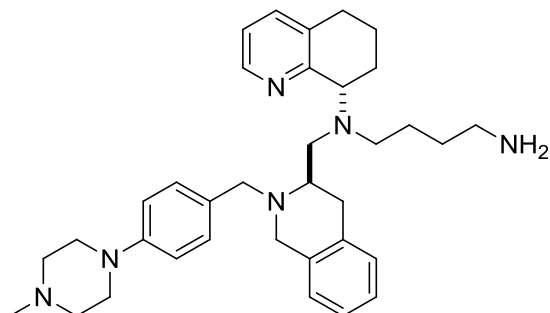
6.90-6.87 (m, 1H), 4.00-3.98 (m, 1H), 3.86 (dd, 2H, 17.6, 16 Hz), 3.71 (dd, 2H, 16, 8 Hz), 3.06-2.98 (m, 2H) 2.88-2.80 (m, 2H), 2.69-2.49 (m, 7H), 2.01-1.90 (m, 4H), 1.82-1.74 (m, 1H), 1.66-1.59 (m, 1H), 1.44-1.33 (m, 4H);  $^{13}\text{C}$  NMR [100 MHz,  $\text{CDCl}_3$ ]  $\delta$  169.69, 158.74, 158.12, 157.30, 147.18, 136.75, 134.35, 134.29, 133.92, 129.71, 126.58, 126.49, 125.87, 121.73, 120.22, 61.53, 61.46, 58.68, 56.82, 56.73, 52.60, 51.76, 42.21, 31.31, 30.46, 29.30, 24.89, 21.84; HRMS (ESI)  $[\text{M}+\text{H}]^+$ , calc'd for  $\text{C}_{28}\text{H}_{37}\text{N}_6$  457.30742, found 457.30712; HPLC/MS purity (> 95%)  $r_t = 0.516$  at 254nM, 75-95% MeOH over 3 minutes.



**N1-(((R)-2-((2-phenylpyrimidin-5-yl)methyl)-1,2,3,4-tetrahydroisoquinolin-3-yl)methyl)-N1-((S)-5,6,7,8-tetrahydroquinolin-8-yl)butane-1,4-diamine (138):**

$^1\text{H}$  NMR [600 MHz,  $\text{CDCl}_3$ ]  $\delta$  8.77 (s, 2H), 8.46-8.52 (m, 3H), 7.54-7.48 (m, 3H), 7.29-7.28 (m, 1H), 7.14-7.08 (m, 1H), 7.14-7.08 (m, 3H), 7.01-6.99 (m, 1H), 6.92 (dd, 1H,  $J = 7.2$  Hz), 5.29 (s, 2H), 4.035-4.01 (m, 1H), 3.79-3.65 (m, 4H), 3.10-3.08 (m, 1H), 3.00 (dd, 1H,  $J = 11.4, 5.4$  Hz), 2.91-2.86 (m, 2H), 2.74-2.72 (m, 1H), 2.67-2.55 (m, 4H), 2.03-1.98 (m, 2H), 1.84-1.81 (m, 1H), 1.69-1.65 (m, 3H), 1.46-1.36 (m, 4H); NMR [100 MHz,  $\text{CDCl}_3$ ]  $\delta$  163.98, 158.09, 157.94, 147.31, 137.94, 136.56, 134.53, 134.07, 131.07, 130.71, 129.57, 128.36, 126.78, 126.42, 126.11, 121.87, 61.83, 56.57, 52.96, 51.31, 31.97, 29.81, 26.85, 21.33; ; HRMS (ESI)  $[\text{M}+\text{H}]^+$ , calc'd for

C<sub>34</sub>H<sub>41</sub>N<sub>6</sub>; 553.33872, found 553.33965; HPLC/MS purity (> 95%) *r*<sub>t</sub> = 0.566 at 254nM, 75-95% MeOH over 3 minutes.



**N1-(((R)-2-(4-(4-methylpiperazin-1-yl)benzyl)-1,2,3,4-tetrahydroisoquinolin-3-yl)methyl)-N1-((S)-5,6,7,8-tetrahydroquinolin-8-yl)butane-1,4-diamine (139):**

<sup>1</sup>H NMR [400 MHz, CDCl<sub>3</sub>] δ 8.44 (dd, 1H, *J* = 2.8, 1.6 Hz), 7.24-7.20 (m, 3H), 7.08-7.01 (m, 3H), 7.08-7.02 (m, 3H), 6.98-6.95 (m, 1H), 6.89-6.85 (m, 3H), 3.98-9.52 (m, 1H), 3.65-3.56 (m, 4H), 3.41 (s, 1H), 3.19-3.17 (m, 4H), 3.05-2.93 (m, 2H), 2.84-2.79 (m, 2H), 2.71-2.67 (m, 1H), 2.58-2.55 (m, 7H), 2.52-2.46 (m, 3H), 2.39 (s, 3H), 2.17-2.11 (m, 2H), 1.99-1.92 (m, 2H), 1.83-1.75 (m, 1H), 1.64-1.59 (m, 1H), 1.40-1.30 (m, 4H); NMR [100 MHz, CDCl<sub>3</sub>] δ 158.23, 150.46, 147.17, 136.50, 134.77, 134.37, 130.72, 129.78, 129.46, 126.60, 126.02, 125.50, 121.52, 116.08, 61.65, 61.60, 56.83, 55.62, 55.31, 52.61, 52.40, 50.83, 49.44, 49.36, 46.30, 42.17, 31.68, 29.72, 29.35, 26.33, 25.36, 21.25; HRMS (ESI) [M+H]<sup>+</sup>, calc'd for C<sub>30</sub>H<sub>49</sub>N<sub>6</sub>; 553.40132, found 553.40381; HPLC/MS purity (> 95%) *r*<sub>t</sub> = 0.678 at 254nM, 75-95% MeOH over 3 minutes.

## 4.7 Biological Experimental

### **Efficacy Evaluation in Human Peripheral Blood Mononuclear Cells (PBMC's) for compound 35 (VT-03-066)**

Experiments performed at Southern research Institute, Frederick MD.

Fresh human PBMCs, seronegative for HIV and HBV, are isolated from screened donors (Biological Specialty Corporation, Colmar, PA). Cells are pelleted/washed 2-3 times by low speed centrifugation and re-suspension in PBS to remove contaminating platelets. The Leukophoresed blood is then diluted 1:1 with Dulbecco's Phosphate Buffered Saline (DPBS) and layered over 14 mL of Lymphocyte Separation Medium (LSM; Cellgro by Mediatech, Inc.; density 1.078+/-0.002 g/ml; Cat.# 85-072- CL) in a 50 mL centrifuge tube and then centrifuged for 30 minutes at 600 X g. Banded PBMCs are gently aspirated from the resulting interface and subsequently washed 2X with PBS by low speed centrifugation. After the final wash, cells are enumerated by trypan blue exclusion and re-suspended at  $1 \times 10^7$  cells/mL in RPMI 1640 supplemented with 15 % Fetal Bovine Serum (FBS), and 2 mM L- glutamine, 4  $\mu$ g/mL Phytohemagglutinin (PHA, Sigma). The cells are allowed to incubate for 48-72 hours at 37 C. After incubation, PBMCs are centrifuged and re-suspended in RPMI 1640 with 15% FBS, 2 mM L-glutamine, 100 U/mL penicillin, 100  $\mu$ g/mL streptomycin, and 20 U/mL recombinant human IL-2 (R&D Systems, Inc). IL-2 is included in the culture medium to maintain the cell division initiated by the PHA mitogenic stimulation. PBMCs are maintained in this medium at a concentration of  $1-2 \times 10^6$  cells/mL with biweekly medium changes until used in the assay protocol. Cells are kept in culture for a maximum of two weeks before being deemed too old for use in assays and discarded. MDMs are depleted from the culture as the result of adherence to

the tissue culture flask. For the standard PBMC assay, PHA stimulated cells from at least two normal donors are pooled (mixed together), diluted in fresh medium to a final concentration of  $1 \times 10^6$  cells/mL, and plated in the interior wells of a 96 well round bottom microplate at 50  $\mu$ L/well ( $5 \times 10^4$  cells/well) in a standard format developed by the Infectious Disease Research department of Southern Research Institute. Pooling (mixing) of mononuclear cells from more than one donor is used to minimize the variability observed between individual donors, resulting from quantitative and qualitative differences in HIV infection and overall response to the PHA and IL-2 of primary lymphocyte populations. Each plate contains virus/cell control wells (cells plus virus), experimental wells (drug plus cells plus virus) and compound control wells (drug plus media without cells, necessary for MTS monitoring of cytotoxicity). In this in vitro assay, PBMC viability remains high throughout the duration of the incubation period. Therefore, infected wells are used in the assessment of both antiviral activity and cytotoxicity. Test drug dilutions are prepared at a 2X concentration in microtiter tubes and 100  $\mu$ L of each concentration (nine total concentrations) are placed in appropriate wells using the standard format. 50 L of a predetermined dilution of virus stock is placed in each test well (final MOI = 0.1). The PBMC cultures are maintained for seven days following infection at 37°C, 5% CO<sub>2</sub>. After this period, cell-free supernatant samples are collected for analysis of reverse transcriptase activity and/or p24 antigen content. Following removal of supernatant samples, compound cytotoxicity is measured by addition of MTS to the plates for determination of cell viability. Wells are also examined microscopically and any abnormalities are noted. MTS staining for PBMC viability to measure cytotoxicity: At assay termination, assay plates are stained with the soluble tetrazolium-based dye MTS (CellTiter 96 Reagent, Promega) to determine cell viability and quantify compound toxicity. The mitochondrial enzymes of metabolically active cells metabolize MTS to

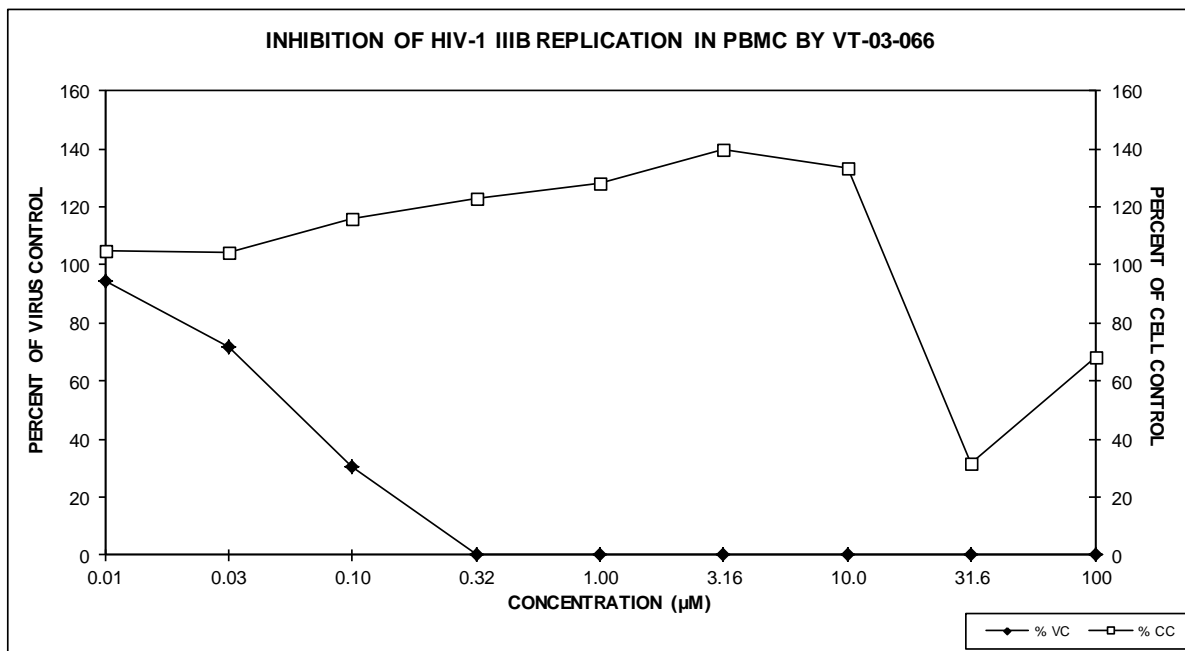
yield a soluble formazan product. This allows the rapid quantitative analysis of cell viability and compound cytotoxicity. The MTS is a stable solution that does not require preparation before use. At termination of the assay, 20  $\mu$ L of MTS reagent is added per well. The microtiter plates are then incubated 4-6 hrs at 37°C. The incubation intervals were chosen based on empirically determined times for optimal dye reduction. Adhesive plate sealers are used in place of the lids, the sealed plate is inverted several times to mix the soluble formazan product and the plate is read spectrophotometrically at 490/650 nm with a Molecular Devices Vmax or SpectraMaxPlus plate reader. Data Analysis Using an in-house computer program: IC<sub>50</sub> (50% inhibition of virus replication), IC<sub>90</sub> (90% inhibition of virus replication), IC<sub>95</sub> (95% inhibition of virus replication), TC<sub>50</sub> (50% cytotoxicity), TC<sub>90</sub> (90% cytotoxicity), TC<sub>95</sub> (95% cytotoxicity) and therapeutic index values (TI = TC/IC; also referred to as Antiviral Index or AI) are provided. Raw data for both antiviral activity and toxicity with a graphical representation of the data are provided below summarizing the individual compound activity.

### INHIBITION OF HIV-1 IIIB REPLICATION IN PBMC BY VT-03-066

RT Values(cpm)										
CONC (µM)	0.0	0.01	0.03	0.10	0.32	1.00	3.16	10.0	31.6	100
SAMPLE 1	11605	11107	10017	5402	0	0	0	0	0	0
SAMPLE 2	10088	9721	7608	2090	0	0	0	0	0	0
SAMPLE 3	11037	10025	5865	2559	0	0	0	0	0	0
MEAN	10909.8	10284.0	7829.7	3350.0	0.0	0.0	0.0	0.0	0.0	0.0
% VC	100.0	94.3	71.8	30.7	0.0	0.0	0.0	0.0	0.0	0.0

TOXICITY VALUES (Cell Titer 96 - O. D. @ 490/650 nm)										
CONC (µM)	0.0	0.01	0.03	0.10	0.32	1.00	3.16	10.0	31.6	100
SAMPLE 1	0.714	0.702	0.691	0.761	0.836	0.862	0.958	0.924	0.225	0.509
SAMPLE 2	0.772	0.829	0.830	0.915	0.998	1.017	1.100	1.044	0.247	0.513
SAMPLE 3	0.776	0.845	0.838	0.948	0.941	1.017	1.107	1.053	0.248	0.526
MEAN	0.754	0.792	0.786	0.875	0.925	0.965	1.055	1.007	0.240	0.516
% CC	100.0	105.0	104.3	116.0	122.7	128.0	139.9	133.6	31.8	68.4

DRUG: VT-03-066	50%	90%	95%
TC (µM)	25.7	> 100	> 100
IC (µM)	0.06	0.22	0.26
ANTIVIRAL INDEX (AI)	453	> 456	> 378



Client: Emory  
 Project Number: 14018.13  
 Investigator: Lackman-Smith  
 Setup Date: 03/18/14



Virus/Strain: HIV-1 / IIIB  
 Virus Date/Titer: 7/18/08, 2.5 uL/well  
 Technician: Mankowski  
 PBMC2Drugs9Conc - ver 6.6

**CYP450 Assay (3A4, 2D6, and 2C19) on compound 137 (VT-04-008).**

Experiments performed by Ricerca, Inc.

CYP450, 3A4. Human recombinant CYP450 3A4 expressed in insect BTI-TN-5B1-4 is used. Test compound and/or vehicle is preincubated with 8 nM enzyme in phosphate buffer 7.4 for 15 minutes at 37°C. The reaction is initiated by addition of 50 uM 7-benzyloxy-4-(trifluoromethyl)-coumarin and cofactor solution (1.3 mM NADP, 3.5 mM glucose-6-phosphate buffer pH 7.4 for 15 minutes at 37°C, 3.3 mM MgCl<sub>2</sub> for a 30 minute incubation period and terminated by further addition of 80% acetonitrile. Determination of the amount of 7-hydroxy-4-trifluoromethyl-coumarin formed is read spectrofluorimetrically. CYP450, 2D6 % 2C19 - Human recombinant CYP450 3A4 expressed in insect BTI-TN-5B1-4 is used. Test compound and/or vehicle is preincubated with 8 nM enzyme in phosphate buffer 7.4 for 15 minutes at 37°C. The reaction is initiated by addition of 50 uM 7-benzyloxy-4-(trifluoromethyl)-coumarin and cofactor solution (1.3 mM NADP, 3.5 mM glucose-6-phosphate buffer pH 7.4 for 15 minutes at 37°C, 3.3 mM MgCl<sub>2</sub> for a 30 minute incubation period and terminated by further addition of 80% acetonitrile. Determination of the amount of 7-hydroxy-4-trifluoromethyl-coumarin formed is read spectrofluorimetrically.

**Displacement of <sup>125</sup>I-SDF-1 Binding by Compound 137 (VT-04-008).**

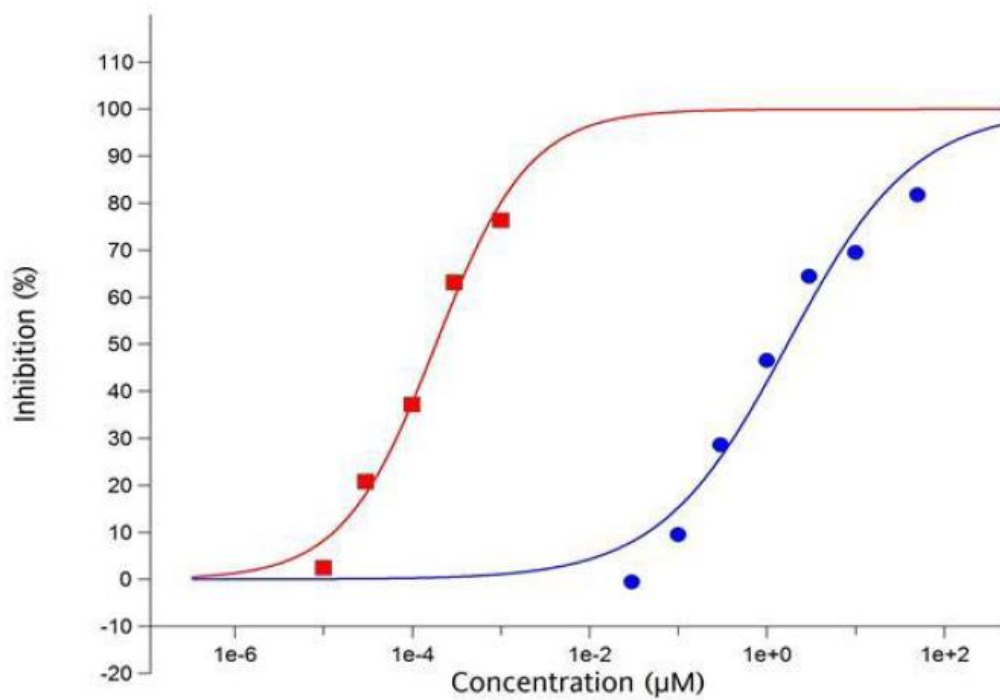
Experiments performed at Ricerca, Inc. Taipai, Taiwan.

Human chemokine CXCR4 expressed in Chem-1 cells are used in modified HEPES buffer pH 7.4. A 0.5 µg aliquot is incubated with 0.03 nM [<sup>125</sup>I]SDF-1α for 90 minutes at 25°C. Non-specific binding of a test compound is estimated in the presence of 30 nM SDF-1α. Membranes are filtered and washed, filters are then counted to determine [<sup>125</sup>I]SDF-1α specifically bound. Non labeled SDF-1, AMD3100, and Compound xx were screened at various concentrations and an IC<sub>50</sub> curve were determined, as shown below for compound 15. AMD3100 was found to have an IC<sub>50</sub> of 454 nM.

Experiments performed at Eurofin Panlabs, Inc.

**Compound: VT-04-008, PT #: 1179567**

118070	CYP450, 2C19	350015	hum	2	1 µM	-5			
118080	CYP450, 2D6	350016	hum	2	1 µM	47			
118090	CYP450, 3A4	350017	hum	2	1 µM	-12			
244550	Chemokine CXCR4	349964	hum	2	50 µM	82	1.70 µM	1.29 µM	0.61
			hum	2	10 µM	69			
			hum	2	3 µM	64			
			hum	2	1 µM	47			
			hum	2	0.3 µM	29			
			hum	2	0.1 µM	9			
			hum	2	0.03 µM	-1			

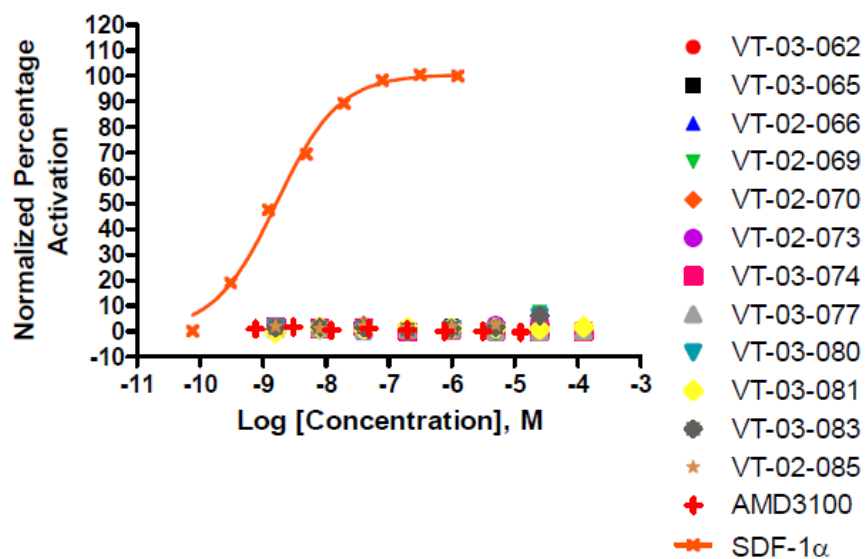
**Assay: 244550** - 1 Chemokine CXCR4

Compound Name	IC <sub>50</sub>	K <sub>i</sub>	n <sub>H</sub>
● VT-04-008 (1179567)	1.70 μM	1.29 μM	0.61
■ SDF-1α	0.18 nM	0.14 nM	0.83

## Calcium Flux Data for Compound 137 (VT-03-066)

CXCR4 Agonist Data (Percentage Activation Normalized to  $E_{max}$  Control)

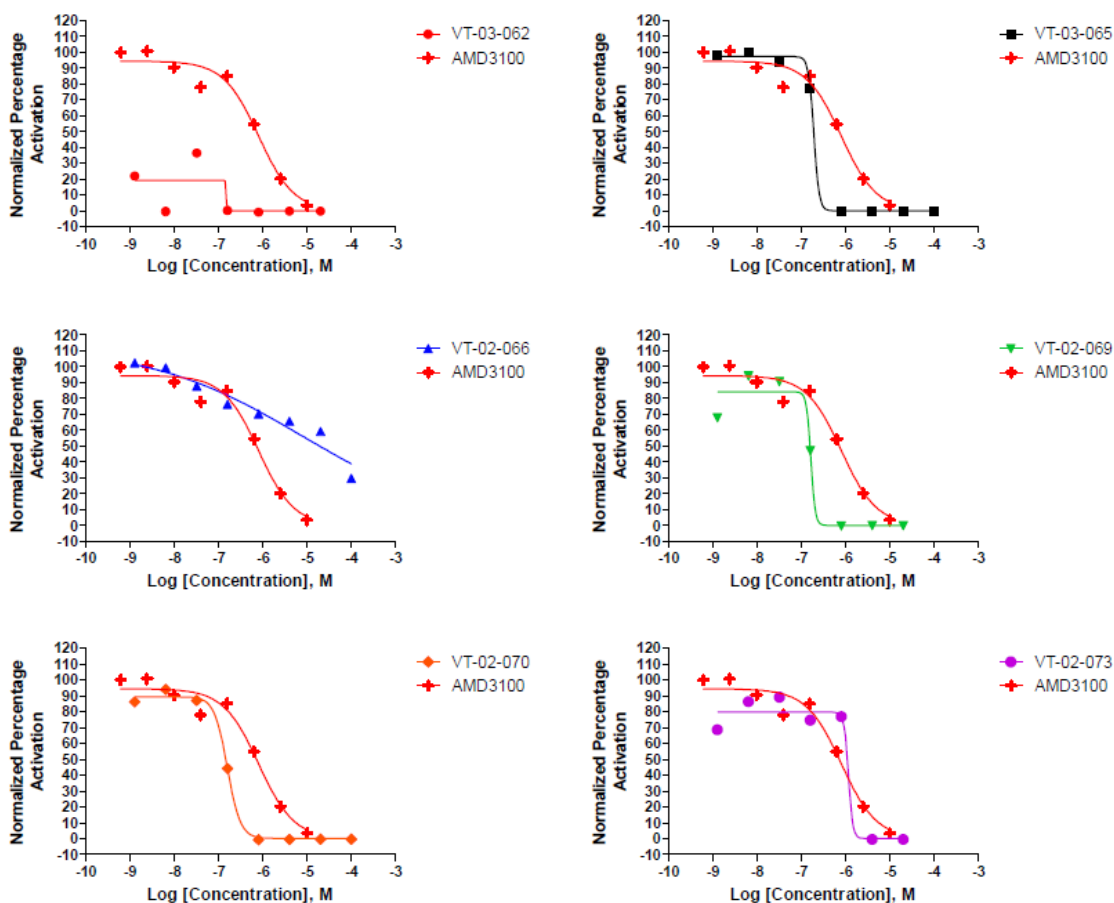
Plate 1



<u>Compound ID</u>	<u>Predicted EC<sub>50</sub> Potency Value</u>
VT-03-062	-*
VT-03-065	-
VT-02-066	-
VT-02-069	-*
VT-02-070	-
VT-02-073	-*
VT-03-074	-
VT-03-077	-
VT-03-080	-*
VT-03-081	-
VT-03-083	-*
VT-02-085	-*
AMD3100	-
SDF-1α	1.7nM

\* Top dose(s) of compound formed a precipitate when added to HBSS FLIPR buffer making it difficult to determine if any agonist or antagonist activity seen was due to receptor activation or inhibition, respectively, or if activity seen was non-receptor mediated. Those points were removed due to unreliability of data.

### CXCR4 Antagonist Data (Percentage Activation Normalized to EC<sub>80</sub> Control)



<u>Compound ID</u>	<u>Predicted IC<sub>50</sub> Potency Value</u>
VT-03-062	<1.6nM *
VT-03-065	190nM
VT-02-066	~7.7μM
VT-02-069	160nM*
VT-02-070	160nM
VT-02-073	1.2μM*
AMD3100	300nM

\* Top dose(s) of compound formed a precipitate when added to HBSS FLIPR buffer making it difficult to determine if any agonist or antagonist activity seen was due to receptor activation or inhibition, respectively, or if activity seen was non-receptor mediated. Those points were removed due to unreliability of data.

## References

1. Choi, W. T.; Tian, S.; Dong, C. Z.; Kumar, S.; Liu, D.; Madani, N.; An, J.; Sodroski, J. G.; Huang, Z., Unique ligand binding sites on CXCR4 probed by a chemical biology approach: implications for the design of selective human immunodeficiency virus type 1 inhibitors. *Journal of virology* **2005**, *79* (24), 15398-404.
2. Scholten, D. J.; Canals, M.; Maussang, D.; Roumen, L.; Smit, M. J.; Wijtmans, M.; de Graaf, C.; Vischer, H. F.; Leurs, R., Pharmacological modulation of chemokine receptor function. *British journal of pharmacology* **2012**, *165* (6), 1617-43.
3. Debnath, B.; Xu, S.; Grande, F.; Garofalo, A.; Neamati, N., Small molecule inhibitors of CXCR4. *Theranostics* **2013**, *3* (1), 47-75.
4. Pierce, K. L.; Premont, R. T.; Lefkowitz, R. J., Seven-transmembrane receptors. *Nature reviews. Molecular cell biology* **2002**, *3* (9), 639-50.
5. Kenakin, T., Functional selectivity and biased receptor signaling. *The Journal of pharmacology and experimental therapeutics* **2011**, *336* (2), 296-302.
6. Christopoulos, A.; Kenakin, T., G protein-coupled receptor allosterism and complexing. *Pharmacological reviews* **2002**, *54* (2), 323-74.
7. Burger, J. A.; Peled, A., CXCR4 antagonists: targeting the microenvironment in leukemia and other cancers. *Leukemia* **2009**, *23* (1), 43-52.
8. Muller, C. E.; Schiedel, A. C.; Baqi, Y., Allosteric modulators of rhodopsin-like G protein-coupled receptors: opportunities in drug development. *Pharmacology & therapeutics* **2012**, *135* (3), 292-315.
9. Wu, B.; Chien, E. Y.; Mol, C. D.; Fenalti, G.; Liu, W.; Katritch, V.; Abagyan, R.; Brooun, A.; Wells, P.; Bi, F. C.; Hamel, D. J.; Kuhn, P.; Handel, T. M.; Cherezov, V.; Stevens, R. C., Structures of the CXCR4 chemokine GPCR with small-molecule and cyclic peptide antagonists. *Science* **2010**, *330* (6007), 1066-71.